TESLA - COLLABORATION

Transparencies from the
TESLA Meeting, July 7-9, 1999 at DESY

DESY

July 1999, TESLA 99-13

TESLA Meeting at DESY, July 7 - 9, 1999

M. Leenen 25.6.1999

Preliminary Agenda
for the TTF Collaboration Meeting
DESY, 7th - 9th July, 1999

<u>July 7th, Seminarroom 2, Building 2a</u> (Please notice different room)

9:00	Welcome and Introduction	D. Trines
9:15	Summary of Linac Operation	G. Schmidt / S. Schreiber
10:00	Status of Cavities and Auxiliaries	D. Proch
10:20	Superstructure Concept	J. Sekutowicz
10:40	Coffee Break	
11:10	Shutdown Activities	H. Schlarb
11:30	Progress on Controls	K. Rehlich
12:00	Undulator Status	U. Hahn
12:20	Photon Diagnostics	R. Treusch
12:40	Organisation of Working Groups	

- Cavities and Auxiliaries
  B. Aune/D. Bloess/P. Schmüser
- Commissioning and Experimental Program for TTF Linac
  M. Castellano/T. Garvey/G. Schmidt

14:00 Main Auditorium
Colloquium in Memory of Björn H. Wiik

July 8th, (Rooms to be announced)

9:00 Working Groups
17:00 Meeting of Technical Board
19:00 Social Event (Annex of DESY canteen)

July 9th, Seminarroom 4a+b, Building 1b

9:00	News from Collaborating Institutions	
	Saclay / Orsay	B. Aune
	INFN	C. Pagani
	FNAL	H. Edwards
	CERN	D. Bloess
	FZ Karlsruhe	K.- P. Jüngst
	Others as requested	
10:40	Coffee Break	
11:10	Summary of Working Groups	
12:40	Next Meeting	
	AOB	

R. Brinkmann 25.06.99

July 8th, Seminarroom 5, Bld. 1b

9:00 TESLA-500 Working Group

Conveners: R. Brinkmann, O. Napoly

Preliminary programme: (final programme will be announced at the meeting)

Spent beam line and collimation; E. Merker
Positron injector linac; V. Paramonov
Damping ring design update; W. Decking
Positron Source before the IP; R. Brinkmann
Multi-bunch beam dynamics in main linac; N. Baboi
Beams with different energies (FEL/collider); V. Tsakanov
Estimate of beam halo; R. Brinkmann
Non-linear Energy Collimation; N. Walker
Beam Position Measurement at the IP; T. Scholz

Discussion on work to be done for TDR; all participants

Scientific Colloquium in Memory of Prof. Dr. Bjørn H. Wiik

Wednesday, July 7, 1999
at 2:00 pm

Am Mittwoch, dem 7. Juli 1999, findet um 14:00 Uhr das wissenschaftliche Kolloquium zum Gedenken an Bjorn H. Wiik statt. Dazu werden etwa 300 auswärtige Gäste aus dem In- und Ausland kommen.

Da im DESY-Hörsaal nur etwa 350 Personen Platz finden, wird das Kolloquium in den Seminarraum 4 und auch nach Zeuthen in Wort und Bild übertragen.

Ferner wird in das Foyer des DESY-Hörsaals und auch in den Vorraum vor dem Seminarraum 4 eine Tonübertragung geschaltet, um allen Besuchern die Möglichkeit zu geben, das Kolloquium zu verfolgen.

Wegen des so geringen Platzangebotes im DESY-Hörsaal werden die DESY-Mitarbeiter gebeten, insbesondere den Seminarraum 4 bzw. in Zeuthen das Foyer zu besuchen, um so in Gastfreundschaft den auswärtigen Gästen den DESY-Hörsaal zu überlassen.

Das Programm des Kolloquiums sieht folgende Beiträge vor:

Streichquartett Op. 27, 1. Satz von E. Grieg

Eröffnung des Kolloquiums - Prof. Dr. Albrecht Wagner

Worte des Erinnerns • Reminiscence and Recollection

Erster Bürgermeister Ortwin Runde
MDg. Dr. Hermann Schunck, BMBF
Prof. Dr. Jürgen Lüthje, Universität Hamburg
Prof. Dr. Detlev Ganten, HGF
Prof. Dr. Luciano Maiani, CERN
Prof. Dr. Ralph Eichler, Wissenschaftlicher Rat

Maury Tigner	*Impact of Superconductivity on Particle Physics*
Burton Richter	*The Role of Electron-Positron Colliders for Particle Physics*
	Coffee/Tea Break
Chris Llewellyn-Smith	*Deep Inelastic Scattering*
Jochen Schneider	*Synchrotron Radiation Research at Particle Physics Laboratories*
Volker Soergel	*Bjorn H. Wiik and DESY*

Deutsches Elektronen-Synchrotron
Hamburg, Germany

TESLA

March 25th Oberbergamt Clausthal-Zellerfeld

had invited administrative bodies from communities and county and also environmental interest groups to set the scope for the Environmental Impact Study for TESLA

"Scoping Termin"

Project was presented by DESY
Civil engineering by engineering bureau

Positive atmosphere; mainly constructive criticism

Part of the procedure to secure the legal framework for the construction of TESLA

April 19 th Ministry of Education and Research
Frau Bulmahn

intends to recommand to the German Science Council
to evaluateTESLA in 2001

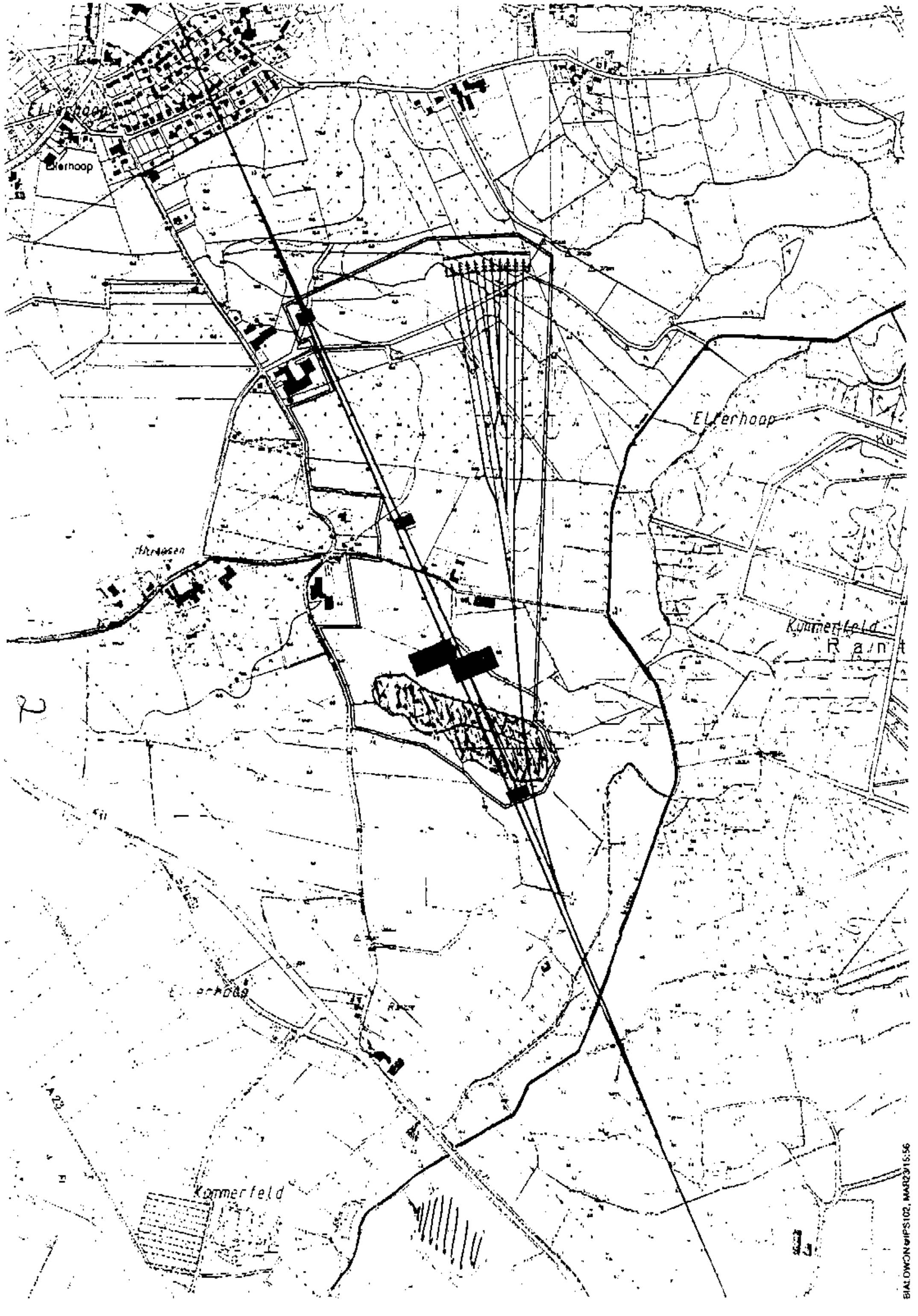

Kurzantrag für den HGF-Vernetzungsfond

Hochfrequenz-Photoinjektoren als Quellen für Elektronenpakete extrem kleiner Länge und Emittanz

Zusammenfassung

DESY plant in Zusammenarbeit mit anderen HGF Zentren und einer grossen Zahl internationaler Partner ein internationales Institut für Angewandte- und Grundlagenforschung in Deutschland. Diese Anlage wird weltweit einmalige Forschungsmöglichkeiten in Bereichen von der Elementarteilchenphysik über die Festkörperforschung, Chemie und Materialwissenschaften bis hin zur medizinischen Diagnostik und Molekularbiologie anbieten. Die laufenden Forschungs- und Entwicklungsarbeiten für TESLA werden zu einem integrierten Systemtest für einen supraleitenden Linac und einem SASE FEL im VUV und weichen Röntgenbereich führen (TESLA Test Facility, TTF).
Für den FEL und den Linac-Betrieb werden Elektronenstrahlen mit höchster Strahlqualität benötigt. Deshalb wird bei DESY ein Entwicklungsprogramm im Bereich der Hochfrequenzelektronenquellen mit dem Ziel einer Optimierung der Strahlqualität und der Betriebsparameter wie z. B. der Betriebssicherheit, verfolgt. Um diese Ziele zu erreichen sind neben einer Weiterentwicklung im Bereich der Simulationsrechnungen und theoretischer Ansätze insbesondere qualitativ hochwertige Messungen der Strahlemittanz unabdingbar. Nach bisherigen Erfahrungen ist ohne ein Experimentierprogramm, also nur aufgrund von Rechnungen, kein nennenswerter Fortschritt zu erwarten.

Beteiligte Institute:

Kurzantrag für den HGF-Fond "Vorbereitung neuer Aktivitäten"

Superconducting RF Cavities of Ultimate Performance

Abstract

DESY plans, together with other HGF centers and a large number of international partners, to build the Tera Electronvolt Superconducting Linear Accelerator TESLA as an international institute for pure and applied science in Germany. This facility, comprising an electron-positron collider with a center-of-mass energy of at least 500 GeV and a Free Electron Laser in the X-ray regime, will offer world-wide unique possibilities for pure and applied research in areas ranging from elementary particle physics via solid state physics, chemistry and materials science to medical diagnostics and molecular biology.

The **Forschungszentrum Jülich** in collaboration with a large number of international partners is pursueing the design of the European Spallation Source ESS as the next generation neutron source to secure Europe's leading role in applying neutron beams to basic and applied research in physics, chemistry, materials science, life sciences, engineering sciences and Earth sciences.

Both facilities rely heavily on superconducting radio-frequency cavities to accelerate high currents of electrons or positrons in TESLA and of negative hydrogen ions in the ESS to high energies. Their main advantages in comparison with normal-conducting accelerating structures are the much reduced operational costs and the improved beam quality.

In order to fully exploit the capabilities of superconducting cavities fabricated from solid niobium, an extensive R&D program is proposed concentrating on the following four topics:

- Development of production methods for niobium of higher purity,
- Improved chemical treatment methods of the inner (radio frequency) surface of the cavities,
- Reinforcement of the mechanical stability of the cavities,
- Development of seamless cavities.

It is intended to collaborate in the R&D program with other HGF institutions (GKSS, HMI), with institutes and universities (Bundesanstalt für Materialforschung, CERN, RWTH Aachen, IN2P3 Orsay, CE Saclay, Universität der Bundeswehr) and with industry (ACCEL, F.I.T. Messtechnik, Heraeus).

— E.P.

Want to have first cost evaluation of the whole project beginning of next year.

Also required manpower for the construction, installation and commissioning period.

INFN will design and evaluate damping rings cryostats cavity production
INR Troitsk will design and evaluate positron linacs
IHEP Protvino will design and evaluate beam dumps collimation system
Orsay/Saclay will design and evaluate injectors beam delivery sytem cavity production

Have established a planning group

BESSY + HMI JOINED WORK ON TTF + FEL BEAMLINES

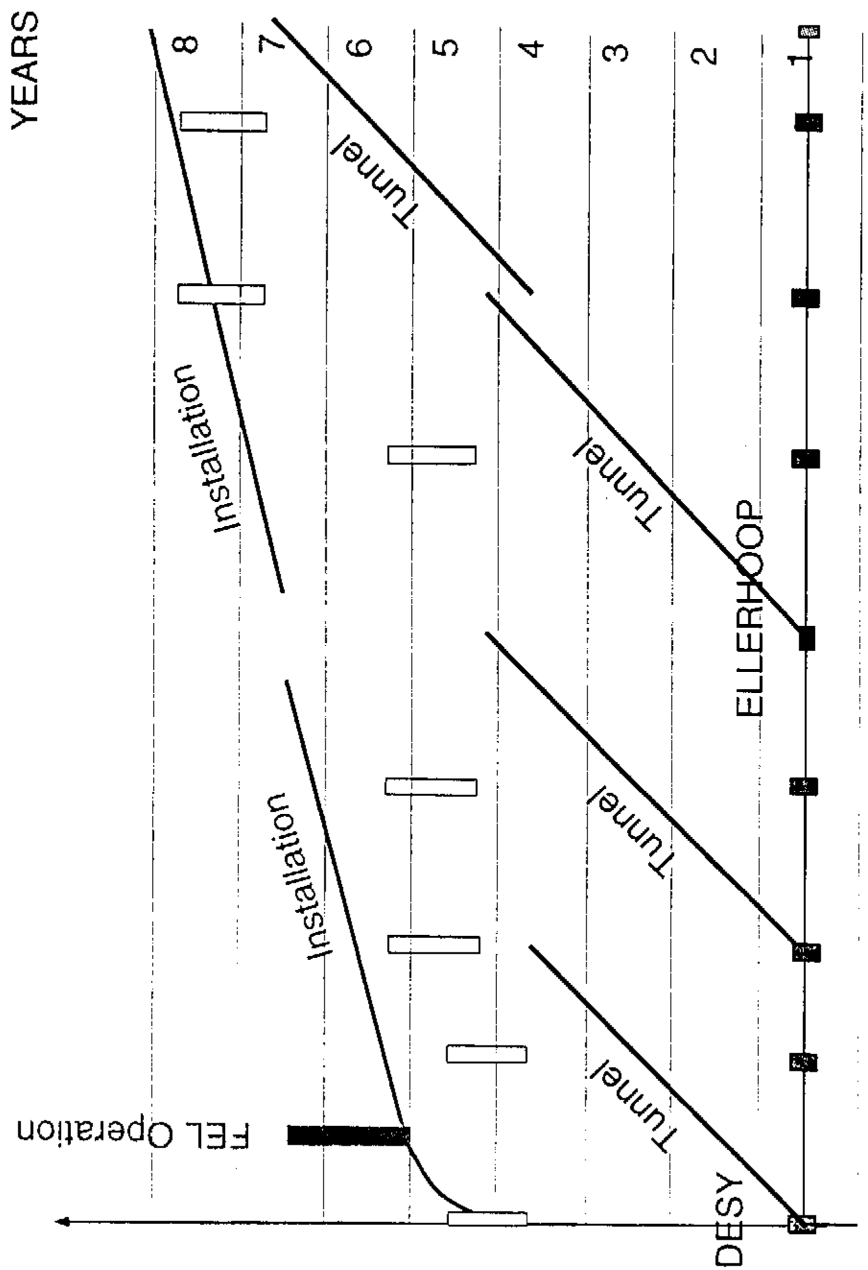

Obtained results from two independent studies on cavity preparation to module assembly

Positiv: no problem to process 20000 cavities within three years

Surprise: fraction of personnel to total cost is dominant
main part therein module assembly

differences between two studies have to be evaluated

Studies underway or in preparation:

cavity production with present technology

parallel studies by INFN and Saclay are envisaged

klystron production

modulator fabrication

wave guide production

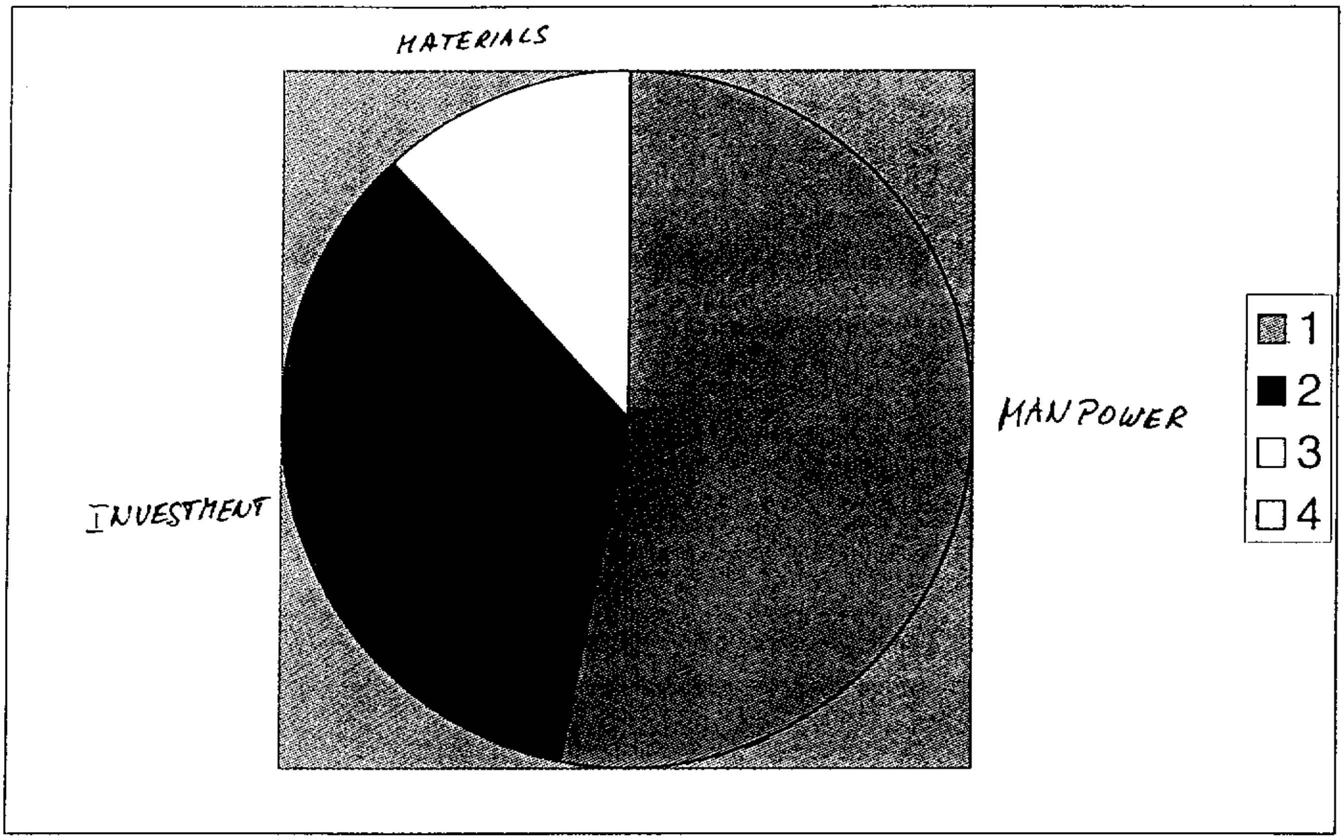
MATERIALS
MANPOWER
INVESTMENT
1
2
3
4

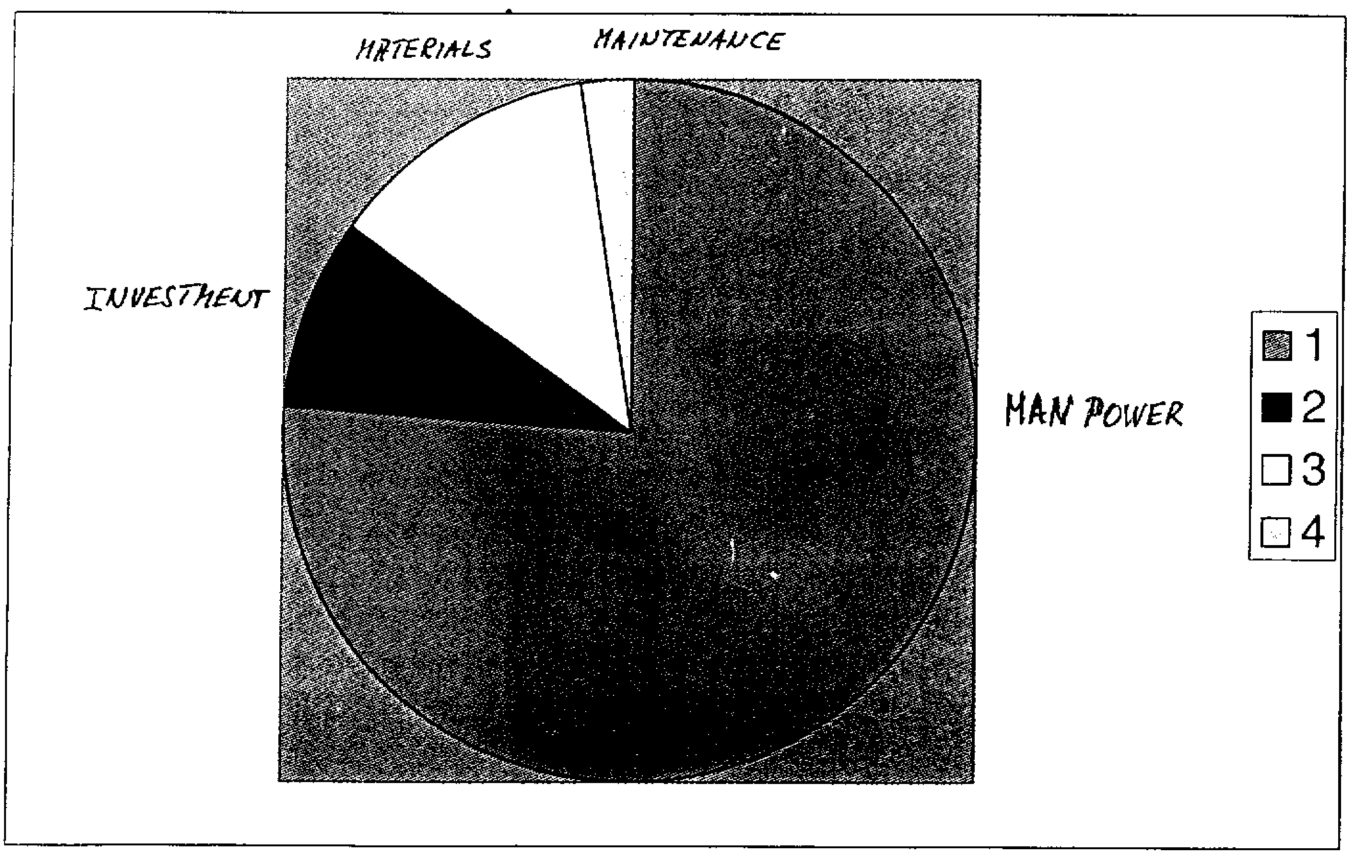
MATERIALS
MAINTENANCE
INVESTMENT
MAN POWER
1
2
3
4

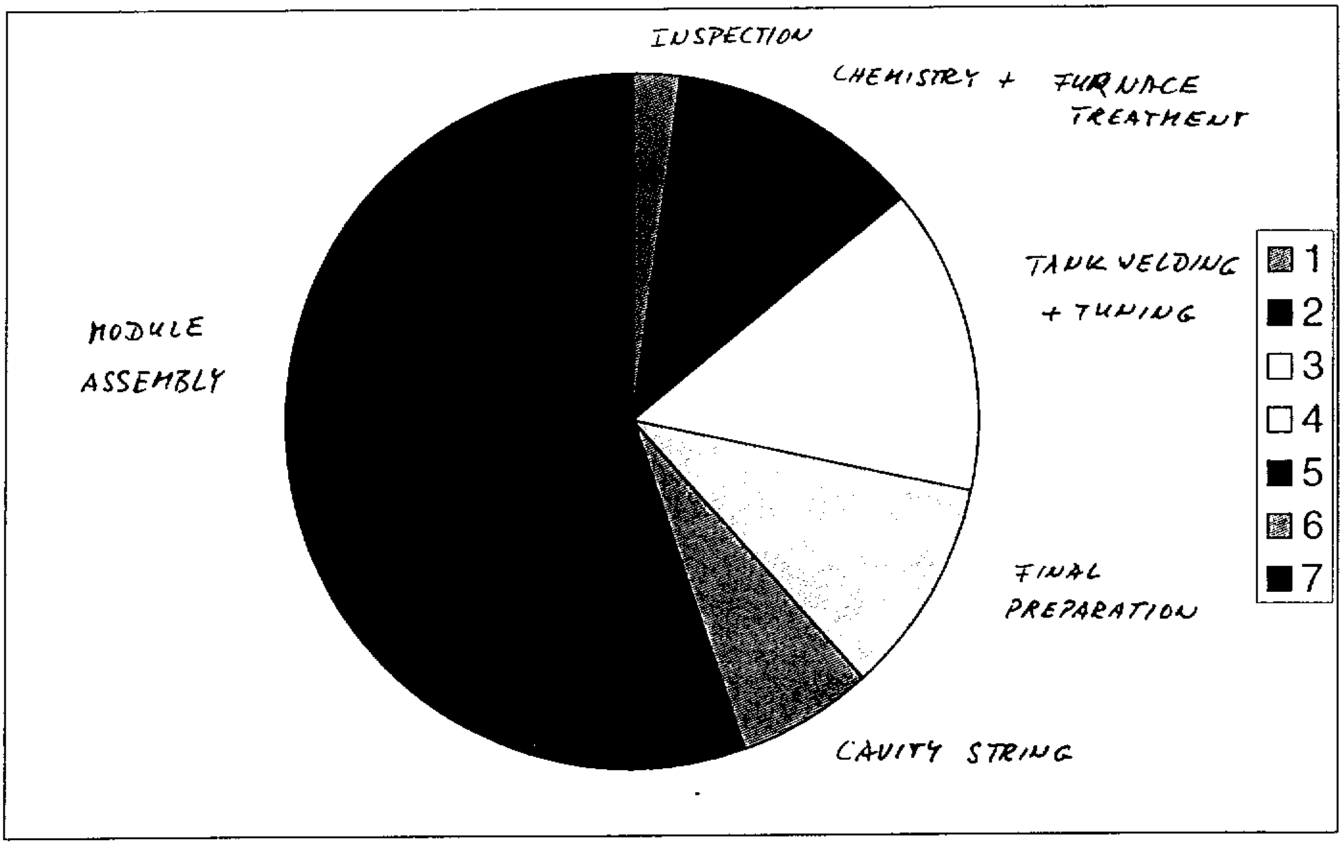

IRNES/MPYNT/HINES2, MAY24/1428

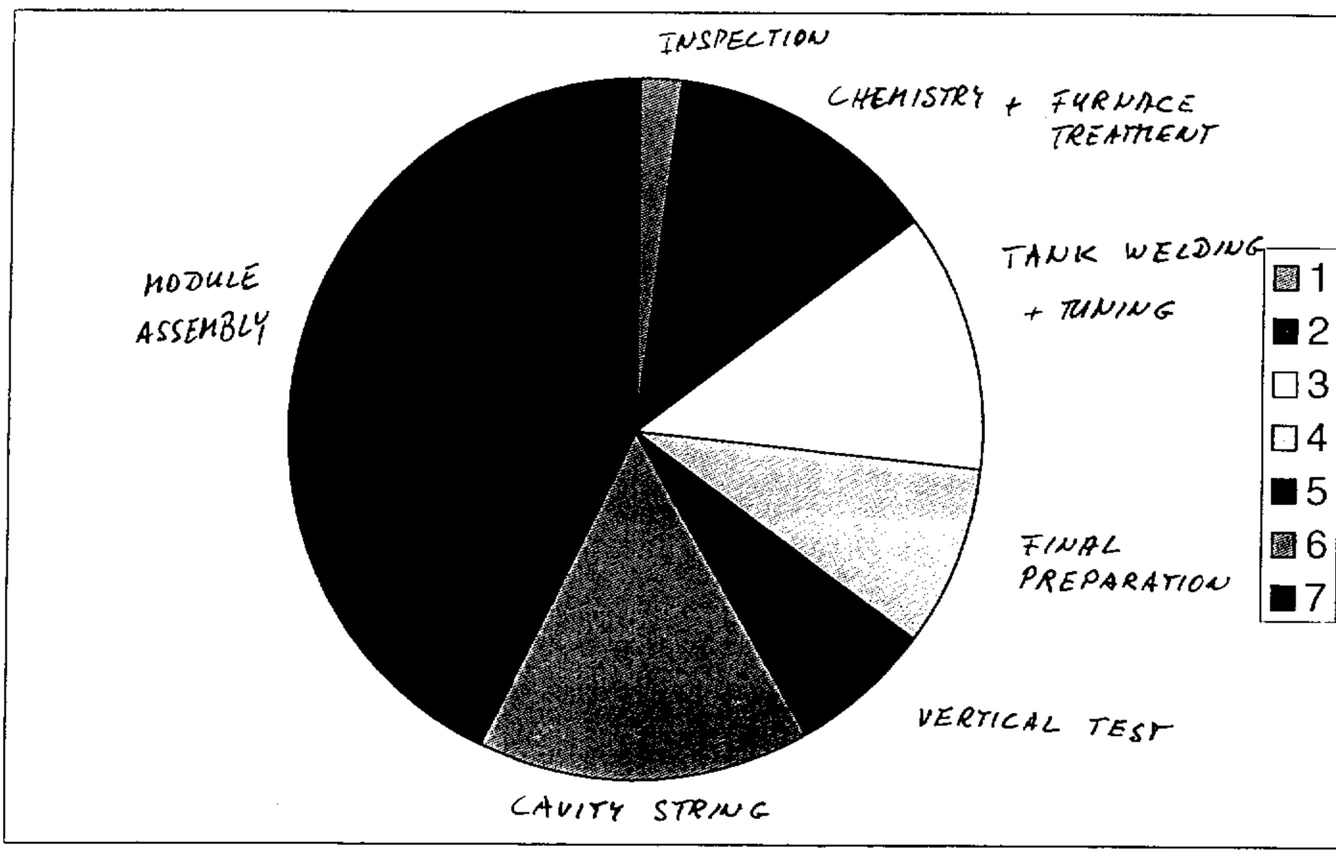

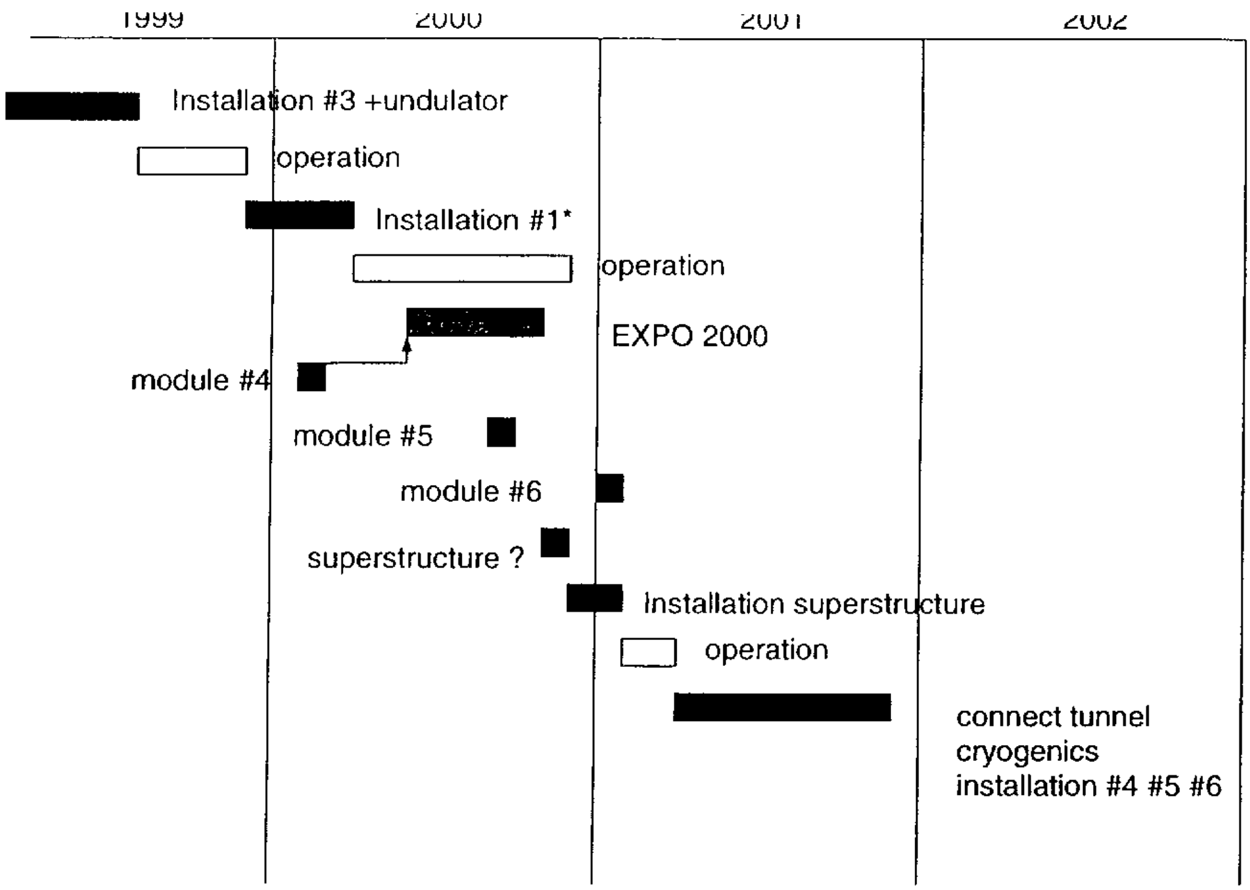

TESLAVB, JUL05/13:56

Linac operation results until 15. March 99

Introduction

Diagnostic changes due to 1 MHz bunch repetition rate
- BPM developments
- Toroids for beam current measurement

Results of emittance measurements:
Comparision between pepper pot and phase space tomography measurements

Summary module operation

Summary of achieved beam parameters

Conclusion

G. Schmidt, -MPY-, 6.07.99

Goal of the run

Preparation of the linac for the installation of the FEL

Commissioning of new beamline elements
1) New injector: FNAL Gun and new diagnostics
2) Bunch compressor II
3) Cryo Module 2

New diagnostics had to be made operational and beam parameters for the FEL had to be established.
->First results have been presented during the TESLA Meeting, March1-3,1999 at DESY

For High Energy collider: HOM and RF steering experiments (presented TESLA Meeting, March 1-3, 1999 at DESY)

Performance of the TTF-FEL Phase I

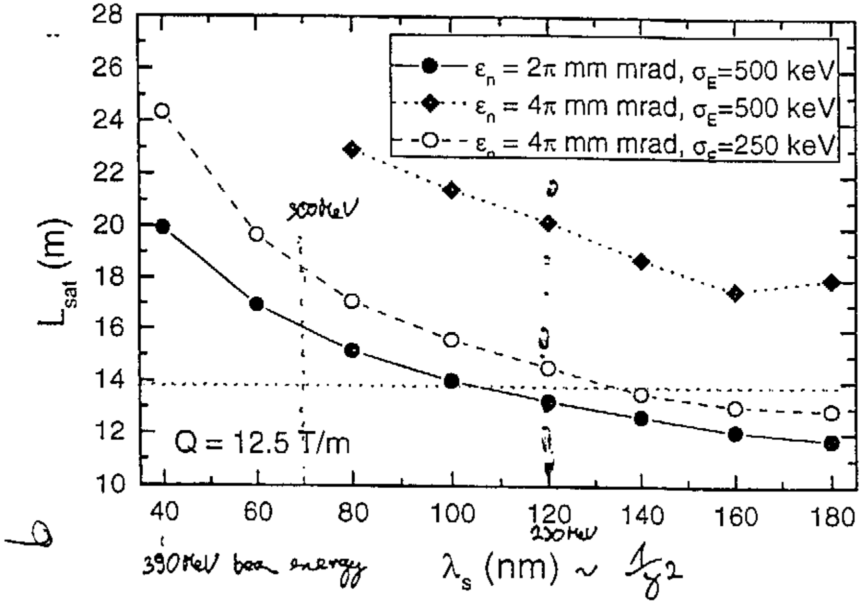

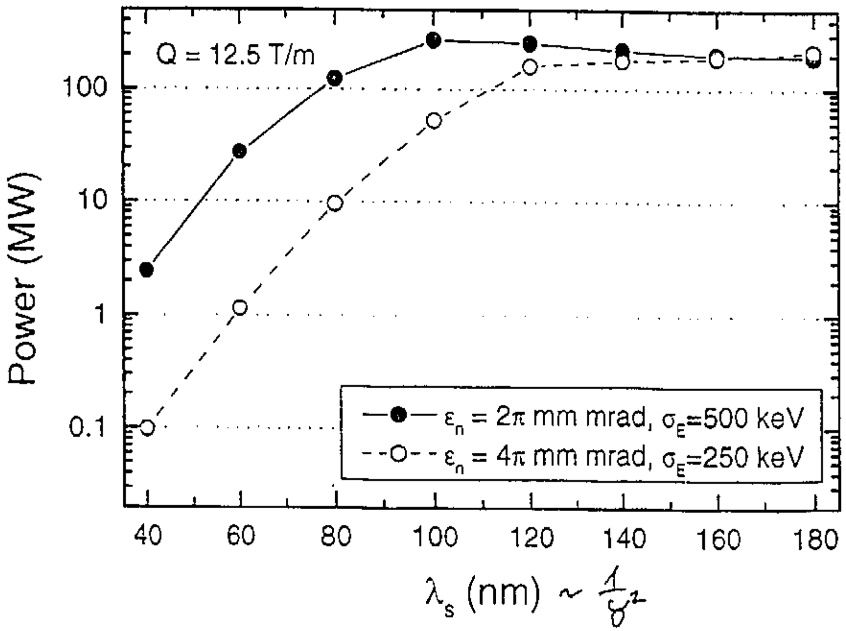

G. Schmidt, -MPY-, 6.07.99

Diagnostic changes due to 1 MHZ bunch repetition rate

BPM developments

The 1 MHz bunch repetition rate was new.
Change in electronics and special delays for the signals to the ADC's were needed.

At the end of the run all BPM's were working.
Calibration with steerer changes were done.

Resolution around 10 micro m can be expected for warm cavity BPM's
All BPM's show modulation of the offset along the macro pulse

Toroids for beam current measurement

Toroid system was adapted to 1 MHz

All Toroids were working at the end of the run and calibration of current was done to 20 %.
Problem occurred with saturation effects at higher beam currents.

B. Faatz

10

Bunch Position Measurements (March 99)

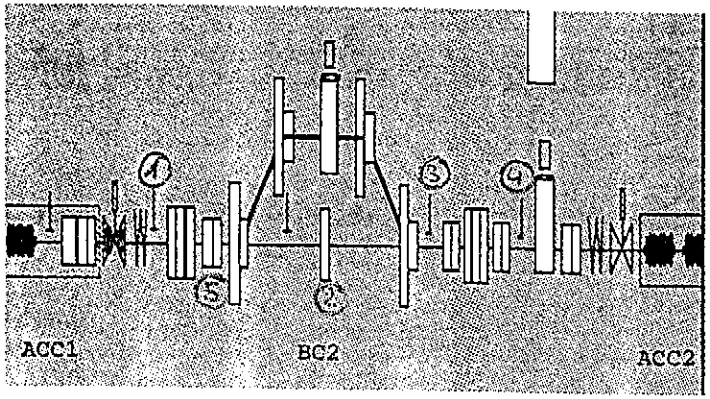

Goal:

Calibration of Reentrant BPM in straight section of BC2
$\Longrightarrow$ 1 V @ 8 nC, @ 1 mm

Beam Energy after Module 1	84.4 MeV
# Bunches	5 – 30
Bunch Spacing	1 μs
Bunch Charge	1 – 8 nC

mostly beam compensation off

used for position measurements:	design resolution
2 Cavity Monitors (No. 1,3):	10 μm
1 Reentrant BPM (No.2):	1 μm
1 Strip Line (No. 4):	20 μm
X/Y steerer (No. 5)	

I. Reyzl

For each steerer setting measure 10 pulses and calculate average bunch position

Move Steerer stepwise

REENTRANT INJ.ADC1: RUN CAL 8nC 110399 I11–Mar–1999 13:55:58

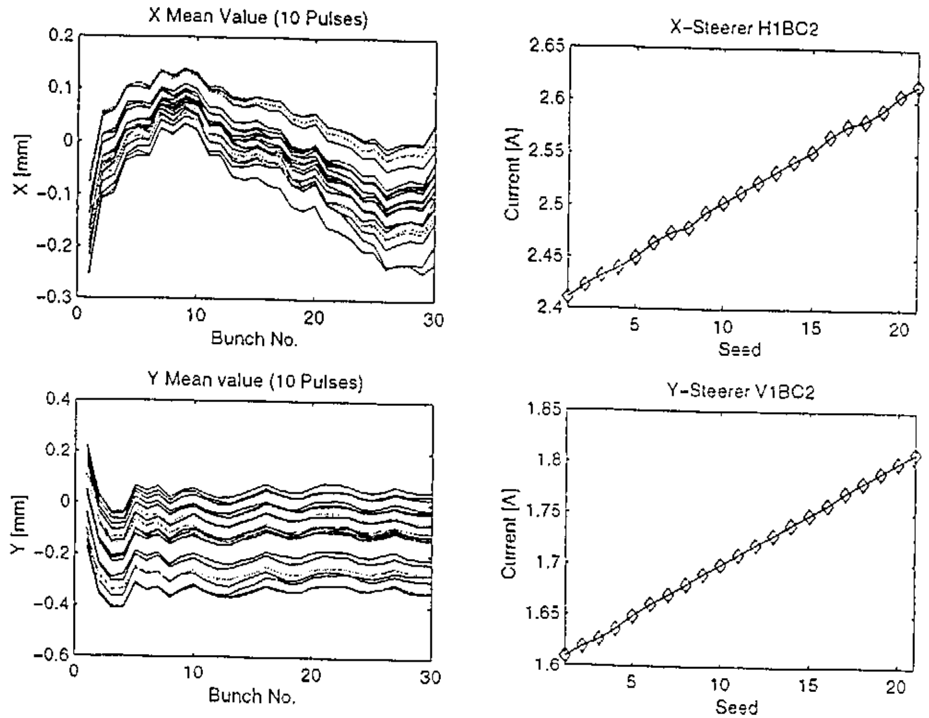

$\Delta I = 0.2A \,\hat{=}\, \Delta X,Y = 400\mu m$

Variation over 30 Bunches : Max - Min ~ 0.3 mm (X/Y)

X: S-Shape

Y: Peak @ 4. Bunch

MORE DATA NEEDED TO IDENTIFY ERROR SOURCES:

- DISPERSIVE EFFECTS
- BEAM OFFSET IN MODULE
- ...

X: PULSE-TO-PULSE VARIATION => POS. SHIFT BY STEERERS

Strip Line ACC2.ADC4: RUN CAL 8nC 110399 I11-Mar-1999 13:55:58

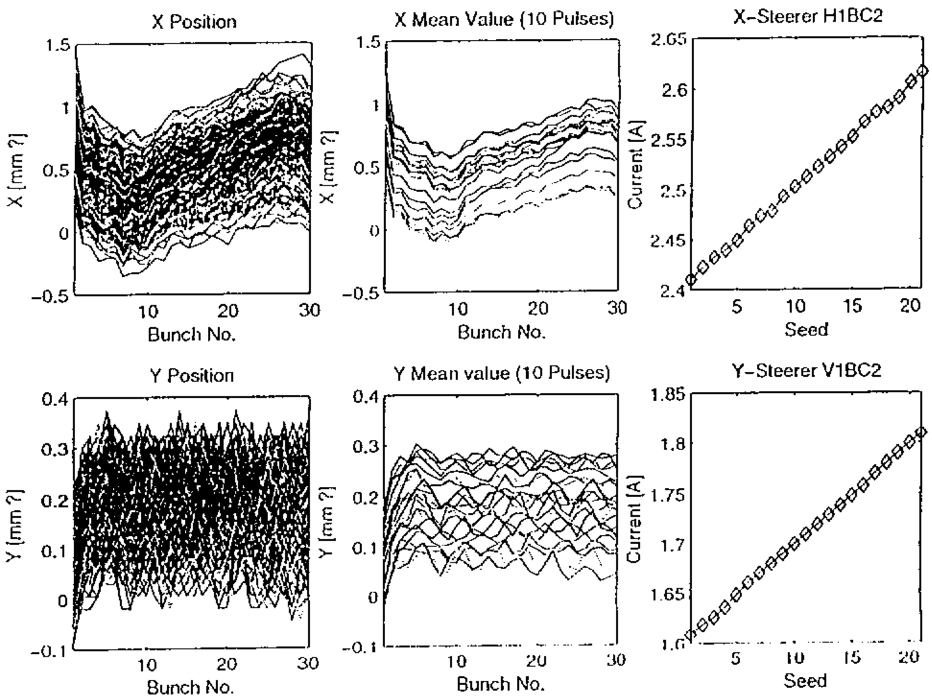

Cavity ACC2.ADC2: RUN CAL 8nC 110399 I11-Mar-1999 13:55:58

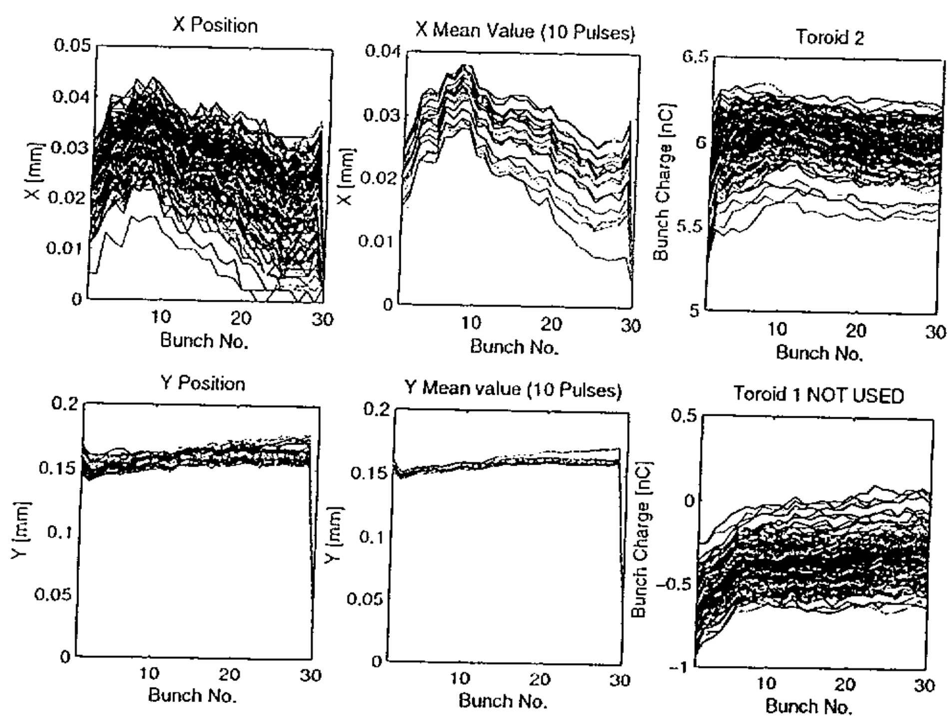

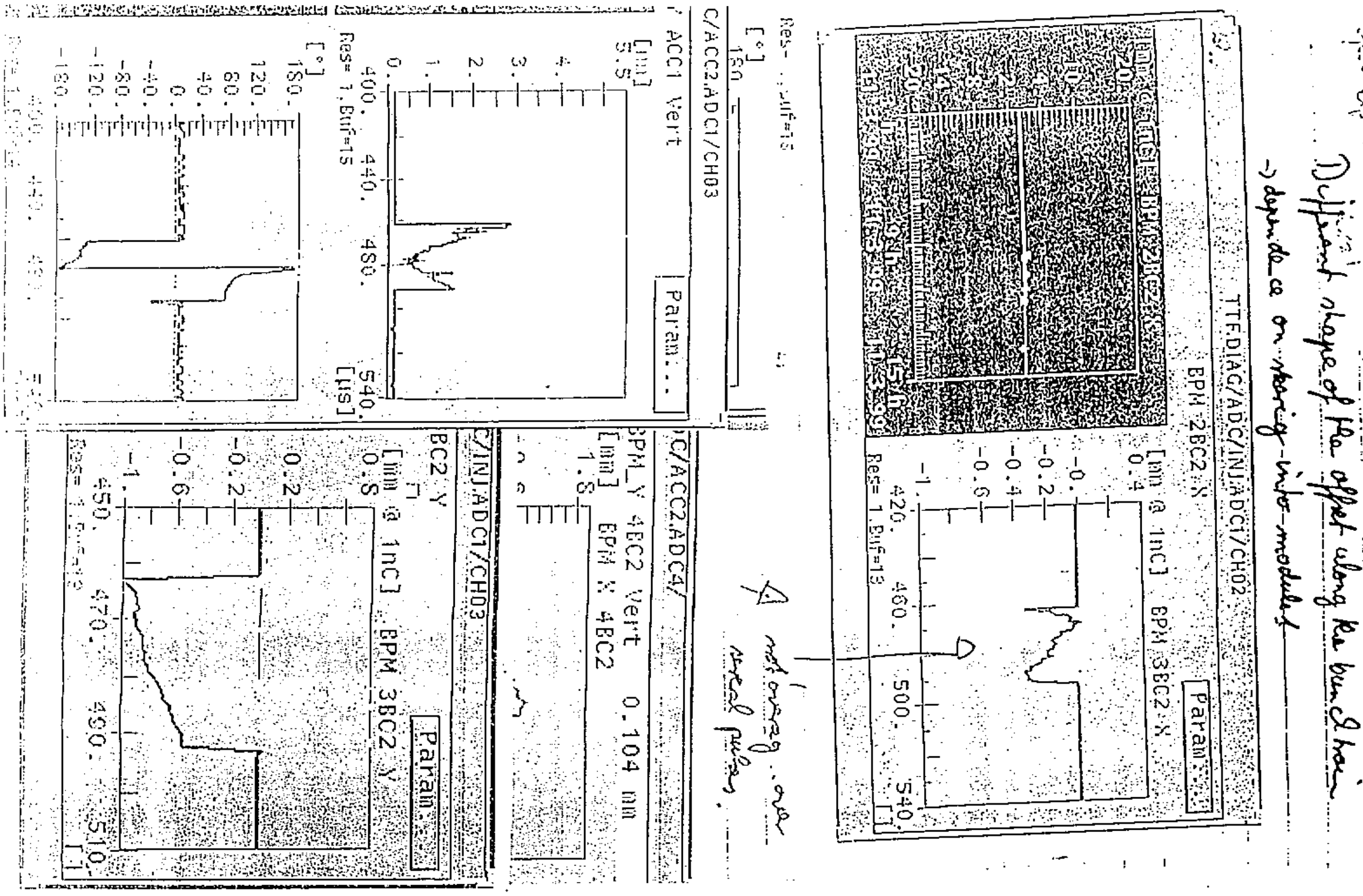

BPM 1BC2, steerer ACC1

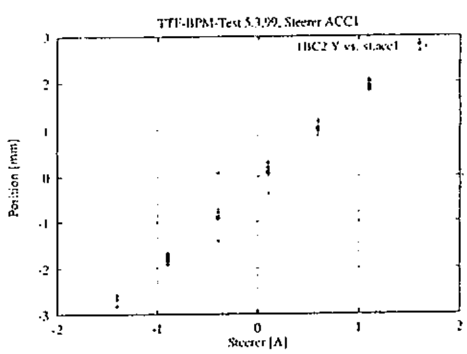

Signals 1BC2/y, position and jitter

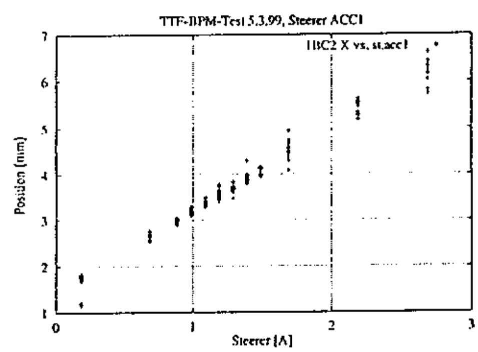

Signals 1BC/x, position and jitter

BPM 1BC2, x, steerer ACC1

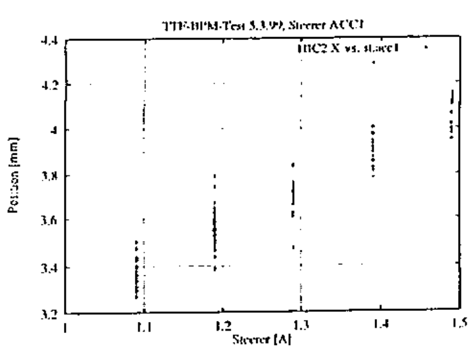

Signals 1BC2/x, position vs. steerer

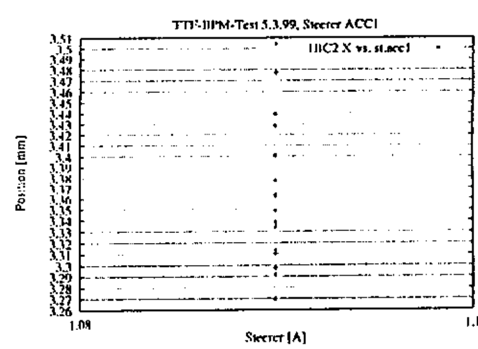

Signals 1BC2/x, position for st-value

BPM 1BC2, x, steerer ACC1

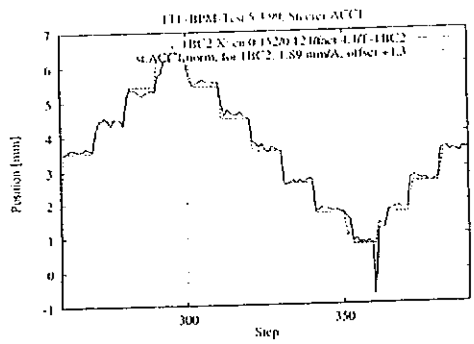

Signals 1BC2/x, steerer ACC1

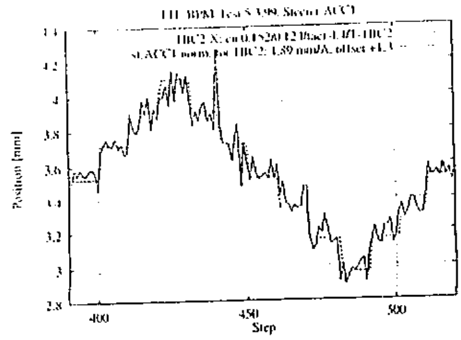

Signals 1BC/x2, steerer ACC1, fine

BPM 1BC2, y, steerer ACC1

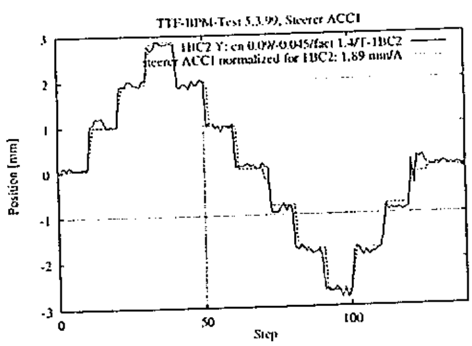

Signals 1BC2/y, steerer ACC1

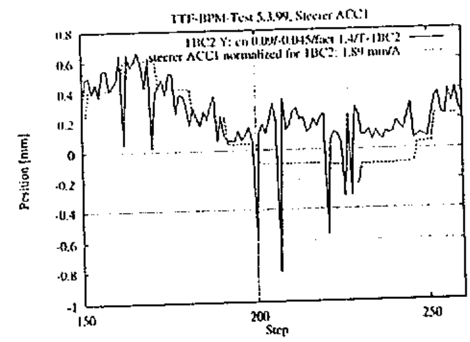

Signals 1BC2/y, steerer ACC1, fine

G. Schmidt, -MPY, 6.07.99

Emittance measurement along the linac

Comparision of pepper pot and phase space tomography measurements at the injector (done)

- ⇩ show good agreement in between error bars
- ⇩ emittance growth with number of bunches
- ⇩ multi bunch emittance was measured

Emittance measurement in BC2 and EXP

No real understanding of emittance growth to up to 80 mm mrad in the exp area.

Improved analysis of pepperpot (slit mask) data taken on 5.3.'99

14

Frank Stephan
FDET

- Introduction + Definitions
- Procedure
- Results
- Errors
- Conclusions
- Outlook

Injector settings

- magnets:
  - trim = 0.0
  - Sol. 1 = 158, 165, 176 ← scan
  - Sol. 2 = 86, 90, 96
  - gun steerer : hor. = −0.3 , vert. = +0.8
  - CC steerer : hor. = 0.0 , vert. = +0.3
  - PP → S.H5 INJ1 = 0.0 , S.V6 INJ1 = 0.0
  - screen → daublet Q.1INJ1 = 0.0 = Q.2INJ1 !
- gun:
  - SP voltage = <u>35 MV</u>
  - power reading at gun ≈ 2.27 MW
  - SP phase = −115° (ok!)
- laser:
  - U_{ctrl} = 1.5 V ⇒ Pk-Pk (ICT_{gun}) ≈ 20 mV
  - Øiris ≈ 3 mm
  - d.h. ≈ 1 nC
- cap. cav.:
  - phase = 141.29° (ok!)
  - gradient = 11.3 MV/m
- data taken on Fr. 5. March 1999 $8^{00} \rightarrow 14^{00}$ by D. Sertore + F. St.

±2 in last digit

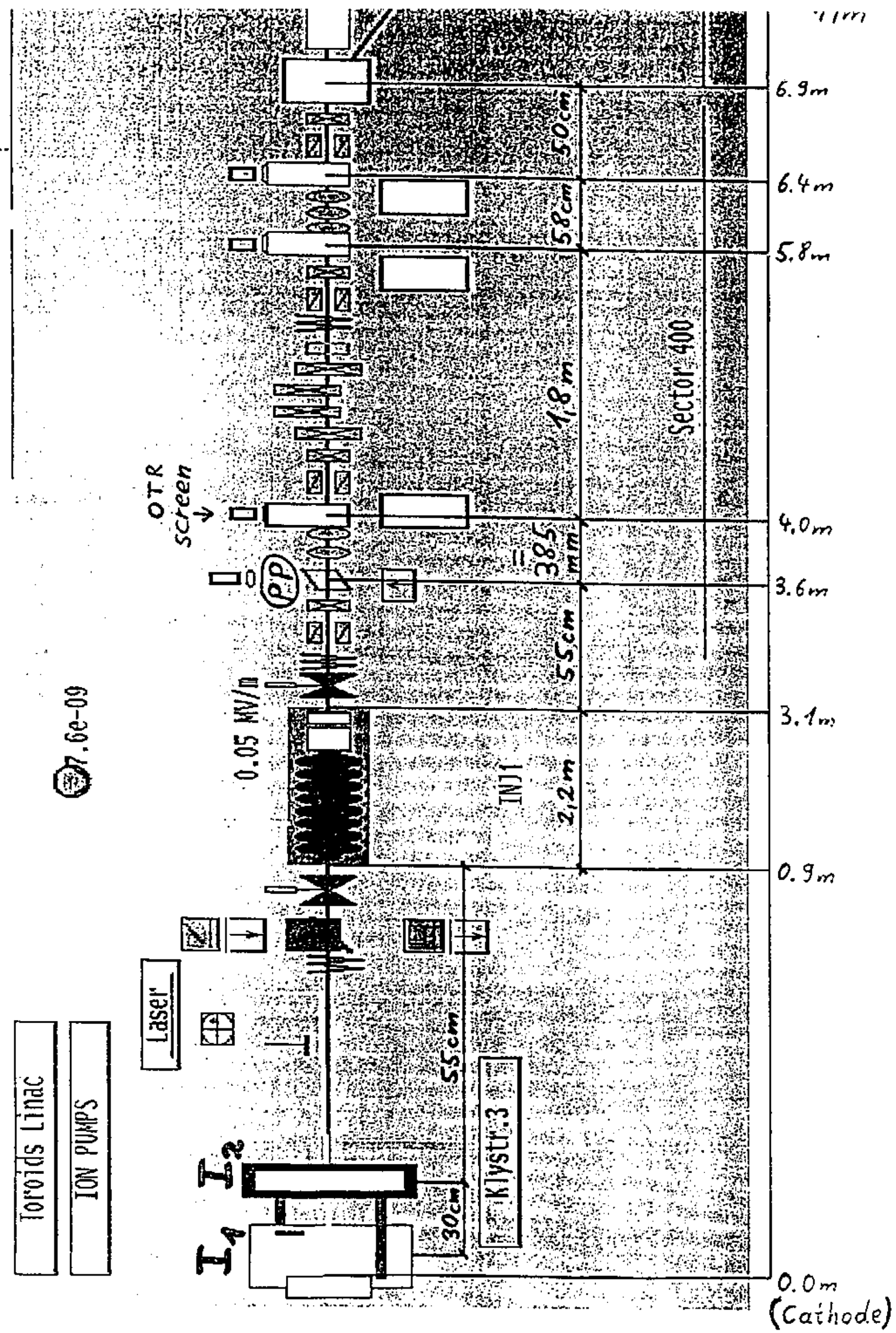

slit distance: 1mm

$$\varepsilon = \sqrt{\langle x^2\rangle \cdot \langle x'^2\rangle - \langle x \cdot x'\rangle^2}$$

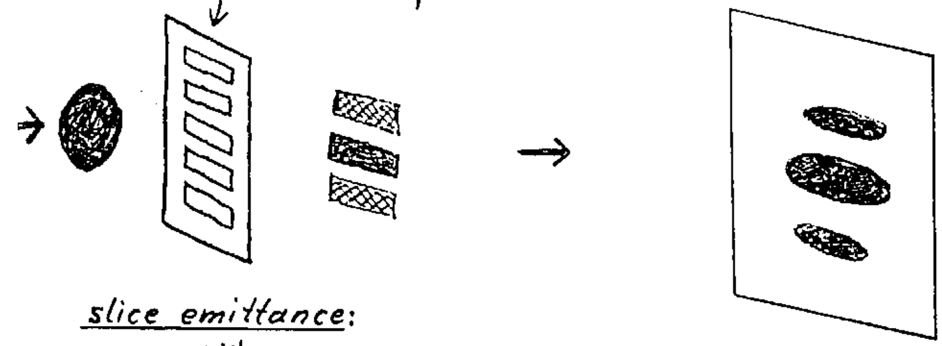

slice emittance:

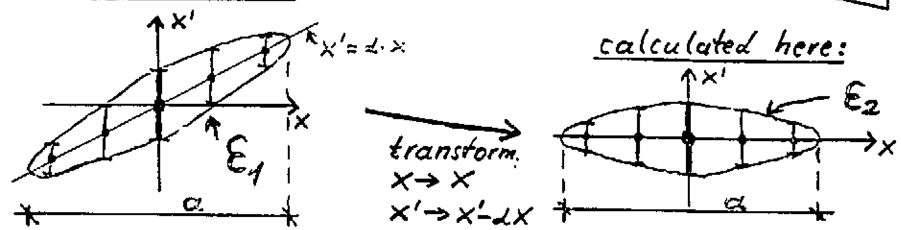

$$\Downarrow$$

$$\boxed{\varepsilon_1 = \varepsilon_2}$$

$$\varepsilon_2 = \sqrt{\langle x^2\rangle \langle x'^2\rangle}$$

$$\langle x^2\rangle = \frac{\sum_{i=1}^{M} (x_i - \bar{x})^2}{M} \xrightarrow[M = N_1+N_2+N_3]{3\ \text{spots}} \frac{N_1(0\text{mm} - \bar{x})^2 + N_2(1\text{mm} - \bar{x})^2 + N_3(2\text{mm} - \bar{x})^2}{N_1 + N_2 + N_3}$$

$$x' = \frac{x - \bar{x}}{385\,\text{mm}} \qquad \left(\Rightarrow \overline{x'_{i}} = 0 = \overline{x'}_{N_1} = \overline{x'}_{N_2} = \overline{x'}_{N_3}\right)$$

↑ distance between slit mask and screen

$$\langle x'^2\rangle = \frac{1}{M}\sum_{i=1}^{M} x_i'^2 \xrightarrow{3\text{spots}} \frac{N_1\cdot\langle x'^2\rangle_1 + N_2\cdot\langle x'^2\rangle_2 + N_3\cdot\langle x'^2\rangle_3}{N_1 + N_2 + N_3}$$

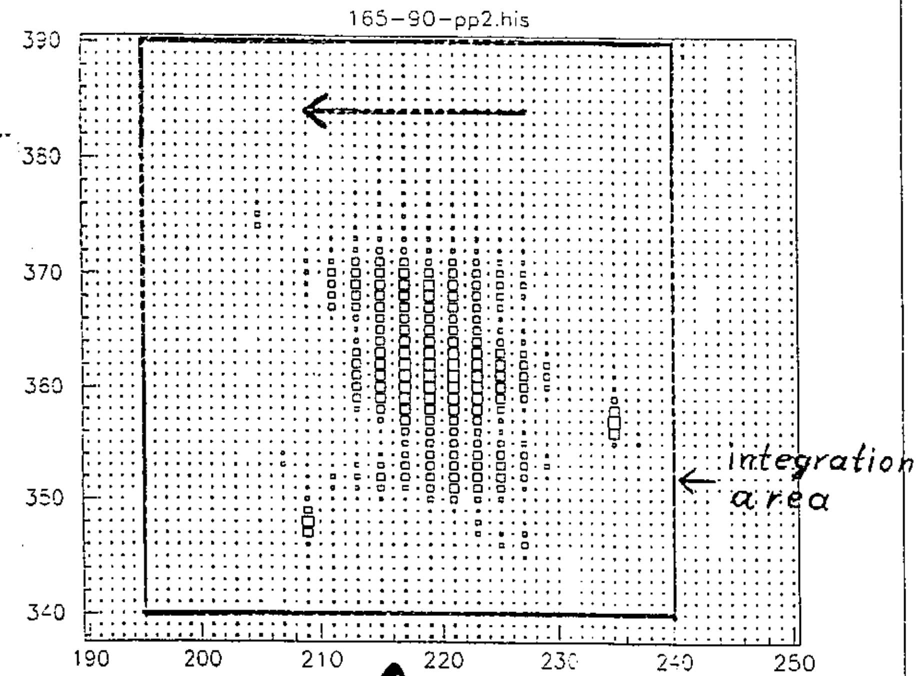

picture 165-90-pp2

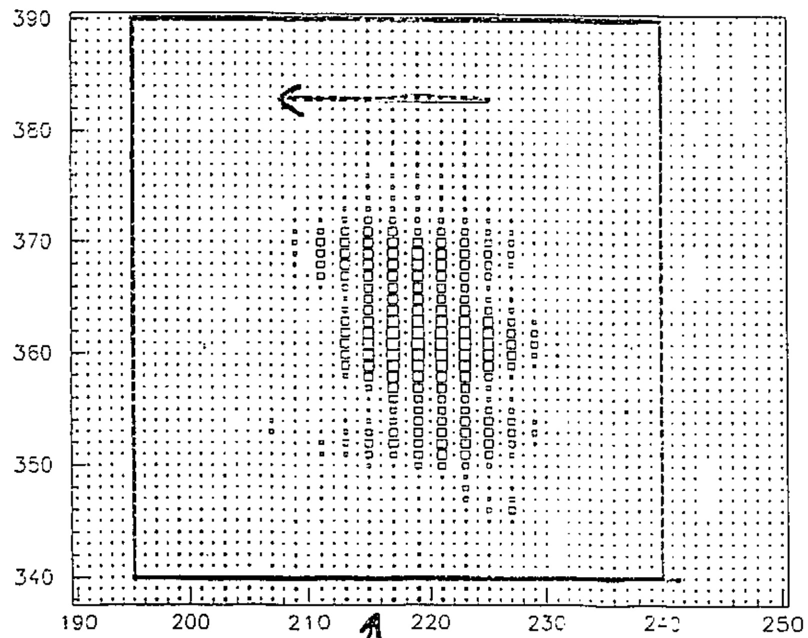

picture without clear x-rays

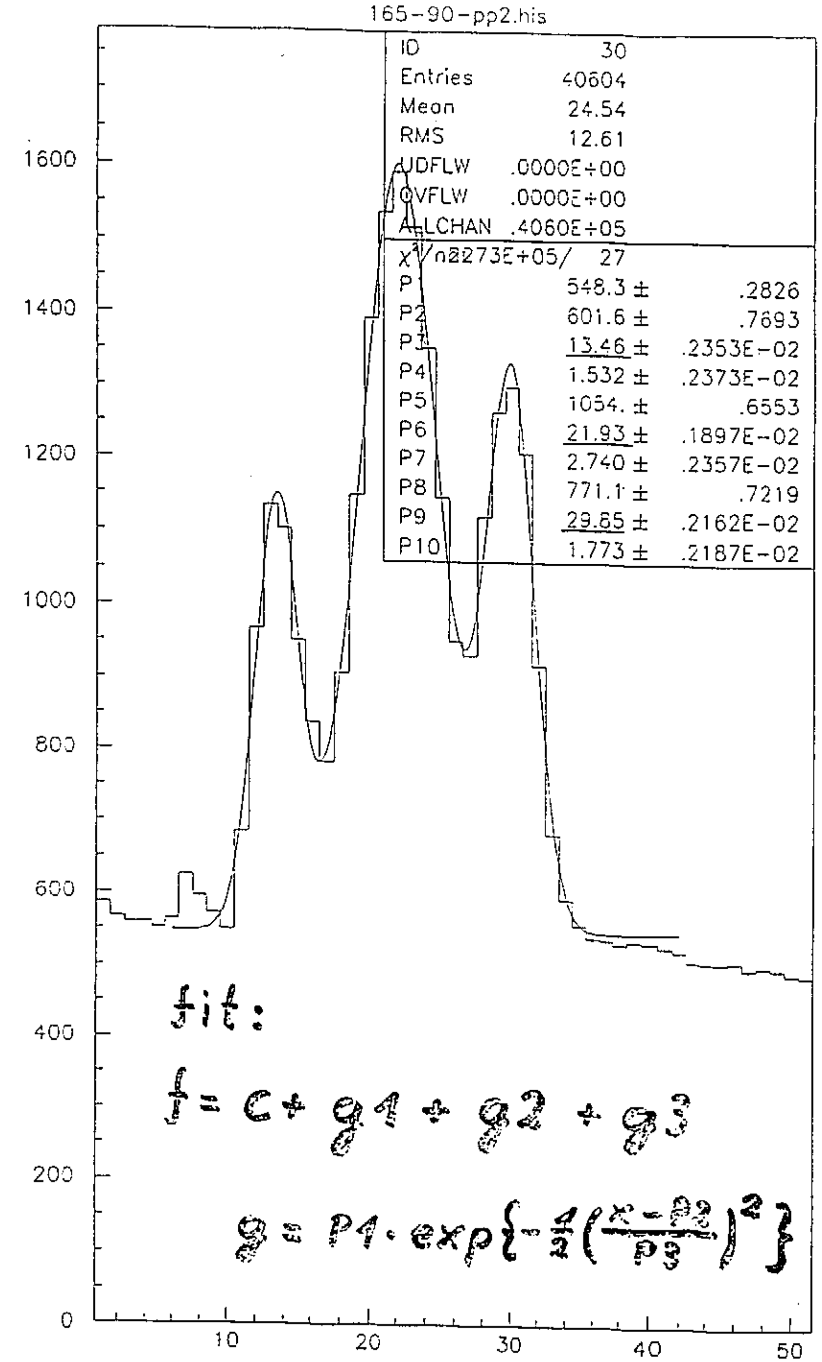

projection on y axis

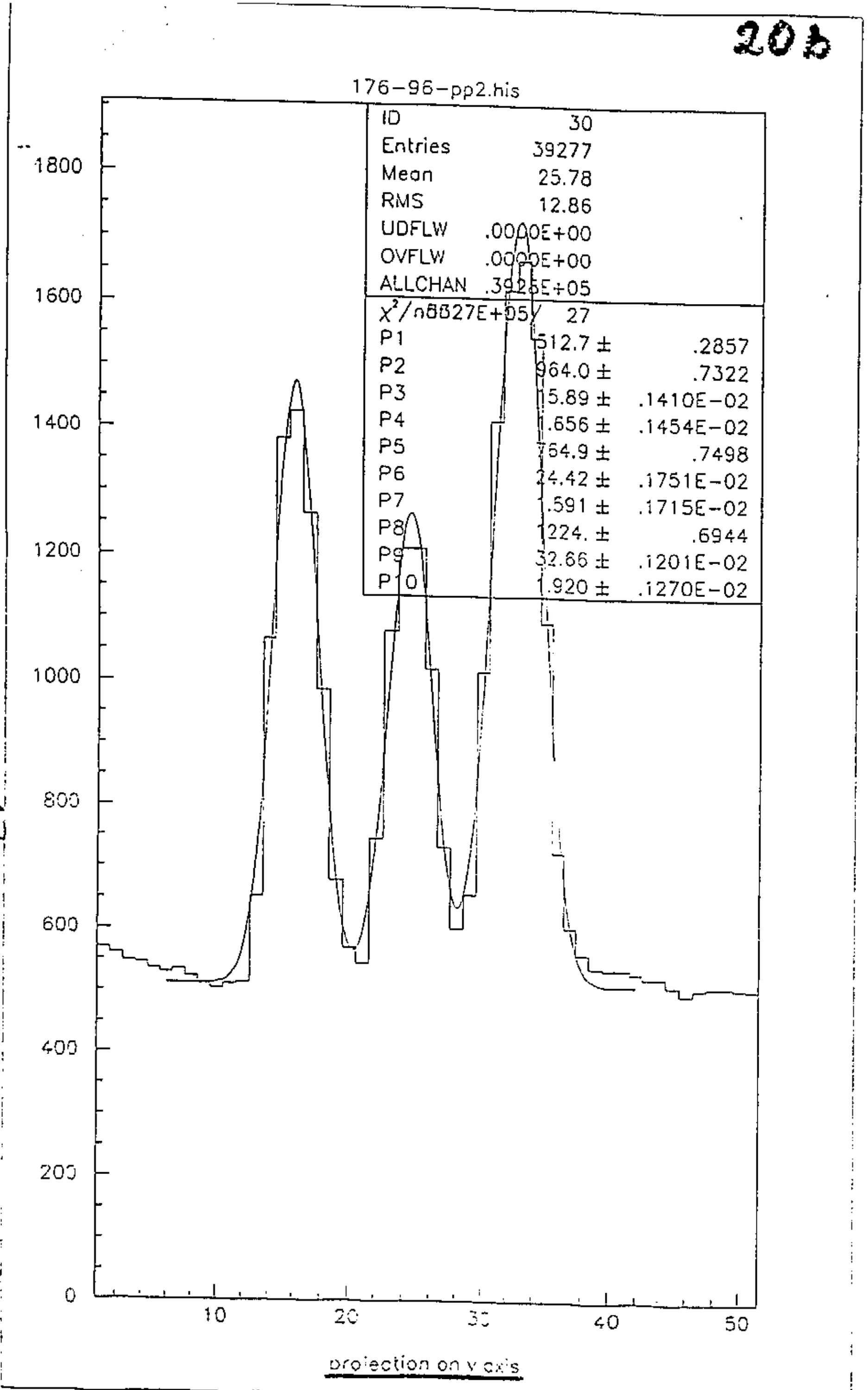
20b
176-96-pp2.his
ID 30
Entries 39277
Mean 25.78
RMS 12.86
UDFLW .0000E+00
OVFLW .0000E+00
ALLCHAN .3928E+05
χ²/ndf .8827E+05/ 27
P1 512.7 ± .2857
P2 964.0 ± .7322
P3 15.89 ± .1410E-02
P4 1.656 ± .1454E-02
P5 764.9 ± .7498
P6 24.42 ± .1751E-02
P7 1.591 ± .1715E-02
P8 1224. ± .6944
P9 32.66 ± .1201E-02
P10 1.920 ± .1270E-02
projection on y axis

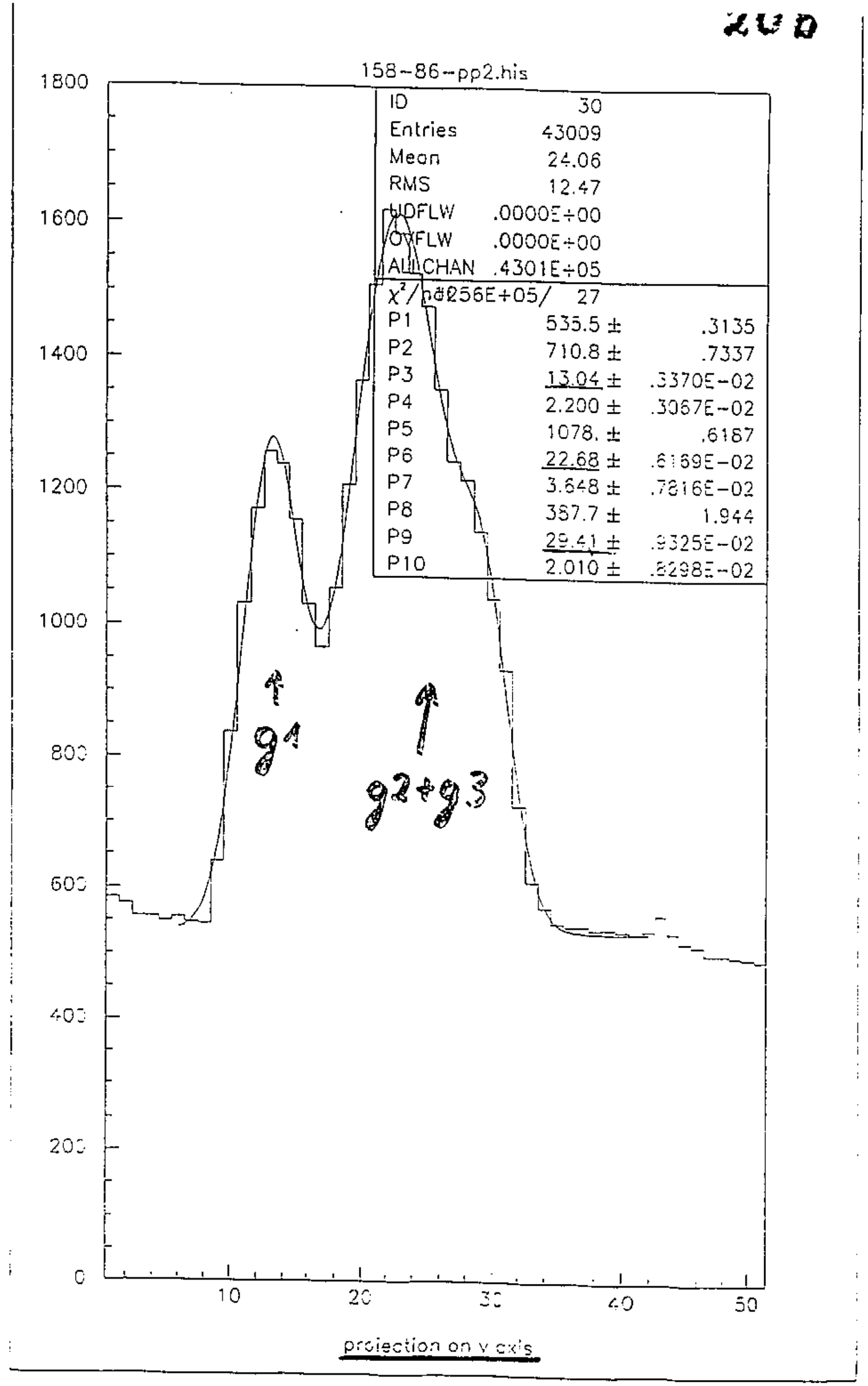
20a
158-86-pp2.his
ID 30
Entries 43009
Mean 24.06
RMS 12.47
UDFLW .0000E+00
OVFLW .0000E+00
ALLCHAN .4301E+05
χ²/ndf .8256E+05/ 27
P1 535.5 ± .3135
P2 710.8 ± .7337
P3 13.04 ± .3370E-02
P4 2.200 ± .3067E-02
P5 1078. ± .6187
P6 22.68 ± .6169E-02
P7 3.648 ± .7816E-02
P8 387.7 ± 1.944
P9 29.41 ± .9325E-02
P10 2.010 ± .8298E-02
g1
g2+g3
projection on y axis

Results

olenoids	name	# bunches	ε (in π mm mrad)	
58 – 86	pp 1	20	0,329	0,31 ±0,02
	pp 2		0,295	
	pp 3		0,300	
	pp 4		0,300	
	pp 5	10	0,285	0,27 ±0,02
	pp 6		0,254	
65 – 90	pp 1	20	0,232	0,23 ±0,02
	pp 2		0,240	
	pp 3		0,211	
	pp 4		0,250	
	pp 5	10	0,129	0,12 ±0,02
	pp 6		0,107	
176 – 96	pp 1	30	0,264 →	0,26
	pp 2	20	0,237	0,23 ±0,02
	pp 3		0,208	
	pp 4		0,245	
	pp 5		0,232	
	pp 6	10	0,147	0,16 ±0,02
	pp 7		0,175	

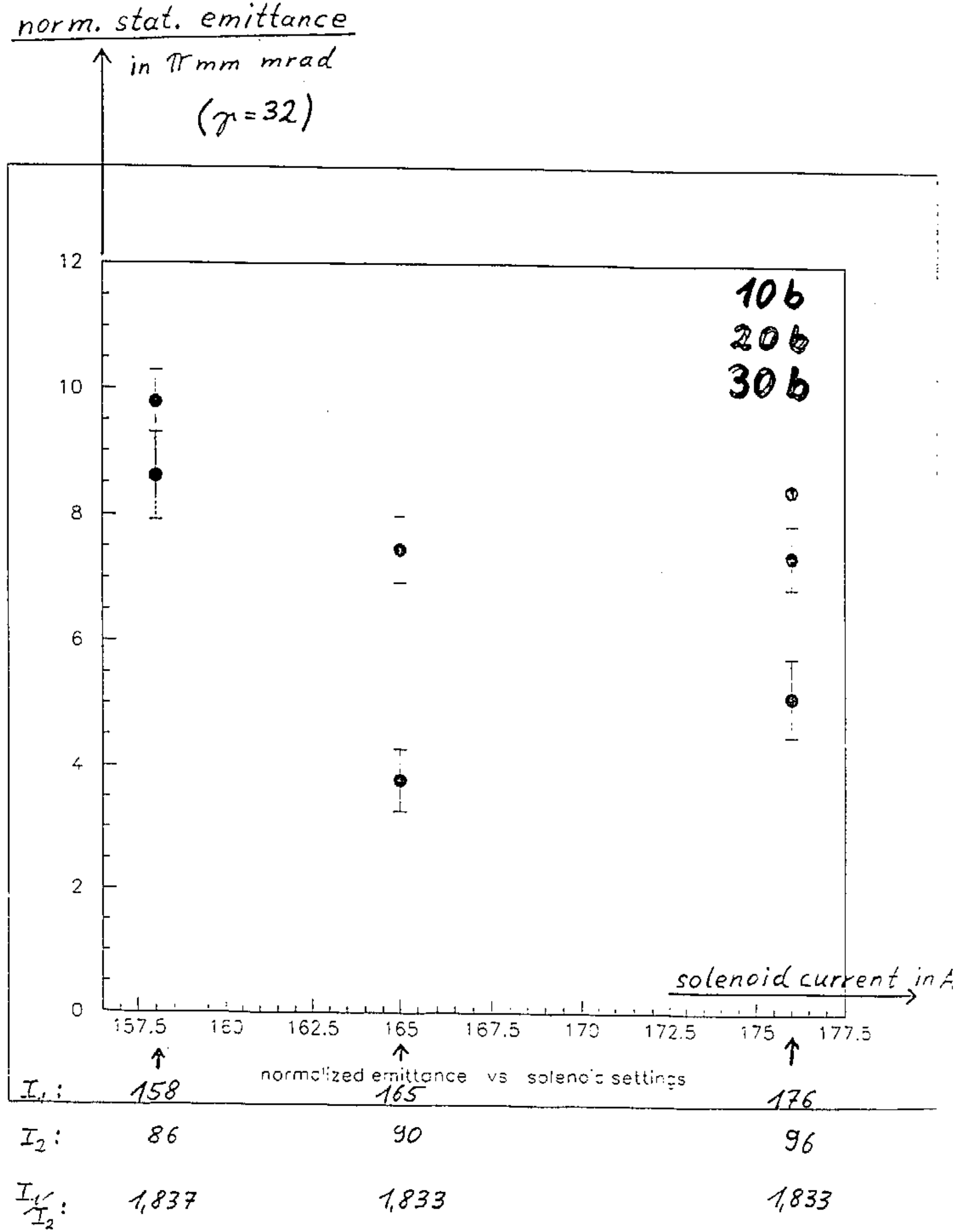

18

norm. emittance (y-plane) measured by tomography (directly after pp measurements)

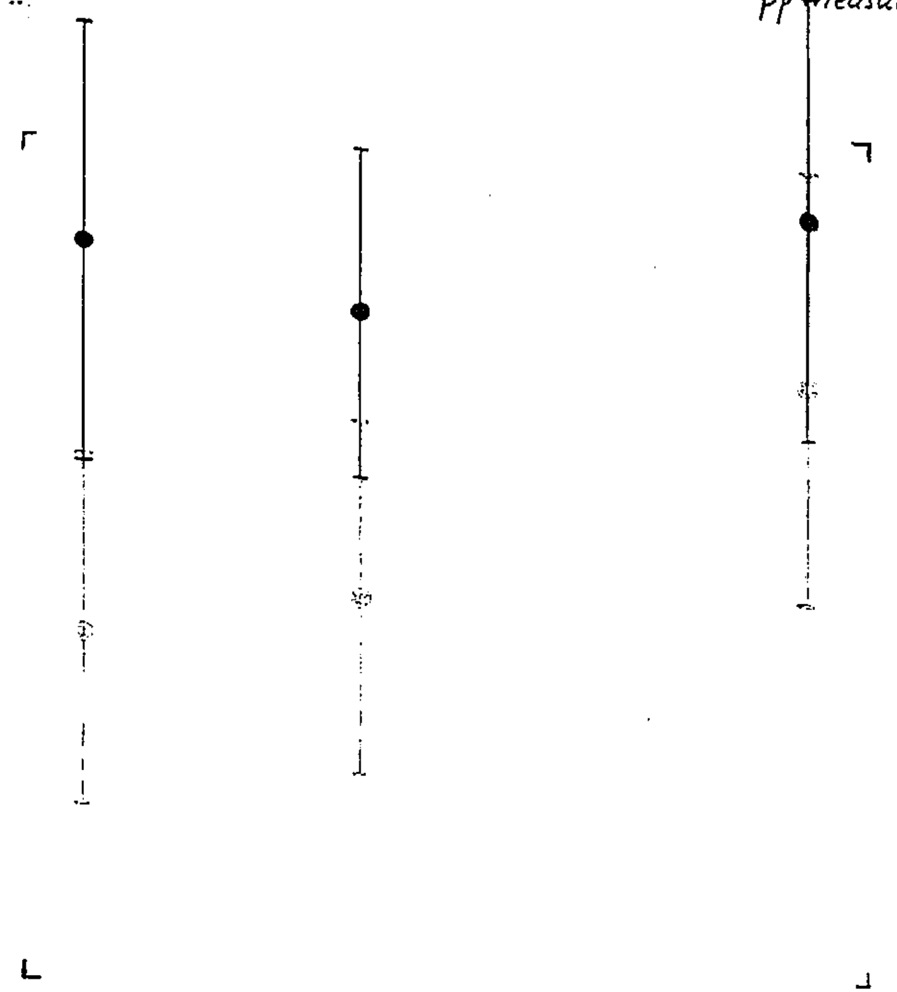

<u>Summary of systematic errors:</u>

$$\varepsilon \rightarrow \varepsilon + \underset{\#slits}{6\%} + \underset{D_{slits}}{5\%} \pm \left(\underset{\#slits}{4\%} \oplus \underset{\ell}{2.6\%} \oplus \underset{w}{5\%} \oplus \underset{D_{slits}}{1\%} \right)$$

$$\Rightarrow \varepsilon \rightarrow \varepsilon + 11\% \pm 7\%$$

Conclusions

smallest measured emittance at $I_1 = 165\,A$, $I_2 = 90\,A$
($\gamma = 32$)

with 10 bunches:

$$\varepsilon_N = [\,4{,}2 \pm 0{,}6(\text{stat.}) \pm 0{,}3(\text{sys.})\,]\ \pi\ \text{mm mrad}$$

with 20 bunches:

$$\varepsilon_N = [\,8{,}3 \pm 0{,}6(\text{stat.}) \pm 0{,}6(\text{sys.})\,]\ \pi\ \text{mm mrad}$$

(comparison with tomography in y-plane:
$\varepsilon_N = (9{,}5 \pm 3)\ \pi\ \text{mm mrad}$)

⇒ higher precission, even higher precission for parameter scans
(but no information about beam dynamics)

⇒ clear increase of emittance with # of bunches
(e.g. slope on rf probe signal)

(single bunch emittance may be not measureable with existing hardware)

⇒ emittance minimum at $I_1 = 165\,A$, $I_2 = 90\,A$ may be because
2 spot shape of electron beam
→ probably not optimal setting (→ higher) for uniform transverse e-beam profile

Outlook

- install slits with 0.5 mm distance correctly and use these slits!
  → smaller uncertainties!
- to analyse data in ttf environment
  CERNLIB (naglib, prolib, packlib, PAW) must be installed
- helpful: look at OTR using a mirror
  → exclude X-rays
- redo parameter scans with homogeneous transverse e^- beam profile

Location of the emittance measurement

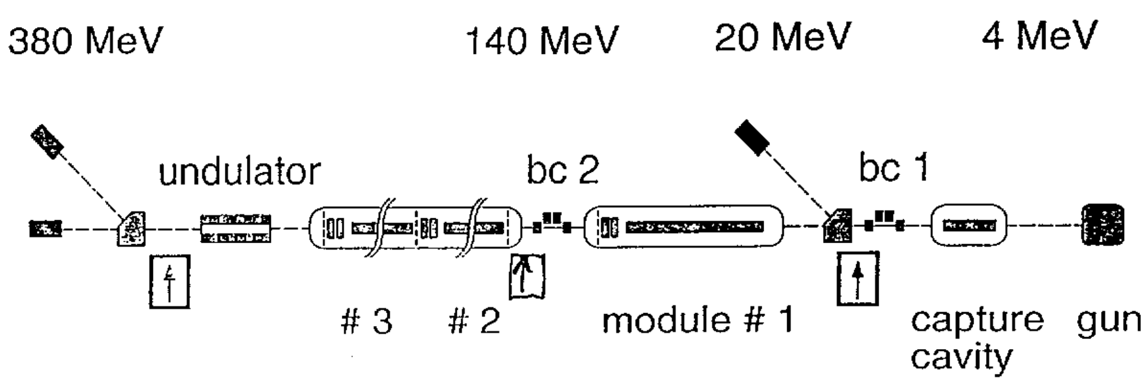

QUADRUPOLE SCAN

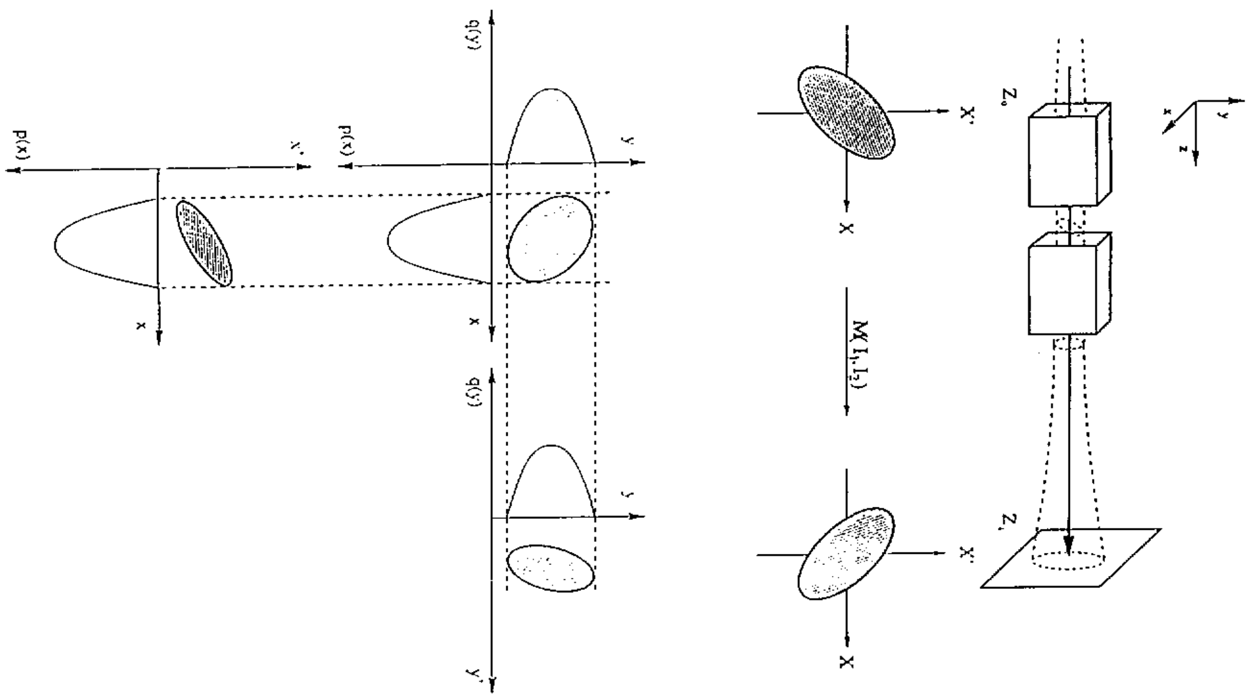

Phase Space Tomography

reconstructed normalized emittance

$\varepsilon_x = (5.5 \pm 2.5)$ mm mrad

$\varepsilon_y = (9.5 \pm 3.1)$ mm mrad

at TTF photo-injector, E = 16 MeV, Q = 1 nC.

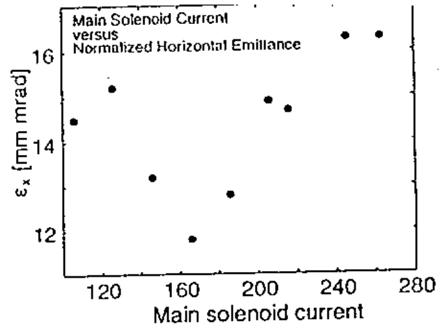

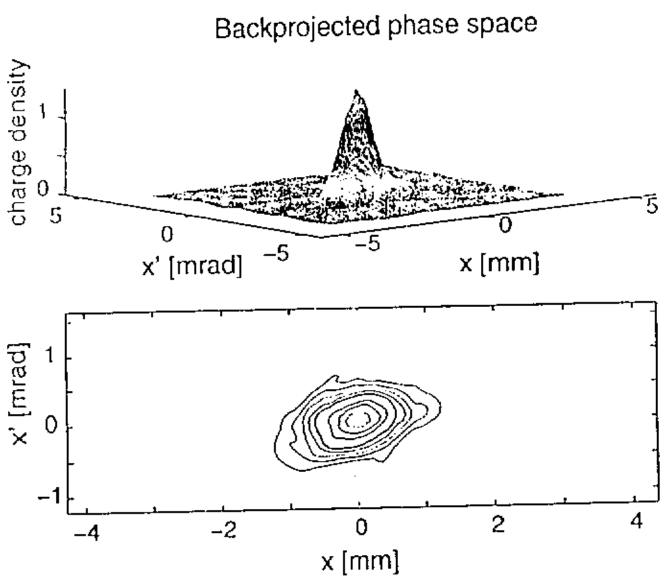

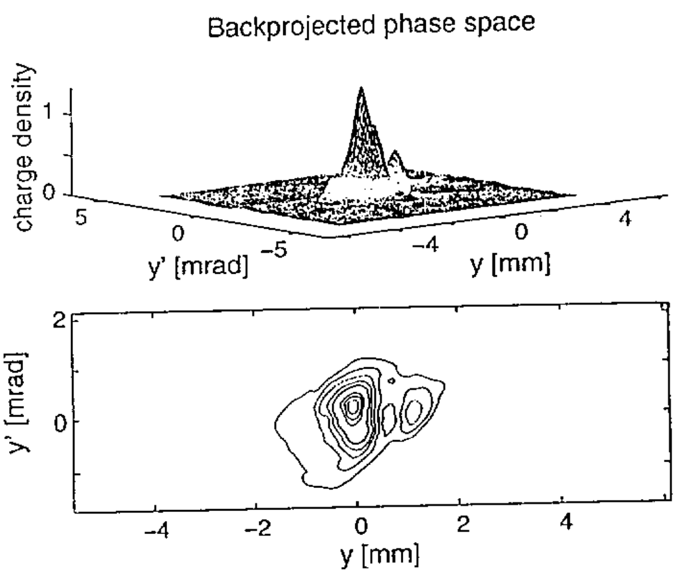

Linac Emittance Measurement:

BC2, Q = 1nC, E = 80 MeV, 15 bunches, horizontal plane, standard injector settings

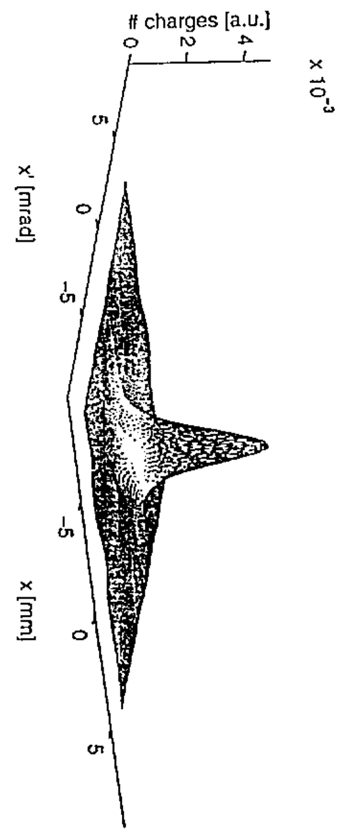

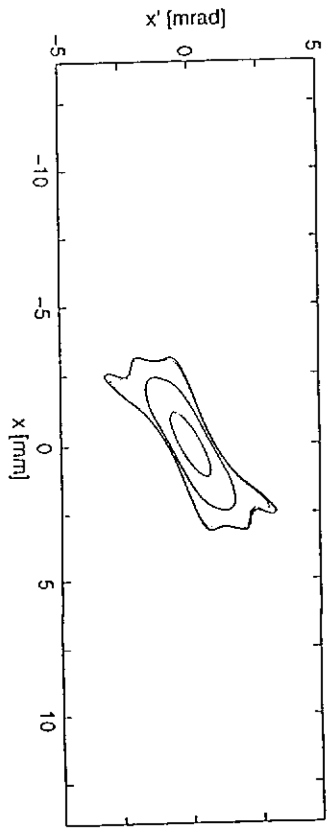

Beam Parameters:

$\varepsilon_x = 80$ mm mrad

$\alpha_x = 1.6$

$\beta_x = 3.1$ m

Linac Emittance Measurement:

BC2, Q = 1nC, E = 80 MeV, 15 bunches, vertical plane, standard injector settings

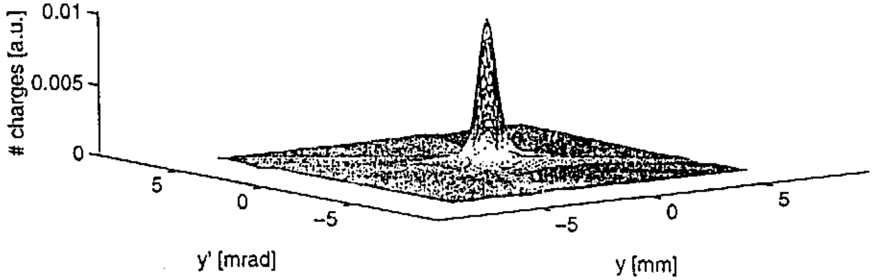

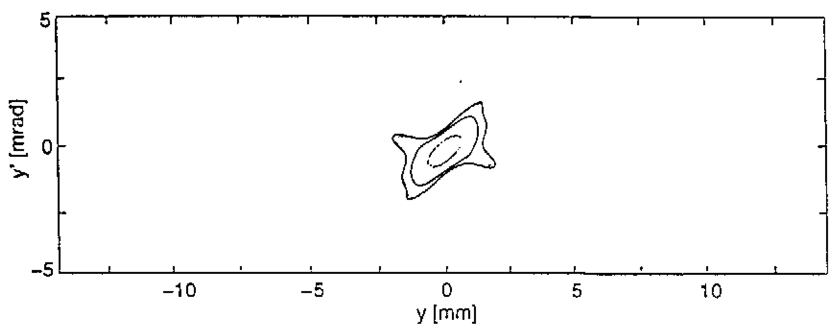

Beam Parameters:

$\varepsilon_x = 45$ mm mrad

$\alpha_x = 1.0$

$\beta_x = 1.5$ m

23

G. Schmidt, -MPY-, 6.07.99

Results of the emittance measurement

1) We measured not a single bunch emittance. What was measured was the multi-bunch phase space volume. Beam jitter causes an emittance growth. A minimum number of bunches is needed to get the signal above the dark current illumination of the OTR foils. The single bunch emittance is therefore smaller
2) The multi-bunch emittance at the injector is between 7 and 10 mm mrad (measured by pepper pot and phase space tomography depending on the number of bunches).
3) A growth of the normalized emittance was observed nearly in all measurements in the bunch compressor and experimental area. (Quad scan and phase space tomograhy)
4) The reason of the emittance growth is not identified. Possible explanations are:

-growth of the multi bunch emittance by offsets in the modules and HOM effects

⇨ find a way to measure single bunch emittance, measure the emittance as a function of the offset in the module or use a BPM reading to see drift of beam center and correct the emittance

-A part of the growth can be explained by errors of the optical system used (depth of field, diffraction, bad optical elements used)

⇨ Improvements of system will be installed for next run

⇨ Nevertheless need deeper understanding of space charge effects and compensation between capture cavity and module 1.

G. Schmidt, -MPY-, 6.07.99

Summary of module operation

Max gradient in module 2 with beam (1nC at 10 to 30 micro seconds pulse length: 18.6 MV/m
(Shown with 2 Klystrons for module1 and 2. On module 2 no regulation was used)

Max gradient without beam 20.5 MV/m (500 to 800 micro seconds flat top)
But: Long term operation with gradients larger than 18 MV/m not possible due to e- and vacuum events in the main couplers further processing needed
Dark current from module 2 at high gradient was significantly reduced due to processing.

Standard gradient: ~10 MV/m
The beam energy was limited between 160 and 180 MeV during stable operation with 1 Klystron by cavities in module 1 and the equal power distribution between modules

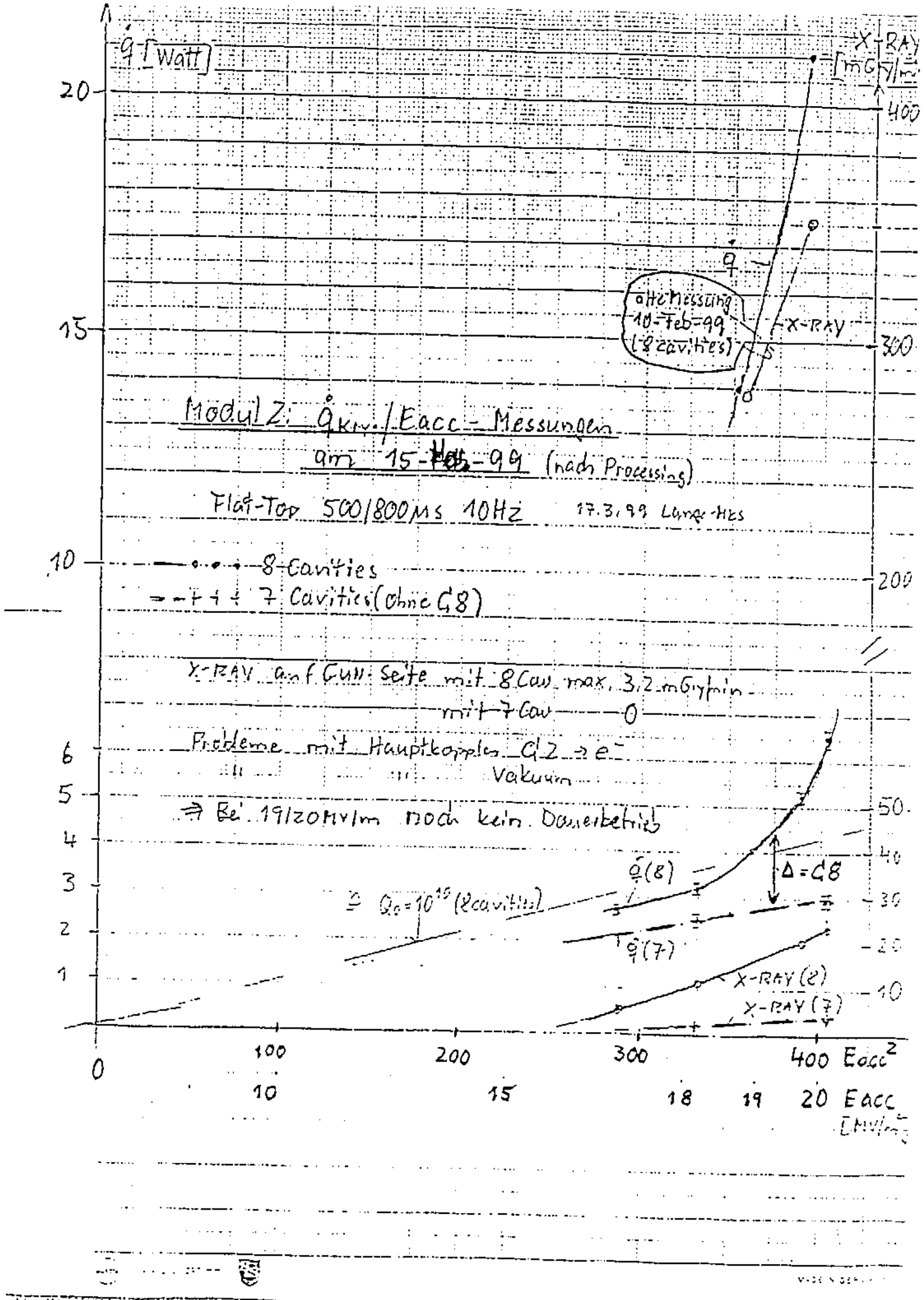

24

Summary of achieved beam parameters

For 1 nC case:

Energy spread ≤ 0.3 % at injector and linac EXP3 (estimated with OTR) =>sufficient for FEL

Standard beam energy between 160 and 180 MeV limited by cavities in module 1
=> new module 1 should allow to go to 230 MeV

Emittance at injector = 5 mm mrad for 10 bunches - 9 mm mrad in second plane
Emittance growth observed along the linac but not understood => Space charge effect?
=>enough for undulator installation but not good enough to reach saturation.

For 8 nC:

Energy spread ≤ 1 % at the injector
And the possibility of beam transport along the linac was shown.
=> needed for RF calibration

25

Conclusion

Diagnostic improved during last run. Nearly all BPM's and toroids were working at the end of the run.

Bunch compressor works predictable and compression shown.

The Phasing between module 1 and 2 for the Bunch compressor operation was difficult and reproducibility was not always possible.

Understanding of different methods to measure the bunch length is improving

Ready for lasing?
Yes and no. Main problem seems to be the understanding of optics and beam emittance along the machine. (real or by measurement methods or beam jitter!?) ??
A method to measure the twiss parameters at different points along the machine exists.
→ FEL will show if emittance growth exists.

RF, bunch compressor and in principle the injector have proven the ability to deliver a sufficient beam quality for the startup of the FEL experiment.

Run 1/99
RESULTS Part I
Gun
Cathode
Laser
Bunch length

S. SCHREIBER
DESY
TTF meeting
7.7.99

TTF Injector II

Train of 800 electron bunches, train length = 0.8 ms
Repetition rate 10 Hz
Bunch charge = 8 nC
Bunch length = 1 mm
Energy = 20 MeV
Emittance (x,y) = 20 π mm mrad

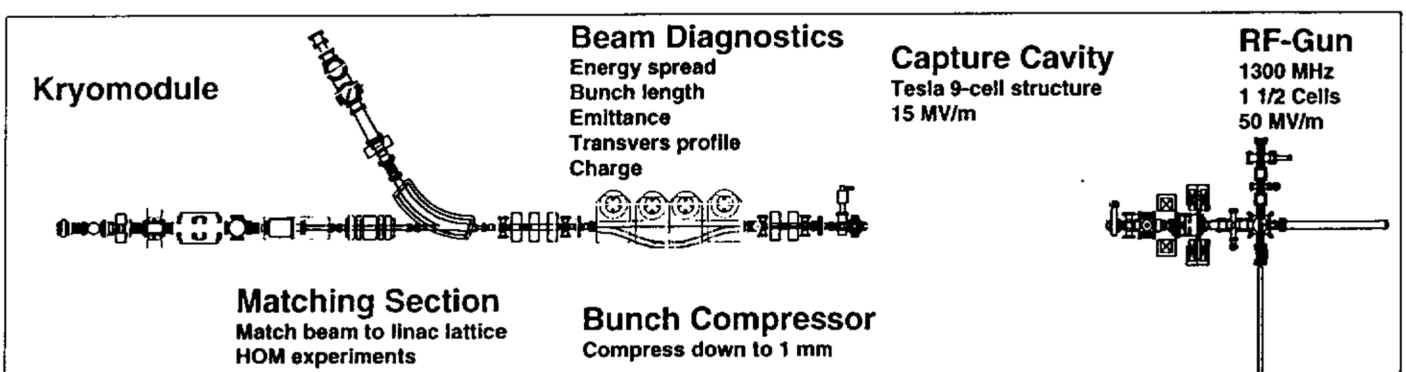

Laser
262 nm (UV)
≈5 μJ/pulse → 8 nC/bunch
800 pulses/train (1 MHz)
10 Hz rep. rate

Cathode System
Material: Cs2Te
QE > 1 %

S. Schreiber
14-Jun-1998

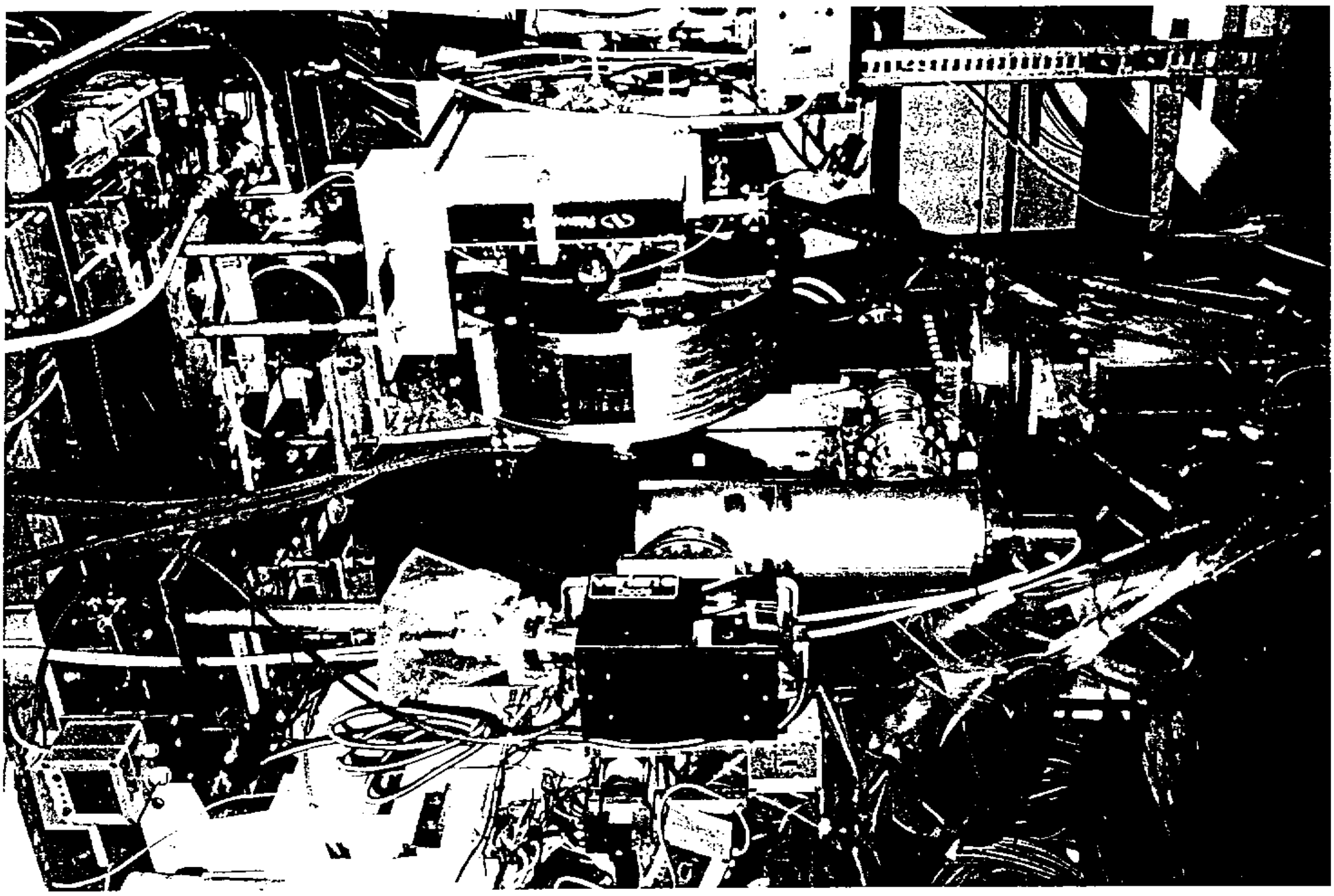

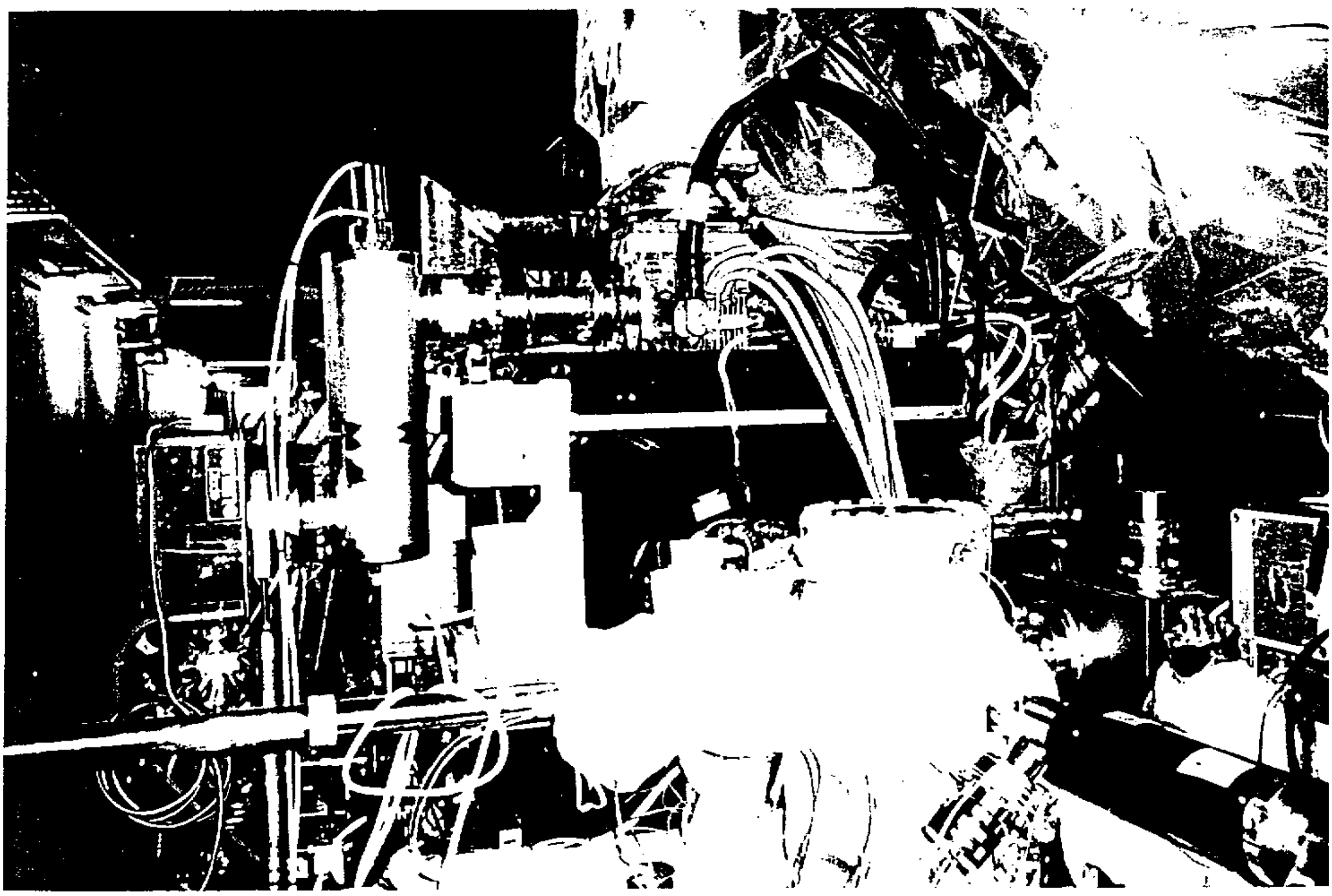

27 TTF · DESY · Cathode System assembled to rf gun · Dec 98

RF Gun Low Level RF System

Digital control system

- 2 TMS C40 DSPs
- table driven feedforward
- control by adjusting feedforward table between pulses ("adaptive feedforward")

28

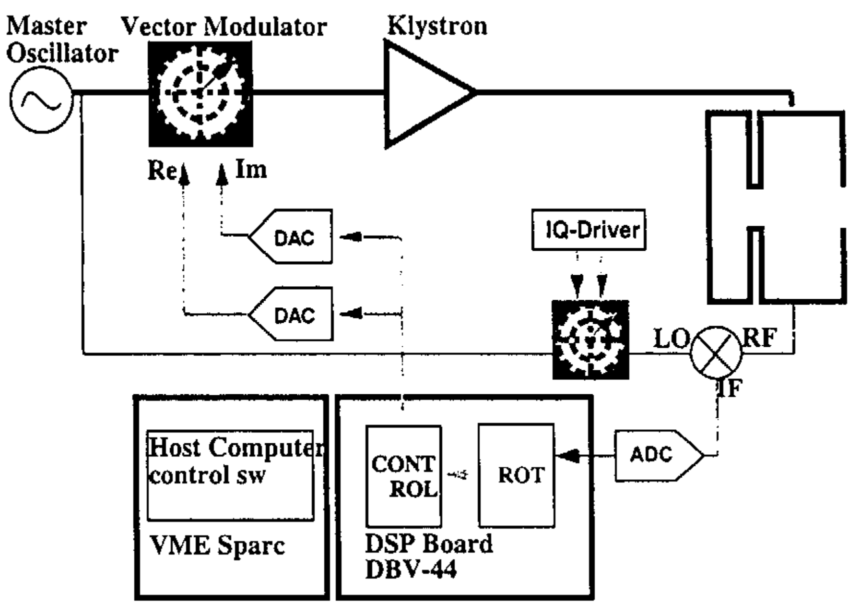

G. von Walter

25 March 1999 2:40 pm

General running experience

- the last run started mid Dec. 98 until mid Mars '99 ≈ 2000 h
- the conditioning of the rf gun + window went smooth, we reached nominal gradient (35 MV/m or 2.2 MW), short pulse (50 μs) at 1Hz before Xmas
- the availability of the rf gun + laser was close to 100%, except one modulator repair + one laser repair
- the injector delivered beam to test the two installed TESLA modules, to test the new bunch compressor and for various experiments (HOM, bunch length, emittance etc.)

⇨ the overall performance of the new injector is satisfactory

- further improvements (→ emittance for FEL operation) and more detailed studies on beam parameters and beam dynamics are scheduled for the next run in summer '99

29

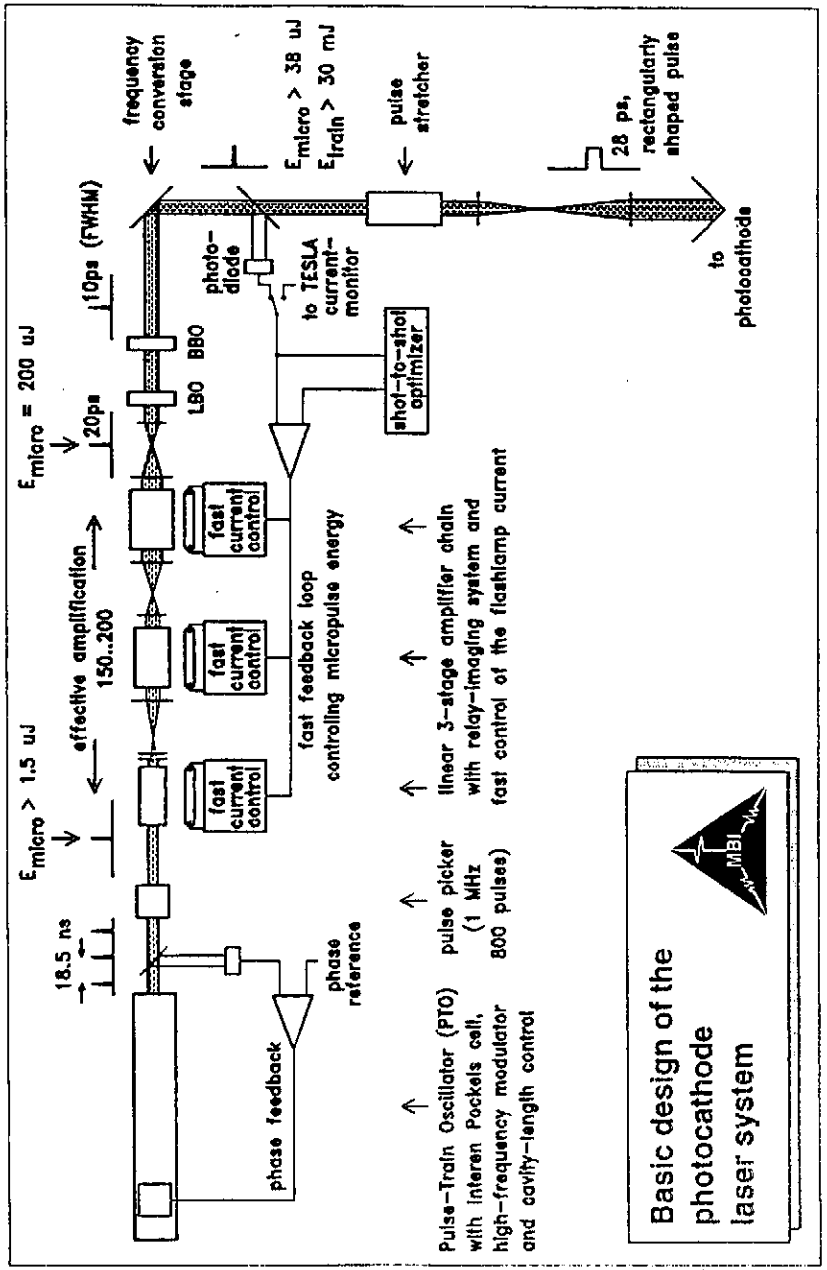

Pulse train (SHG) measured at the output of the laser system

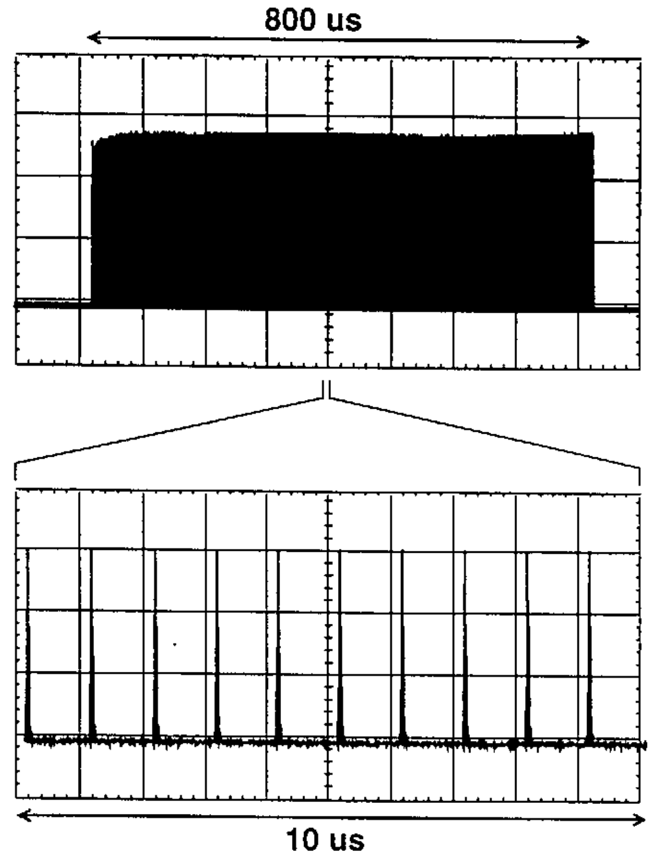

- Energy per micropulse at 1.06 um: E = 200 uJ
- Accuracy of synchronization: dt = 1 ps
- Pulse width (FWHM) at 1.06 um: t = 25 ps
  at 0.26 um: t = 12 ps
- Energy stability from shot to shot
  at 1.05 um: ± 1 %
  at 0.53 um: ± 2 %

30

The Lasersystem

Performance

- Energy:
  - up to 100 μJ per micropulse, largely sufficient for 8 nC
  - stability (shot to shot/within train) better than 5 % rms
- Phase:
  - stability better than 1 ps
  - drift seen with short pulses, fixed by forcing laser phase to 0 using the phase feedback system
  - occasional drift of resonator length
- Transverse profile:
  - flat top, uniformity not satisfactory yet
  - spatial filter in UV to be included, conversion green to UV to be optimized
- μ Pulse length:
  - phase scans suggested a long pulse, confirmed by streak camera and autocorrelation measurements ($\sigma = 15$ ps in UV)
  - fixed by replacing the oscillator laser head
  - now: $\sigma = 10$ ps in IR, 7.1 ± 0.6 ps in UV

The Lasersystem II: Reliability

- Uptime:
  - is running since mid December (except Xmas)
  - in total 2000 hours with 1 Hz or $8{\cdot}10^6$ shots
  - uptime 99 %, available for beam 97 %
- Failures:
  - flashlamps of pulse train oscillator (PTO) exchanged after $8{\cdot}10^6$ shots
  - lost 4 hours + 2 shifts with very unstable conditions
  - complete PTO laser head exchanged to cure pulse length
  - Sparc cpu in laser VME had to be replaced
- Server:
  - laser server and control program is running smoothly and stable
- Interlocks
  - no failure of personal laser safety interlock
  - access to tunnel with laser beam on was not established in a way, that operators could make use of it.
  - no failure of technical laser safety this time (we had one failure in May 1998), SPS is working fine

31

Cathode System

INFN Milano LASA
DESY (Vacuum equ.)

- Cs_2Te cathode: high QE (>1 % over months)
- The cathode system allows to change the cathode without breaking the vacuum
  This is essential to maintain the high quantum efficiency of the Cs_2Te cathode

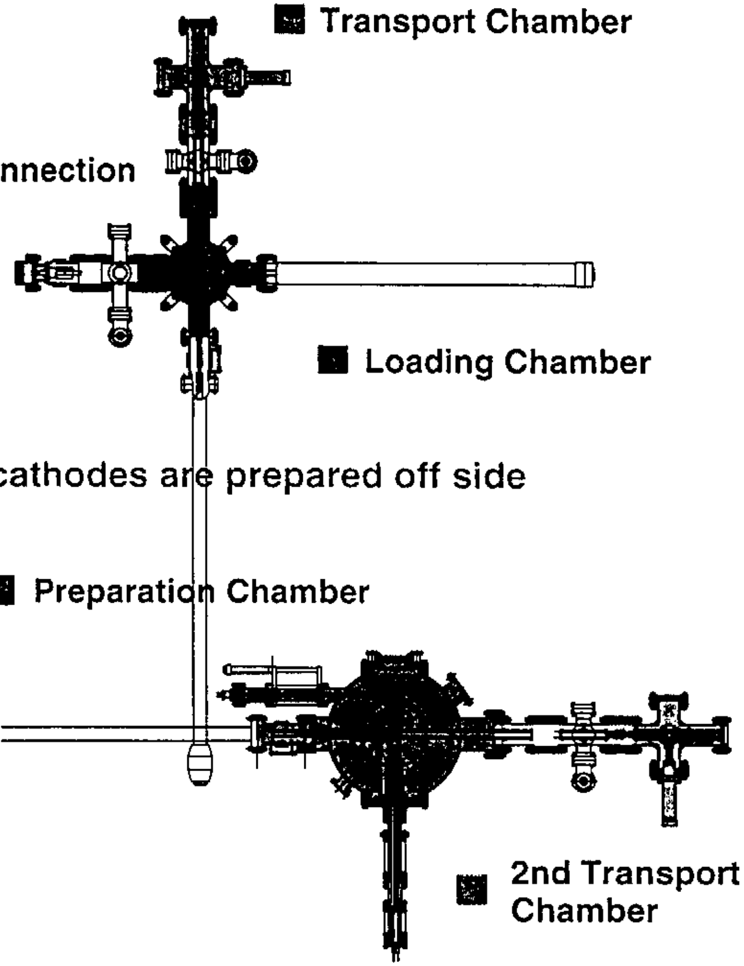

- The cathodes are prepared off side

S. Schreiber
12-Sept-1997

RF Gun Vacuum History

February 1999

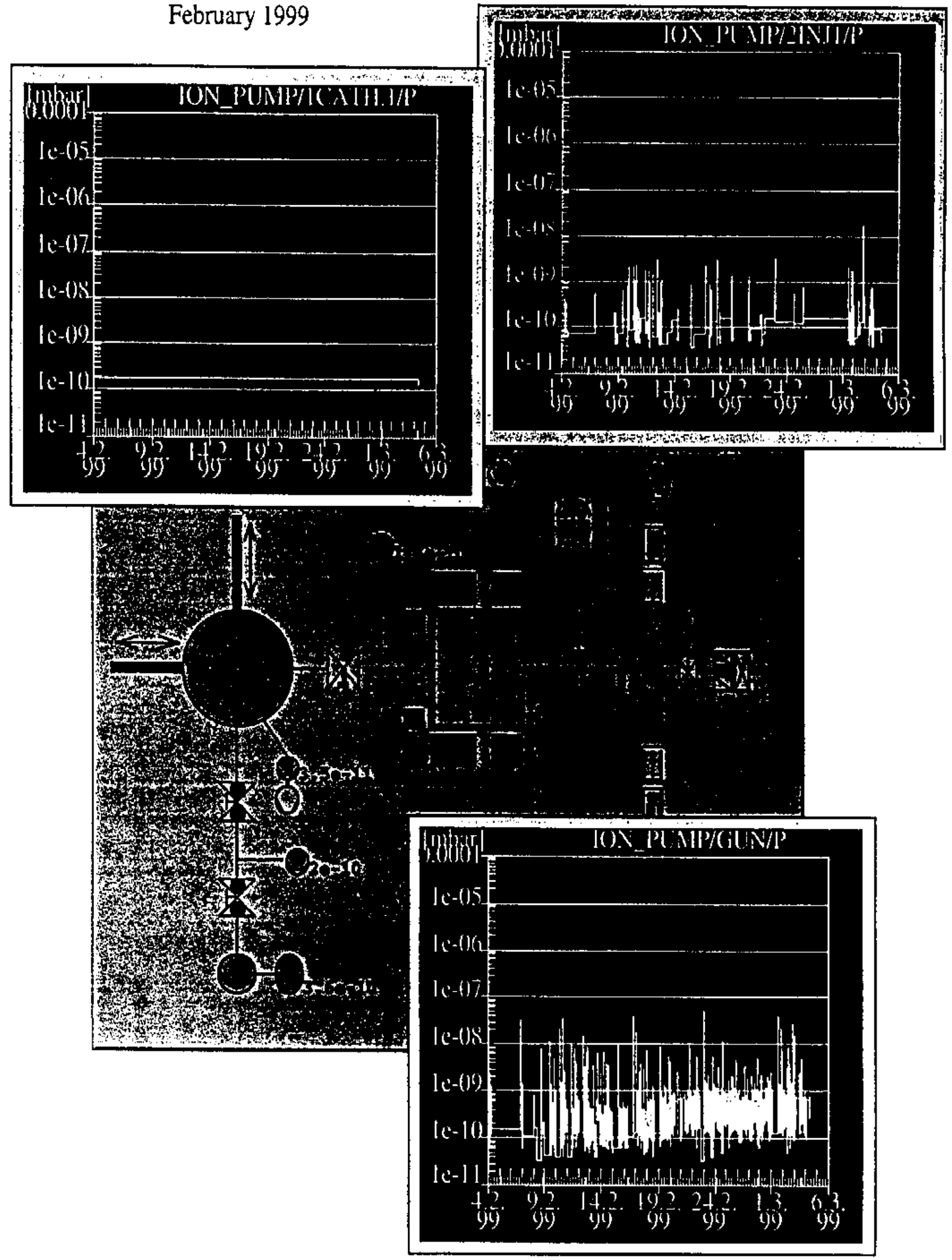

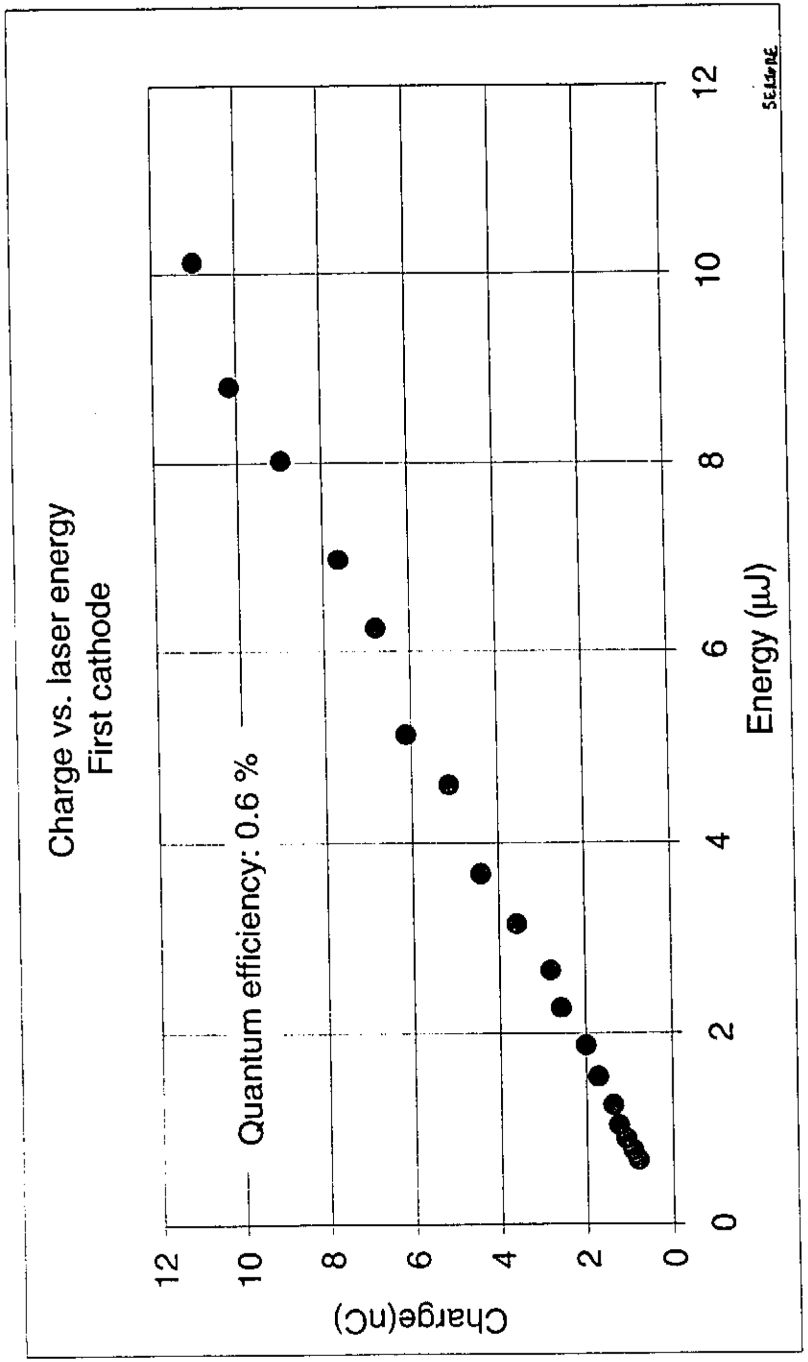

Quantum efficiency of cathode #2

QE = (5.9 ± 0.6)%

over the test period of one week

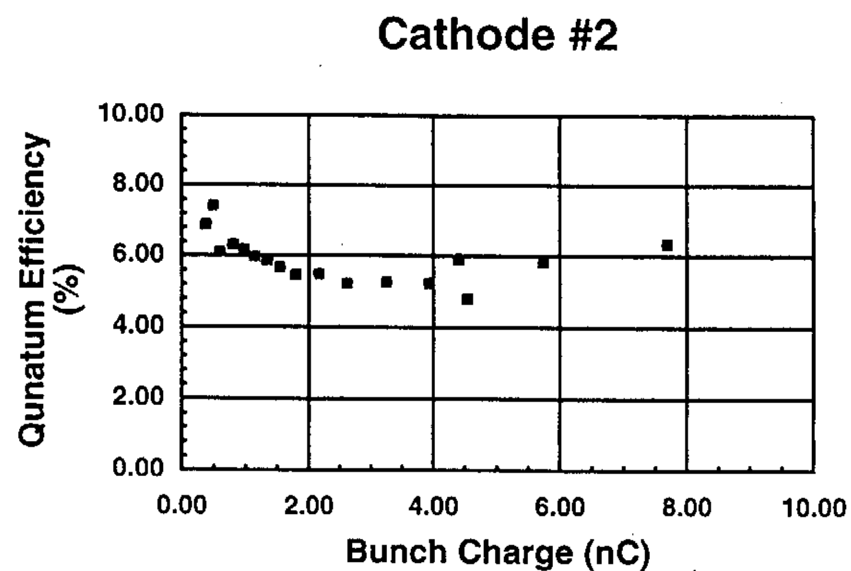

this cathode has a

⇨ Mo. mirror surface finish

→ then Cs_2Te

cathode #1 QE ~ 0.5%

Charge transmission of the gun

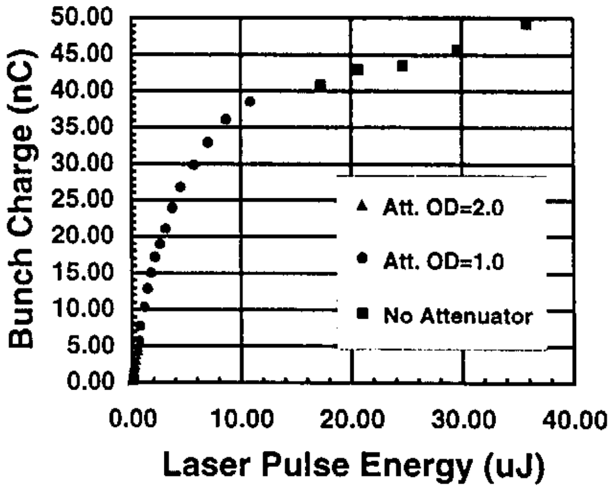

MICHELATO / SCHREIBER / SERTORE

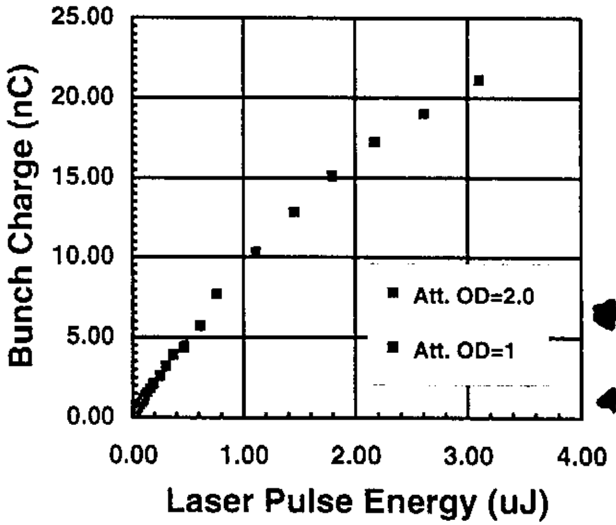

← 8 nC } nominal
← 1 nC

⇨ linear up to ~16 nC   laser spot ∅ 10 mm

Observation of space charge effects:

energy laser good for 2.4 nC: constant
→ charge extraction reduced for lower fields

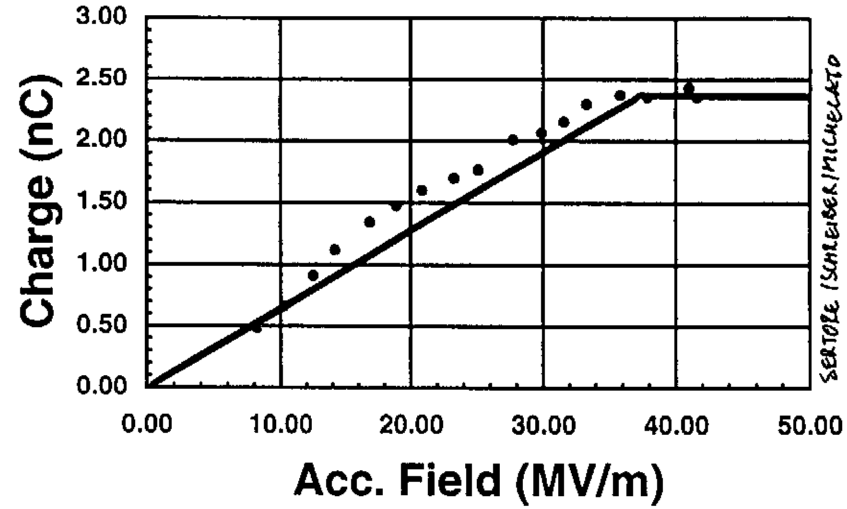

SERTORE / SCHREIBER / MICHELATO

∅ laser on cathode = 3 mm

— from Gauss' law

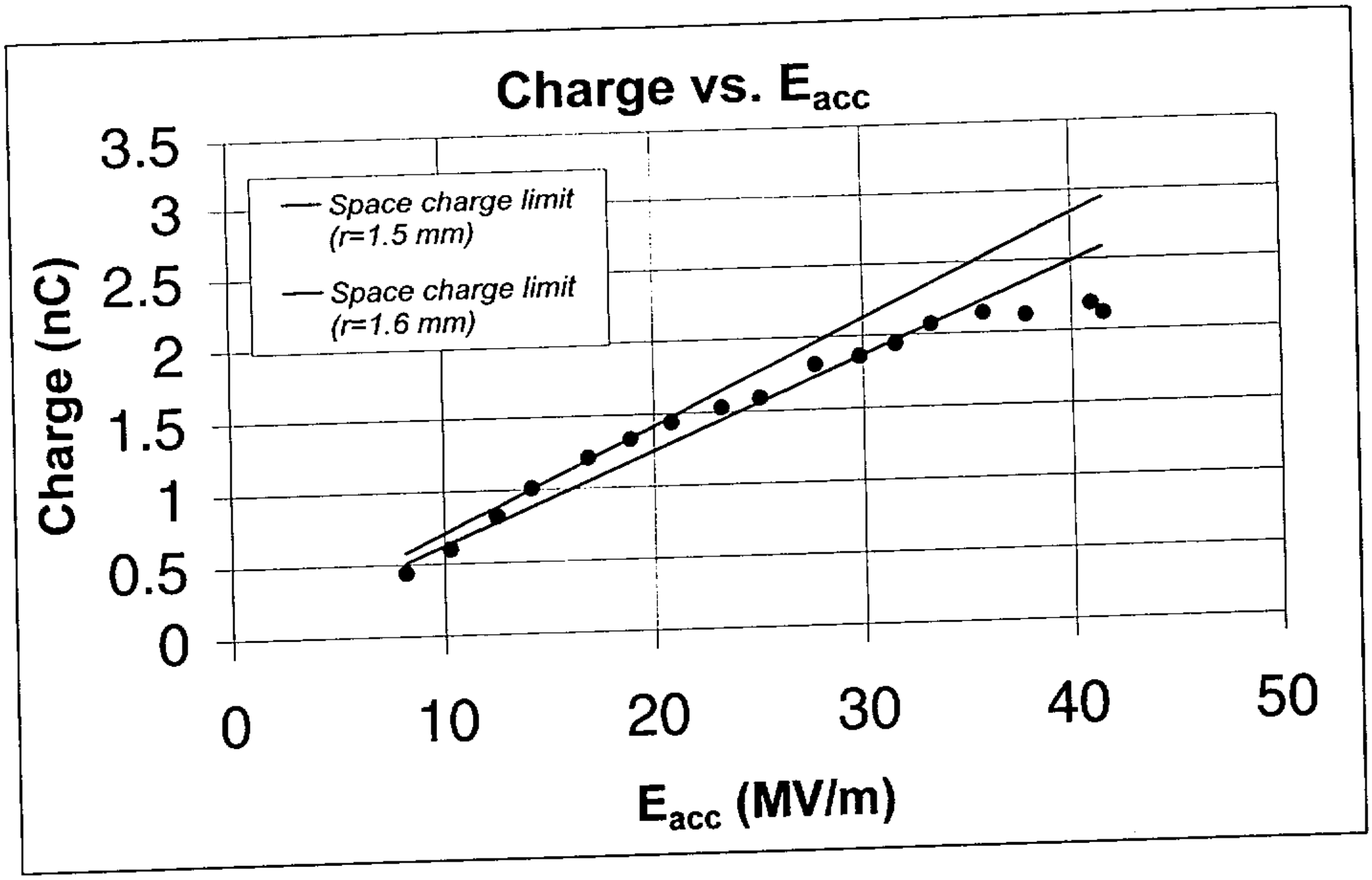

Charge vs. E_{acc}
Space charge limit (r=1.5 mm)
Space charge limit (r=1.6 mm)
3.5
3
2.5
2
1.5
1
0.5
0
Charge (nC)
0
10
20
30
40
50
E_{acc} (MV/m)

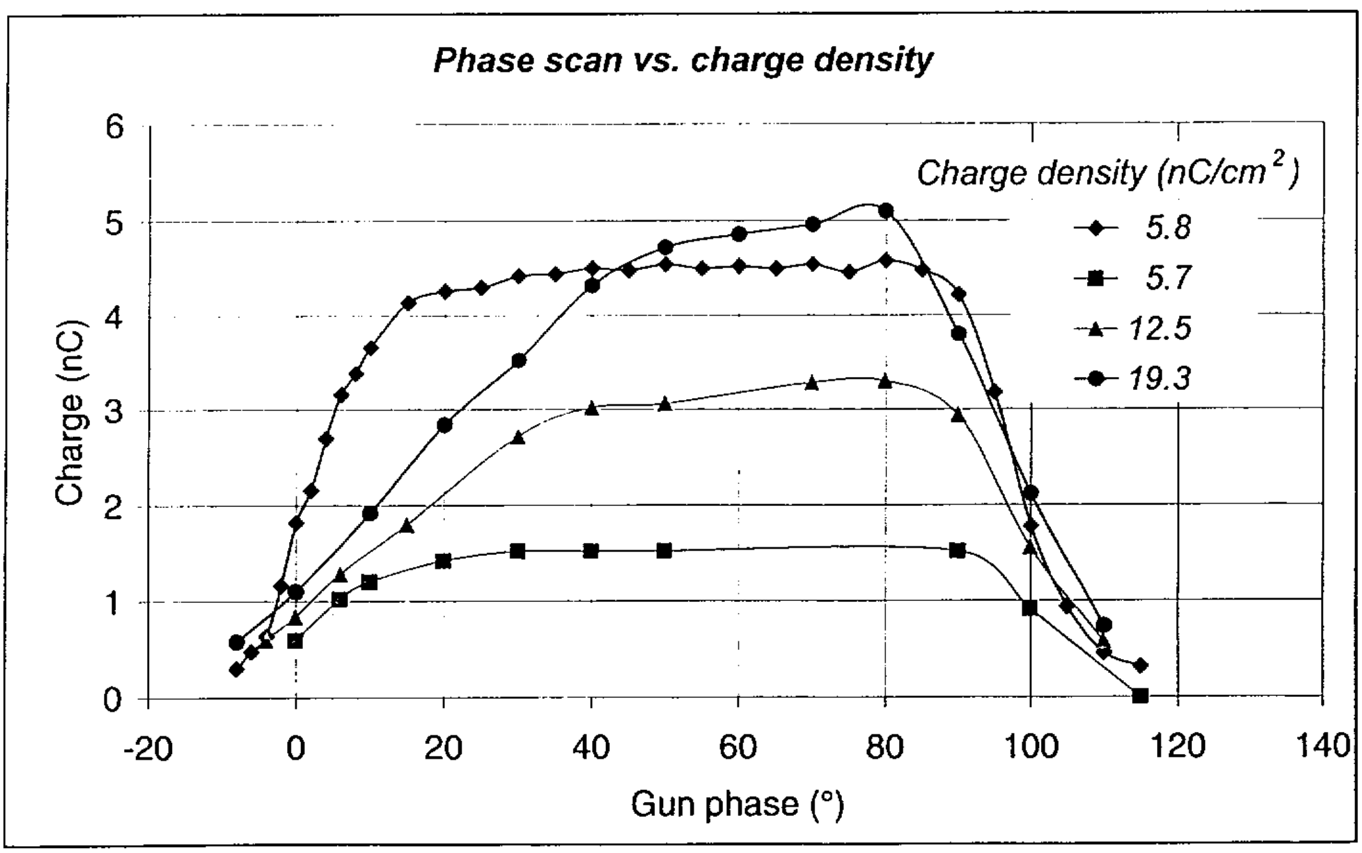

Phase scan vs. charge density
Charge density (nC/cm^2)
5.8
5.7
12.5
19.3
6
5
4
3
2
1
0
Charge (nC)
-20
0
20
40
60
80
100
120
140
Gun phase (°)

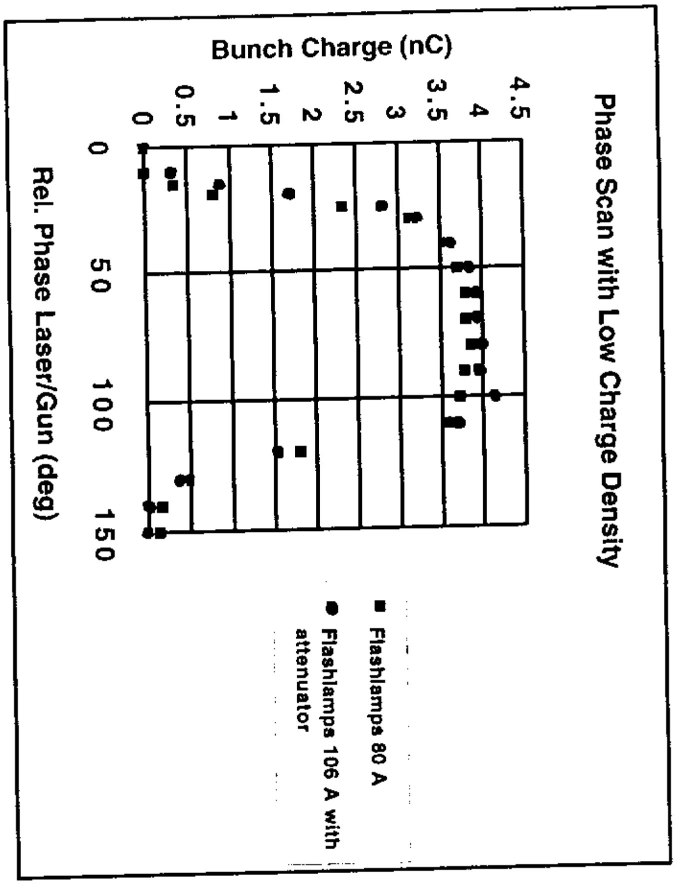

example for two different laser energies but same charge density (by use of an attenuator)

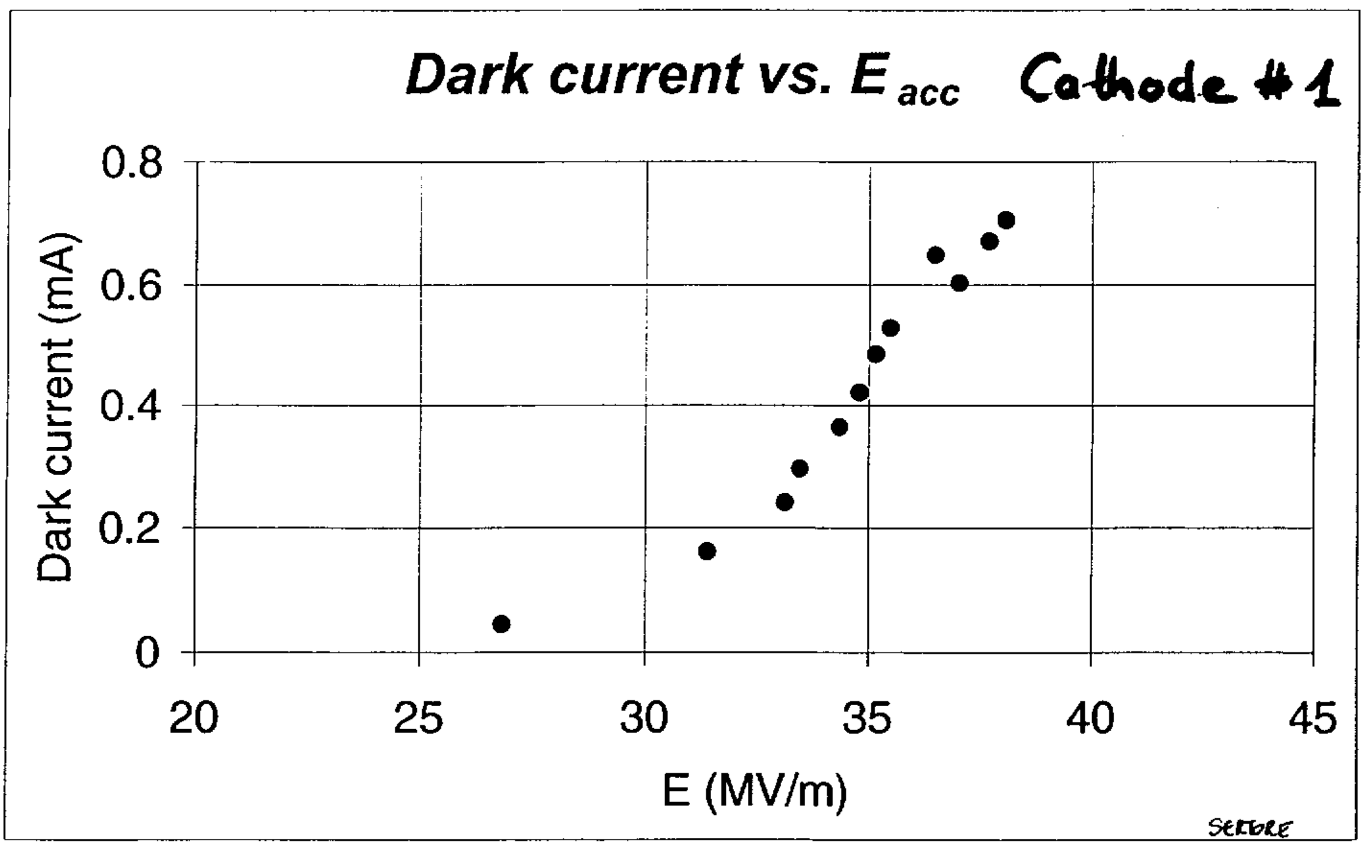

dark current c BC2

36

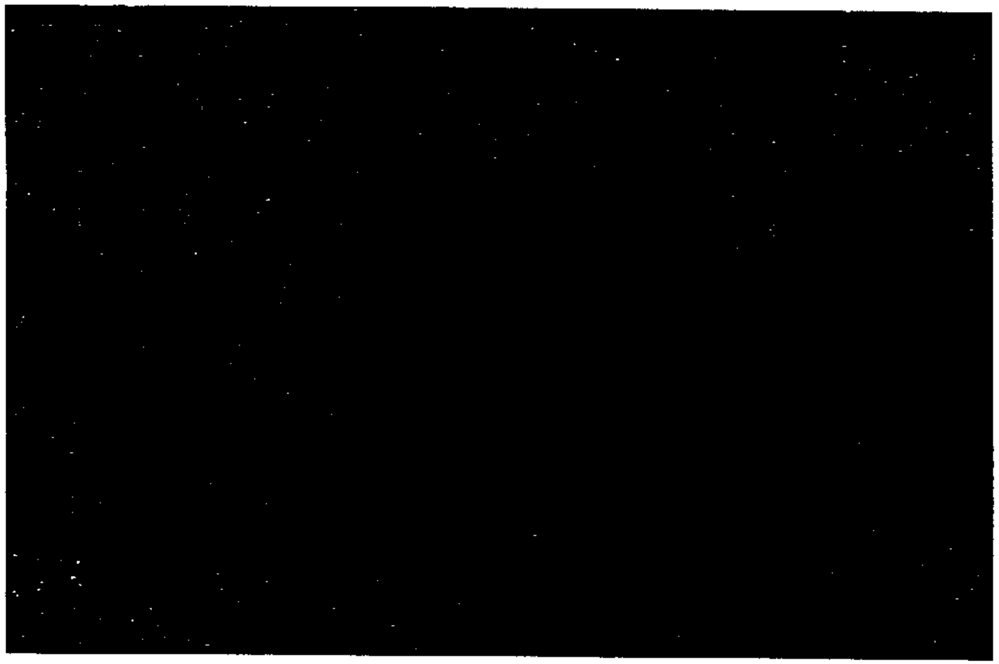

Cathode #1

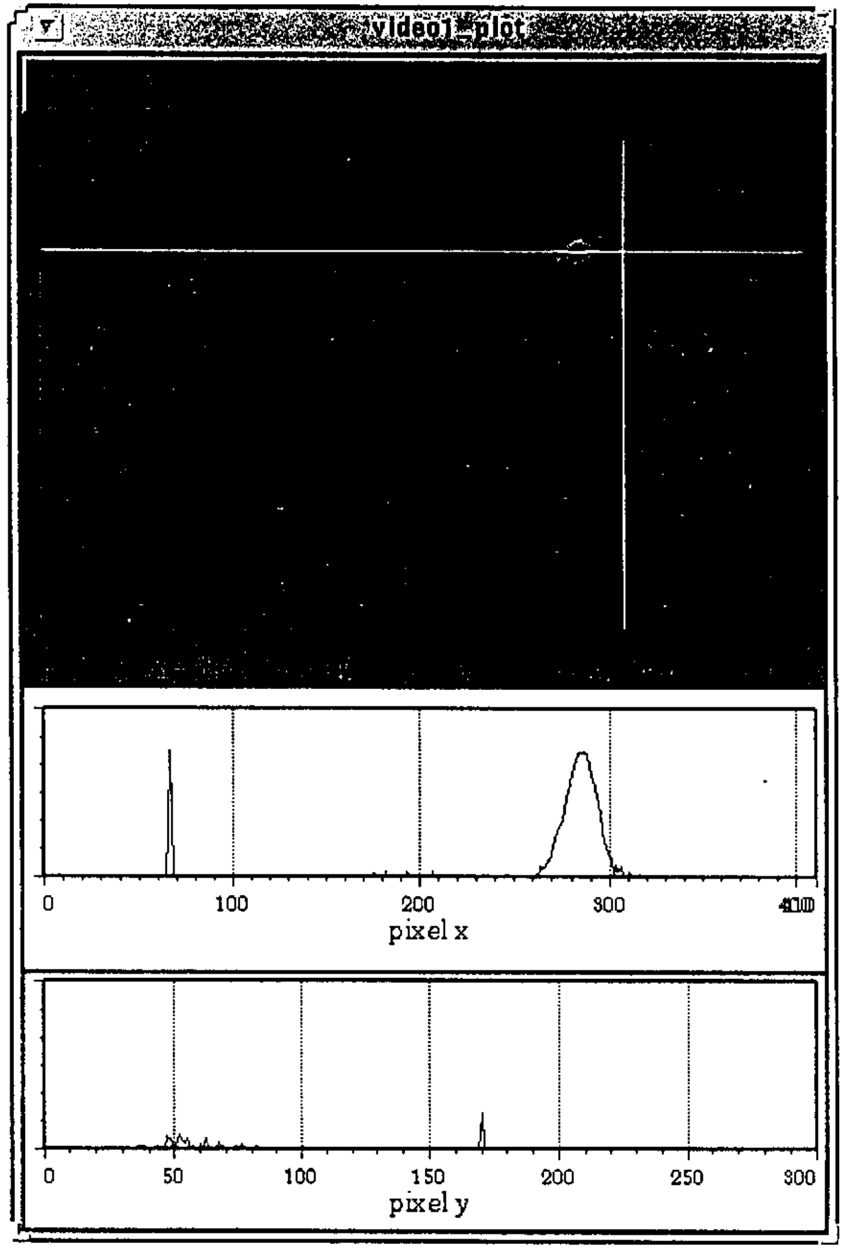

Dark Current

- Cathode #1 ~ mA
- Cathode #2 50 μA @ 42 MV/m

  < 20 μA @ 35 MV/m

34

Dark Current Cathode #2

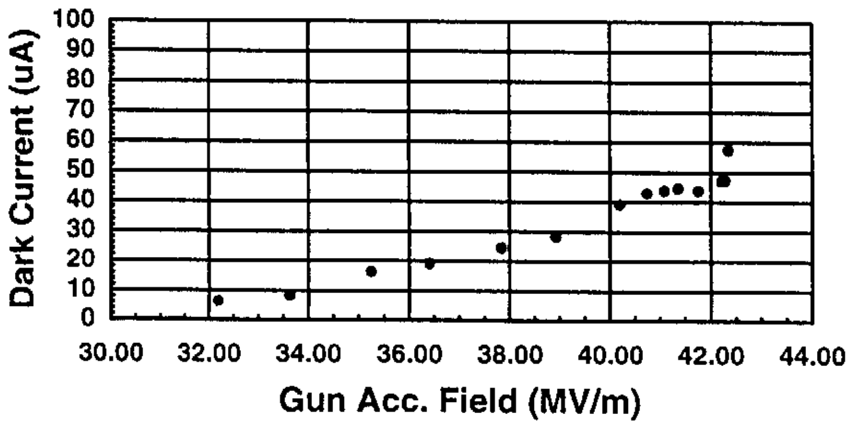

SERTORE/SCHREIBER/MICHELATO

Gun Forw. Power 2.5 MW (37 MV/m)

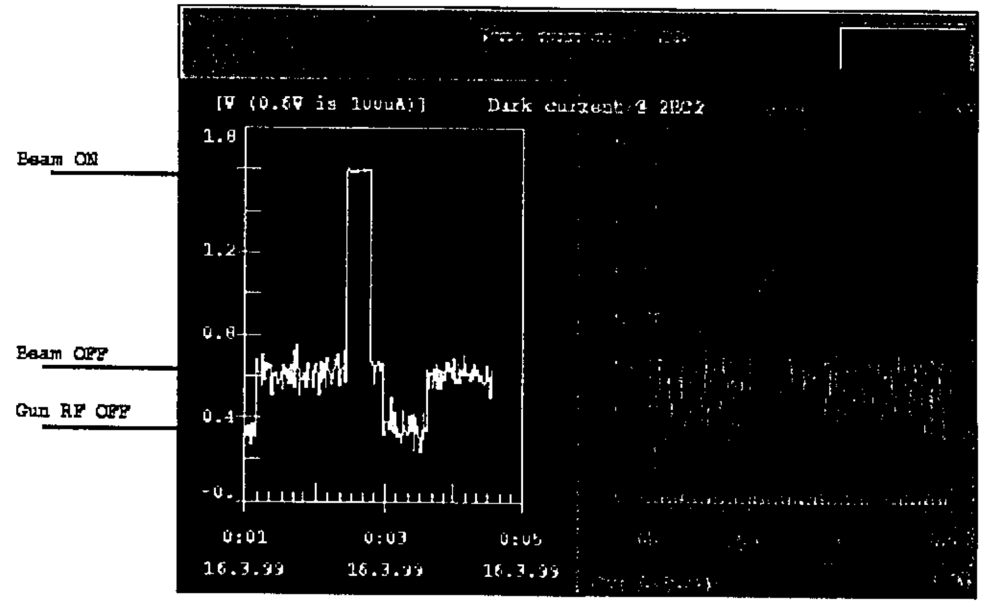

Dark Current = [redacted] 0.6 V ≙ 100 μA (not linear)

dark current measured with reentrant cavity BPM ≈ 0.3 V ≙ 30 μA

Cathode #2, 37 MV/m 0.2 V ≙ 20 μA

→ consistent with ICT measurement 20-25 μA

16.Mar.99 00:04.46

Cathode #2

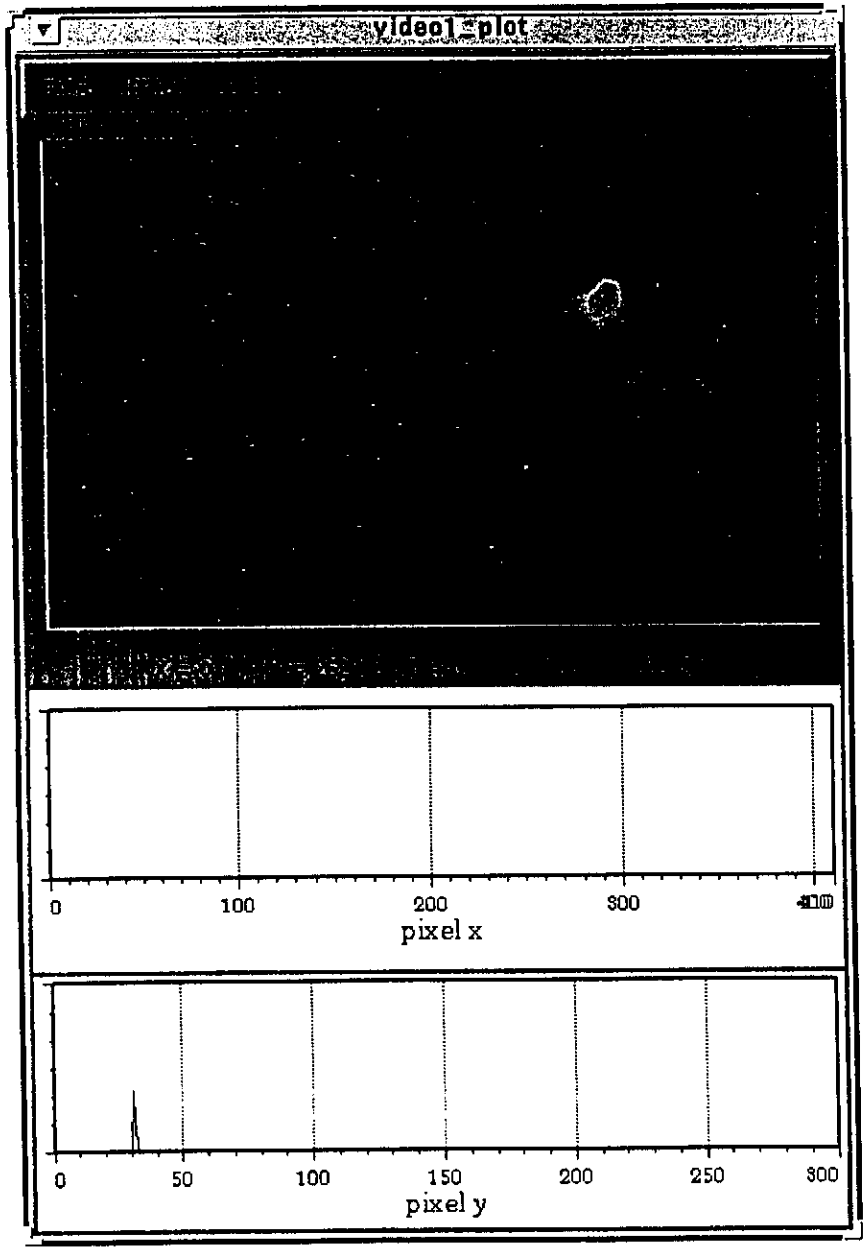

Cathode #2, rf on, beam off

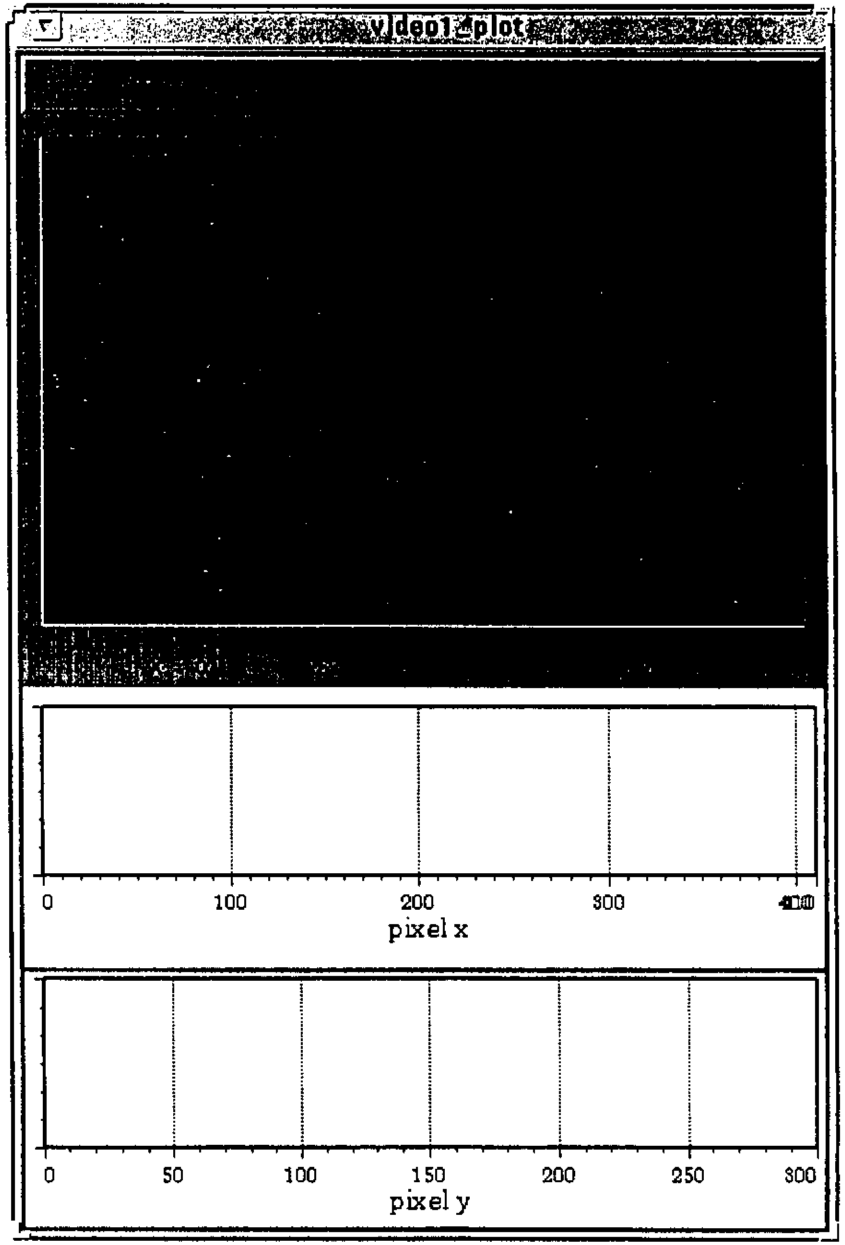

Example of beam current

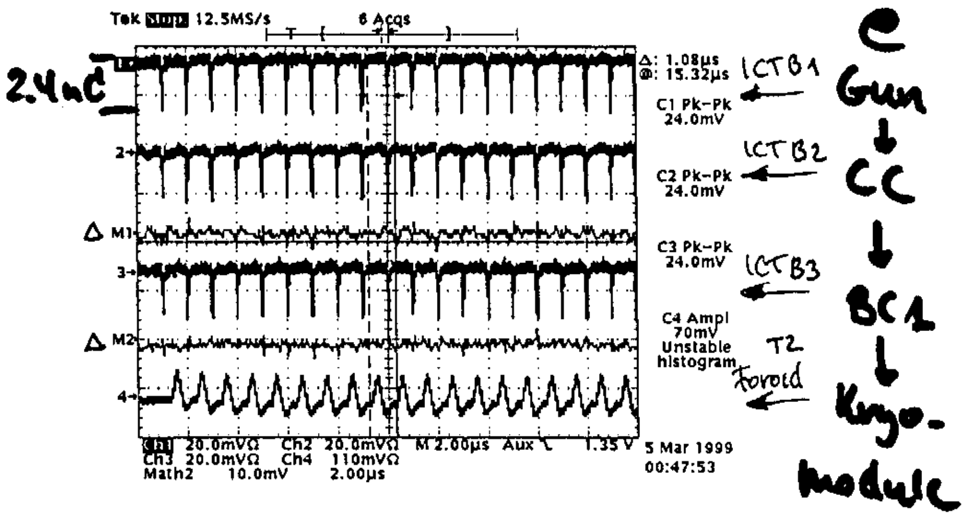

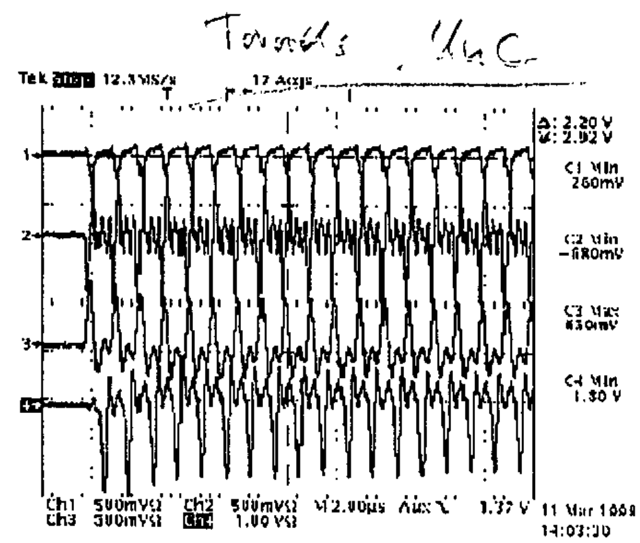

example for 11nC
T2, T3, T4, T7

- measured with ICT's & toroids
- transmission in the injector ~ 100%

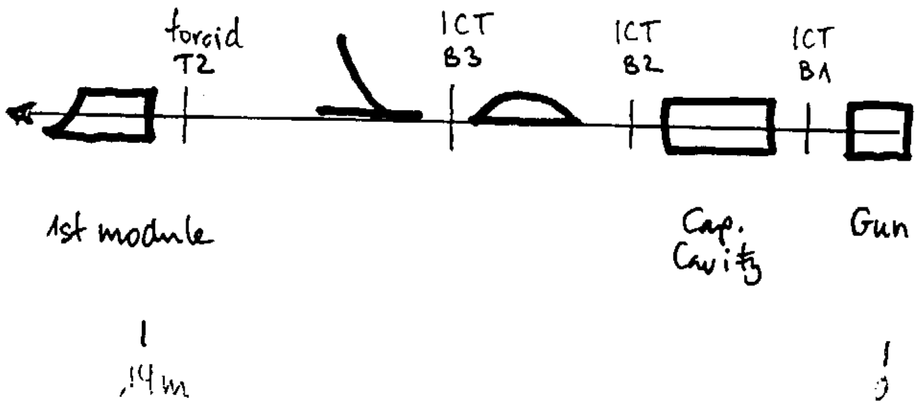

ICT B2

example for current monitoring with ICT B2 (downstream CC)

40

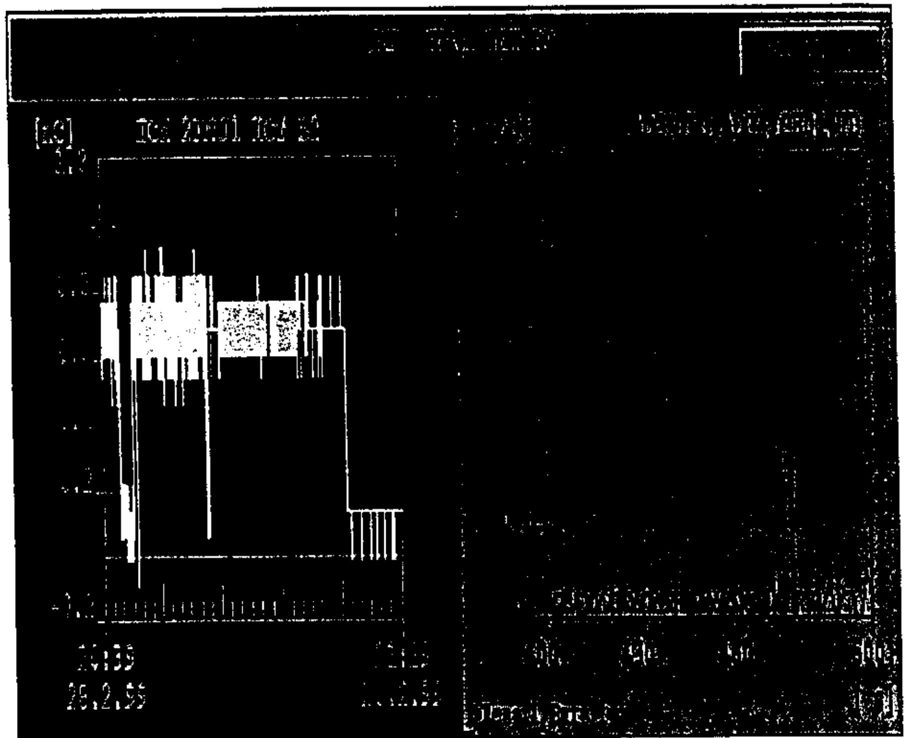

20 min.

stability $\pm 0.1\,nC$ of $0.7\,nC$ / min max

rms $\sigma \approx 0.03\,nC \hat{=} 5\%$

28.Feb.99 23:33.01

S. Schreiber
11.6.99

Bunch length measurements Run 1/99

measurements were done with the following methods:

- Streak Camera
  - Synchrotron radiation @ Dipol (HE)
  - Laser pulses
- Martin-Puplett-Interferometer
  - HE Section (EXP)
- Josephson Junction → no results yet
- others ?

Autocorrelation method for laser pulse length measurements

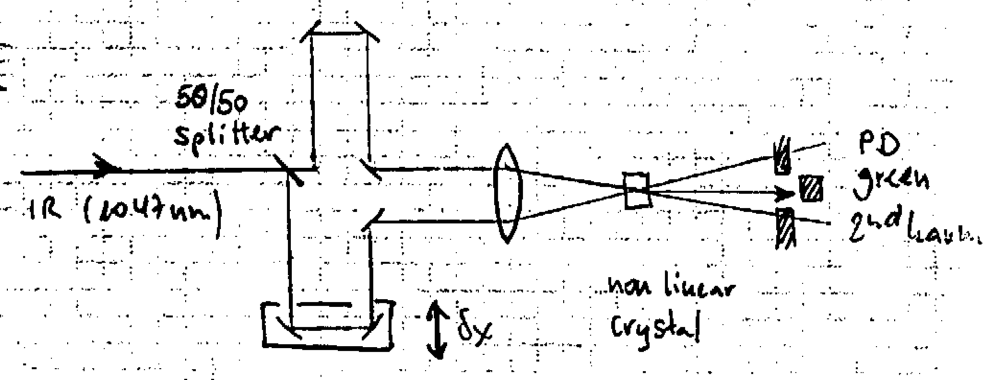

measure green signal @ PD (photo diode) as a function of delay

⇨ direct measure of pulse length

($\frac{1}{2} \cdot 300\mu m$ delay ~ 1 ps)

but: we cannot measure the pulse length as simple as this

Laser

autocorrelation - before repair

@ 1047 nm

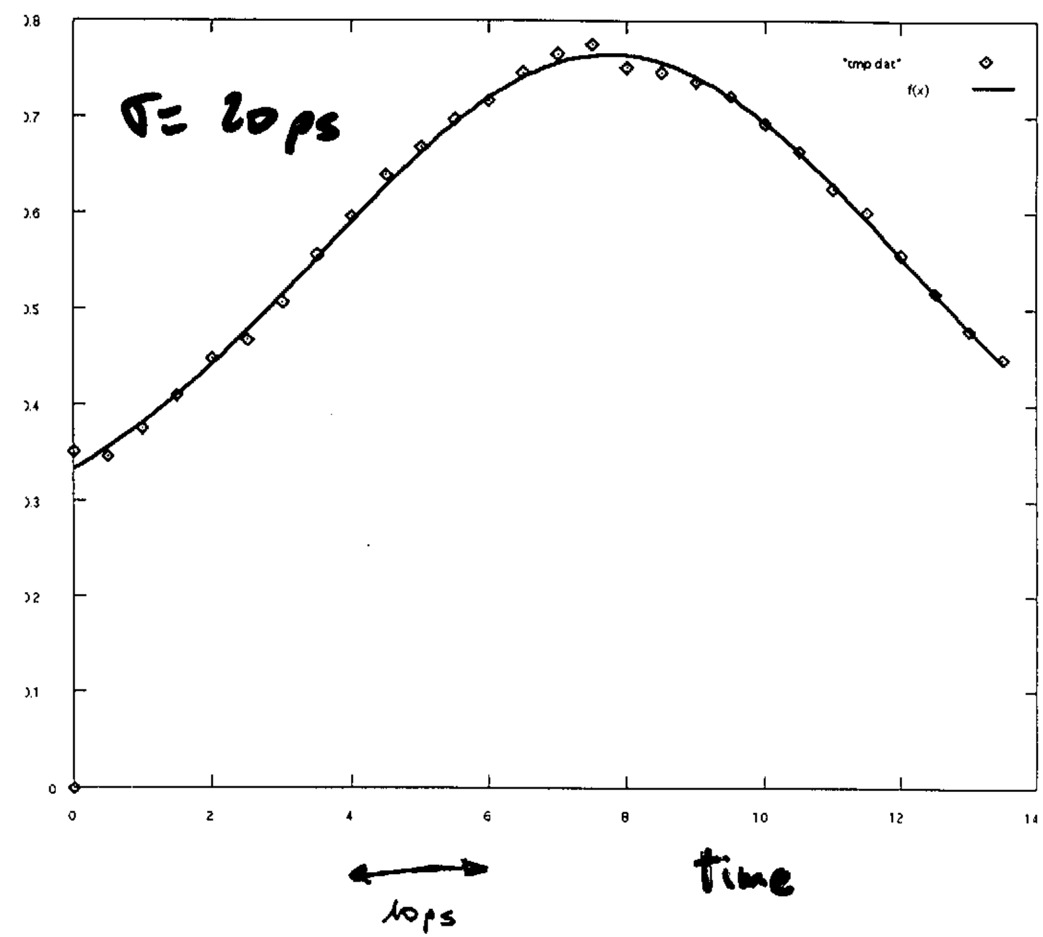

42

Laser

autocorrelation - after repair

@ 1047 nm

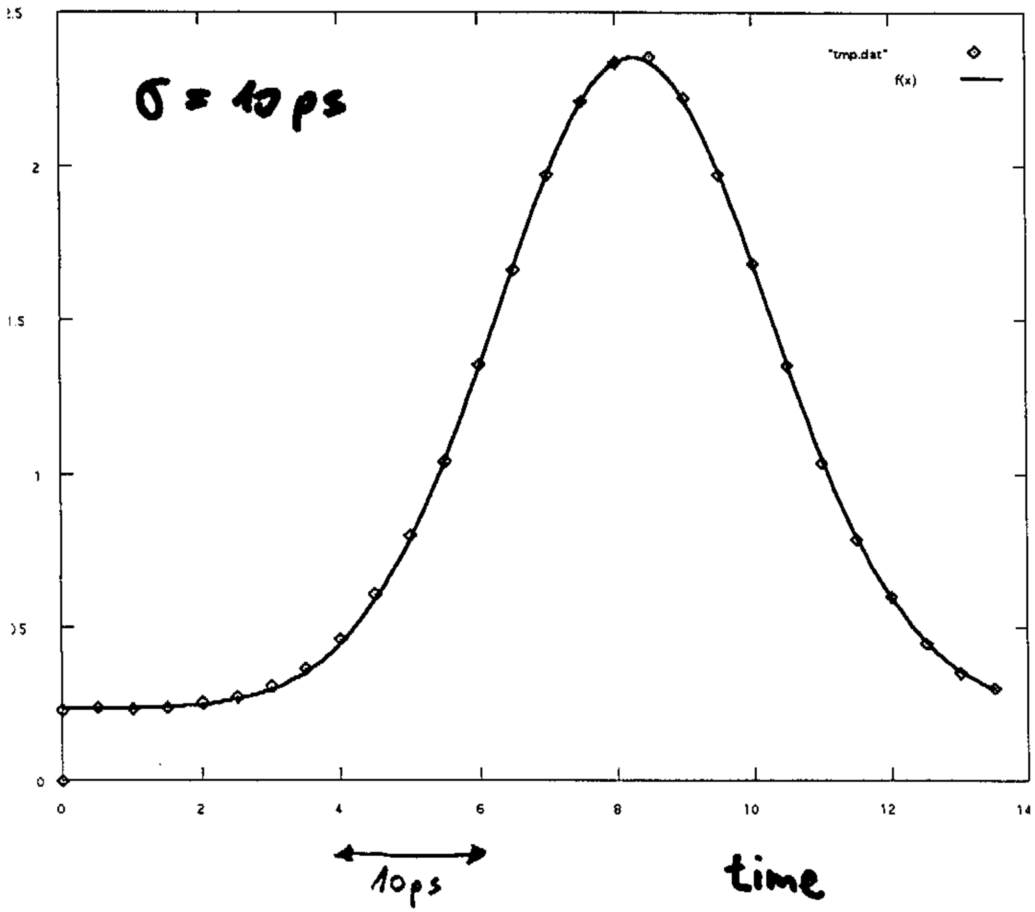

Principle layout of a Streak Camera

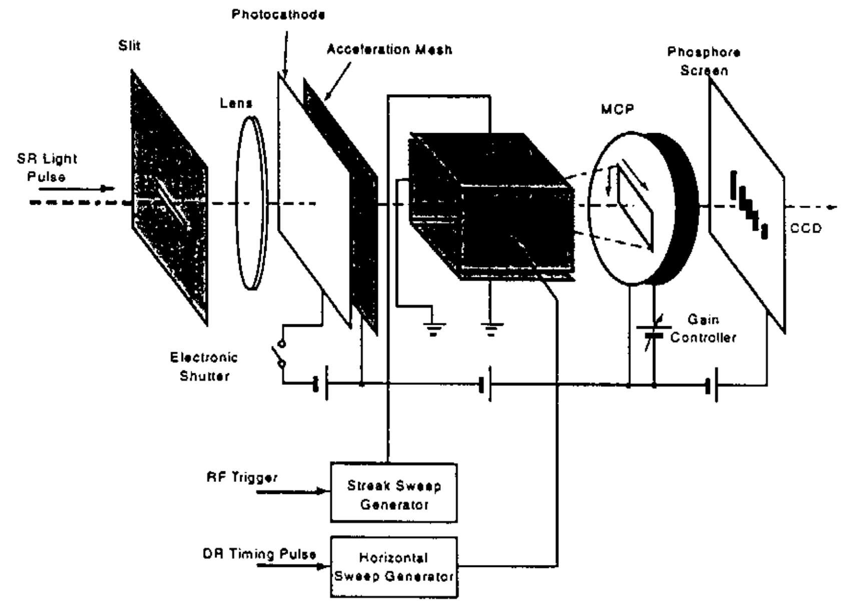

- ARP Streak Camera from LAL/Orsay
- Resolution of the photo tube 2 ps
- Measurement performed with
  - Synchrotron Radiation at the HE Dipole
  - Laser

43

Laser

before repair of Osc.

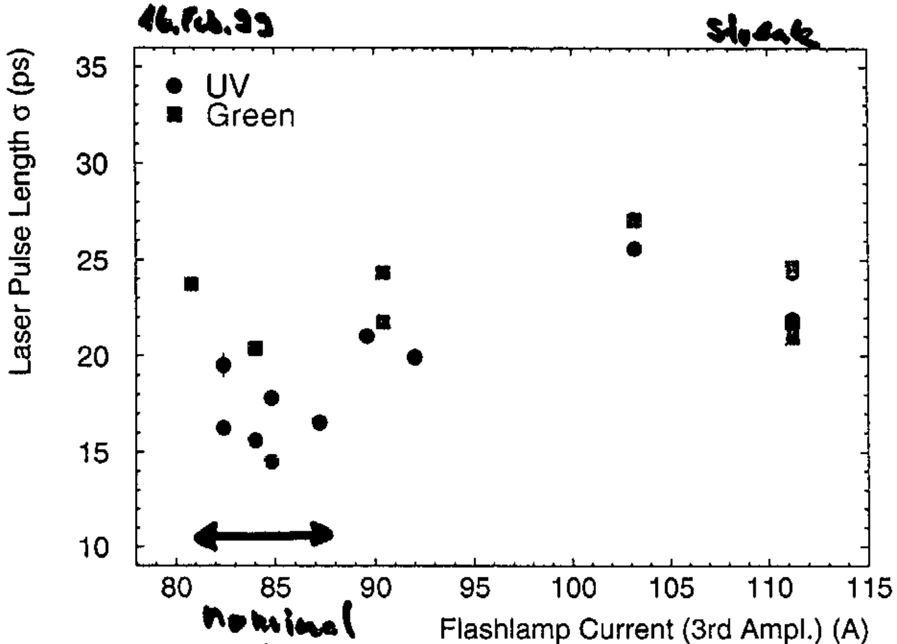

nominal operating current

$\sigma_{uv} = 16\,ps$ for nominal flashlamps current

$\sigma_{green} = 20\,ps$

Laser

after repair of osc.

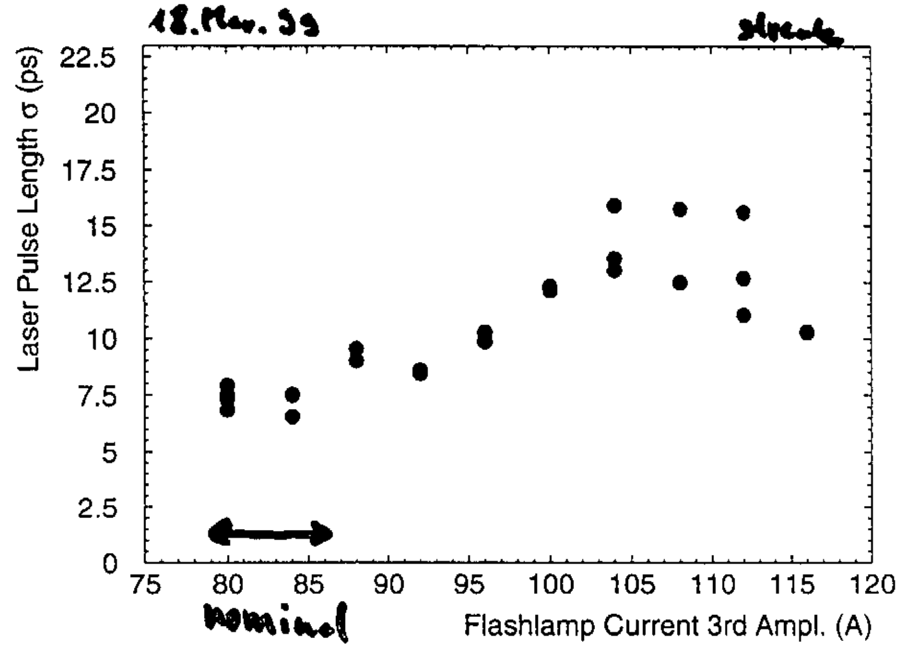

nominal current

$\sigma_{uv} = 7 \pm 1\,ps$

Bunch length measured @ Dipol in EXP3 with Synchrotron radiation

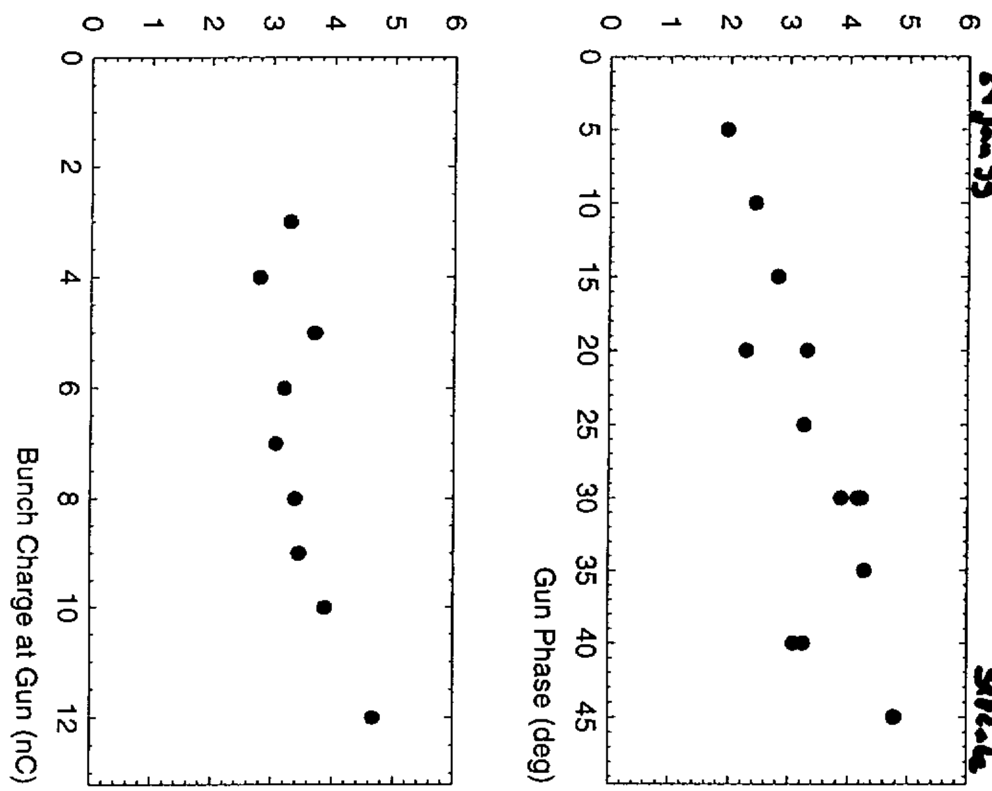

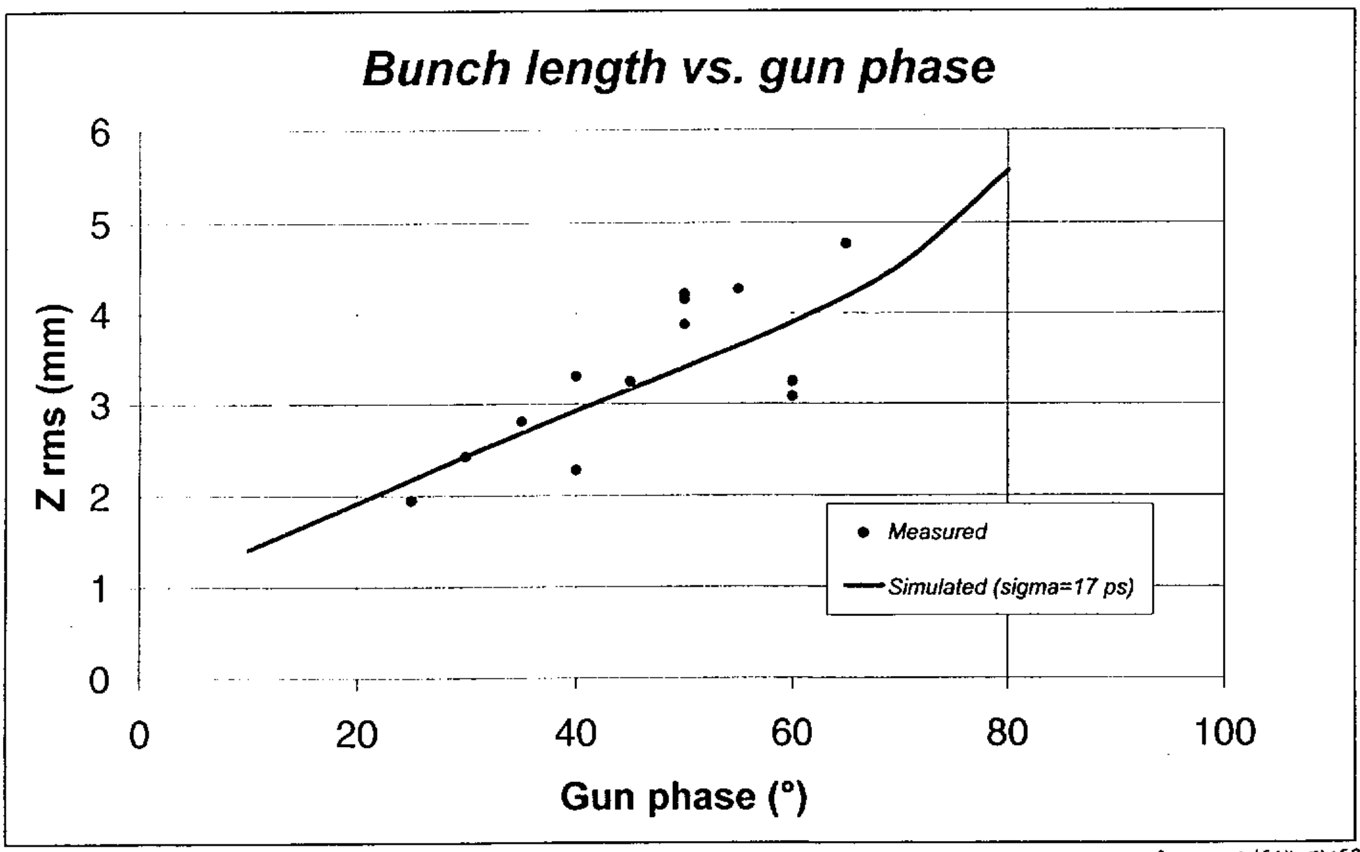

SERTORE / SCHREIBER

Scan of relative Phase Laser/Gun

(Sertore/Schreiber)

S. Schreiber
25-Mar-1999

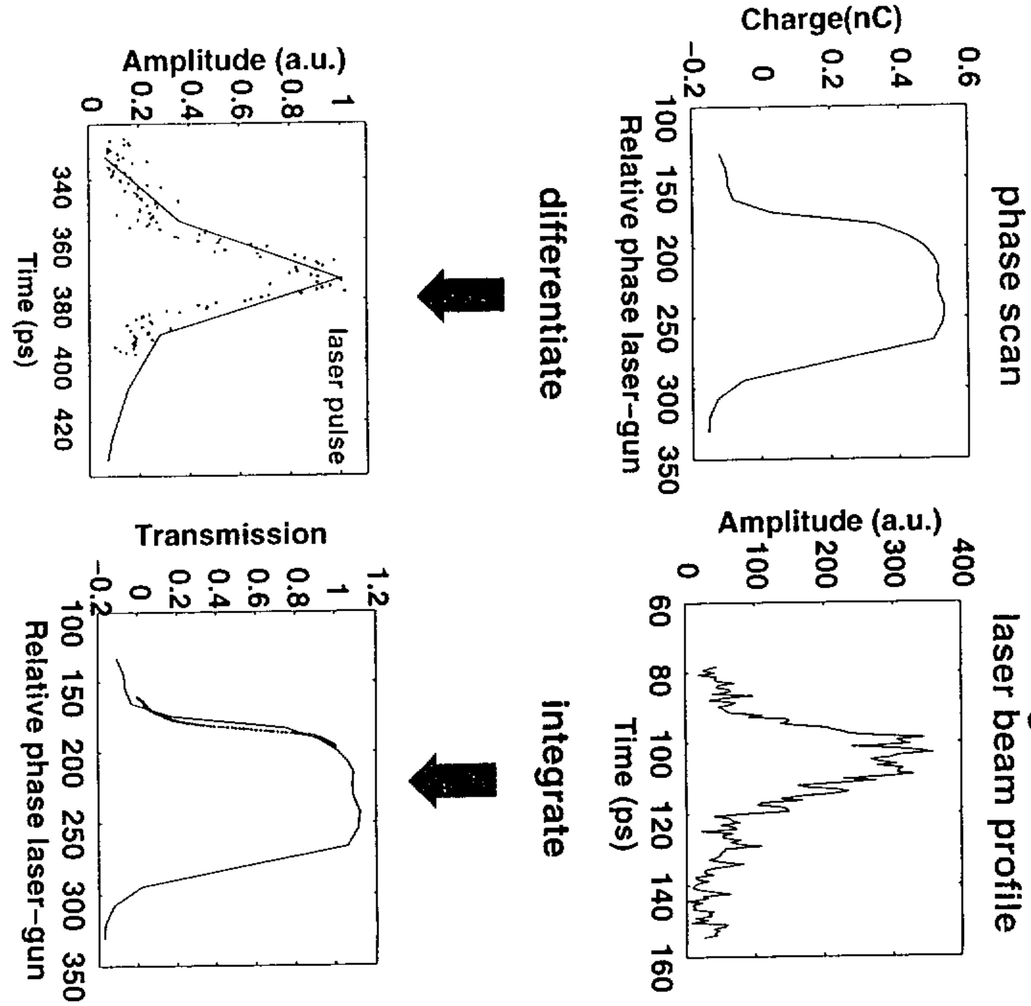

⇨ very nice tool to measure the laser pulse length and to estimate the longitudinal pulse profile

Measurement of the Autocorrelation function

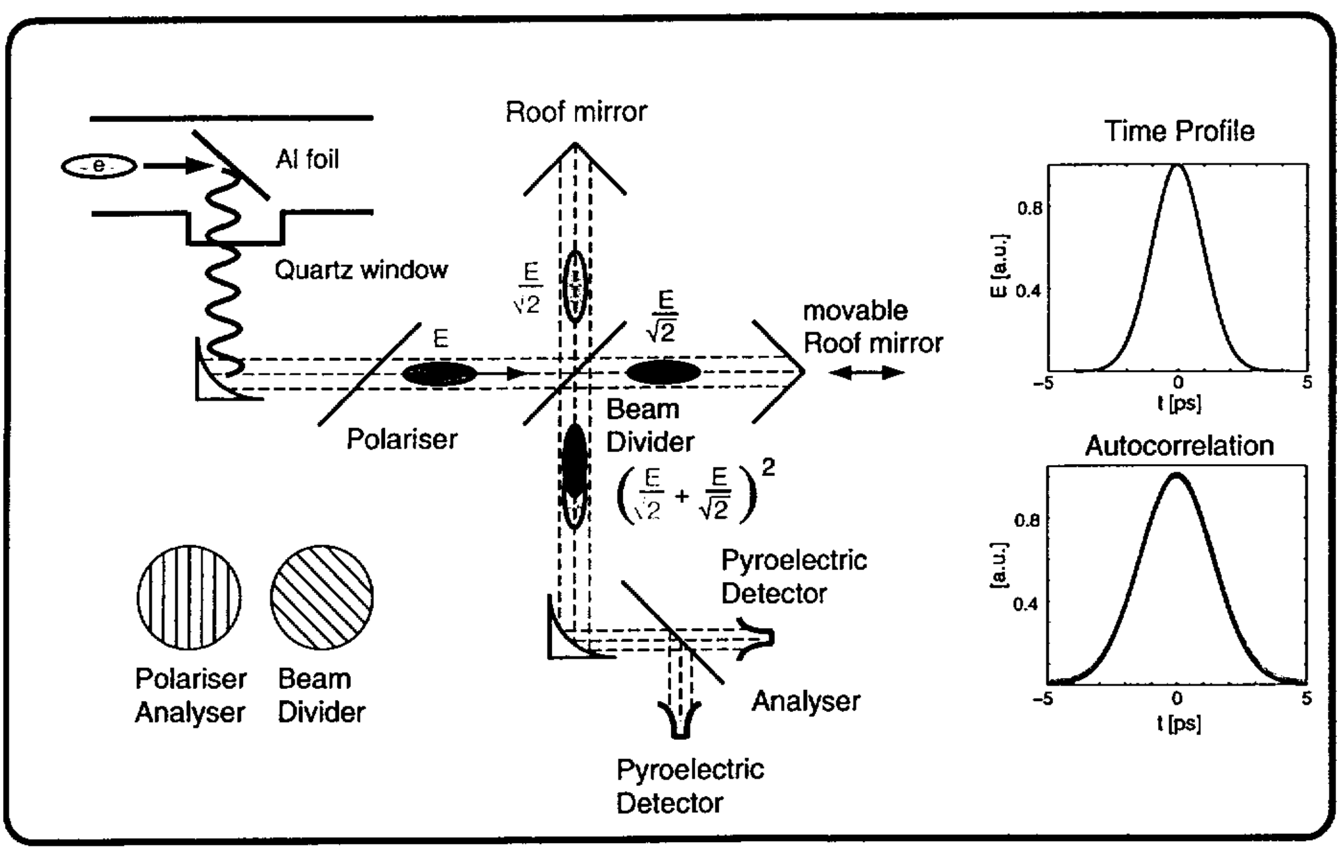

An example of beam diagnostics: Bunch length measurements using coherent transition radiation

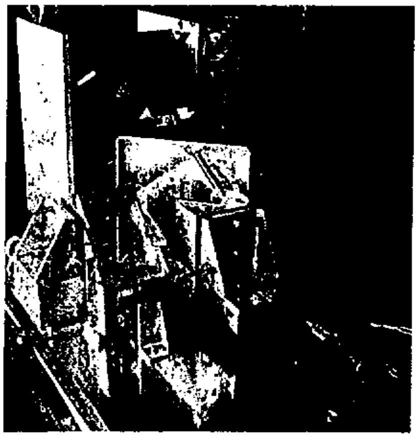

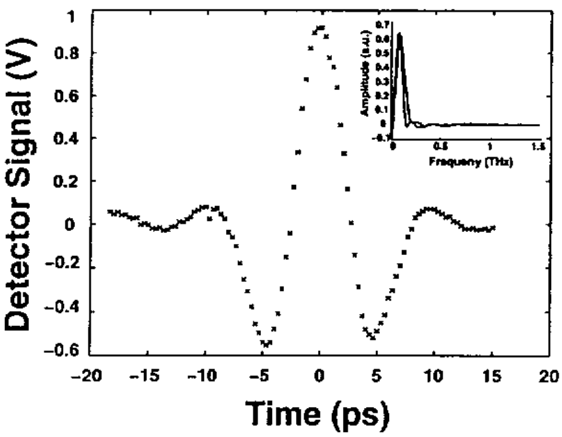

- Martin-Puplett Interferometer
- Transition radiation is produced at an aluminum foil hit by the beam
- The coherent part of the transition radiation is split in a Michelson-type interferometer. After recombination, the interference pattern is measured with pyro-electric detectors.
- From this, the bunch length is determined to be 1.5 ± 0.5 ps (0.45 ± 0.15 mm) rms.

The Difference Interferogram

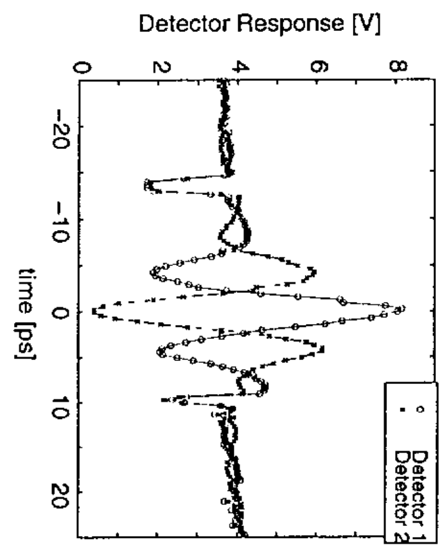

- 2 Detectors measure "anticorrelated" signal
- Correlated fluctuations due to instabilities of the electron beam
- Normalized Difference Interferogram (NDI)

$$NDI = \frac{\text{Detector 1} - \text{Detector 2}}{\text{Detector 1} + \text{Detector 2}}$$

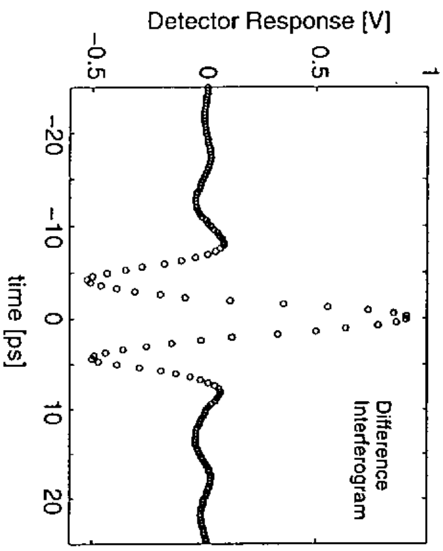

- The NDI is a smooth function, statistical fluctuations within the size of the data points
- Time of measurement: ca. 15 minutes

Kramers-Kronig Reconstruction

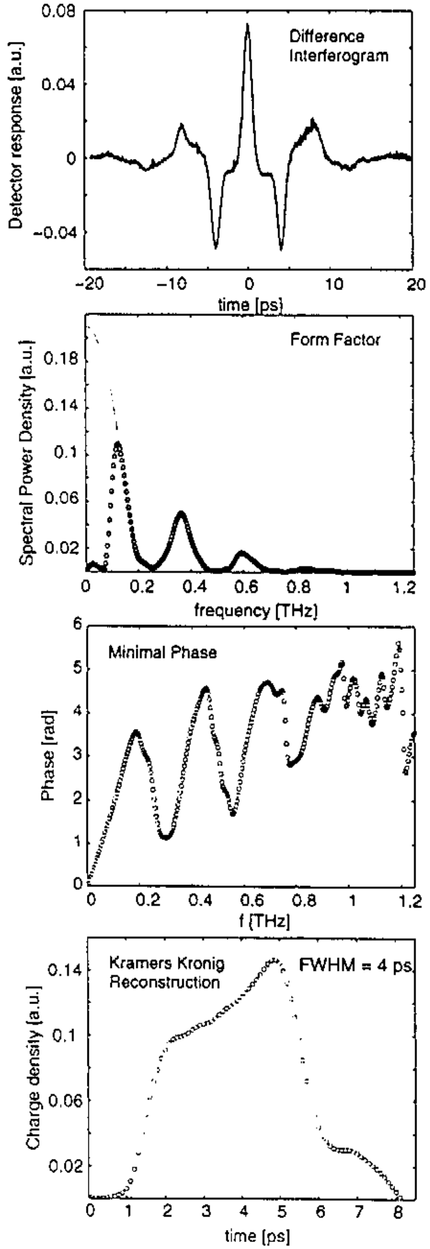

Normalized difference interferogram:

$\Downarrow$ Fourier Transformation

Form factor:

Extrapolation to:

f → 0: 2nd order polynomial function

f → ∞: exponential function

Minimal phase (Kramers-Kronig)

Assumptions:
Causality
Extension of form factor into complex plane

$$\psi_m(\omega) = \frac{2\omega}{\pi} \int_0^\infty \frac{\ln[|f(\omega_0)|/|f(\omega)|]}{\omega^2 - \omega^2} d\omega_0$$

$\Downarrow$ $\sigma_z \approx 2ps \approx 0.6mm$

Fourier Transformation:

$$\rho(t) = \int_0^\infty |f(\omega)| \cos(\psi_m(\omega) + \omega t) d\omega \, .$$

Magnetic bunch compression

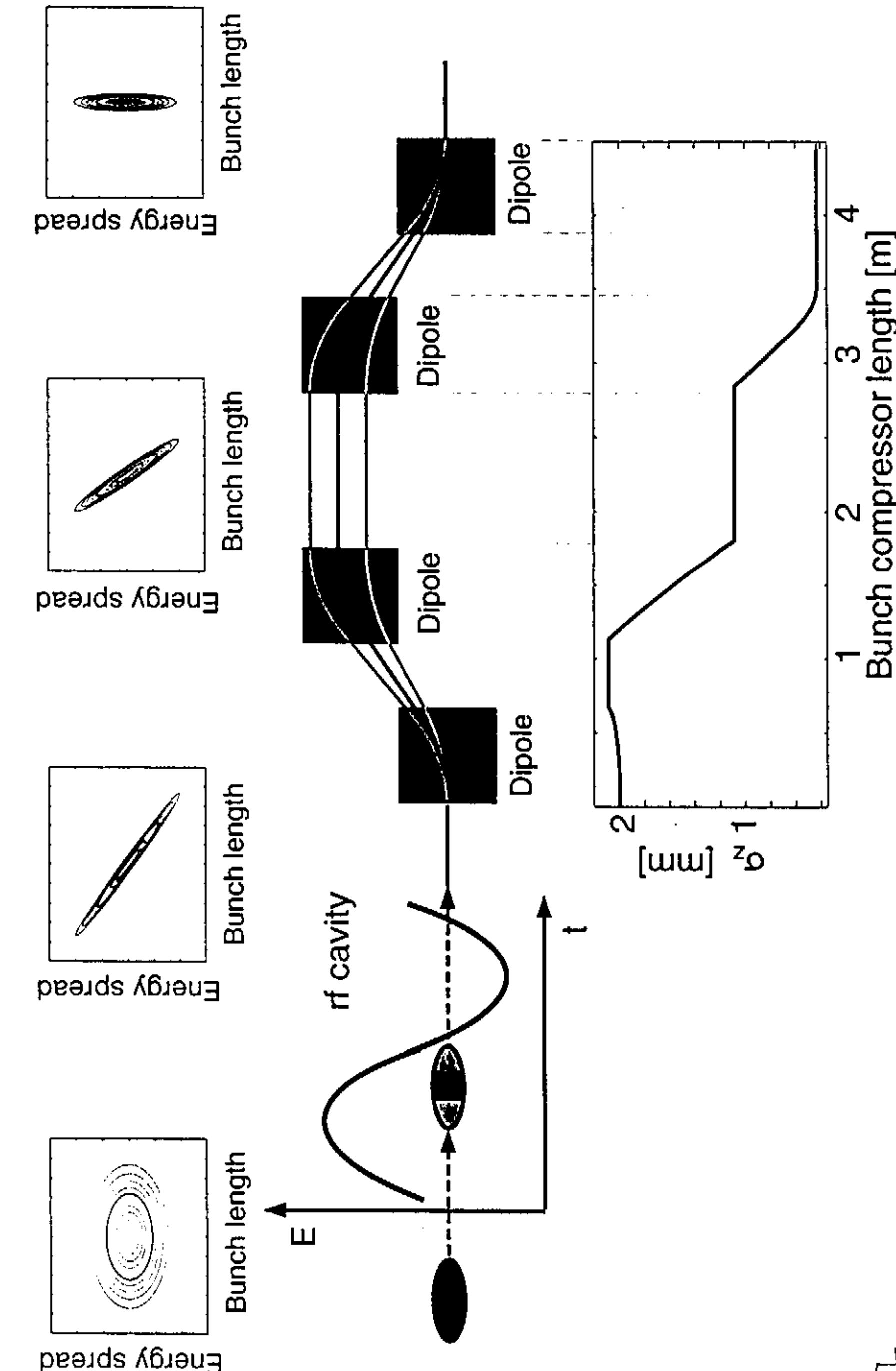

Measurement of the longitudinal charge distribution

(GEITZ)

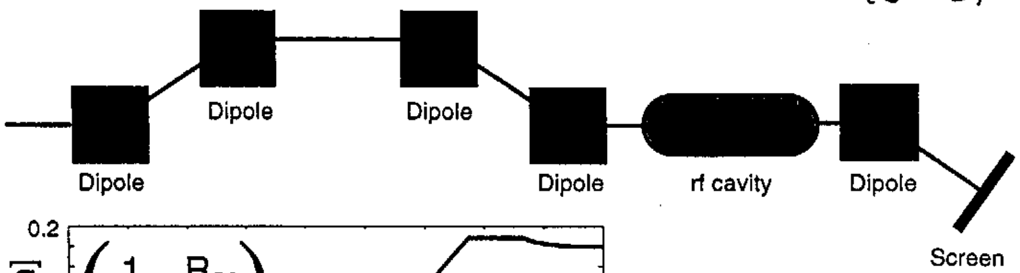

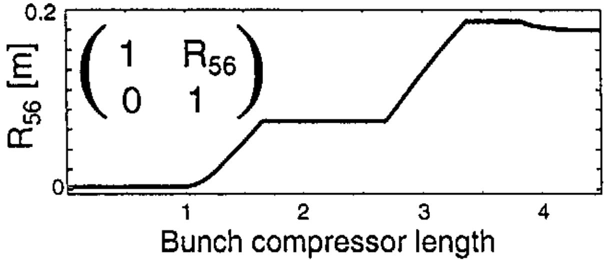

R_{56} transforms initial energy spread into final bunch length

+ off-crest acceleration:

48

$$\begin{pmatrix} 1 & 0 \\ R_{65} & R_{66} \end{pmatrix}$$

R_{65} transforms initial bunch length into final energy spread

$$R_{66} = \frac{\text{initial beam energy}}{\text{final beam energy}}$$

Matrix $\Longrightarrow$ multiplication

$$\begin{pmatrix} L \\ \frac{\Delta E}{E} \end{pmatrix}_{final} = \begin{pmatrix} 1 & R_{56} \\ R_{65} & \rho \end{pmatrix} \begin{pmatrix} L \\ \frac{\Delta E}{E} \end{pmatrix}_{initial}$$

where $\rho = R_{56}R_{65} + R_{66}$

Let $\rho \to 0$: $\Longrightarrow$

$$\boxed{\frac{\Delta E}{E}_f = R_{65} L_i \quad \text{at} \quad R_{56} = -\frac{R_{66}}{R_{65}}}$$

Limits:
- ⇨ Resolution of the spectrometer dipole magnet
- ⇨ Assumption on beam transfer, impact of non-linear wake-fields, transverse-longitudinal coupling

TTF measurements:

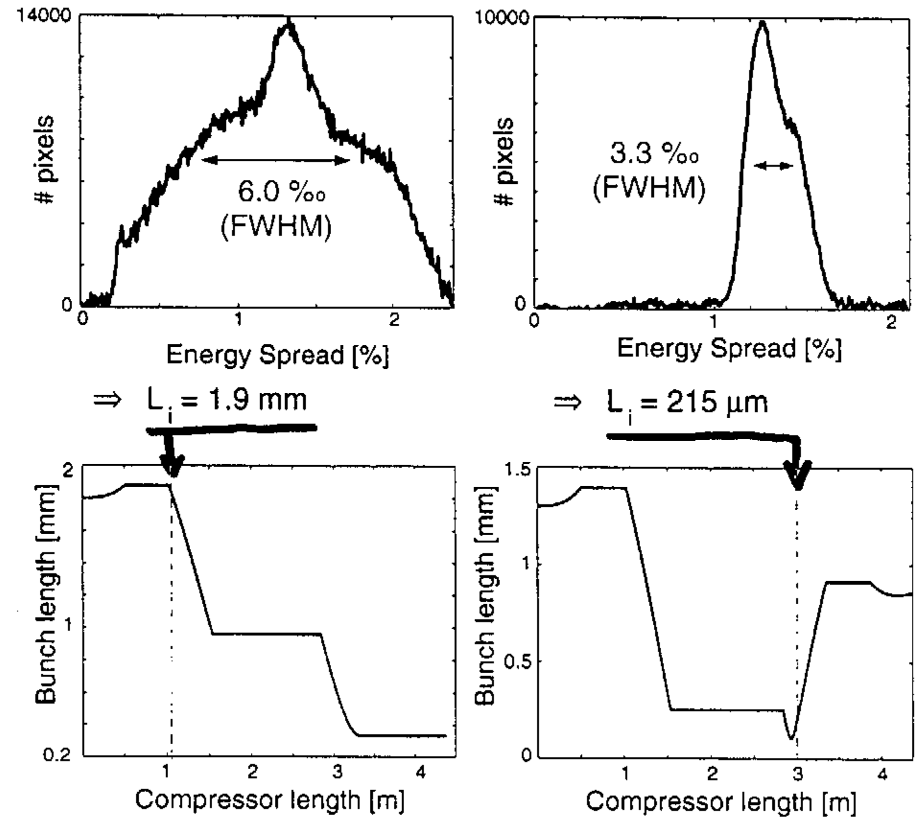

Summary

- :) We had a successfull run with the new injector (mid. Dec '98 – mid March '99)
- :) Smooth conditioning of the gun + rf window design rf pulse length reached (800 μs) at design gradient (35 MV/m)
- :) availability of gun + cathode + laser 98%
- :) the injector delivered routinely beam for TESLA experiments (modules, HOM, bunch compressor studies etc.)

⇨ next run in Summer will concentrate on beam for TTF/FEL experiments with an undulator installed

emittance!

Status of Cavities and Auxiliaries

D.Proch

- I Cavity measurements since last TTF meeting
- II Remaining cavities of second production
- III Third cavity production
  - -order of Nb material
  - -order for cavity production
  - -time schedule
  - -improved eddy current scanner for Nb sheets
- IV Status of input couplers, tuners

Cavities for module 3

4 cavities from ACCEL (S28, S29, S30, S32) and 4 cavities from Dornier (D39, D40, D41, D42) selected for module 3.

Average gradient in the vertical test was: 25.4 MV/m

All cavities are equipped with He vessel

4 cavities are equipped with processed cold part of main coupler

3 (+1) cavities have been tested in CHECHIA

2 additional main coupler are processed and 2 more additional main coupler are under processing -> all cavities will be equipped with a processed cold window

I Cavity measurements since last TTF meeting

5 cavities for Rossendorf (R1, R2, R4, R5, R6)
same design, material, manufacturer, treatment as TTF cavities
but: changed LHe vessel connection, cannot be exchanged with TTF cavities

8 cavities for TTF (A16, A17, A18; S33, S35; C46, C47; Z49)

1 single cell cavity (1S4) of the electro-polishing program

first production Zanon

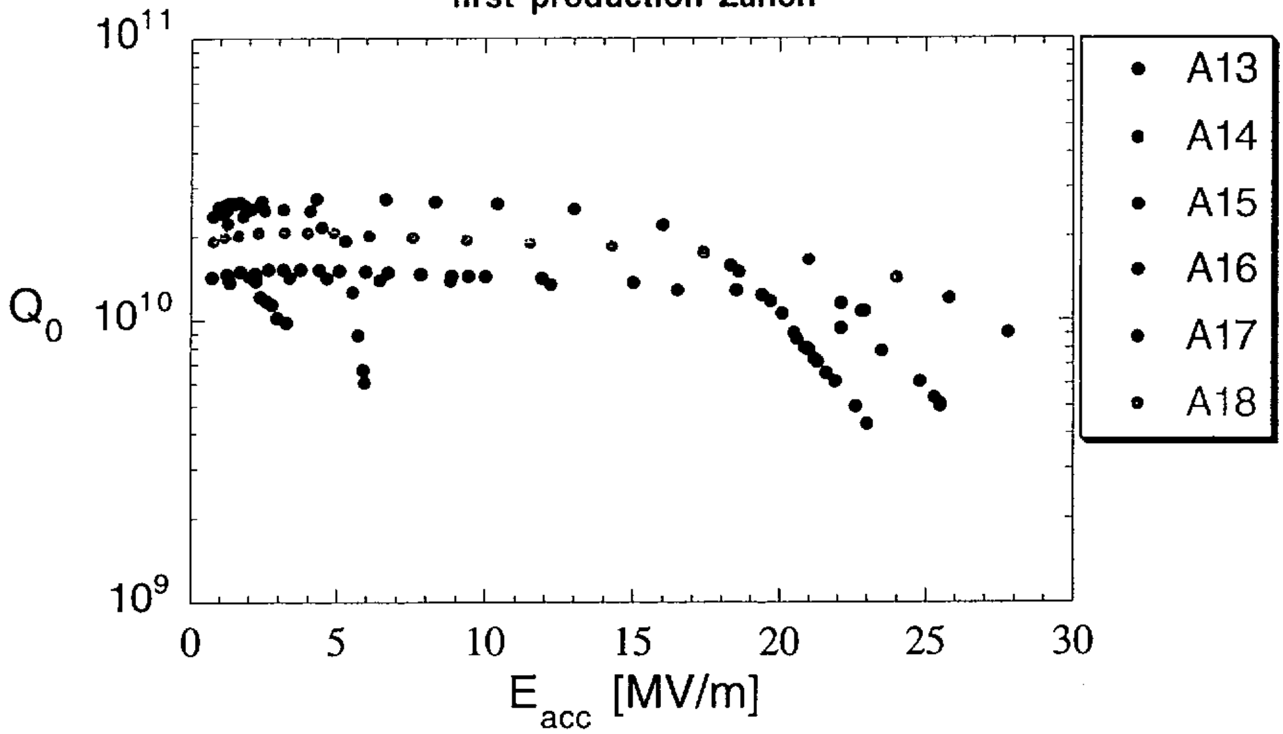

With another calibration, fields above 30 MV/m reached, but this calibration was done with unstable bath-temperature conditions!!

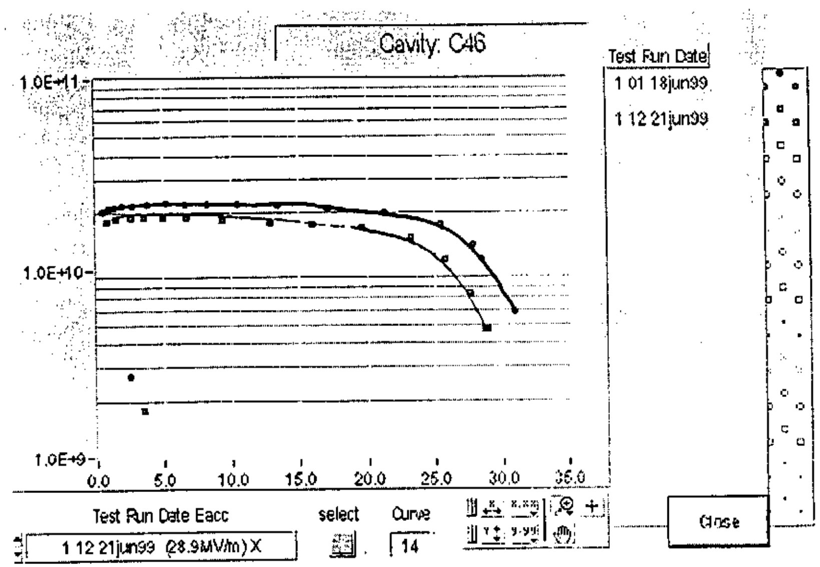

=> 24 MV/m are more likely than >30 MV/m

(remember error is [illegible])

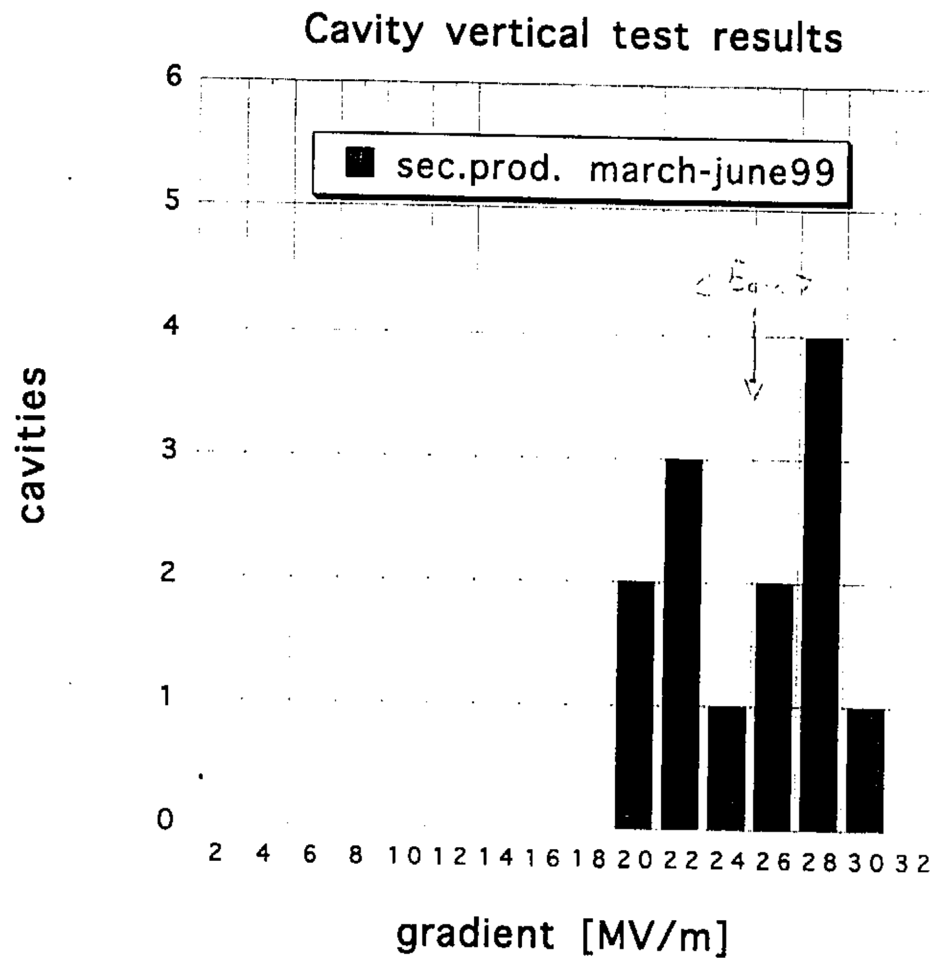

power/quench limit of cavities vert. tests, march-june 99

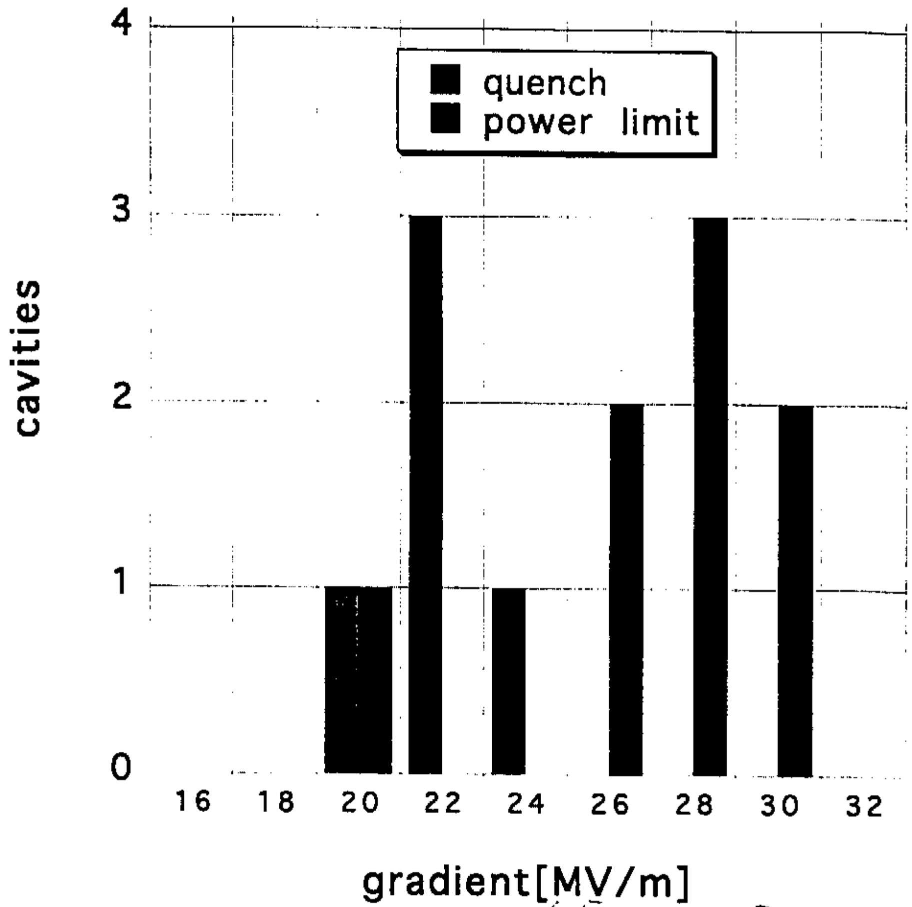

⟨Eacc⟩ = 24

Quench limits

first production – S7, S8, S9, S10, S11, S12, A13, A14

Σ cavities = 17

ΣN = 7

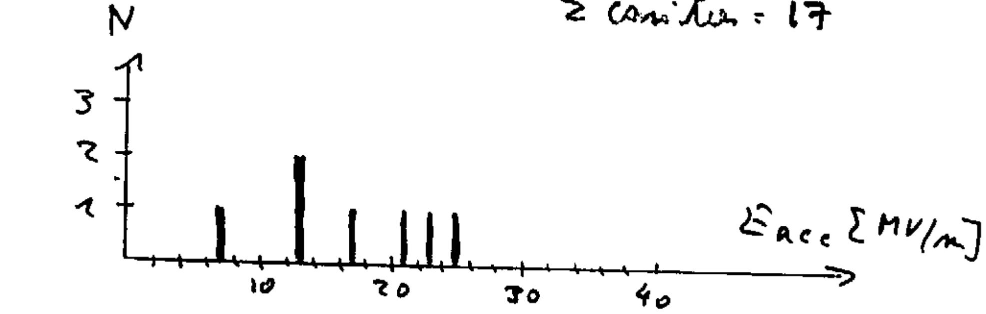

second production – S3?, S36, C45, ... C49, Z50 - Z5?

Σ cavities = 2?

ΣN = 9

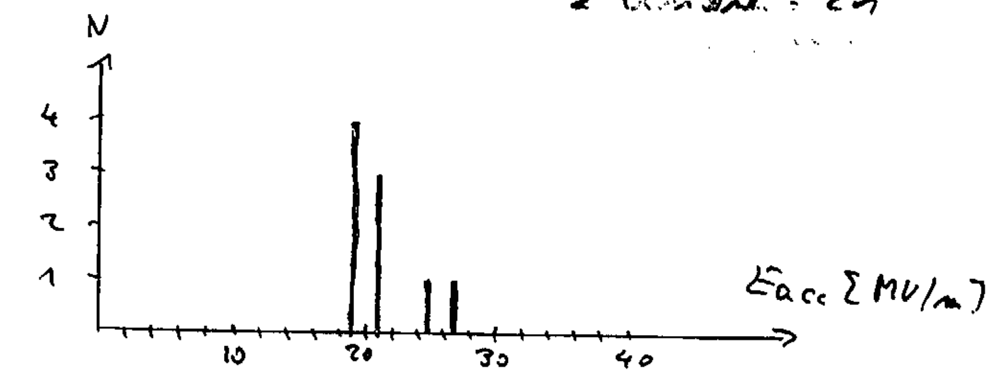

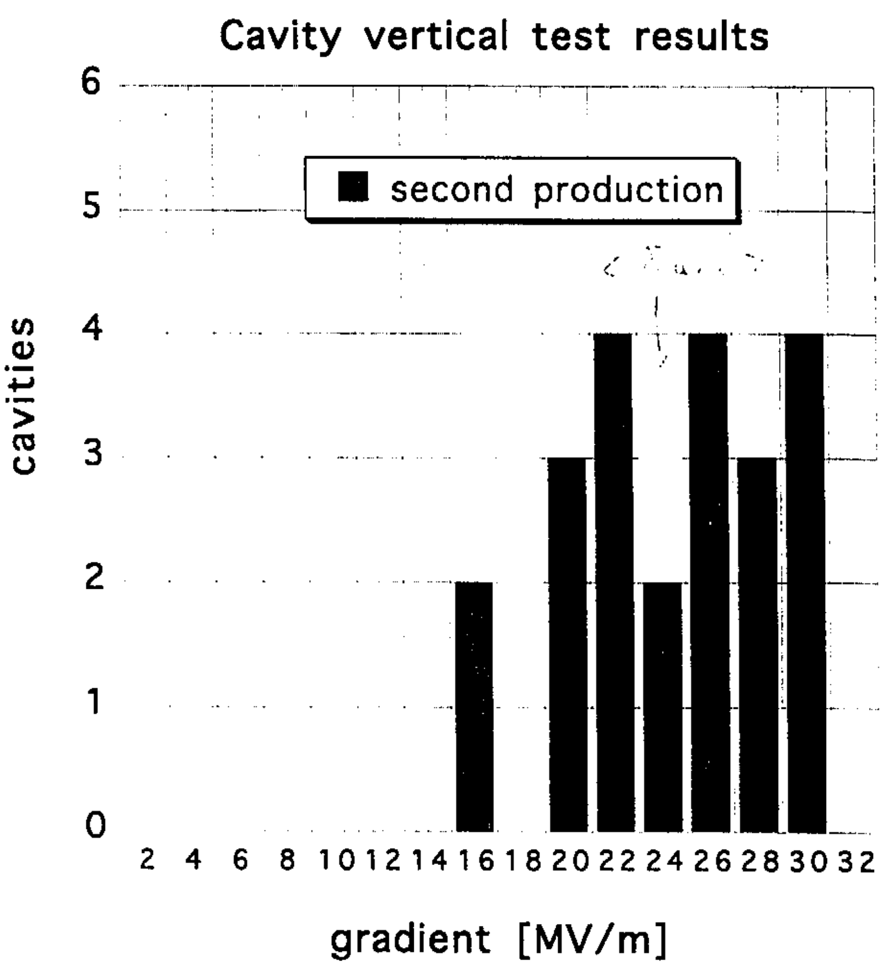

Remaining cavities after modules 1, 2, 3

cavity	Eacc ≥ 25	Eacc ≤ 25	no Eacc	comments
d1		23.1		module 1, new flange
d2	25.6			module 1, new flange
d3		20 (25)		module 1, new flange
a16		22.9		new flange
a17	25.5			new flange
a18	27.8			new flange
s31		14(28)		
s33		20.4		
s35		21.2		
s36			x	
d37		20.3		
d38		19		
c44	25.2			
c45			x	
c46	28.9			
c47		22		
c48			x	
z49		19.4		
z50			x	delivery Sept 99
z51			x	delivery Sept 99
z52			x	delivery Sept 99
z53			x	delivery Sept 99
z54			x	delivery Sept 99
Σ 23	5	10	8	

54

II Remaining cavities of second production

5 cavities with Eacc ≥ 25 MV/m

7 cavities with 25 MV/m ≥ Eacc ≥ 20 MV/m

3 cavities with Eacc ≤ 20 MV/m

8 cavities not yet measured

≥ 23

Cavities needed:

8 cavities for module 1*

8 cavities for module 4

===> one module will operate at Eacc ≥ 25 MV/m
second module will operate at Eacc ≥ 20 MV/m

III Third cavity production

- Nb is ordered for another 30 cavities, delivery already started
- bids for 24 9-cell cavities and 6 modified superstructure cavities are received from ACCEL, CERCA and ZANON
- only one company meets required delivery schedule of
  -first delivery end of January 00
  -delivery rate of 5 cavities per month
- contract will be signed this week, Pönale for late delivery is agreed on by the contractor

Improved eddy current scanner for Nb sheets

- First eddy current scanner operated by scanning the Nb sheet line by line

  ===> start and stop of the scanning head excited mechanical vibrations. This noise limits the ultimate sensitivity.

- New system rotates the Nb sheet continuously (100 rpm), scanning head is placed like the tangential arm of a record player

- first laboratory set up was used to scan the first 160 new Nb sheets:

  ===> higher sensitivity is demonstrated

  faster measuring time (10 instead of 25 minutes)

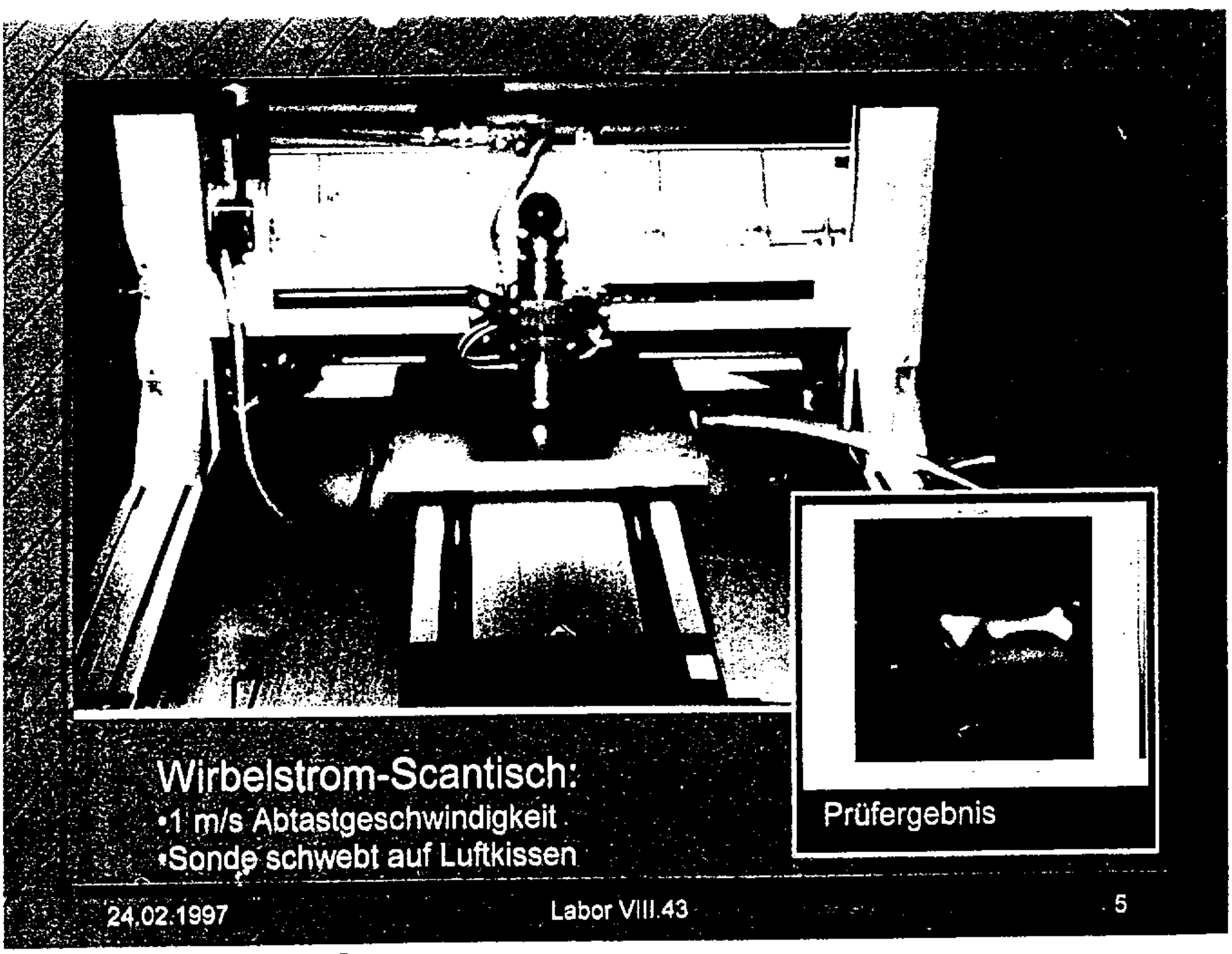

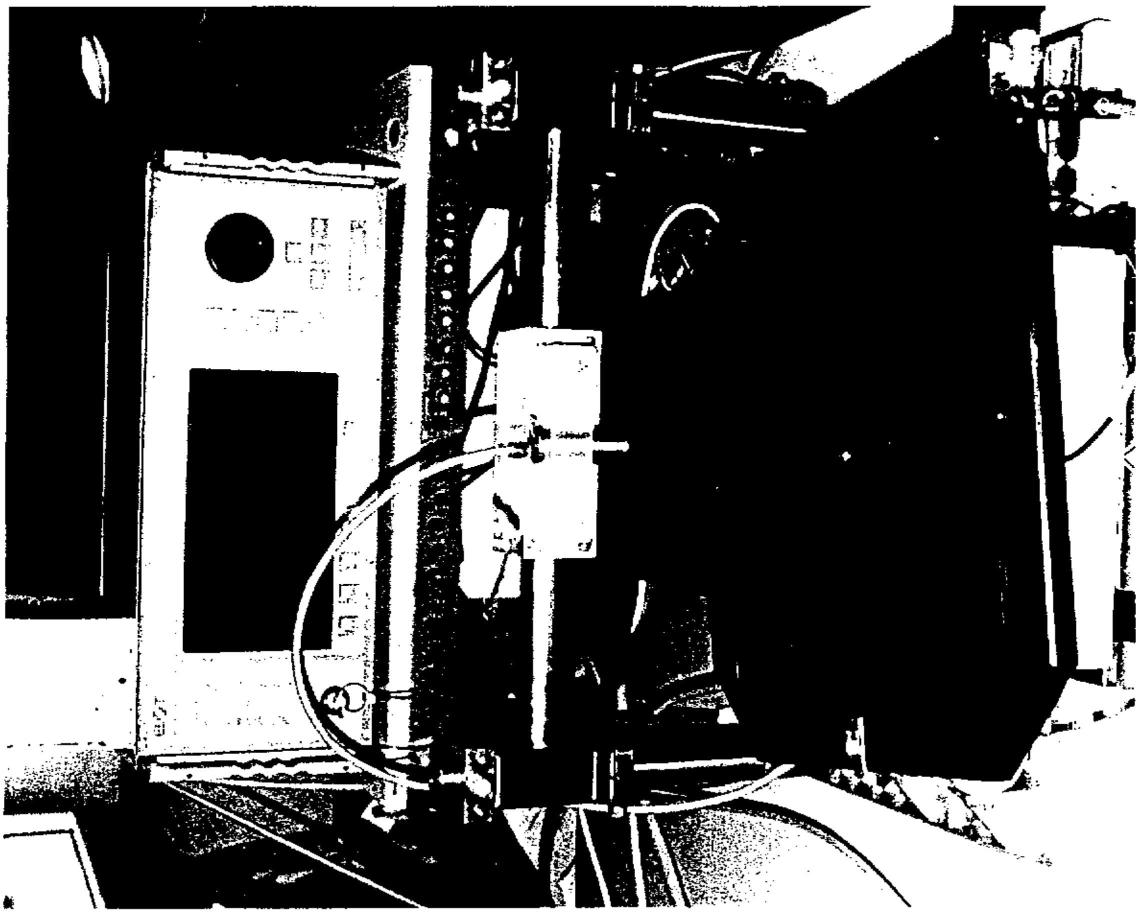

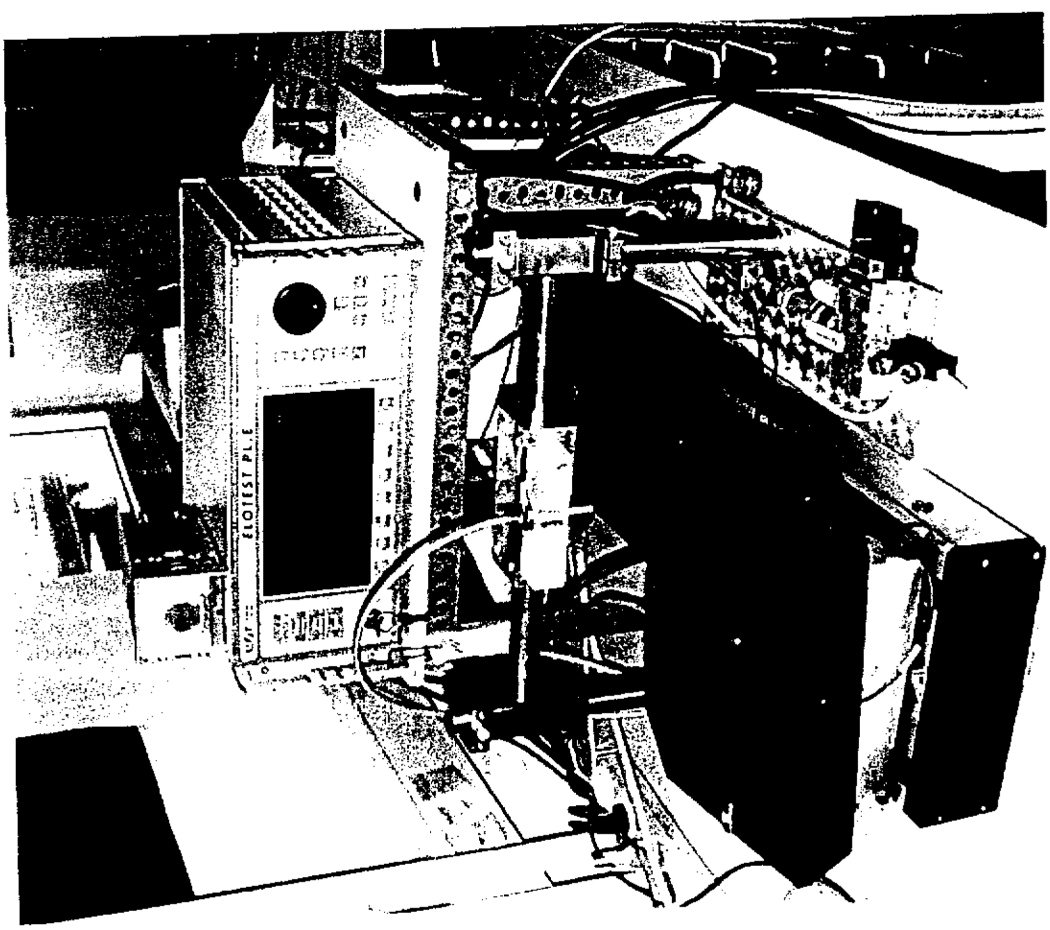
ELOTEST PL.E

Heraeus Sheet Nr. 28

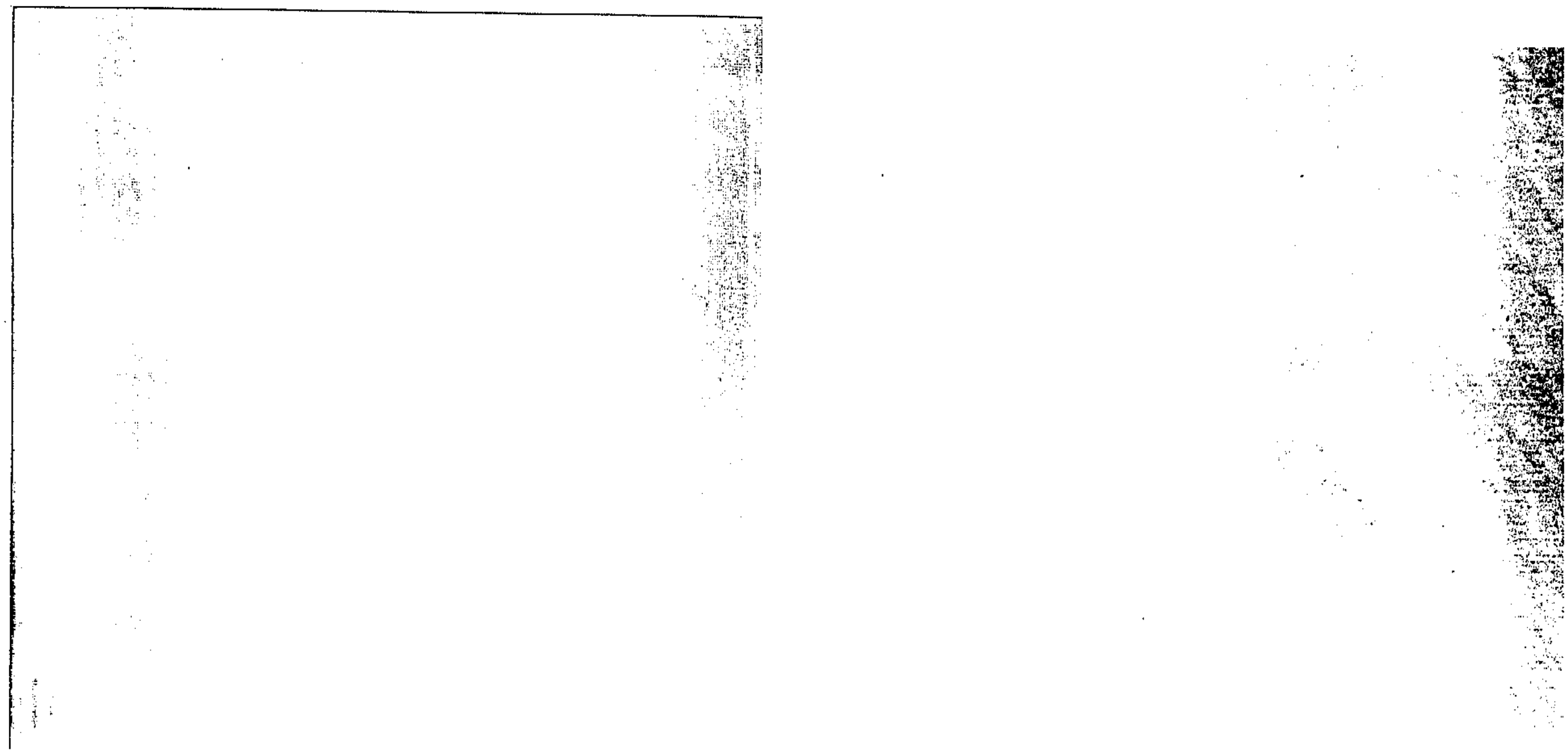

Heraeus Sheet Nr. 28

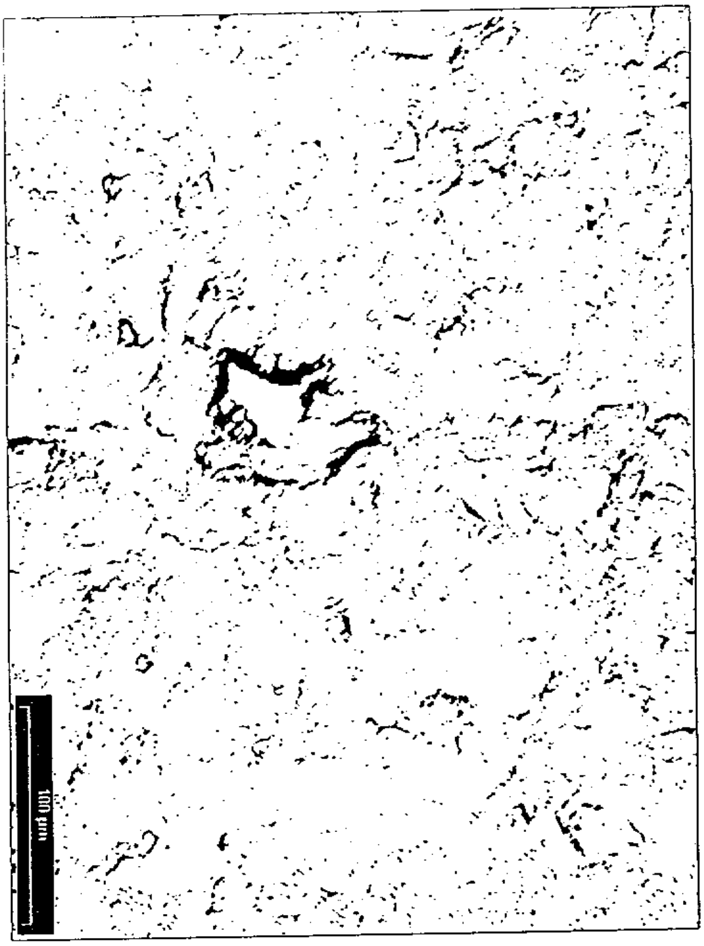

x200

Heraeus Sheet Nr.: 28

IV Status of input coupler, tuner

Input coupler:

TTF2 10 new couplers are fabricated, processing just started, they need wave guide windows

TTF3 20 new couplers are under fabrication, delivery at end of 99, no wave guide windows needed

Short comment about the input coupler workshop, April 26-27,1999:

-RF power of superstructure coupler fixed to 1 MW (2MW, including TESLA upgrade), fixed coupling

-understanding of RF processing: desorption of gases by low energy electron impact

-lambda/2 coax window operated up to 1 MW

- input coupler workshop November 99

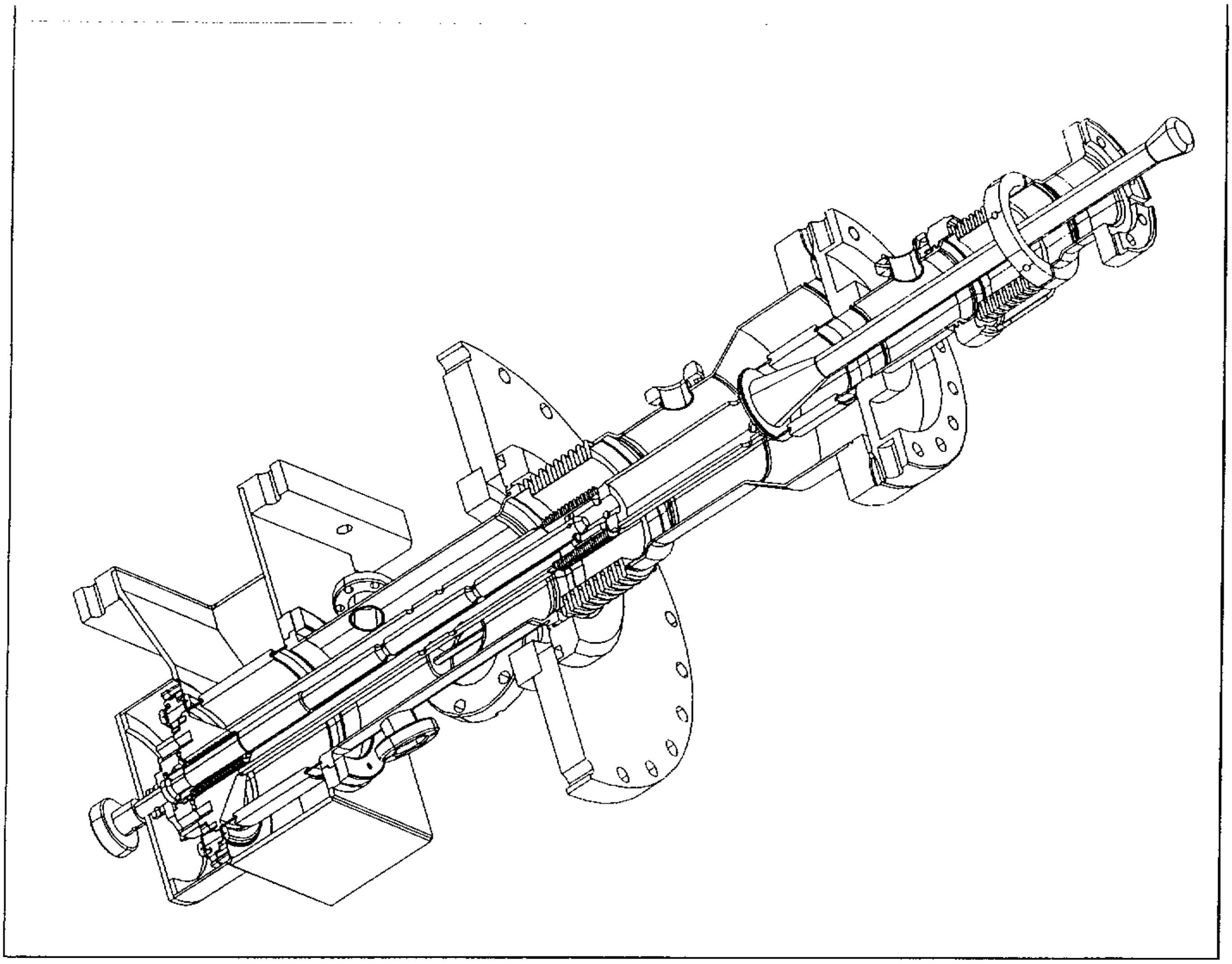

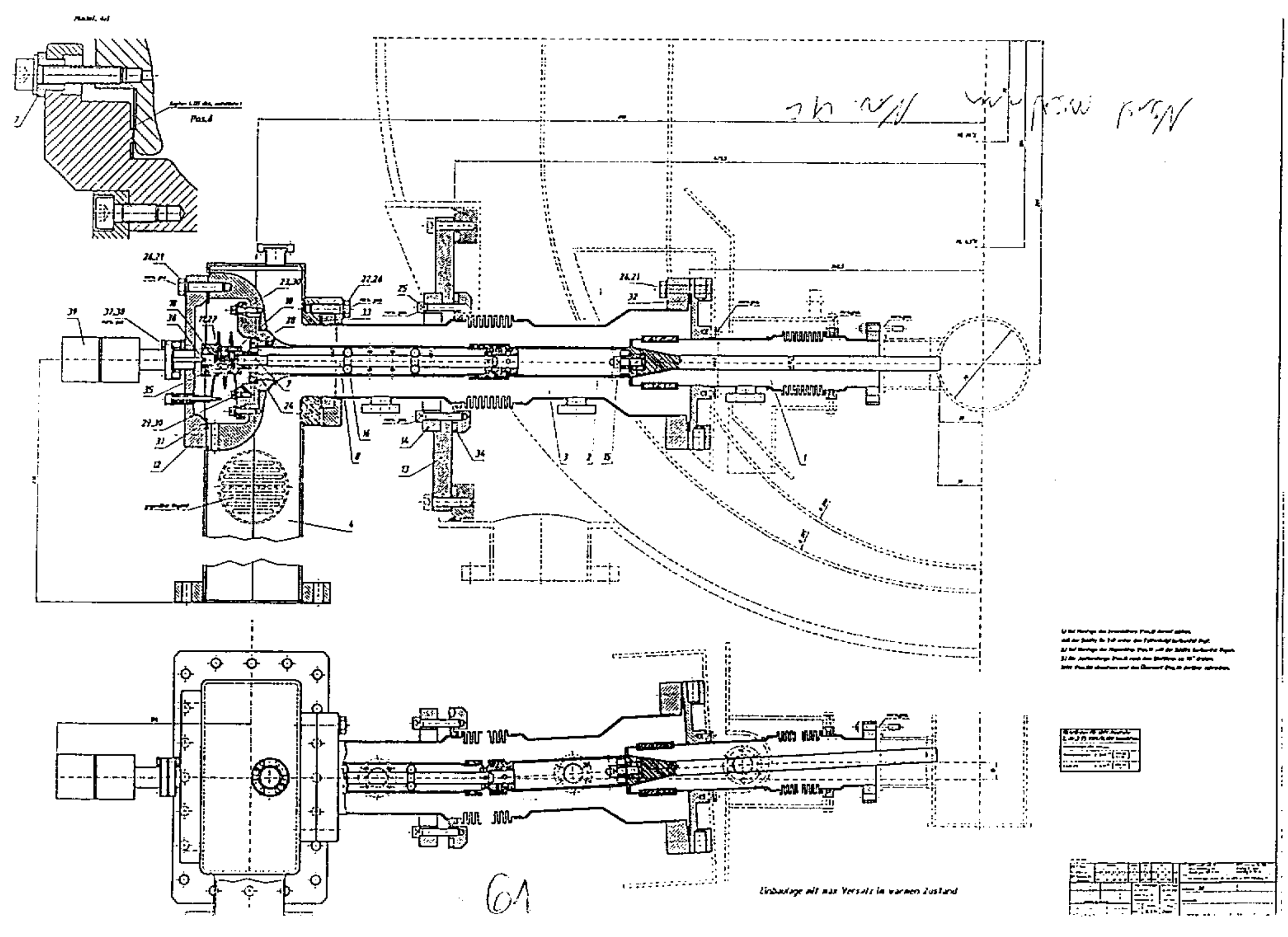

61

Wave guide windows:

20 new windows are under fabrication, delivery in October 99

Tuner:

10 new tuner & drive electronics are under fabrication, delivery in autumn 99

HOM couplers:

the 24 new 9-cell cavities as well as superstructure cavities will be equipped with welded couplers, HOM couplers belong to the cavity fabrication contract

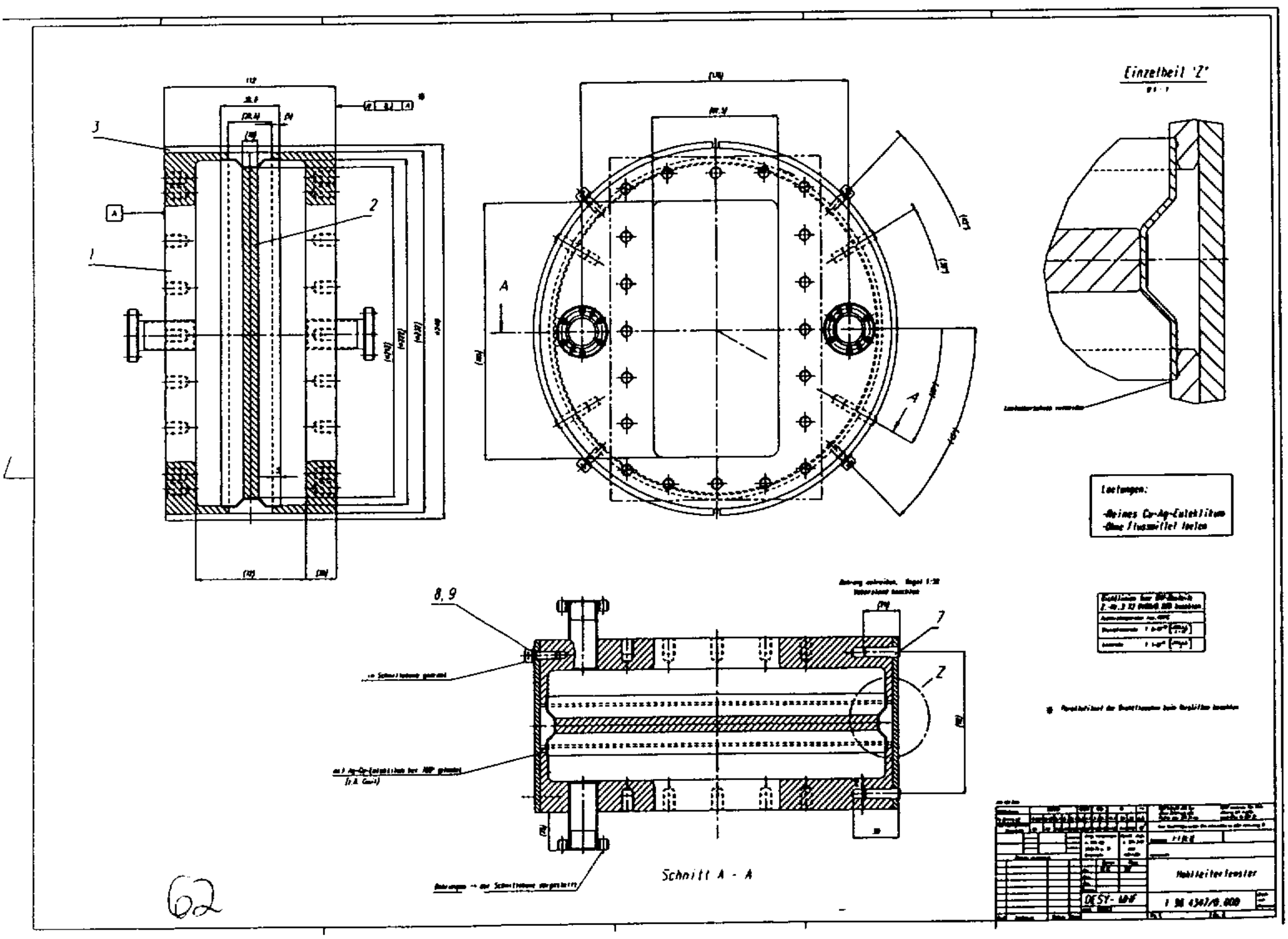

Summary

- <Eacc> of vertical cavity tests approaches the TESLA demand of 25 MV/m
- Quenching of some cavities around Eacc = 20 MV/m needs further investigation
- There are enough cavities available for completion of the next two module 1* and module 4. Average accelerating gradient is expected to be 25 MV/m for one module, slightly below for the other one
- 24 new 9-cells cavities will be fabricated until summer 2000
- Amongst the auxiliary components, the wave guide windows are critical in respect to the time schedule

64

Nb PROTOTYPE OF THE SUPERSTRUCTURE

N. Baboi, R. Bandelmann, H. Chen, B. Dwersteg, M. Ferrario, H. Kaiser, G. Kreps, M. Liepe, C. Martens, A. Matheisen, W.-D. Möller, C. Pagani, H.-B. Peters, E. Plawski, D. Proch, V. Puntus, P. Schmüser, J. Sekutowicz, W. Singer, G. Weichert, A. Zavadsev

I Introduction

Why ?

The hope is that the proposed superstructure will increase:

- number of cells fed by one input coupler (impact on costs),
- the effective gradient in both linacs (impact on performance).

What ?

The aim is to build Nb prototype of the superstructure made of four 7-cell cavities and to test it with the beam in

January-February 2001.

How ?

To minimize the effort we would like :

- to use many of the existing components,
- to make only minor changes in the infrastructure and in the cryostat.

II Components

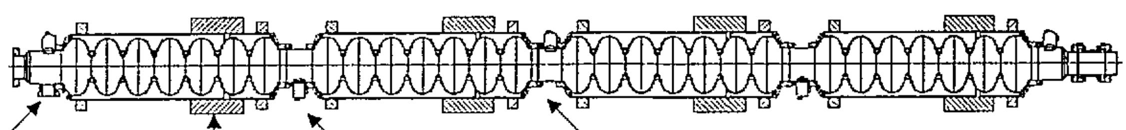

-in this prototype all sub-units (7-cell cavities) are connected by a superconducting junctions (proposed by A. Matheisen) .

- Cavities
  - mid cells and stiffening rings are of the same shape as for TTF cavities,
  - end cells have modified shape to compensate for the bigger diameter of the beam tube.

There will be two types of cavities :

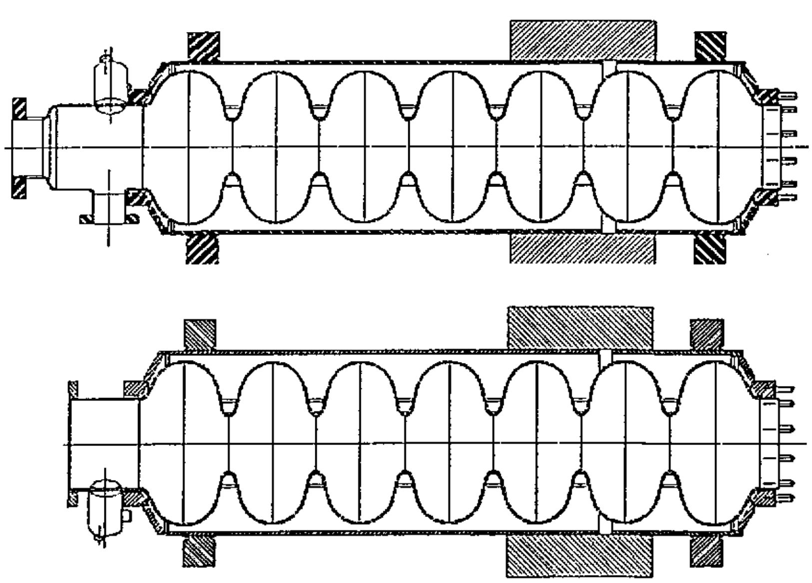

We will order: 2 cavities with the port for input coupler (type I) and 4 of type II.

- Input coupler
  - the superstructure will be fed by coaxial coupler of the DESY TTF III type,
  - the coupler will be placed 45 mm apart from the end cell (axial position), the radial position is changed because new beam tube has bigger radius by 18 mm.
  - penetration depth of the antenna tip for Qext=$2\cdot10^6$ is 6 mm as it is for 9-cell TTF cavities.
  - the only modification is new shape of the flange used for assembly in the cryostat (C. Martens)

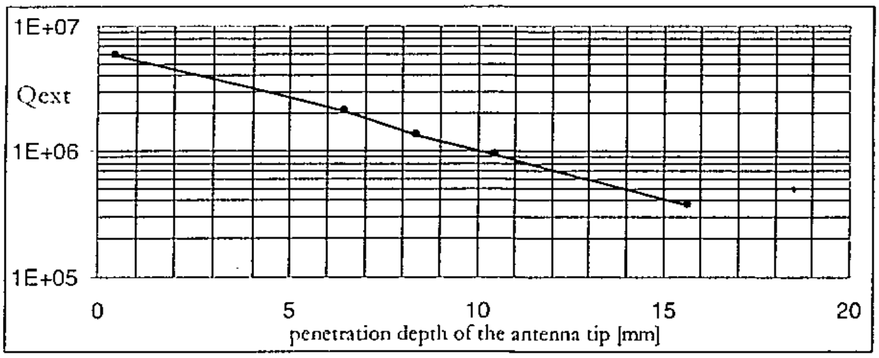

In general the input coupler stays unchanged !!!

C. Martens

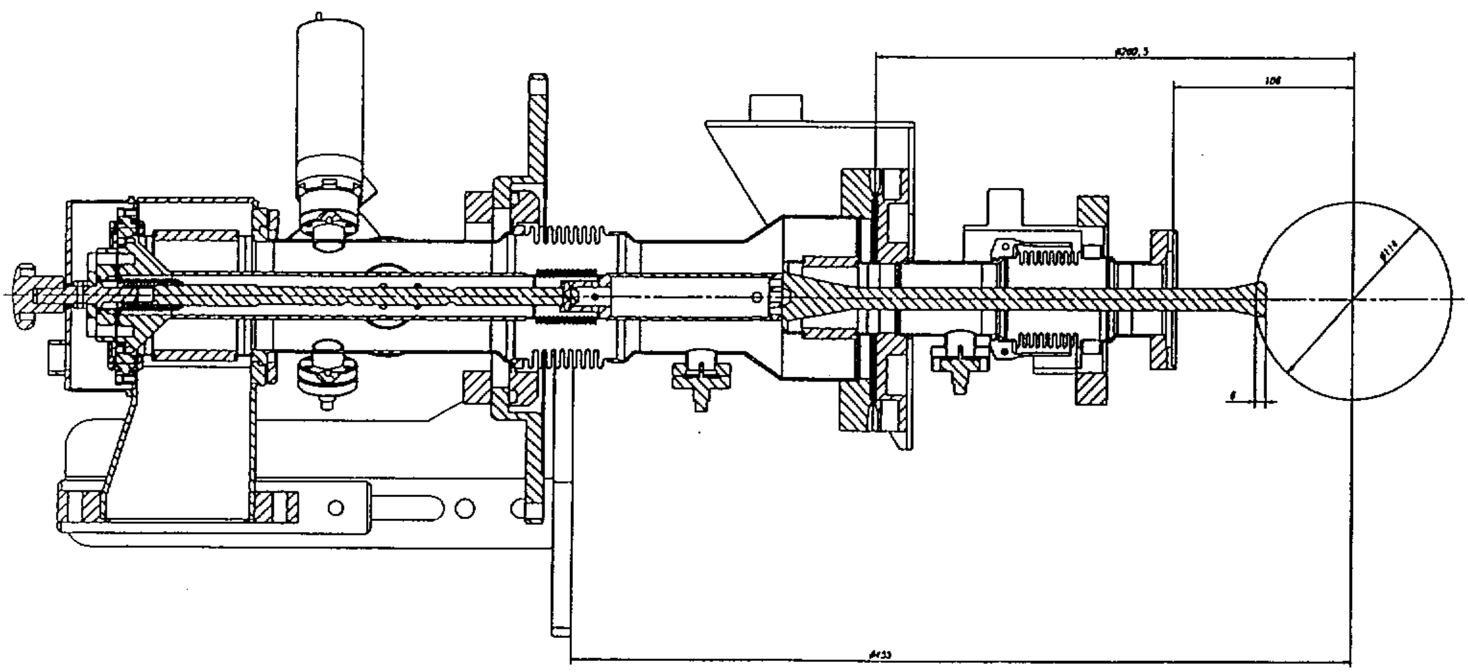

- HOM couplers

First computation of the emittance growth showed that high impedance transversal modes should be damped to the level of $Qext \leq 10^5$. The resulting impedance limit for transversal modes is:

$$Z = (r/q)_{max} \cdot Qext = 17.5\ \Omega/cm^2 \cdot 10^5 \leq 1750\ k\Omega/cm^2$$

The peak power limit for the monopole modes is:

$$Z = (R/Q)_{max} \cdot Qext = 300\ \Omega \cdot 3 \cdot 10^4 \leq 9000\ k\Omega$$

We are still working on the HOM coupler (delay of about 4 weeks). The reason is that part of the space between the cavities is occupied by flanges. This causes that

- HOM couplers must be based on smaller, 40 mm, coaxial line
  (less coupling requires deeper penetration of the antenna and of the loop)

- HOM couplers must be moved from the mid plane of the interconnection towards end-cell
  (antenna tip is exposed to more FM field).

The coupler we have at the moment fulfils requirements on damping, but:

- the antenna penetrates 20 mm in the beam tube,
- it may quench below 25 MV/m since RF losses on the antenna tip for this coupler are 8 times bigger than for 9-cell TTF cavities.

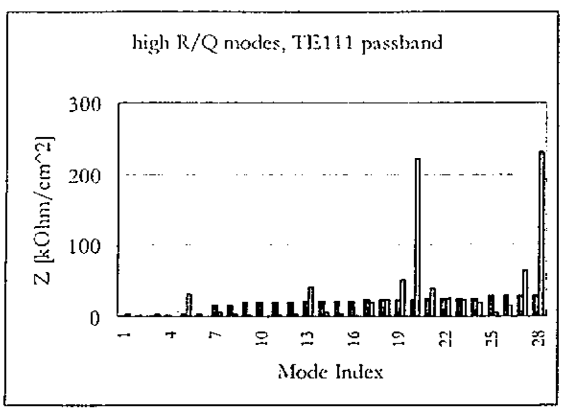

Limit:
↑ 1750 kΩ/cm² ↑

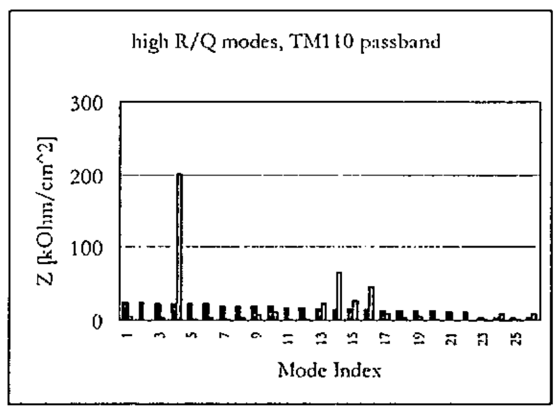

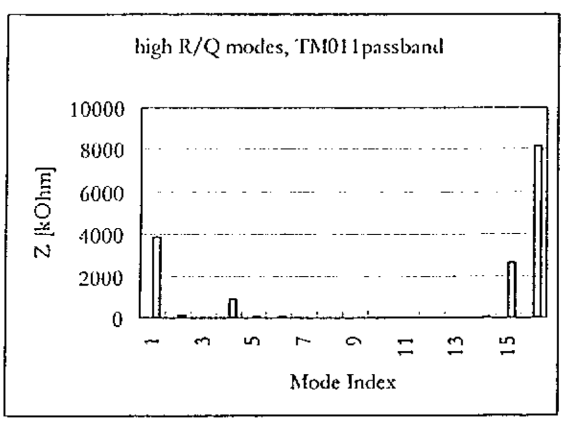

Limit:
← 9000 kΩ

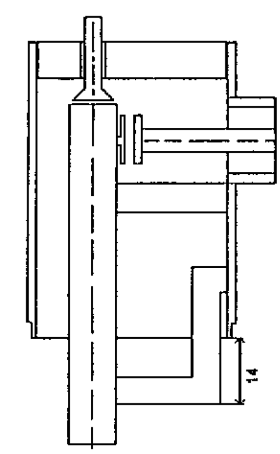

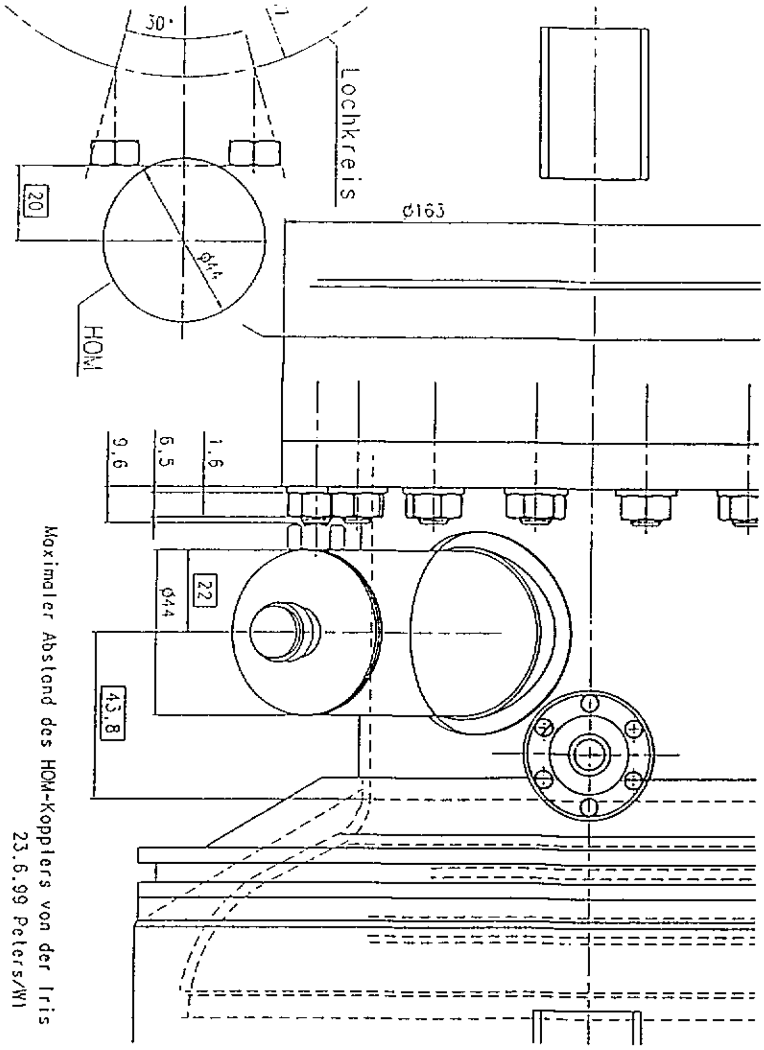

- tuner (critical component of the superstructure, new design H. Kaiser)

- new design of the tuner is unavoidable,
- the space needed for the TTF tuner is $\lambda/2$=115 mm. It is the whole space available between two cavities in the superstructure.

Principle of Tuner:

- cavity fixed at both ends to He-tank
- Length of He-tank varied with tuner.
  → cavity length changes also

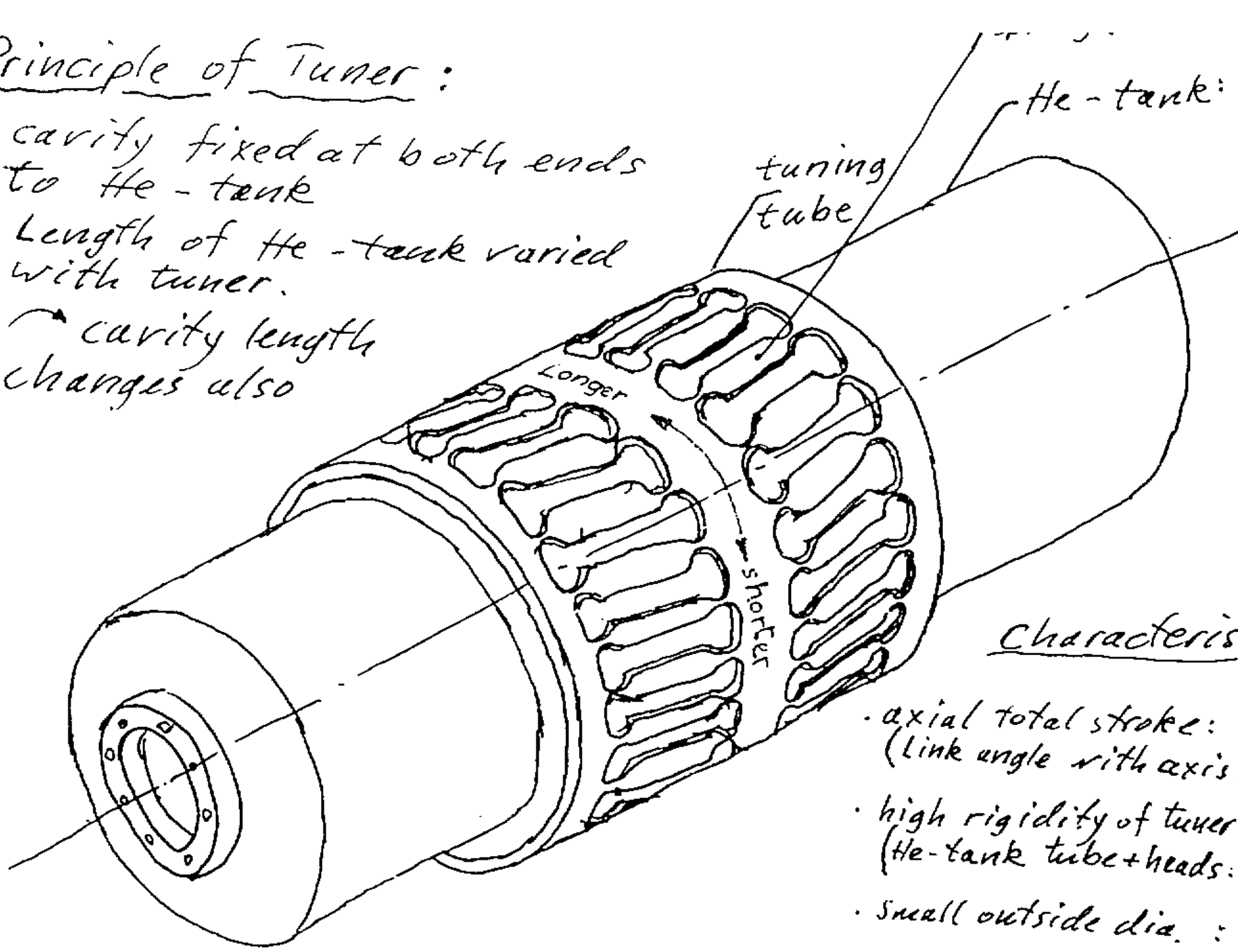

Characteristics:

- axial total stroke: 1.7 mm (link angle with axis: 8°...12°)
- high rigidity of tuner: 2 μm/kN (He-tank tube+heads: 8 μm/kN)
- Small outside dia. : 290 mm
- length: 350 mm

Kai. 7.7.99

- superconducting flange connection for the prototype (A. Matheisen).

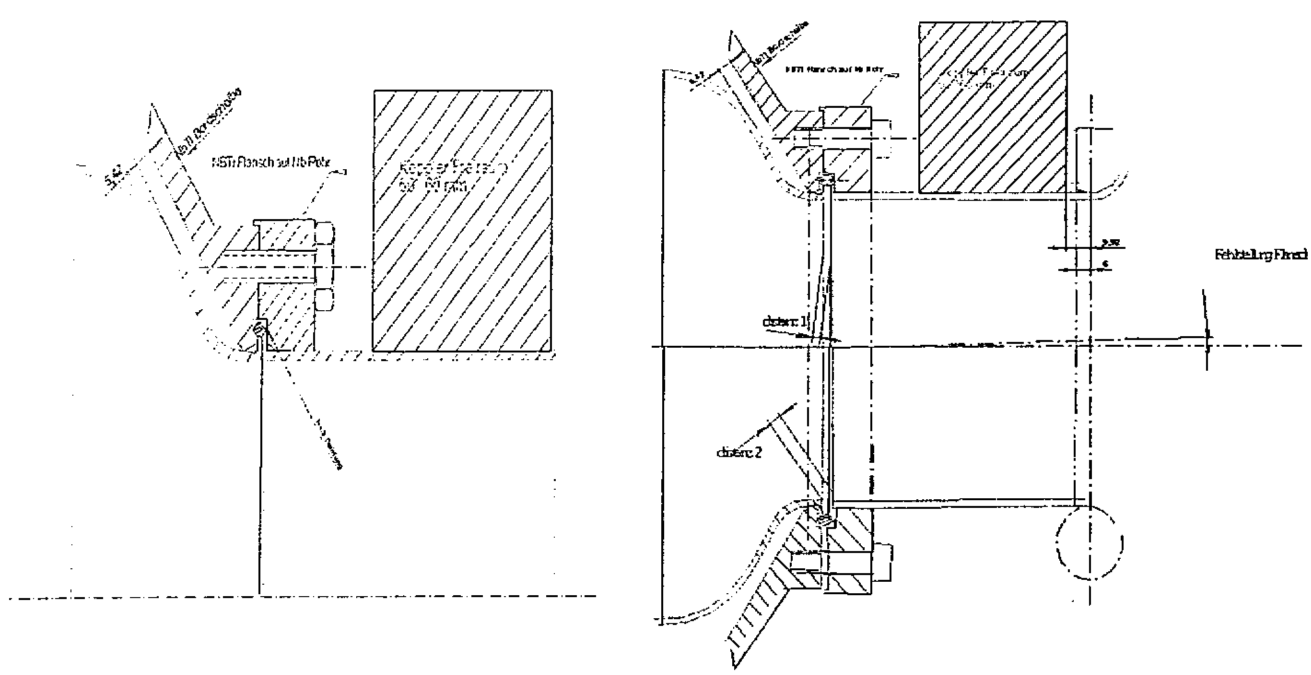

- flanges are made of NbTi. The seal is made of hard Nb
- estimated cw losses of the junction at 25 MV/m are 0.5 W (cavity 94 W, $Q=5\cdot10^9$).

III High Q test of 7-cell sub-units

- cavities will be tested in the vertical cryostat used for the standard 9-cell cavities,
- for the Q vs. E measurements field profile must be balanced as for the operation. Two special end-cups have been constructed to keep field equal in all cells (R. Bandelmann).

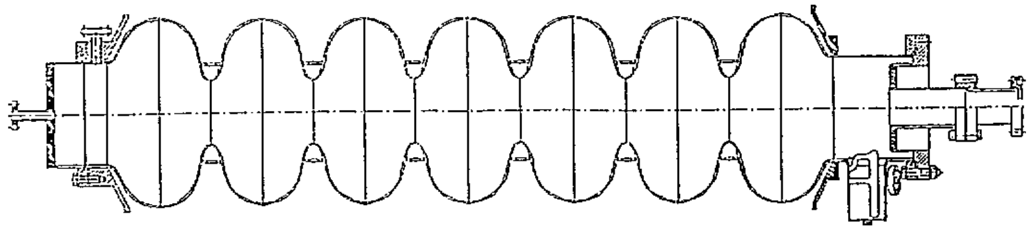

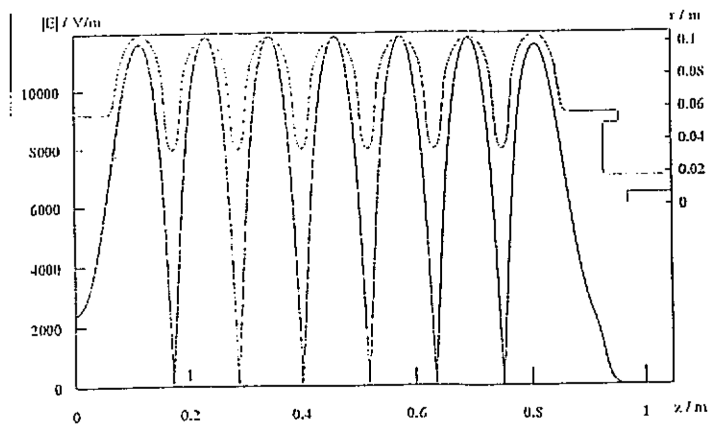

IV Cryomodule

The prototype will be assembled in the spare "old type" cryomodule which should be ready in November 2000 (C. Pagani). The modification of the cryomodule and how the superstructure will be installed (support system) are under discussion (C. Pagani, H.-B. Peters).

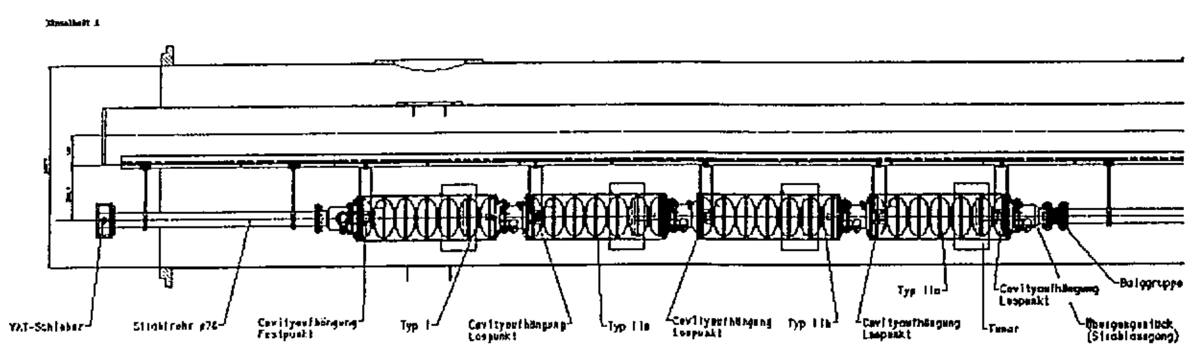

V Summary

- RF measurements on the copper model

- field flatness: all cavities have been tuned for almost 98% field flatness. After assembly and small frequency corrections the achieved field flatness was about 93 %. It can be better.

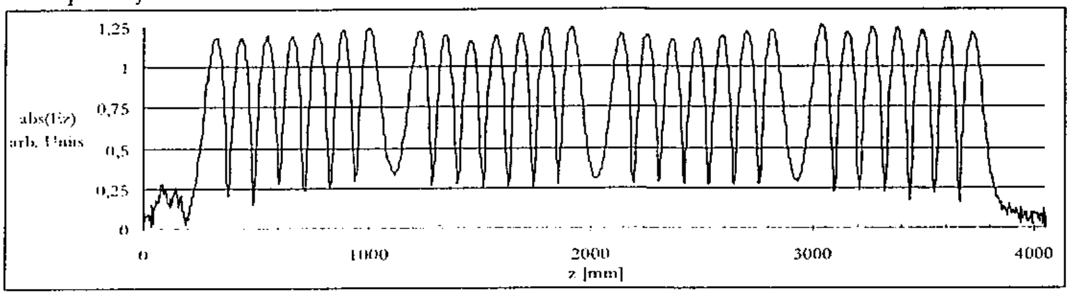

- transients: example cell #28 , computation (HOMDYN M. Ferrario) and measurements.

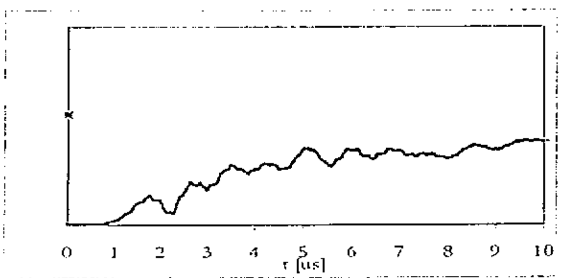

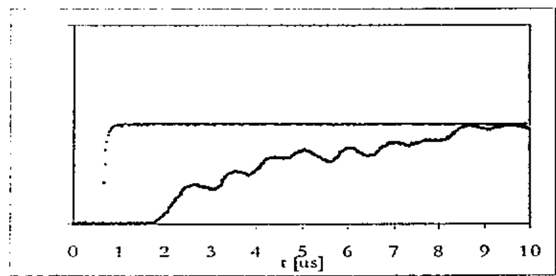

- field profile for HPP

  Example: processing of the cavity #2 (detuned by -200 kHz, C#1 by 6 kHz)

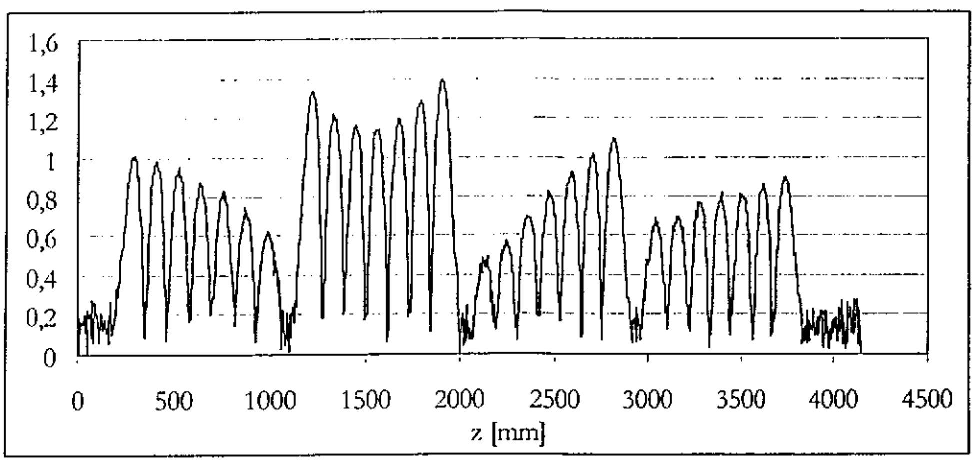

- FM coupler position has been fixed.
- HOM couplers optimization in progress.

- Time Schedule

By the end of 2000 we should install the superstructure in the TTF linac.

- 1 month for the assembly of cryomodule,
- 3 months to test 6 sub-units,
- 8 months to produce 6 sub-units, end-cups for the test,

Conclusion is that by mid/end of July we need:

- new design of HOM coupler,
- new design of the tuner and new helium vessel including conical head plates,
- technical drawings for the cavity production,
- to place order for the cavity production.

Shutdown Activities

Holger Schlarb
July 7, 1999

- Injector
- Acc.-Module 1
- Collimator Section
- Undulator
- Experimental Area 1
- Air-conditioned chamber
- Infrastructure

TESLA TEST FACILITY (HALL 3)

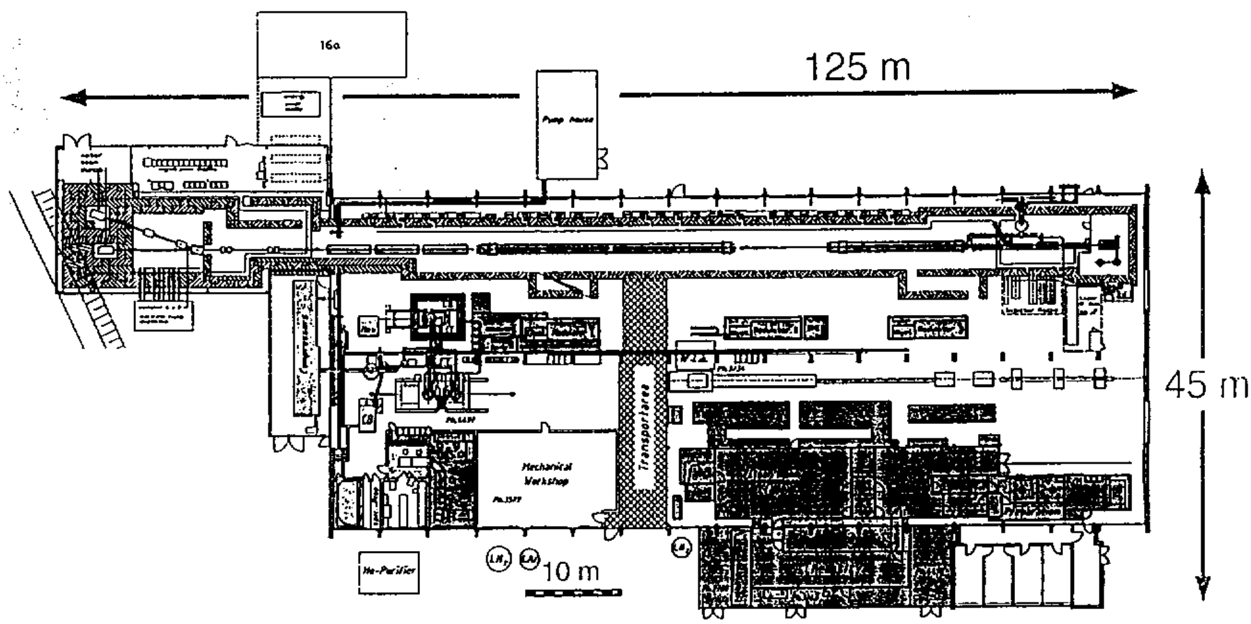

Cavity Treatment and Assembly

Cavity Testing (RF System / He Plant)

TTF Linac

73

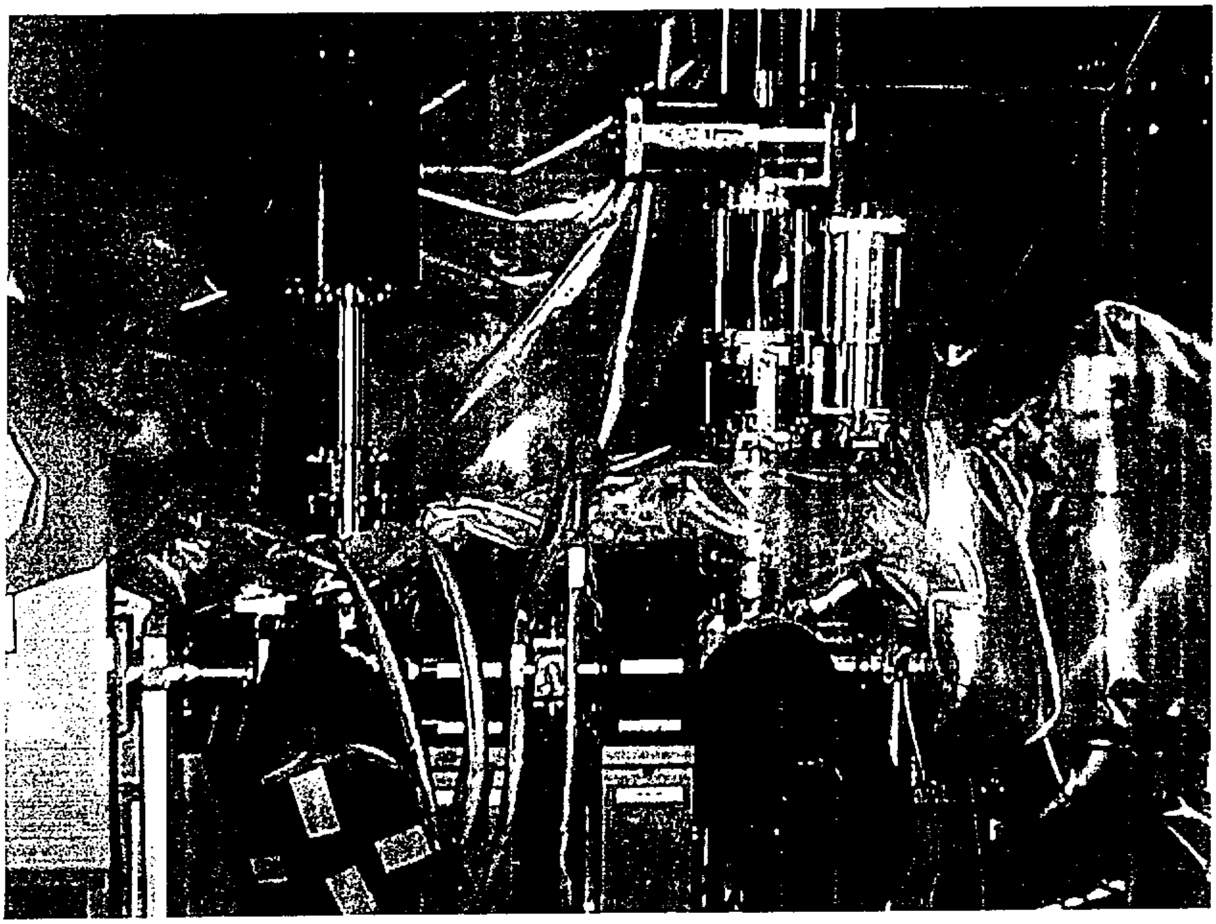

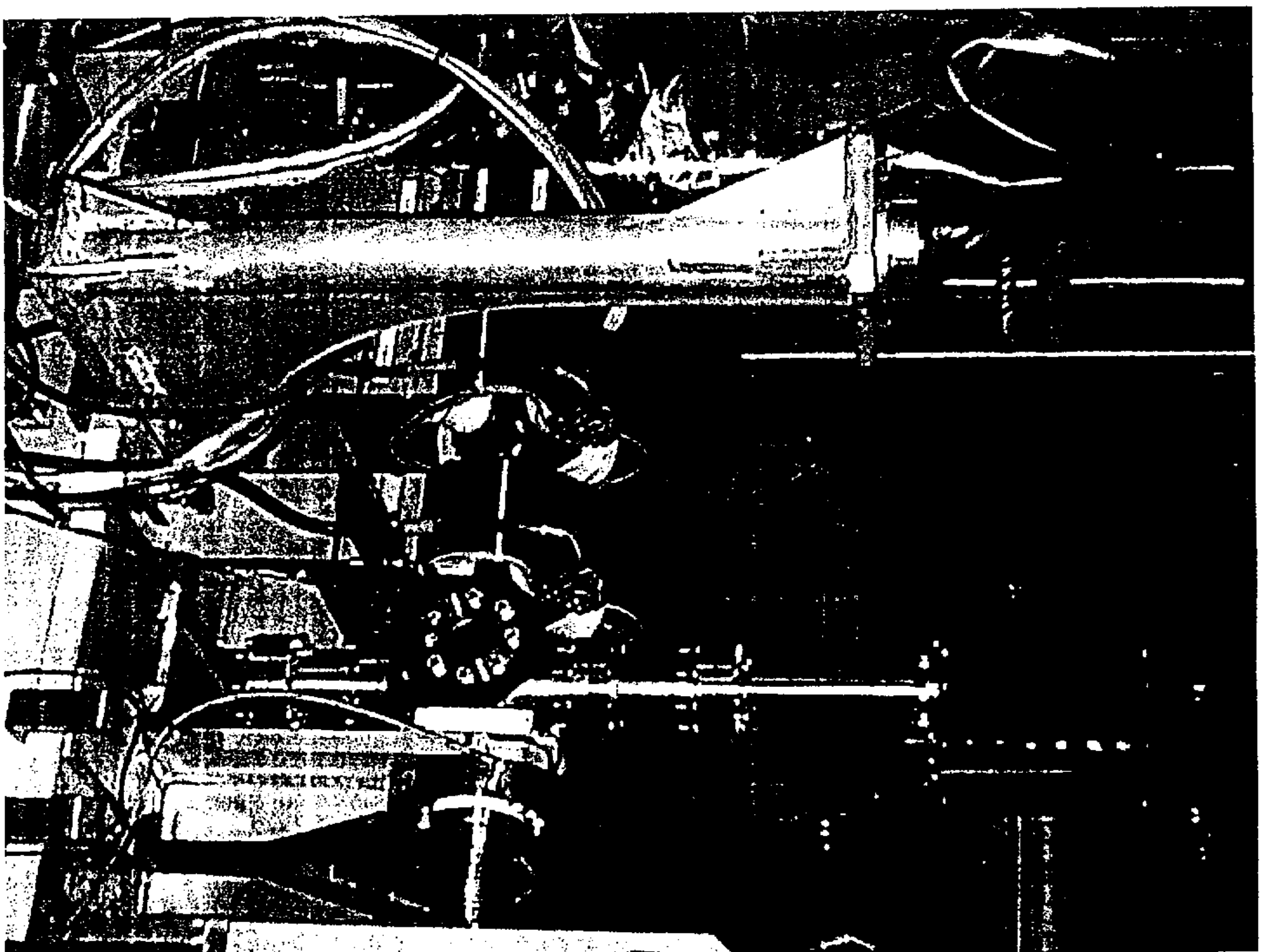

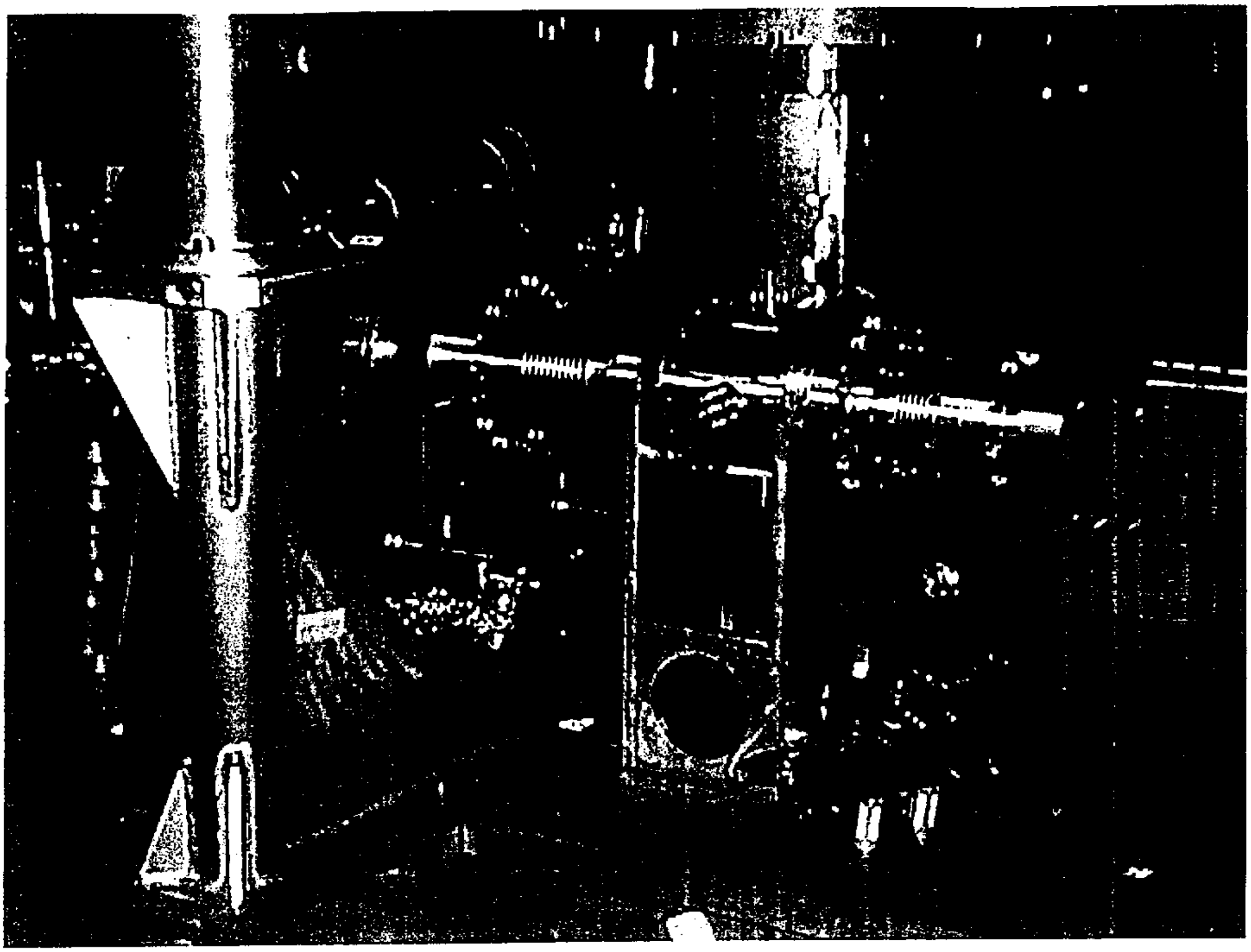

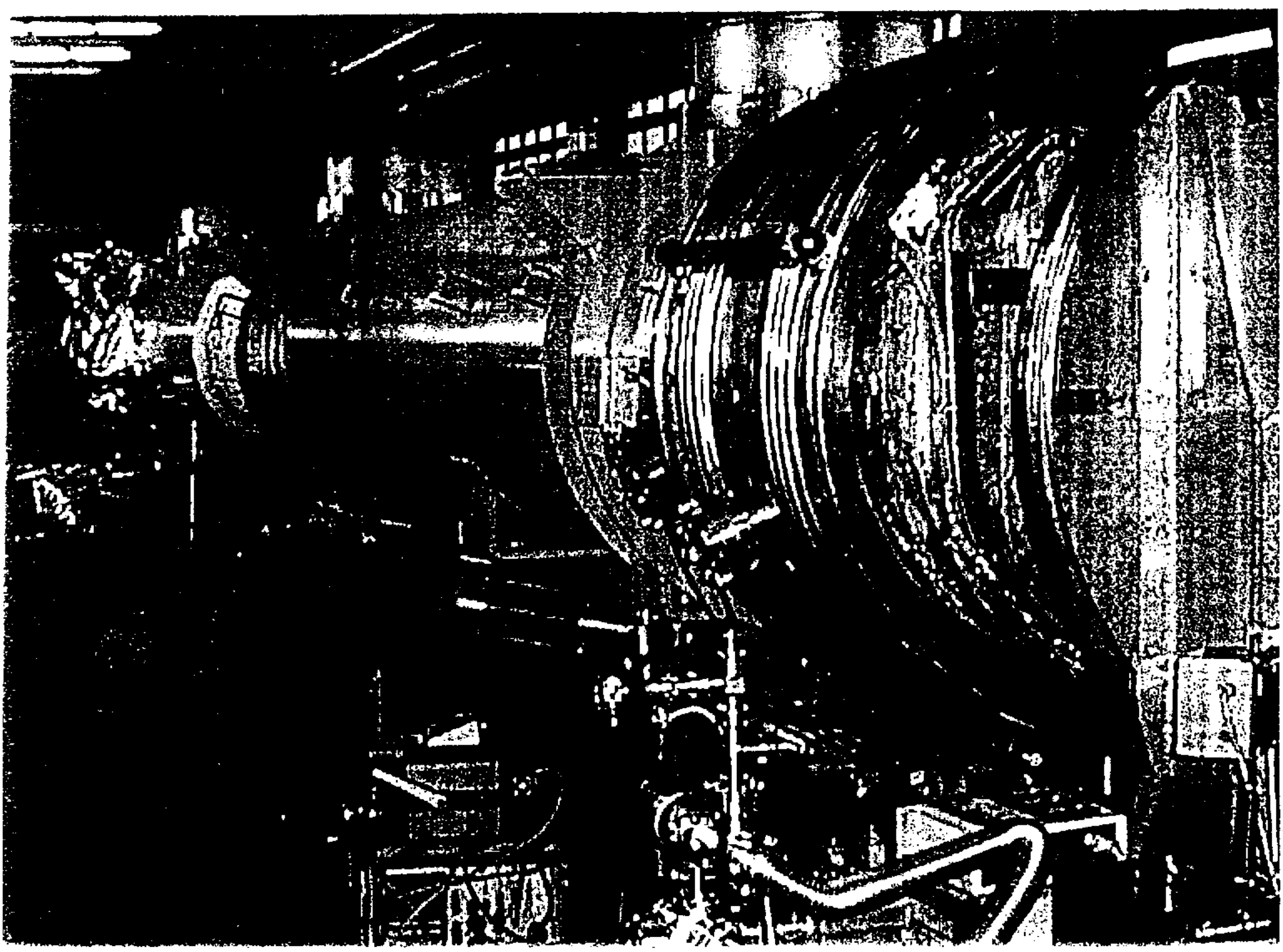

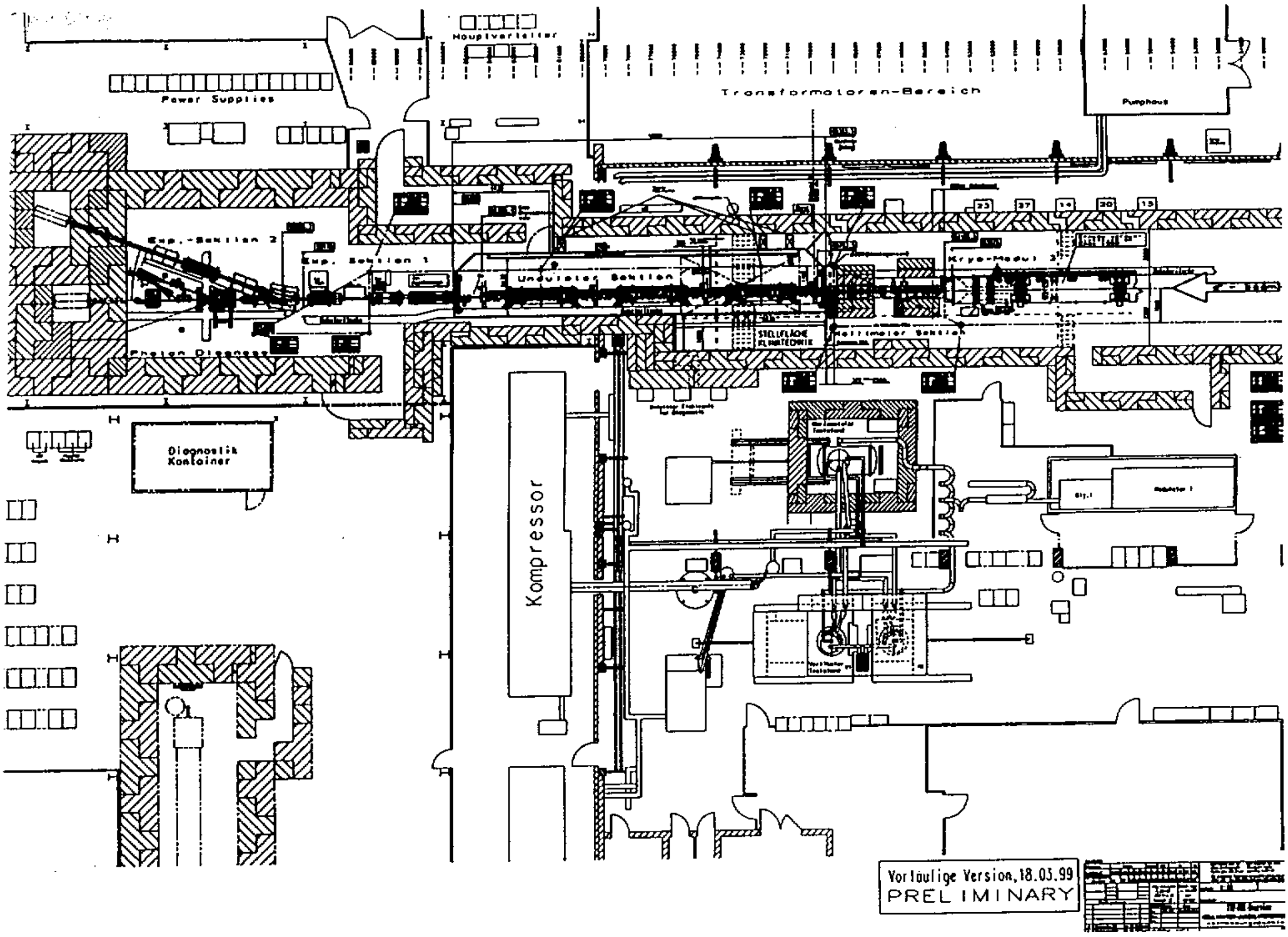
Power Supplies
Hauptverteiler
Transformatoren-Bereich
Pumphaus
Exp.-Sektion 2
Exp. Sektion 1
Undulator Sektion
Kryo-Modul
Photon Diagnose
Kollimator Sektion
Diagnostik Kontainer
Kompressor
Vorläufige Version, 18.03.99
PRELIMINARY

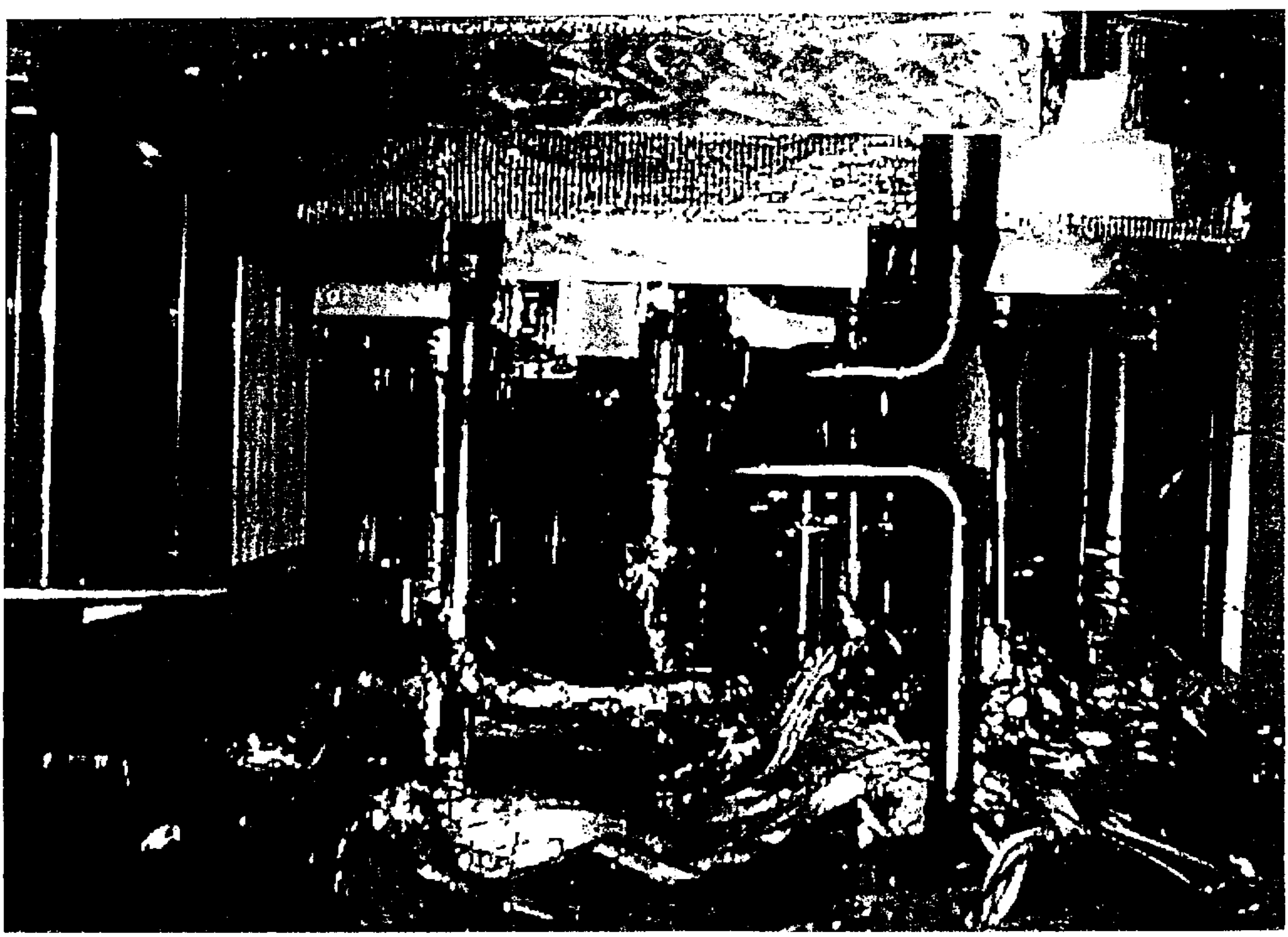

6

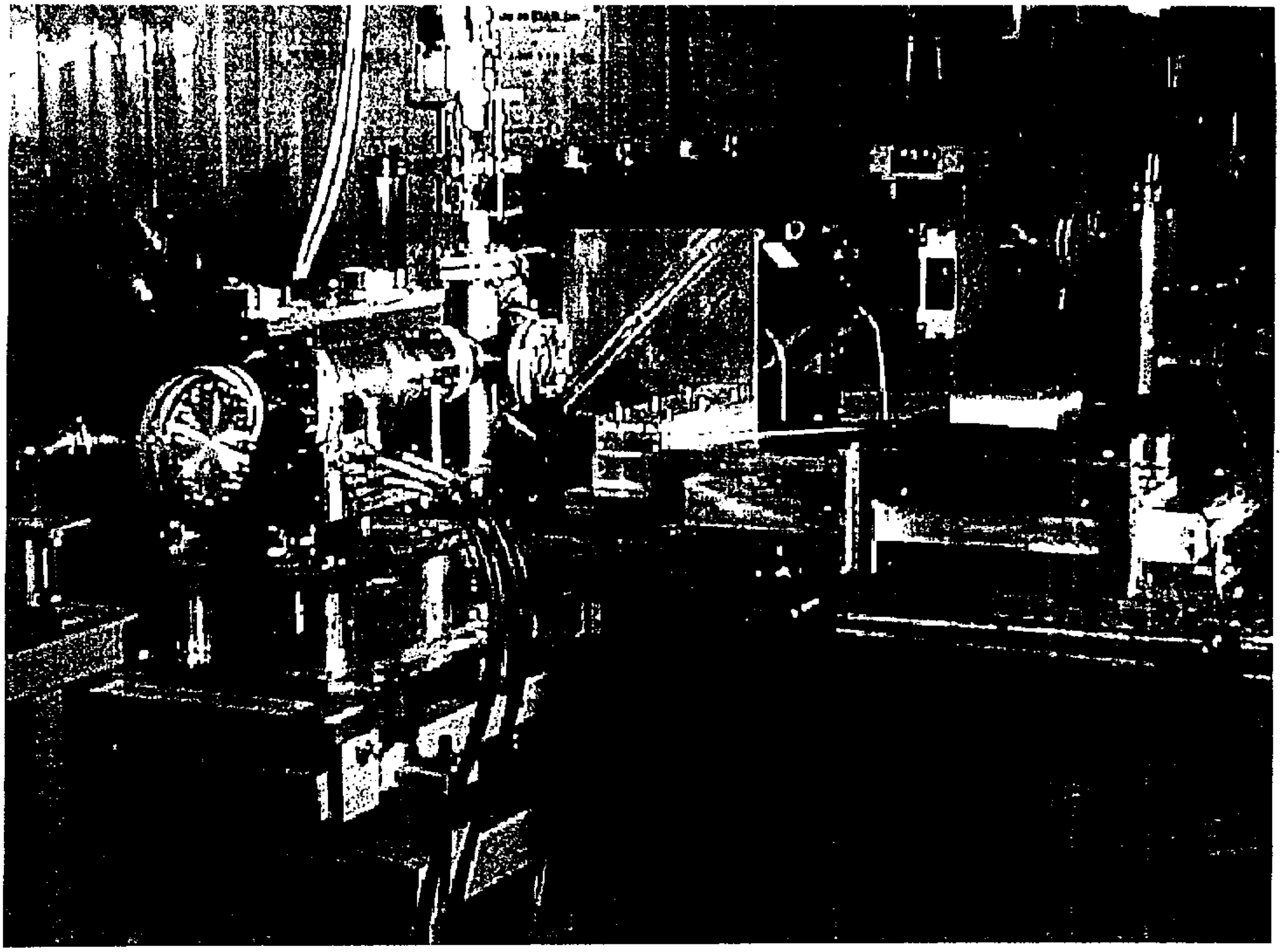

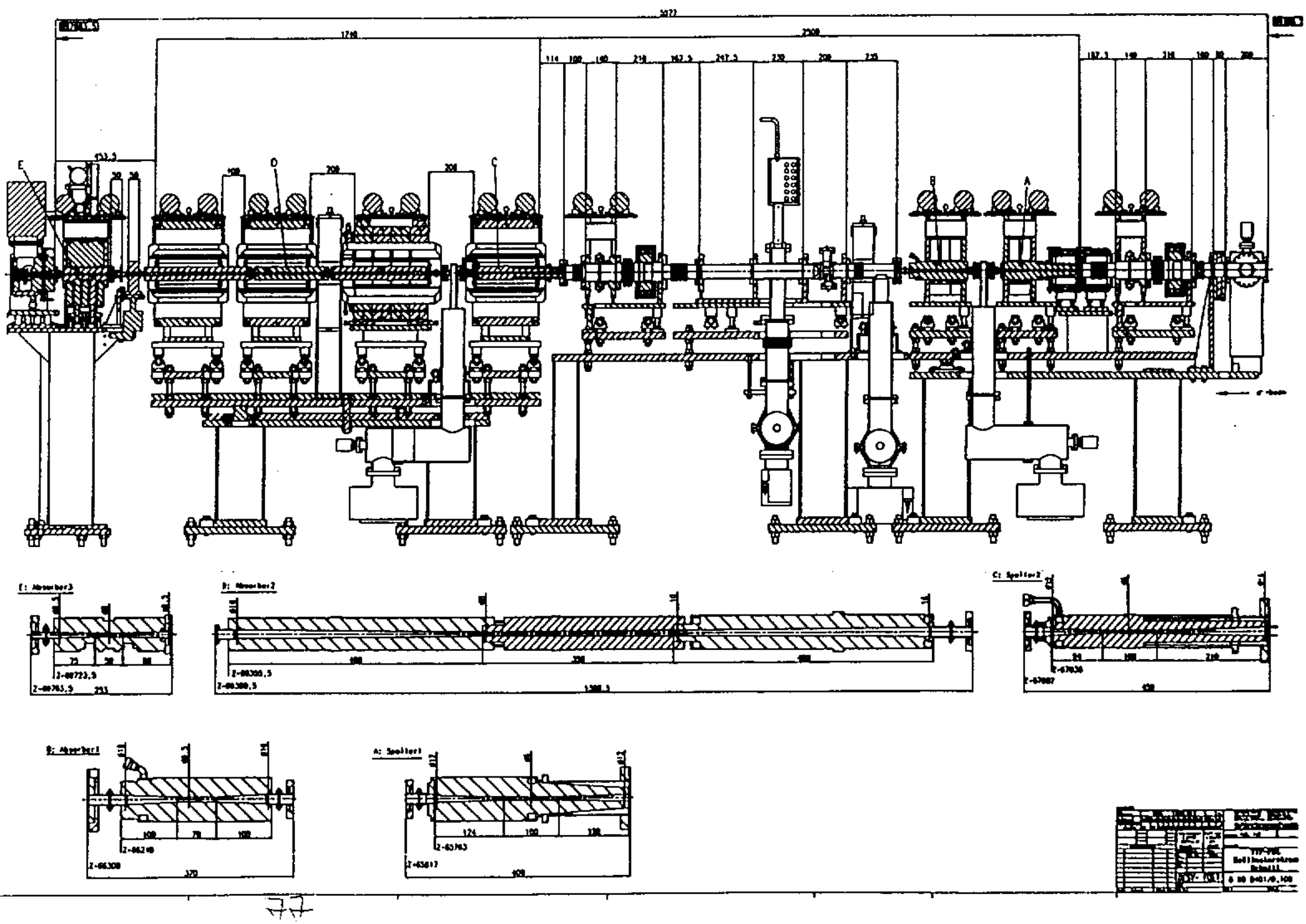
E
D
C
B
A
E: Absorber3
D: Absorber2
C: Spoiler2
B: Absorber1
A: Spoiler1

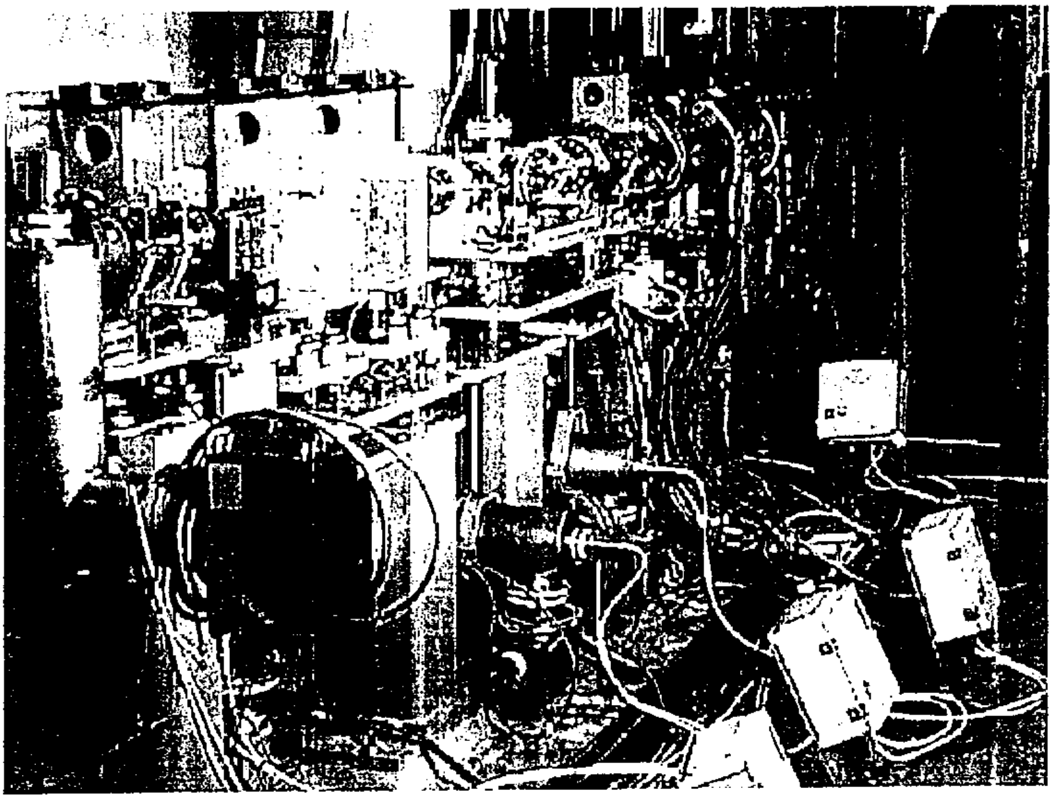

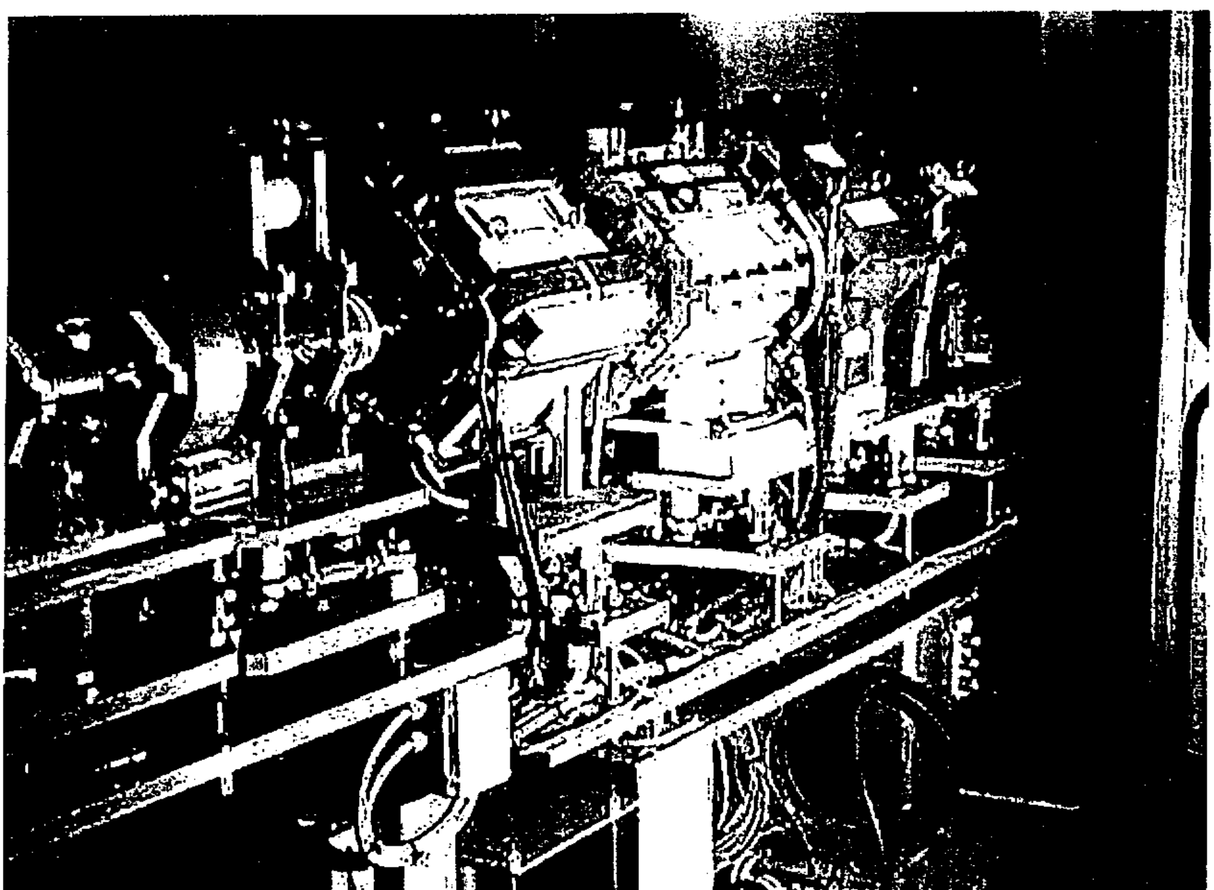

Schnitt B-B (M 1:20)

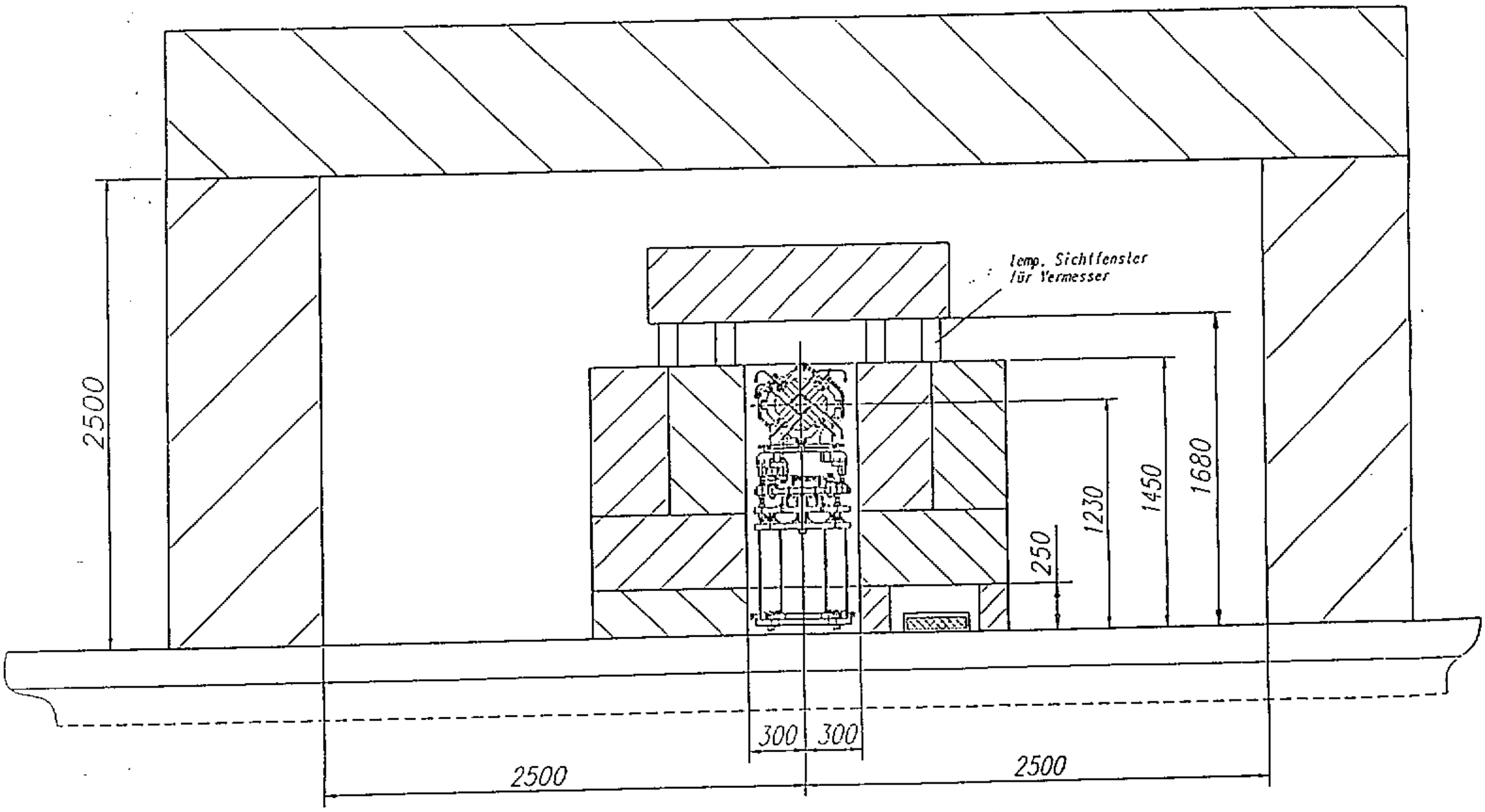

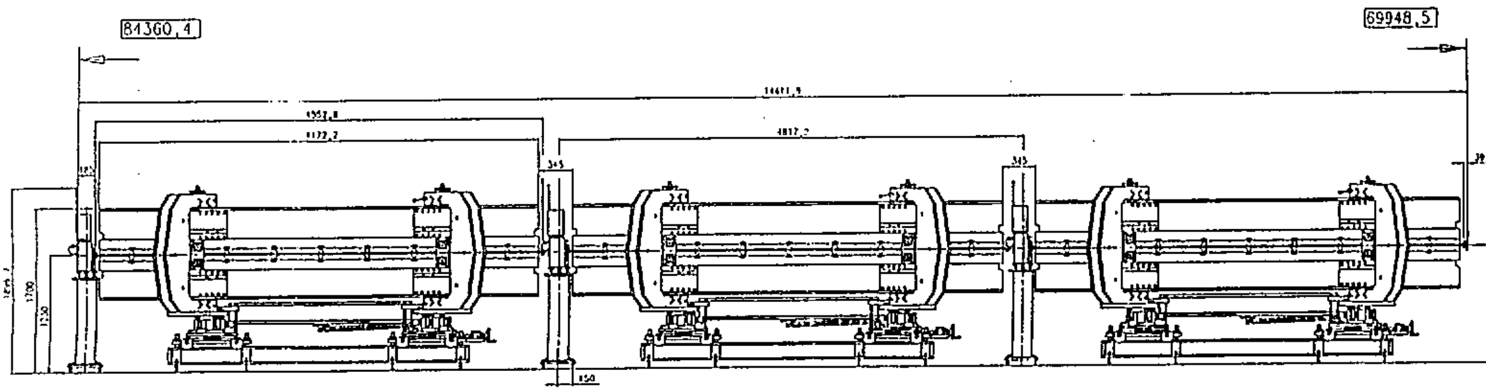

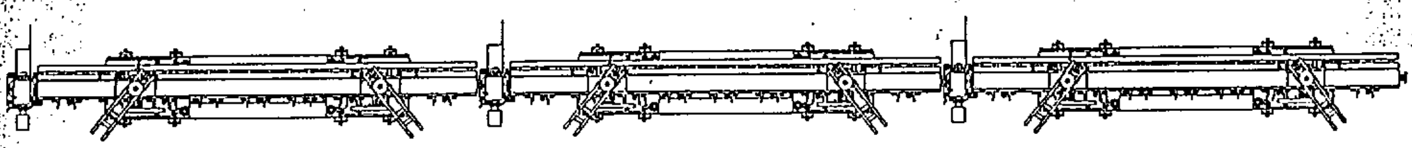

7.0	31.03.99
Revision	Date

TTF-FEL
Undulatorstreck

DESY- FDE1 | 1 98 ----/0.000

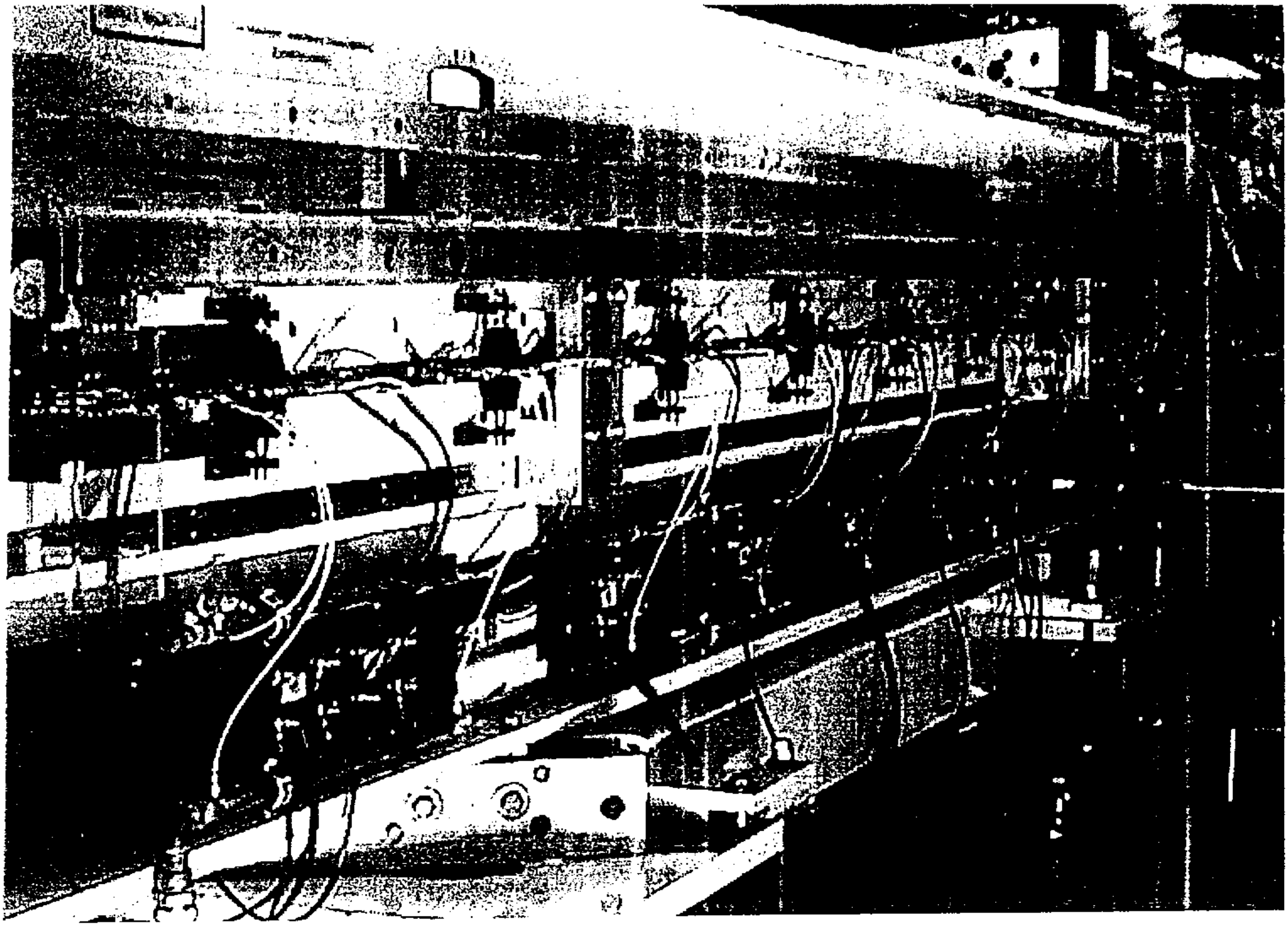

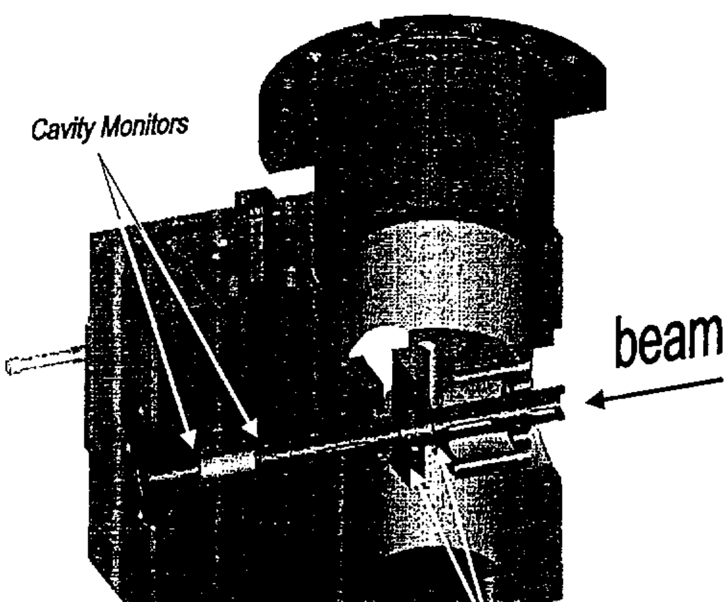
Cavity Monitors
beam
Wirescanner Slits

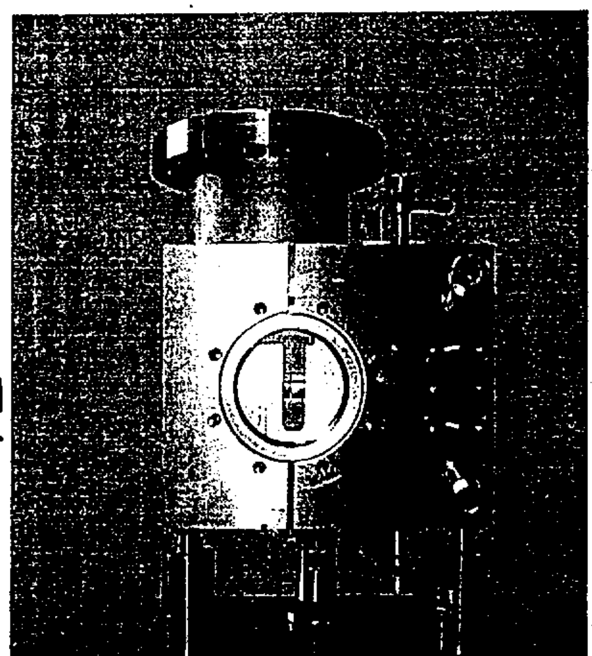

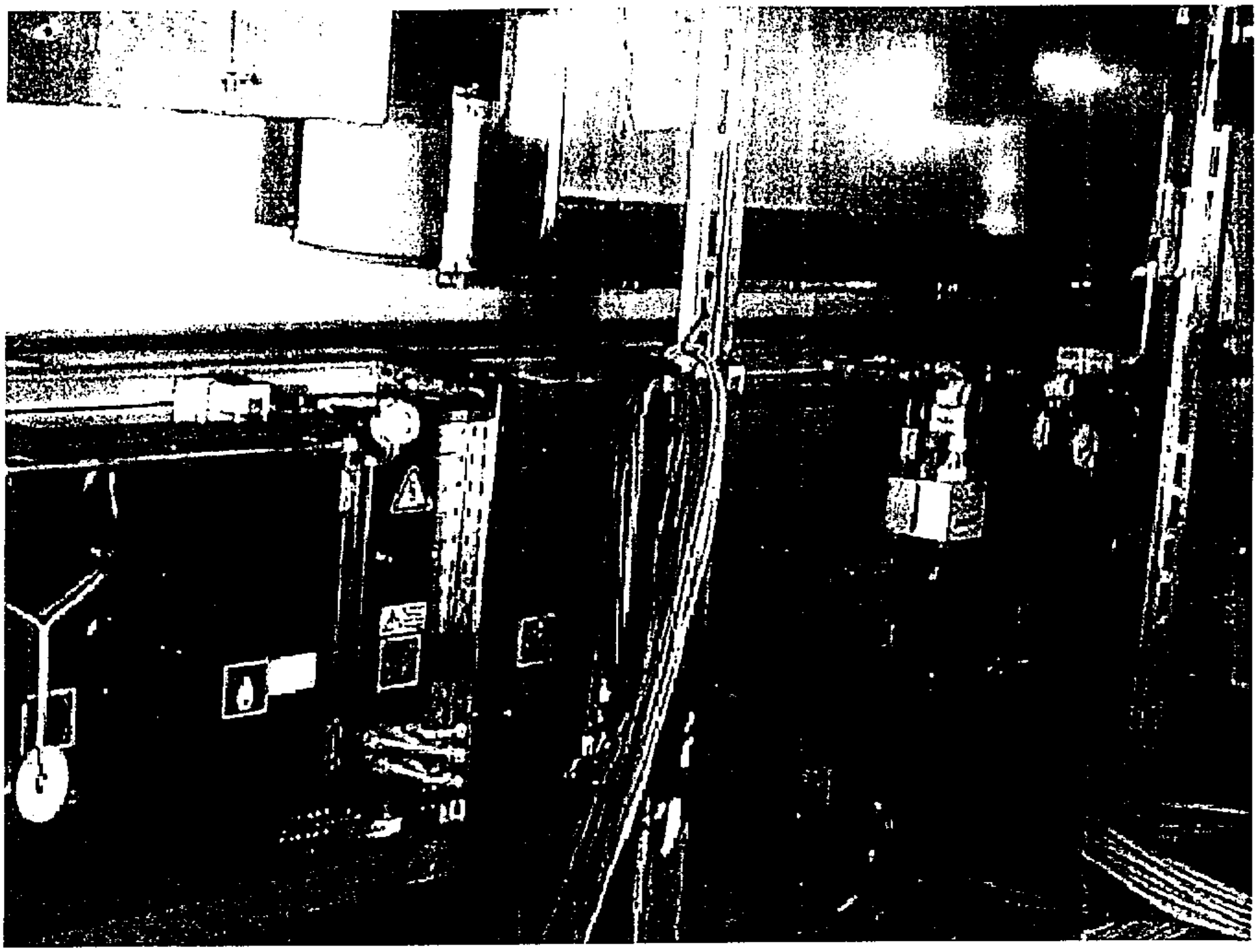

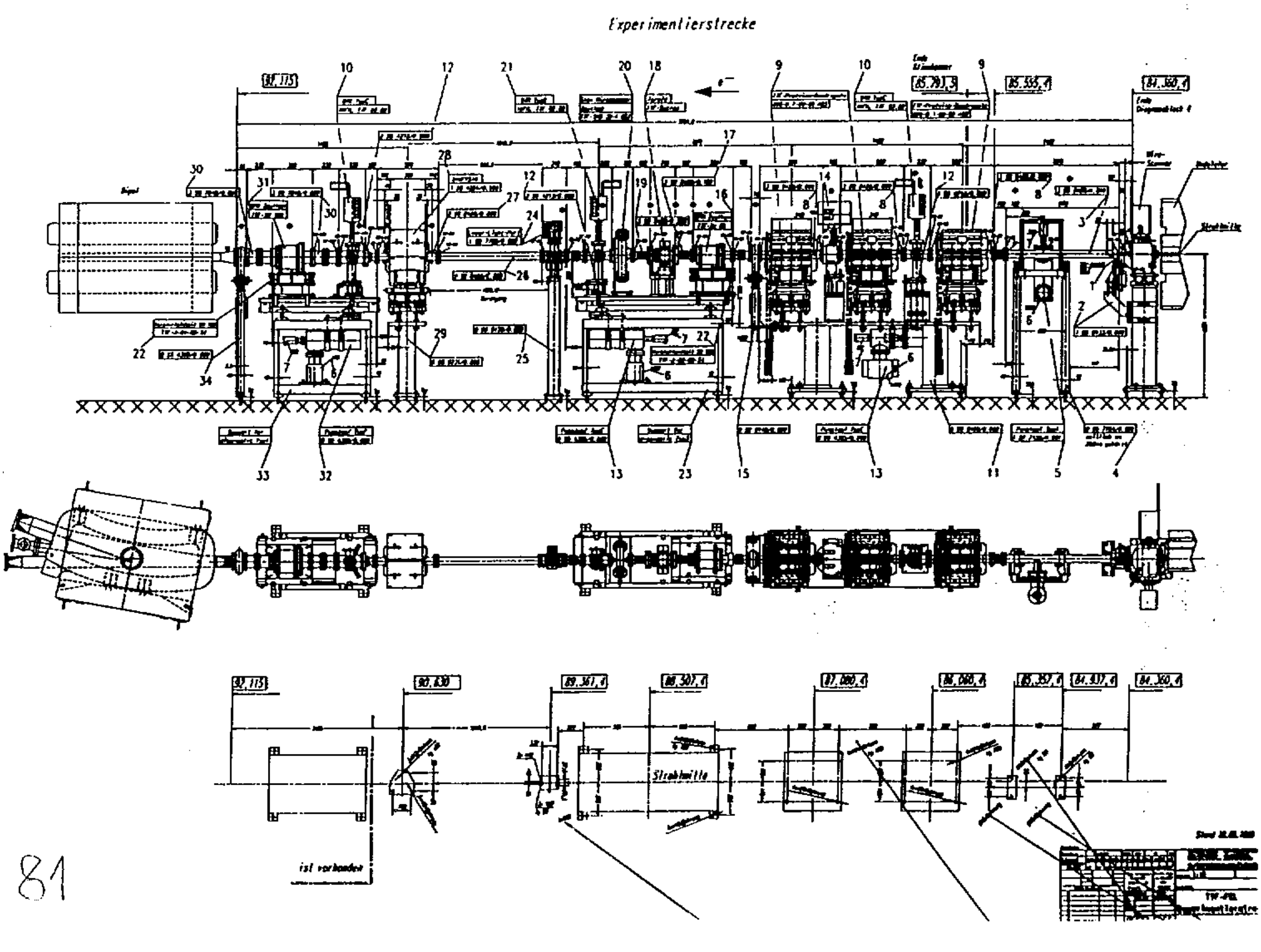
Experimentierstrecke
Strahlmitte
ist vorhanden

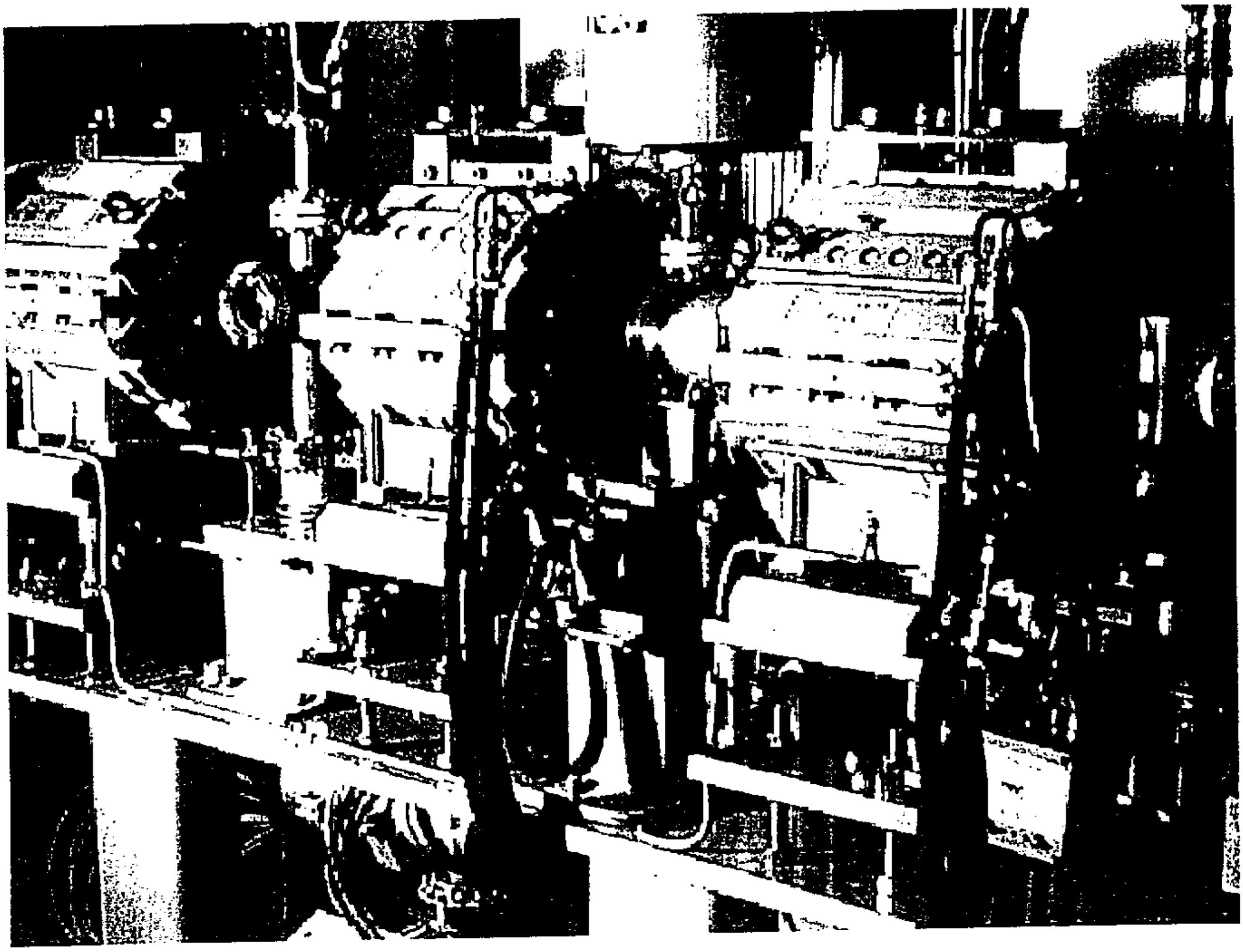

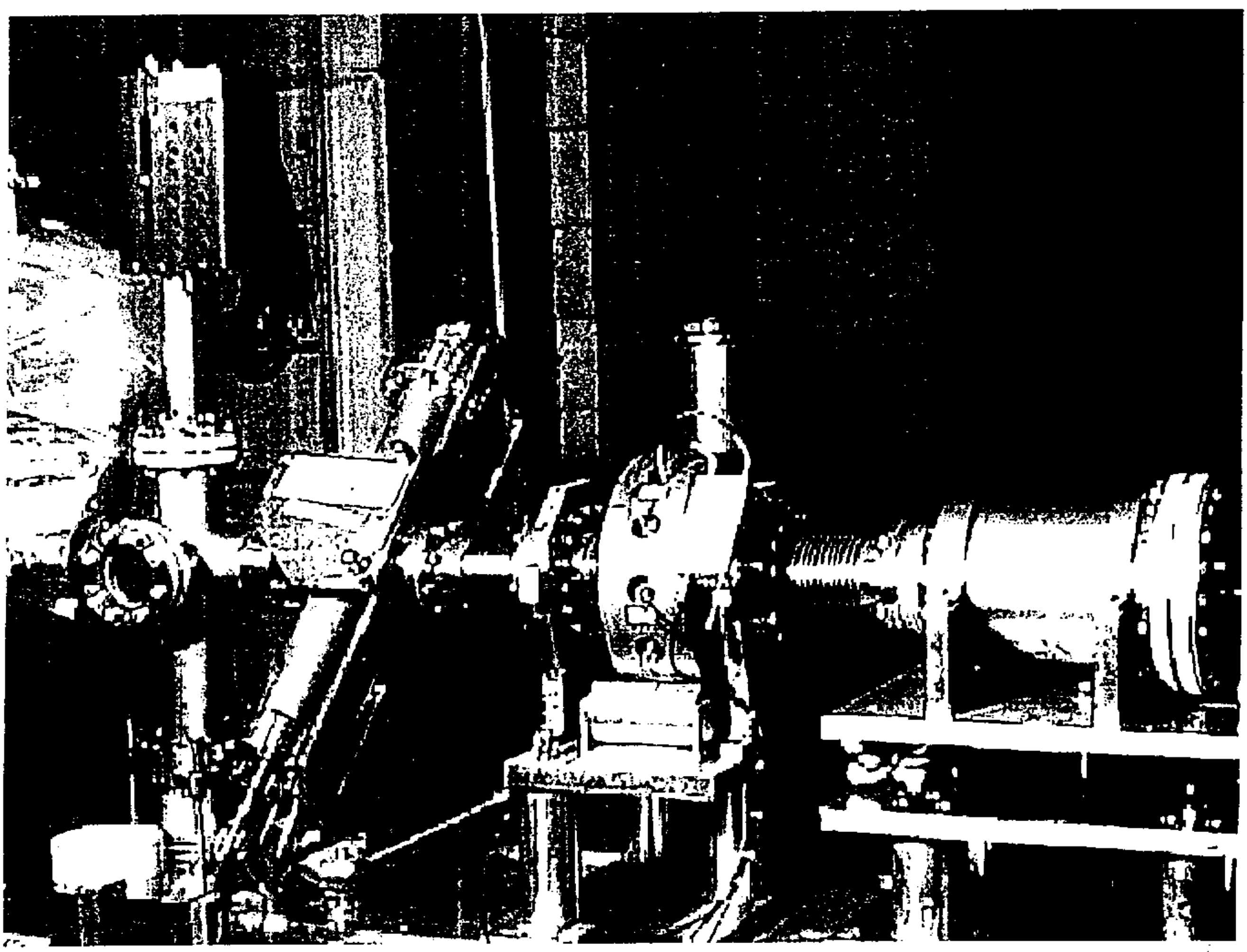

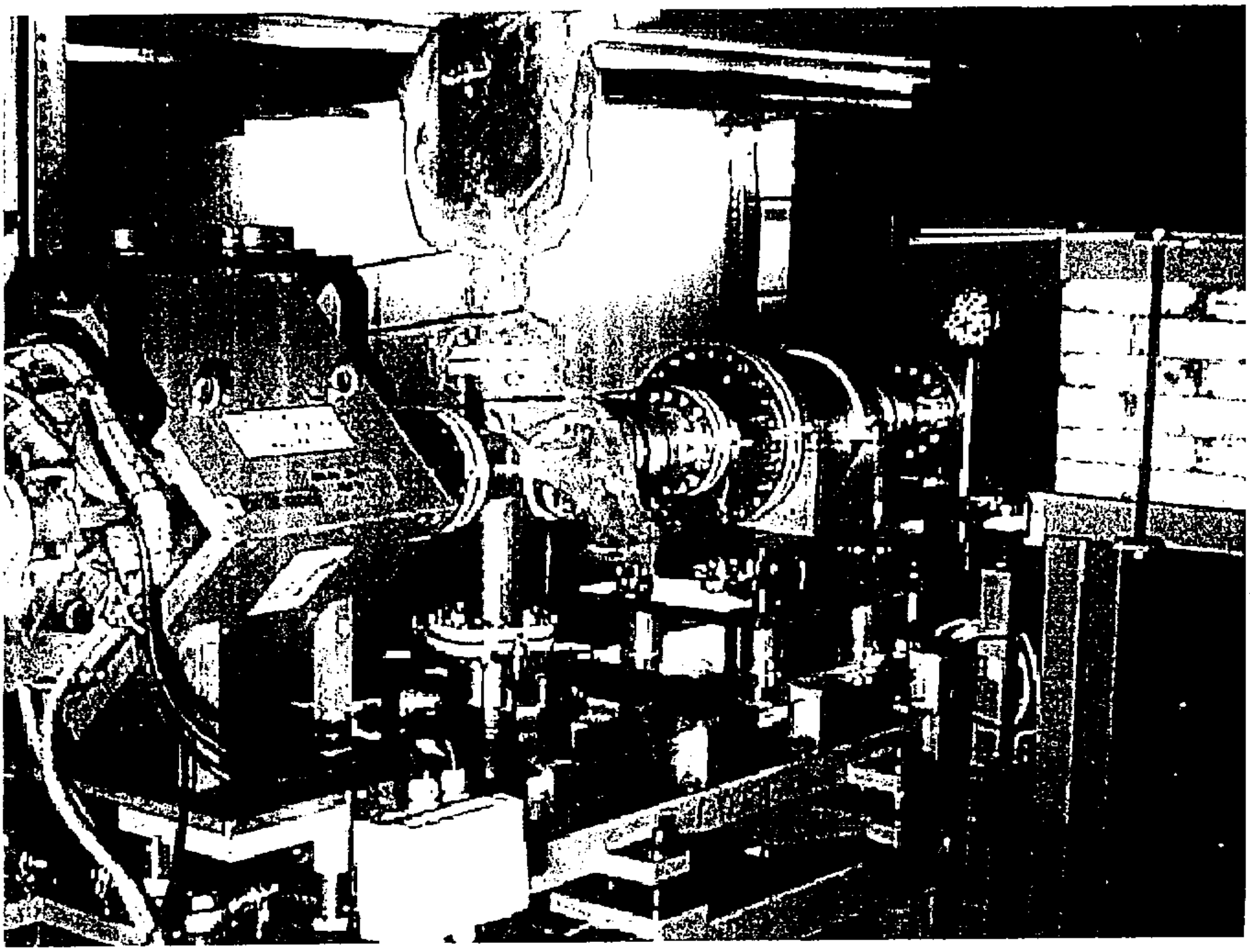

1:30

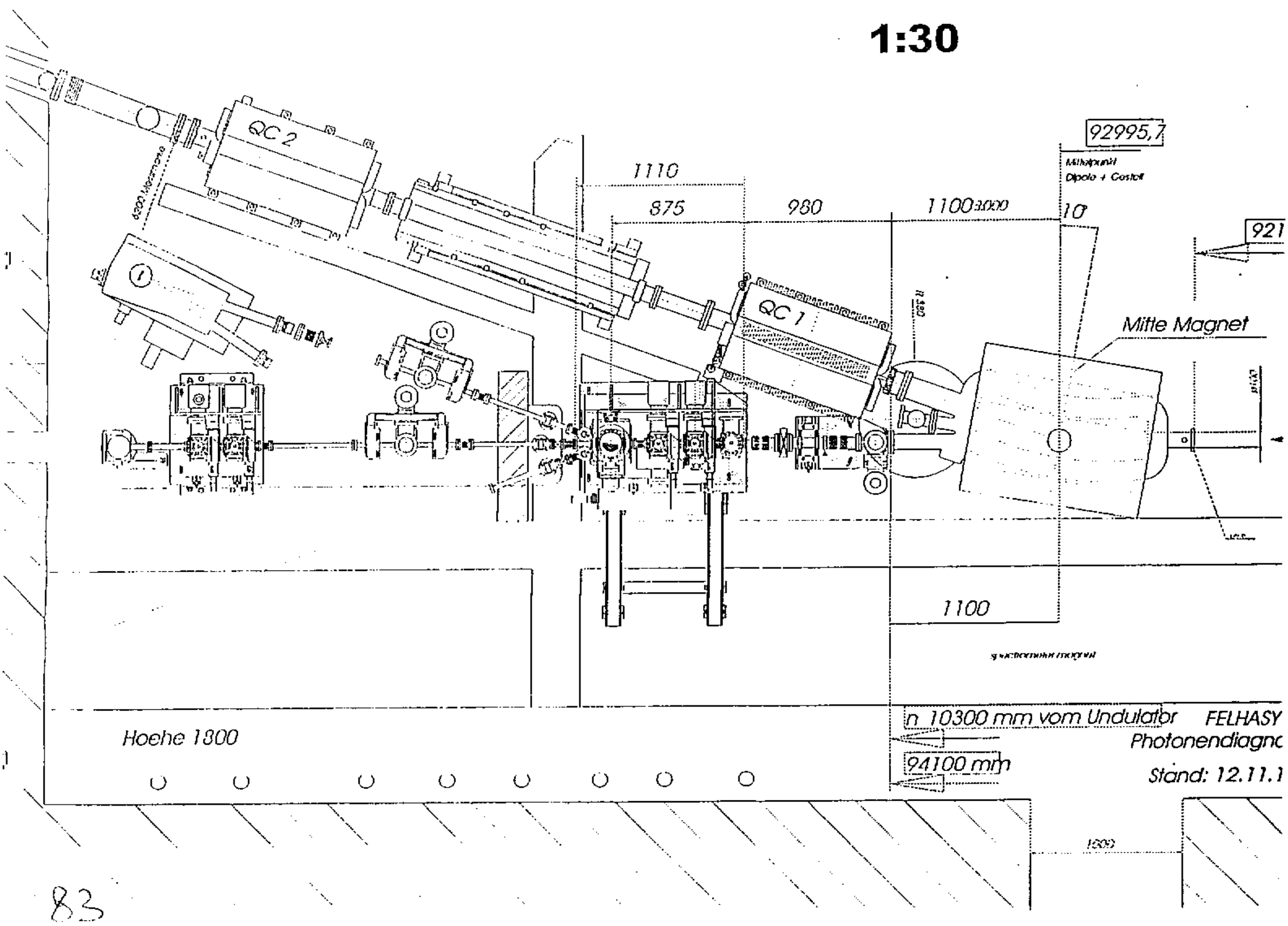
QC 2
QC 1
1110
875
980
1100
3000
10°
92995,7
Mittelpunkt Dipole + Costoff
921
Mitte Magnet
1100
Hoehe 1800
n 10300 mm vom Undulator
94100 mm
FELHASY
Photonendiagnc
Stand: 12.11.1

G. Schmidt, -MPY-, 16.06.99

Time schedule for July/August 99 for the TTF Shut Down (Mar.-July 1999)

Goal: First lasing or electron beam through the undulator before the FEL Conference 99 (23 -28 August).

Status:

Undulator:
- 1st Section in
- 2nd Section in
- 3rd Section ready for installation inside tunnel

Diagnostic Block: All assembled, 2 diagnostic block fiducialized,
4 blocks leak checked after assembly
1 block installed inside tunnel

Collimator: Vacuum components completely installed. Section is leak tight and prealigned

Tentative Schedule for July 99

- Installation work on the injector: 1st and 2nd week of July (28.6-9.7)
- collimator: Concrete shielding inside tunnel 5.7.99
- Undulator: 9.7.99 Vacuum chamber installed and undulator inside the tunnel
- Prealignment of undulator: 12-16.7.99
- Diagnostics blocks installation and vacuum connection: from 16.7.99 to 23.7.99
- collimator: Alignment and last concrete shielding inside tunnel 16.7.99 so that tunnel roof can be closed
- Tunnel roof can be closed now (19.7.99)
- 26 -28.7.99 Alignment of diagnostic blocks

- 26.7-6.8.99 alignment of undulator and diagnostic blocks (laser interferometrie)

Mile stones:

- Tuesday 20.7.99 Interlock ready and tunnel closed. Start to cool down modules.
  Work on the injector, linac (magnet power supplies diagnostic etc.) and modules can start during shifts.
- Monday, 26.7.99 Module cold.
- The undulator would be completely aligned on the 6.8.99
- 2 weeks are then available for tests with the undulator before the FEL 99 conference.

84

Progress on Controls

Kay Rehlich
DESY MVP2

85

- New Components and Modifications in Hardware
- New Features and Improvements in Software

DESY

Laser

Interlock (PLC)

DOOCS Server

Modifications, bug fixes

Scope server

New TTF beam line components/positions

...

RF

DSP (digital signal processor)

5 Systems: linac, Chechia, RF gun, FNAL, lab

RF procedures/operations

Preparation for TESLA requirements (new DSP, in tunnel..)

Modulator controls discussions

Finite State Machine (FSM)

Tool to create finite state server programs

to automate linac operation

DOOCS display

Multi data in a plot

Correlation plots

Drag and drop

Interlock

Beam Inhibit System (BIS)

"Fast OFF" box for the collimator

Undulator

Temperature Controller

Temperature measurement

Integrators for photo multipliers

Network Infrastructure

Network in Hall 3

- faster: 10/100 MBit backbone
- better maintainable: star topology
- Packet switching
- 100 IP nodes connected

Computer Infrastructure

4 VME crates (undulator)

2 consoles in the new control room

Orbit correction (FSM)

Timing

Modification from 10MHz to 9MHz

ProfiBus

Design of a new VME board to control 2 ProfiBus lines including a UNIX driver

is used to control BIS, Pumpstations and other PLCs

Fast ADC (Hamburg & Zeuthen)

8 channel VME ADC board

- for undulator BPMs, RF and ..
- 14 bit resolution, up to 10 MHz
- 5 boards ready: 20. July
- 12 more boards: mid August
- (old board: 12bit, 2MHz, price factor 3 higher)

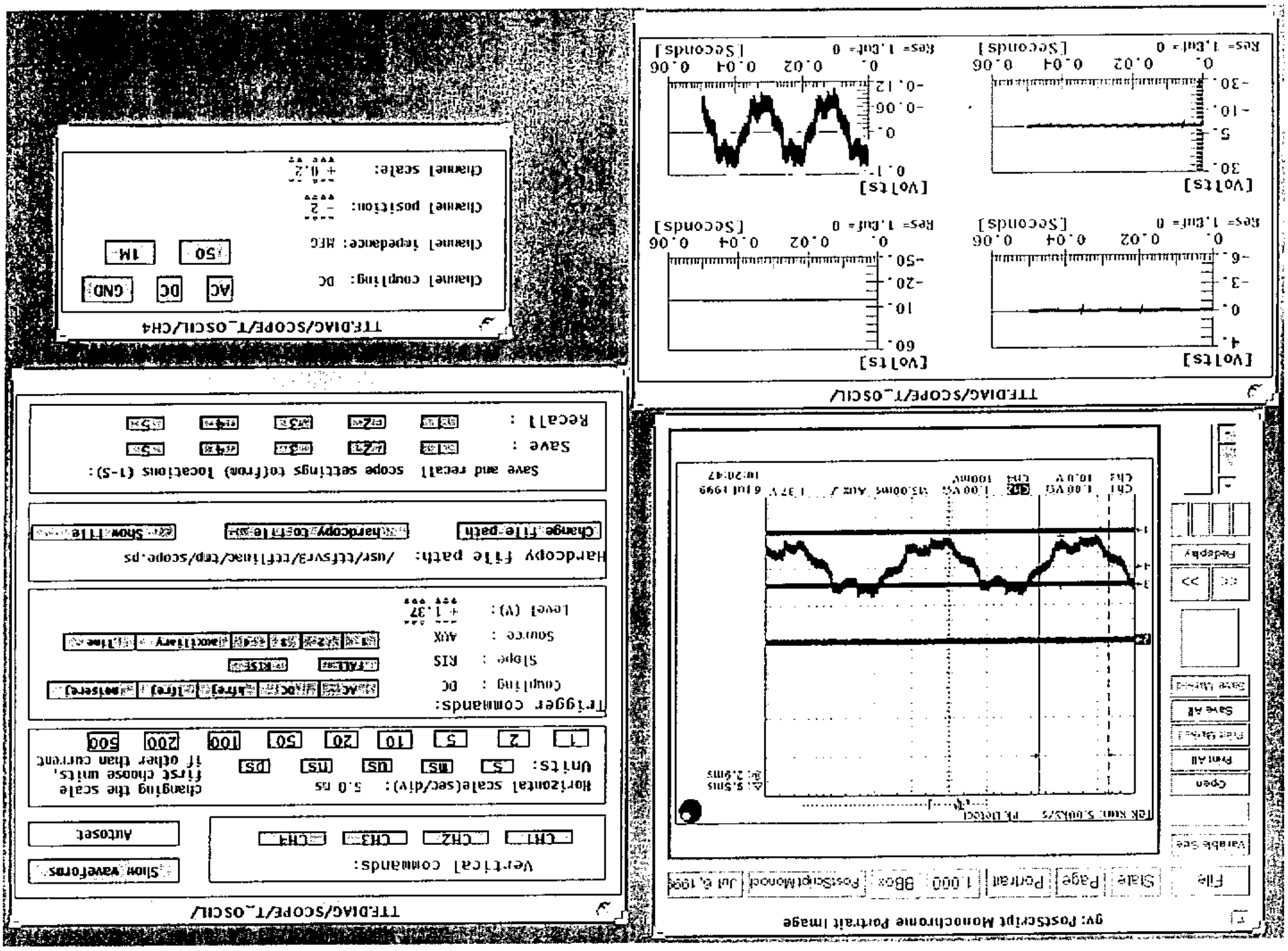

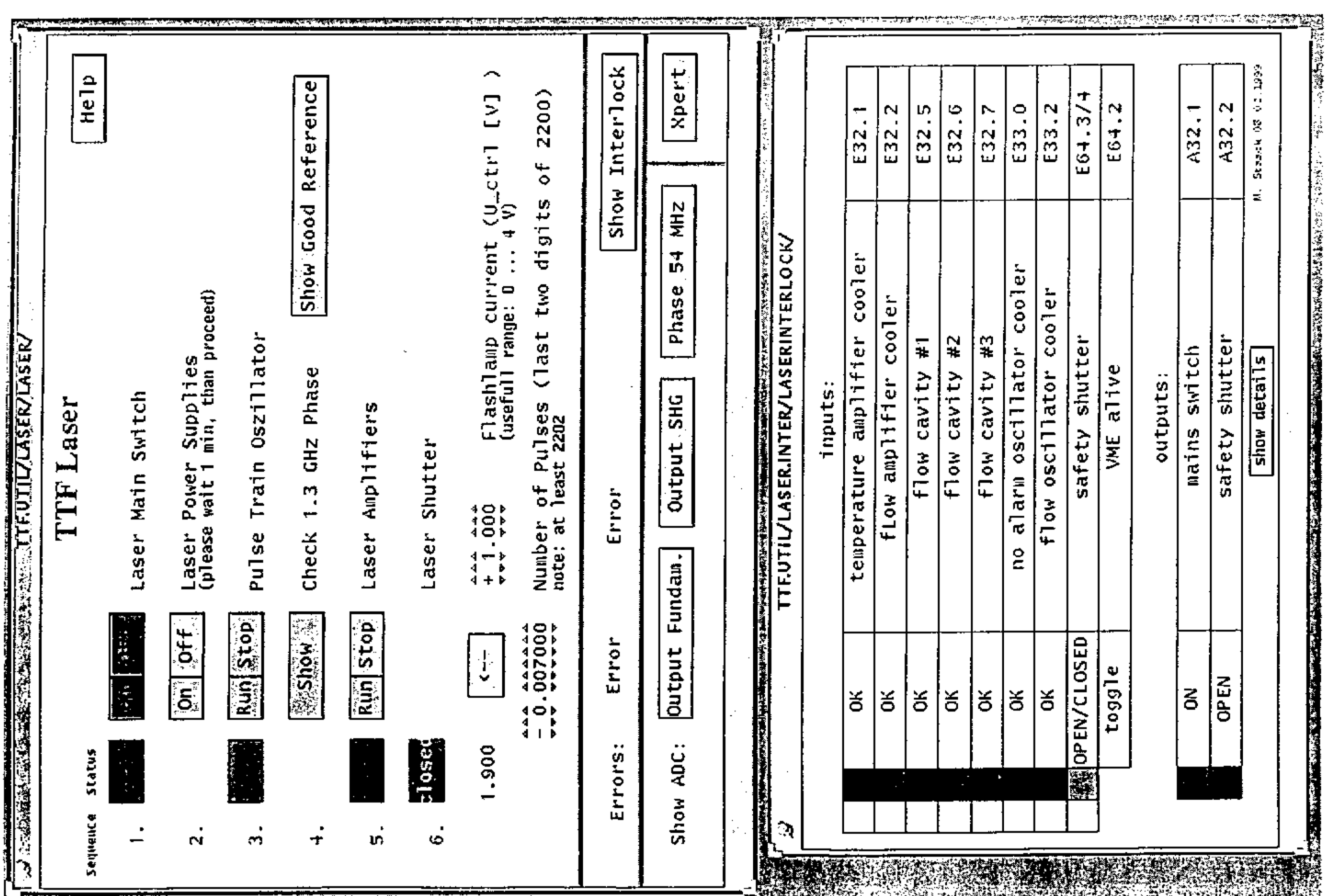

TTF.UTIL/LASER/LASER/
TTF Laser
Help
Sequence Status
1. Laser Main Switch
2. On Off Laser Power Supplies (please wait 1 min, than proceed)
3. Run Stop Pulse Train Oszillator
4. Show Check 1.3 GHz Phase
Show Good Reference
5. Run Stop Laser Amplifiers
6. Laser Shutter
1.900
- 0.007000
+ 1.000
Flashlamp current (U_ctrl [V]) (usefull range: 0 ... 4 V)
Number of Pulses (last two digits of 2200) note: at least 2202
Errors: Error Error
Show Interlock
Show ADC: Output Fundam. Output SHG Phase 54 MHz Xpert
TTF.UTIL/LASER.INTER/LASERINTERLOCK/
inputs:
OK temperature amplifier cooler E32.1
OK flow amplifier cooler E32.2
OK flow cavity #1 E32.5
OK flow cavity #2 E32.6
OK flow cavity #3 E32.7
OK no alarm oscillator cooler E33.0
OK flow oscillator cooler E33.2
OPEN/CLOSED safety shutter E64.3/4
toggle VME alive E64.2
outputs:
ON mains switch A32.1
OPEN safety shutter A32.2
show details

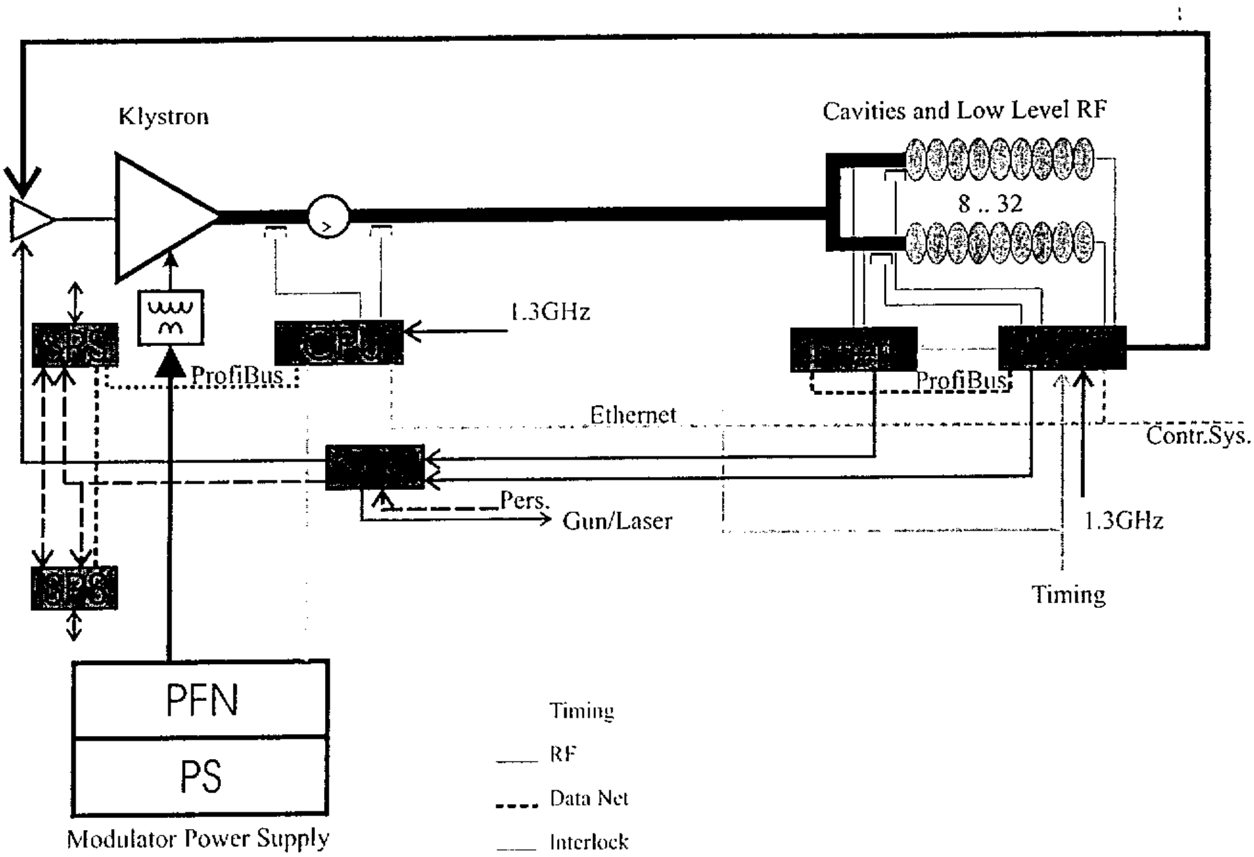

6.4.99 Kay Rehlich

RF System Building Blocks

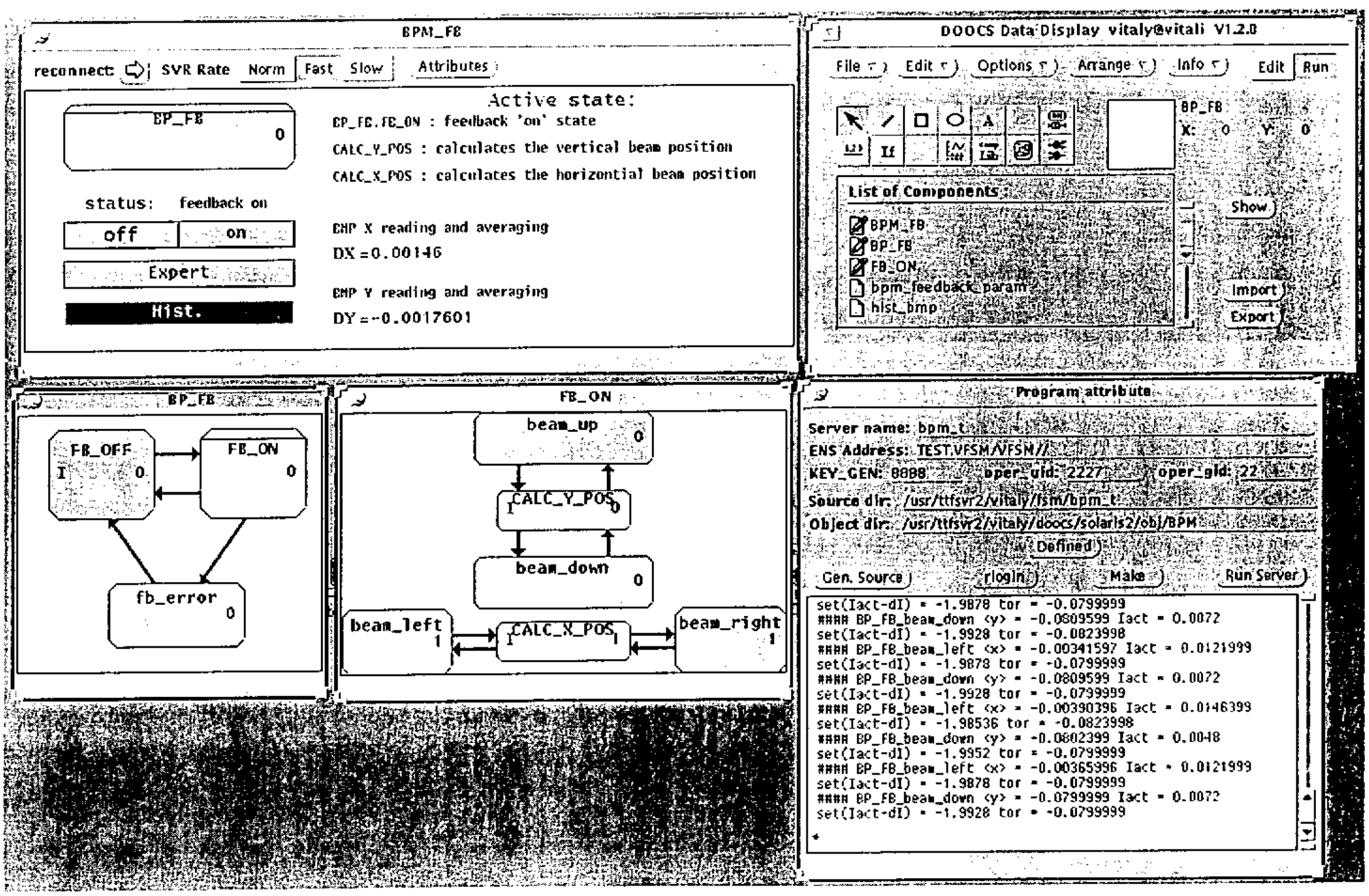

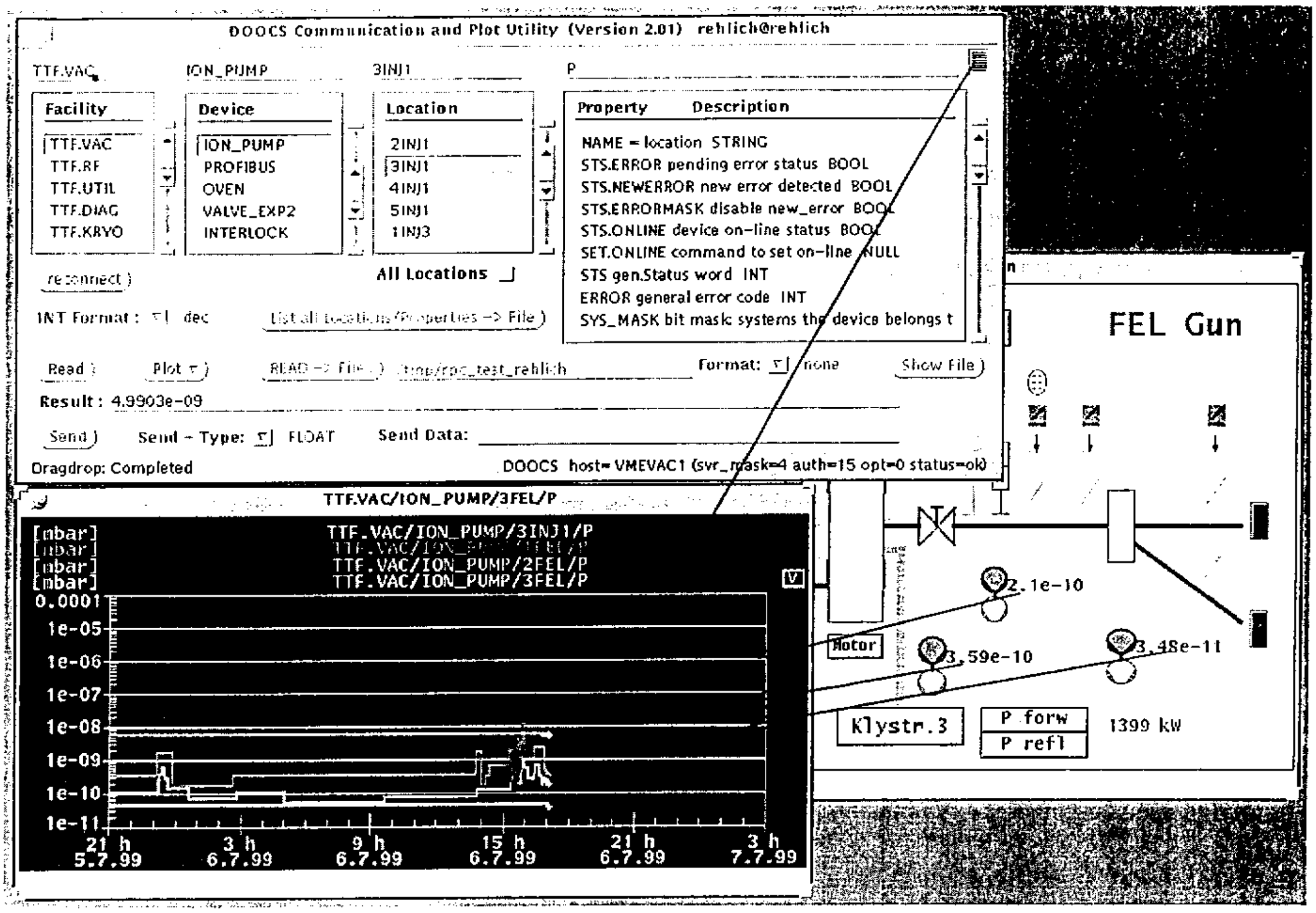

DOOCS Communication and Plot Utility (Version 2.01) rehlich@rehlich
Facility
TTF.VAC
TTF.RF
TTF.UTIL
TTF.DIAG
TTF.KRYO
Device
ION_PUMP
PROFIBUS
OVEN
VALVE_EXP2
INTERLOCK
Location
2INJ1
3INJ1
4INJ1
5INJ1
1INJ3
All Locations
Property Description
NAME = location STRING
STS.ERROR pending error status BOOL
STS.NEWERROR new error detected BOOL
STS.ERRORMASK disable new_error BOOL
STS.ONLINE device on-line status BOOL
SET.ONLINE command to set on-line NULL
STS gen.Status word INT
ERROR general error code INT
SYS_MASK bit mask systems the device belongs t
reconnect
INT Format: dec
Read
Plot
Format: none
Show File
Result: 4.9903e-09
Send
Send - Type: FLOAT
Send Data:
Dragdrop: Completed
DOOCS host= VMEVAC1 (svr_mask=4 auth=15 opt=0 status=ok)
TTF.VAC/ION_PUMP/3FEL/P
[mbar]
TTF.VAC/ION_PUMP/3INJ1/P
TTF.VAC/ION_PUMP/2FEL/P
TTF.VAC/ION_PUMP/3FEL/P
0.0001
1e-05
1e-06
1e-07
1e-08
1e-09
1e-10
1e-11
21 h 5.7.99
3 h 6.7.99
9 h 6.7.99
15 h 6.7.99
21 h 6.7.99
3 h 7.7.99
FEL Gun
2.1e-10
3.59e-10
3.48e-11
Motor
Klystr.3
P forw
P refl
1399 kW

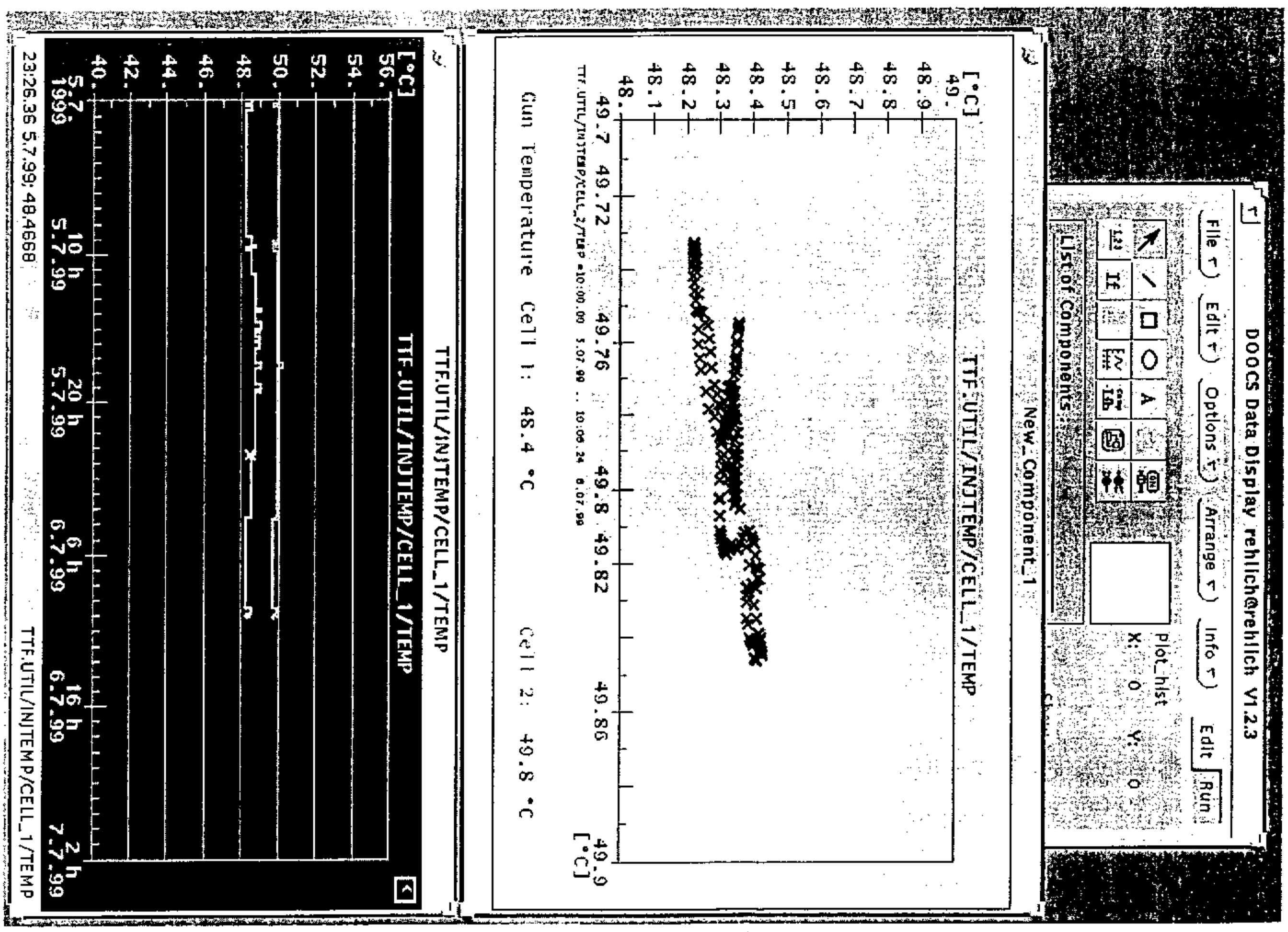

TTF.UTIL/INJTEMP/CELL_1/TEMP
Gun Temperature Cell 1: 48.4 °C
Cell 2: 49.8 °C
DOOCS Data Display rehlich@rehlich V1.2.3
File
Edit
Options
Arrange
Info
Run
List of Components
New_Component_1
Plot_hist
23:26:36 5.7.99: 48.4668

Beam loss detection system at low β-function section

H. Schlarb

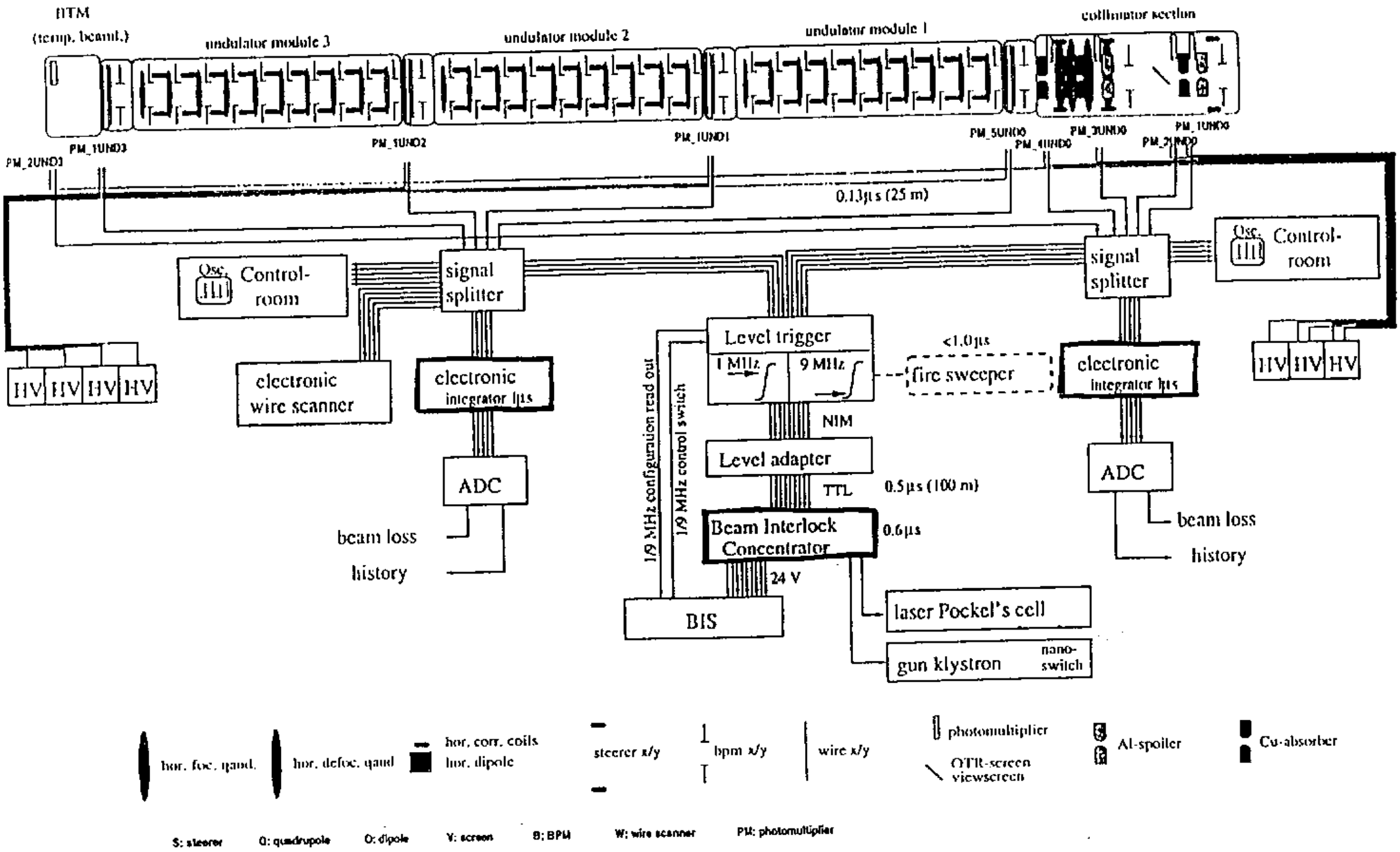

New Network Infrastructure in Hall 3

17.3.1999
Kay Rehlich

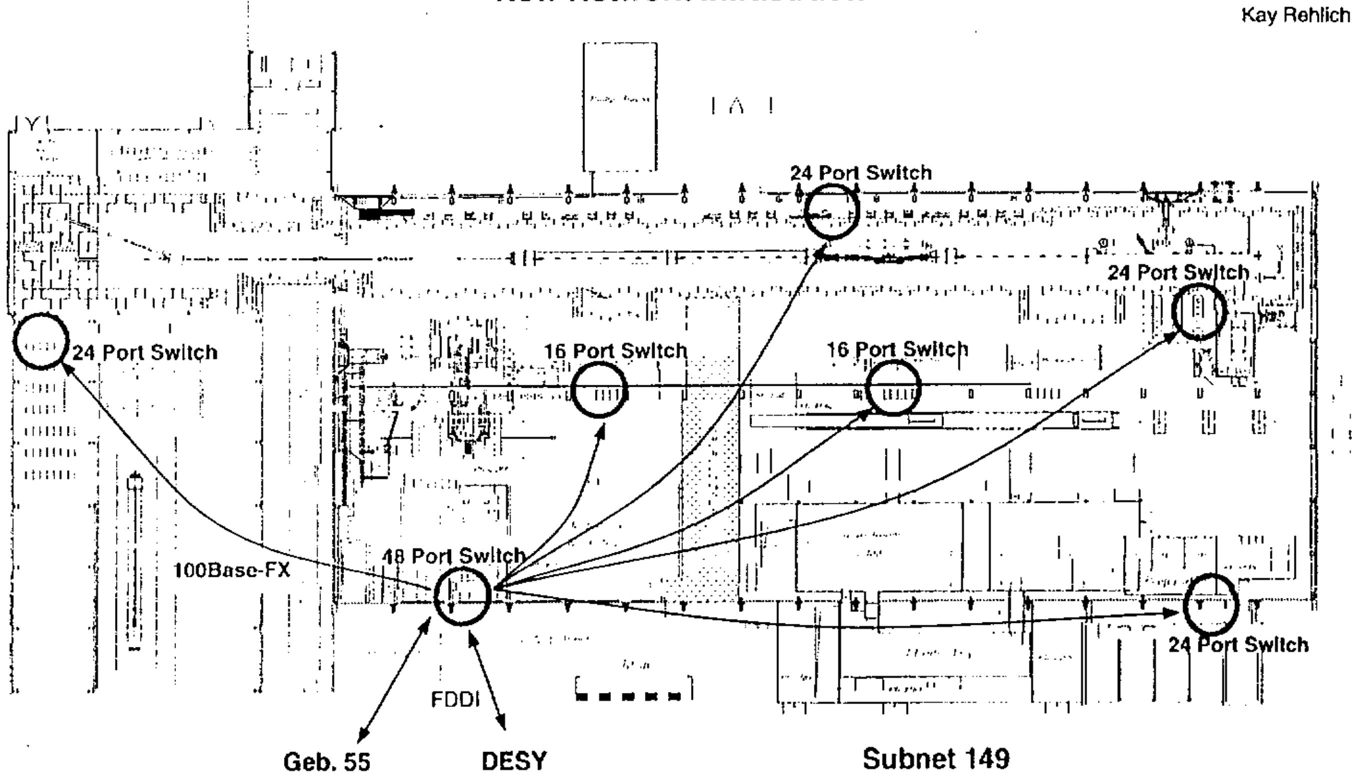

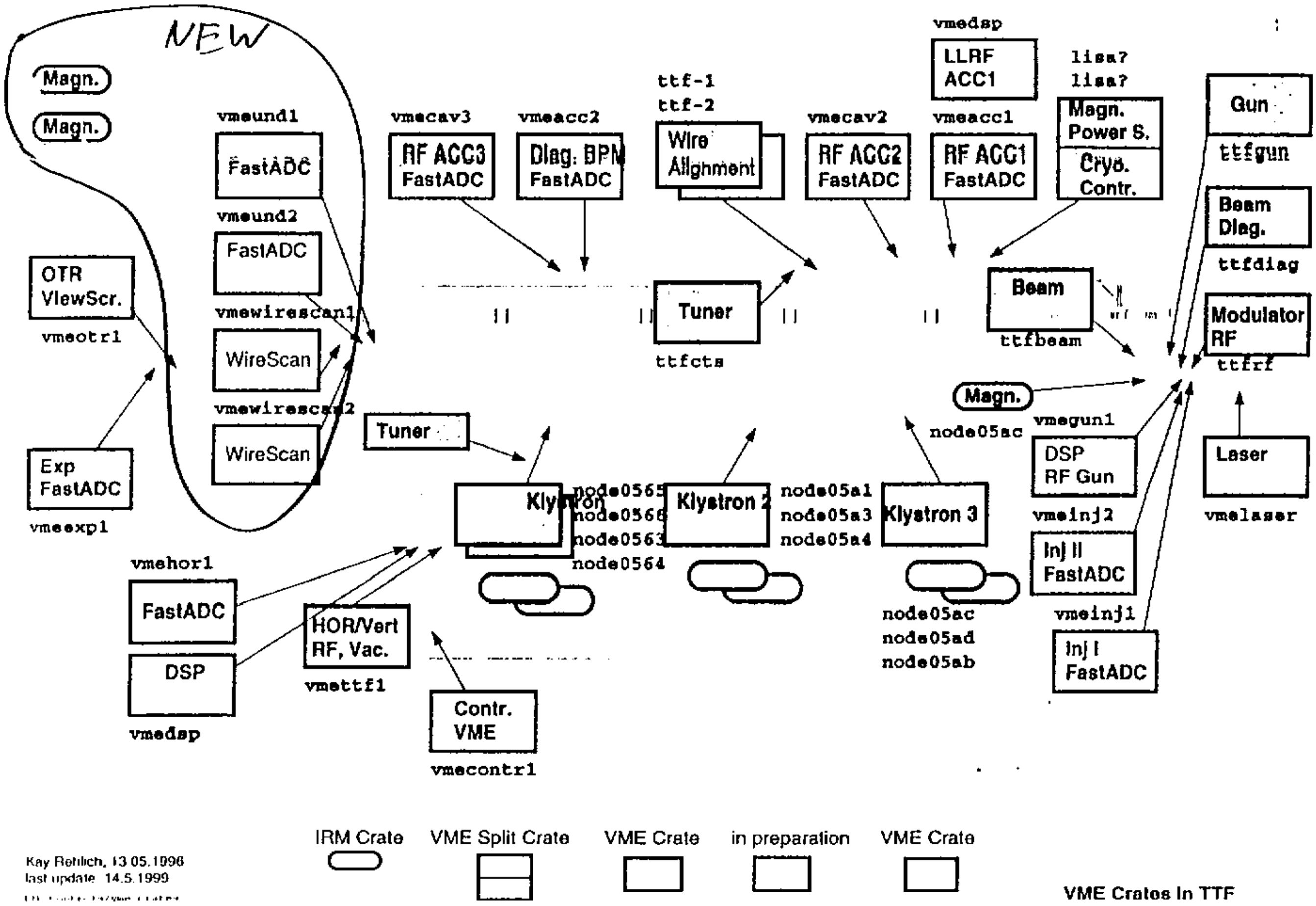

Kay Rehlich, 13.05.1998
last update 14.5.1999

VME Crates In TTF

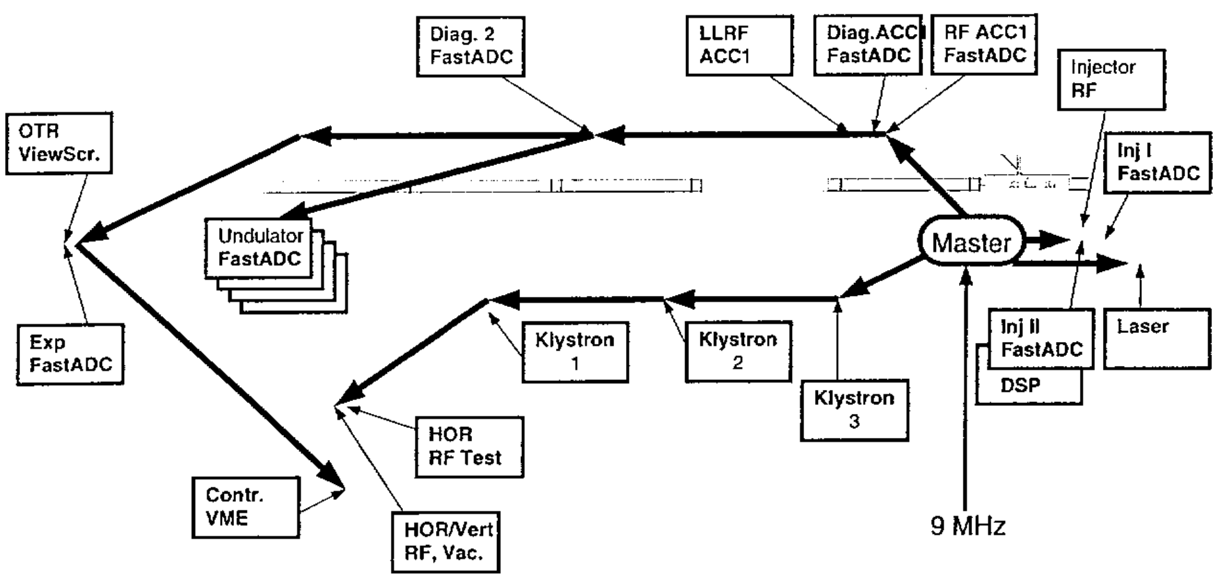

Kay Rehlich, 7.7.1999

Timing System in TTF

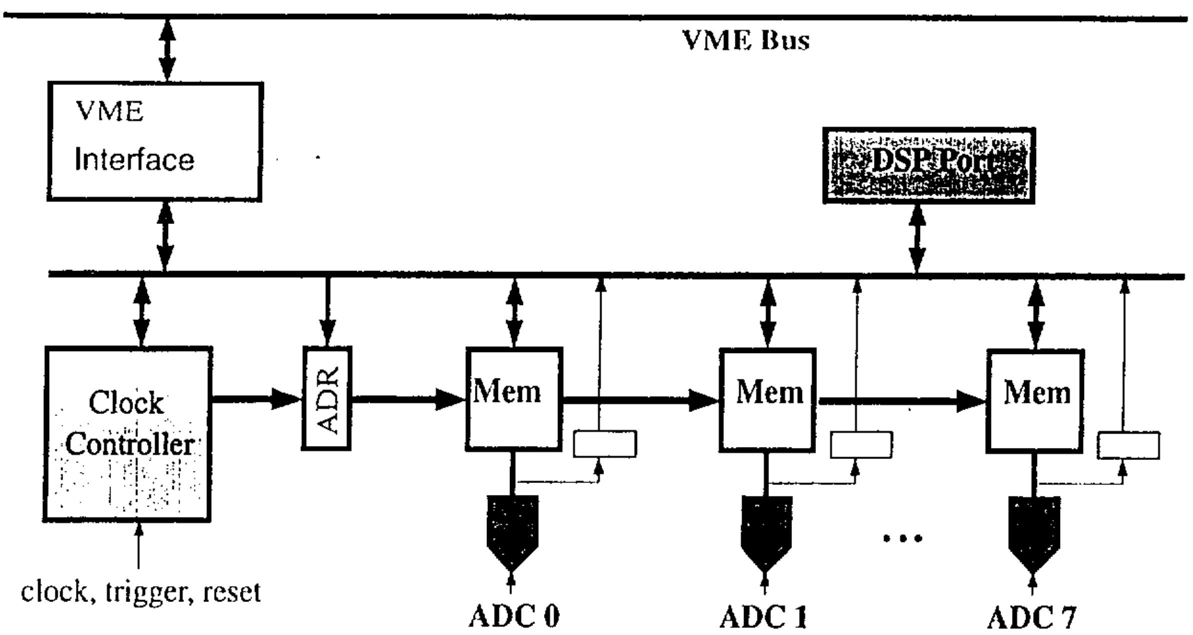

8 Channels of fast ADCs: up to 1 or 10 MHz sampling, 14 bit resolution, 128k word of memory
1 DSP port: for a link to a standard Ti C60 processor

Kay Rehlich, 3.98

New ADC Board Design for Diagnostics and Feedback Systems

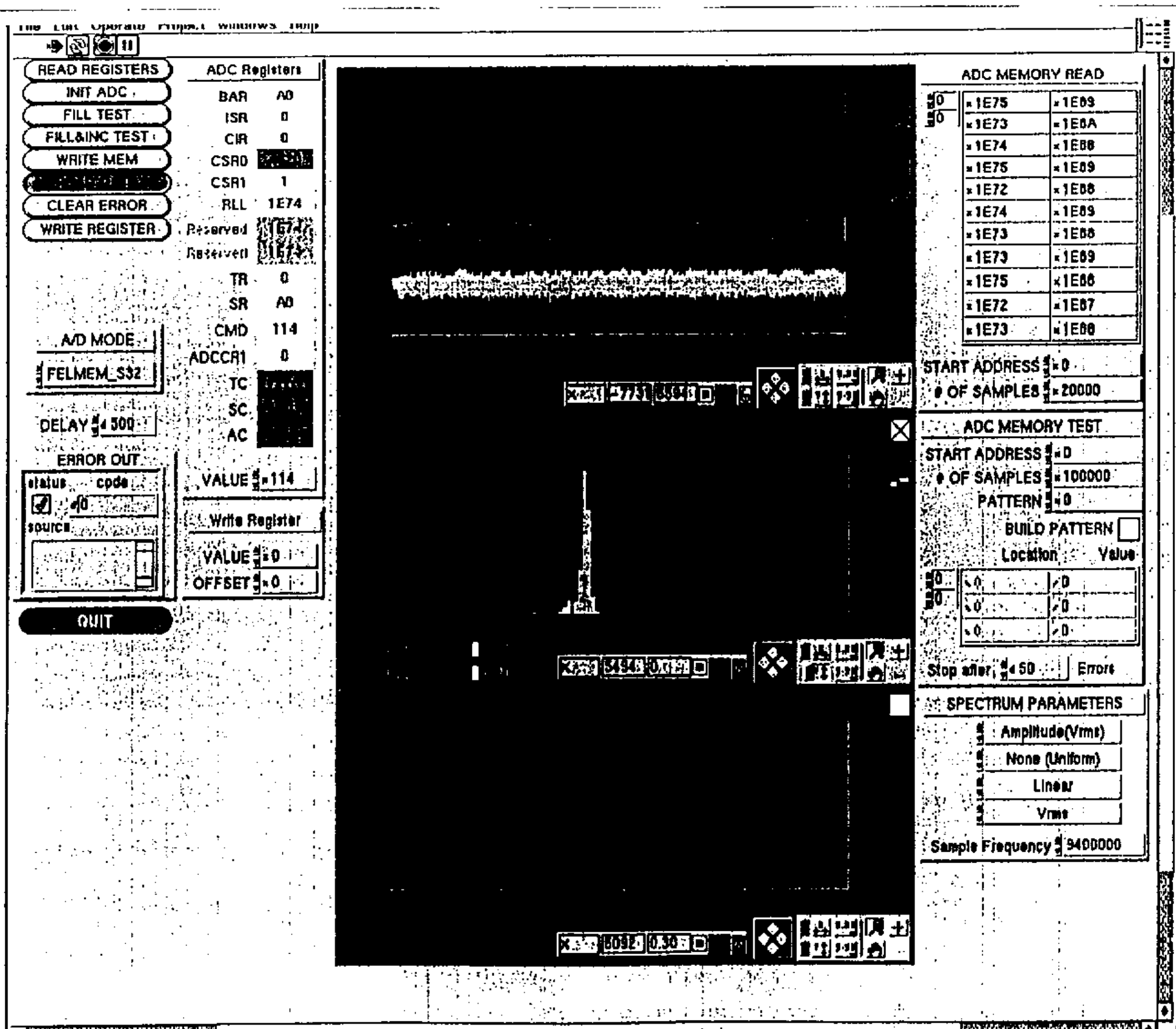

95

Undulator Status

Ulrich Hahn, HASYLAB at DESY
7. 7. 1999

Outline

Introduction

Undulator Vacuumchamber

Monitorblocks

Status of the Magnet Structures

Final Assembly and Set up in the Linac

The Undulator Vacuum System

length: ~ 15m, ∅ 9.5 mm
vacuum: *outgassing rate <1• 10 $^{-11}$ mbar•l/sec•cm^{-2}*
particle free: *according TESLA specification*

4 monitor blocks (185 mm long)
monitoring of the particle beam position in front and at the end of the 3 undulator modules

3 FEL - vacuum chambers 4.5m long 128x11.5mm^2
monitoring of the particle beam position in the gap of the undulator modules
steering of the particle beam in the gap of the undulator modules

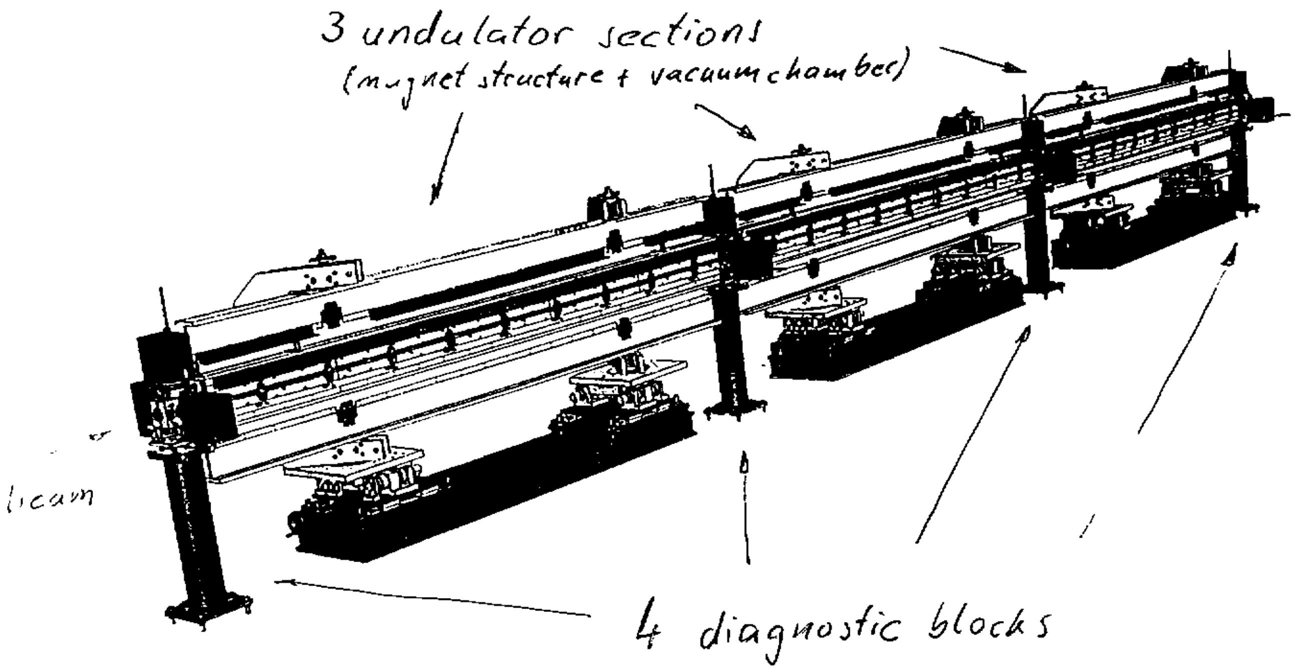

Three FEL - Vacuum Chambers

Material: extruded Aluminum with stainless steel flanges
Chamber crosssection: 128x11.5mm^2, ∅ 9.5 mm
Chamber length: 4492.2 mm
Microroughness of the hole: 0.47µm along the extrusion and 0.98µm perpendicular to the extrusion direction

relative *beam position measurement*

2 chambers with 10 ***pick up monitors*** *(40 electrodes - vertical - horizontal)*
1 chamber with 10 ***waveguide monitors*** *(40 electrodes - vertical - horizontal)*

beam steering

36 watercooled steering coils in each chamber

FEL vacuum chamber

designed and manufactured by DESY-HASYLAB and APS-Argonne Nat'l Lab Chicago

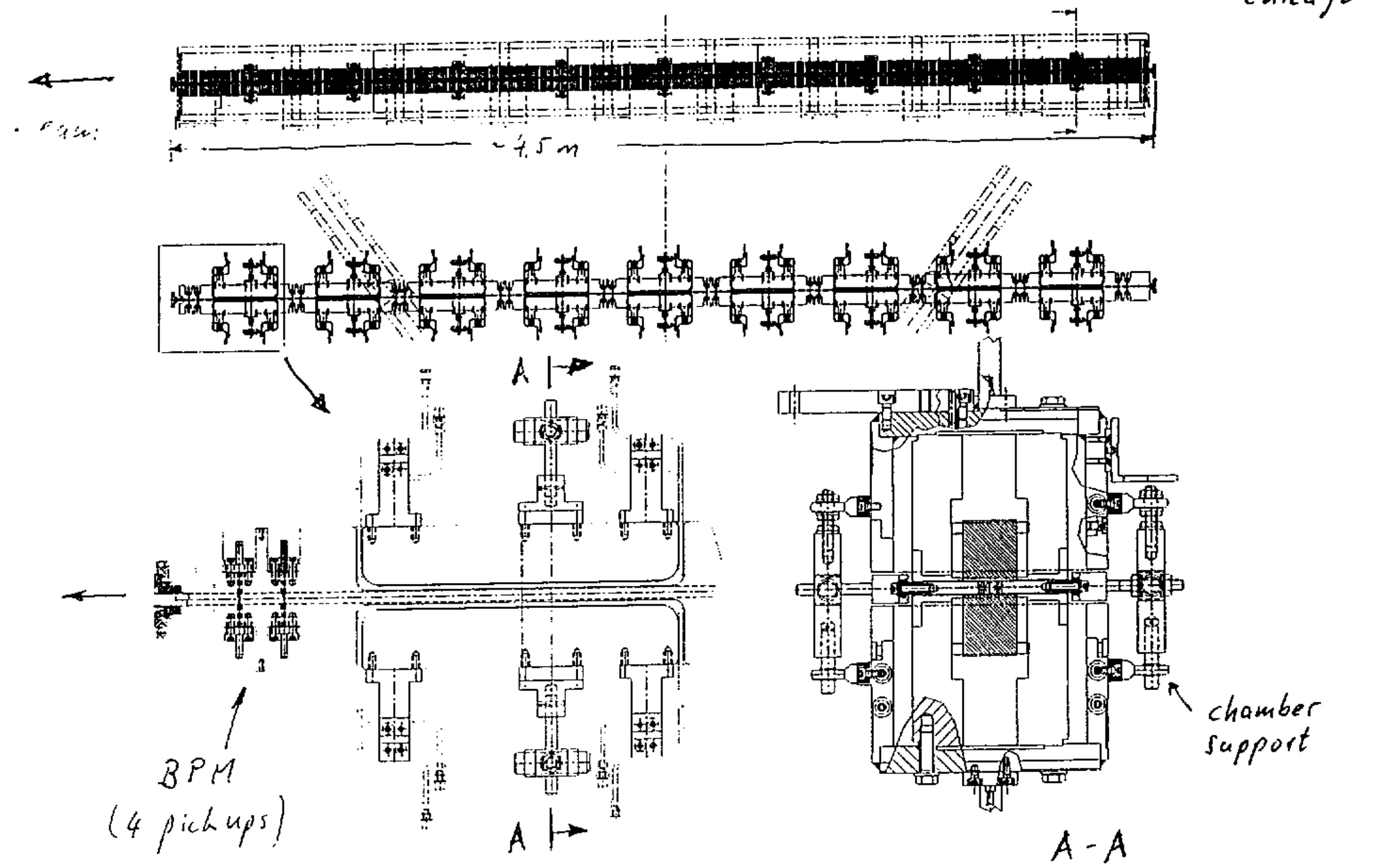

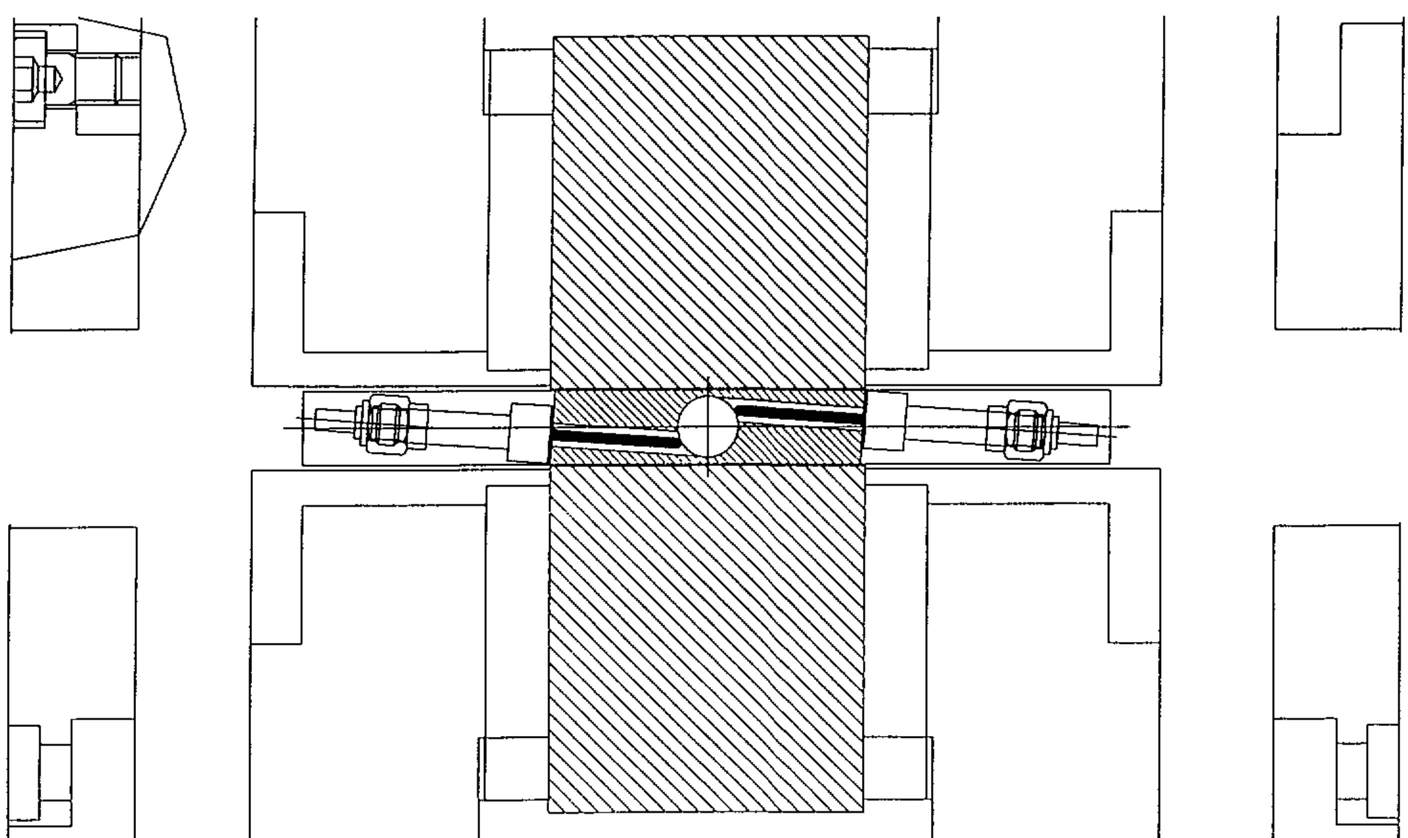

pick up monitor

M. Wendt et. al.

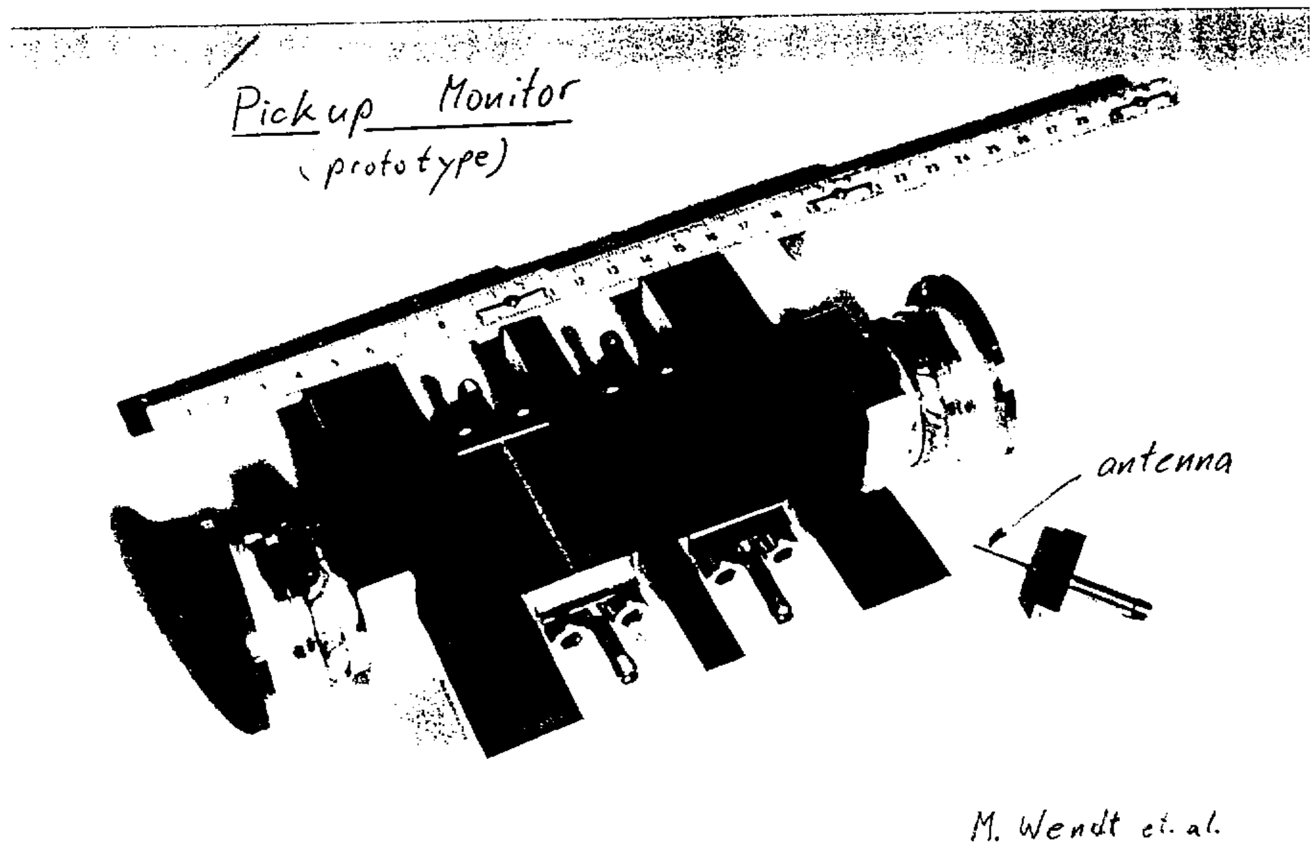
Pickup Monitor
(prototype)
antenna
M. Wendt et. al.

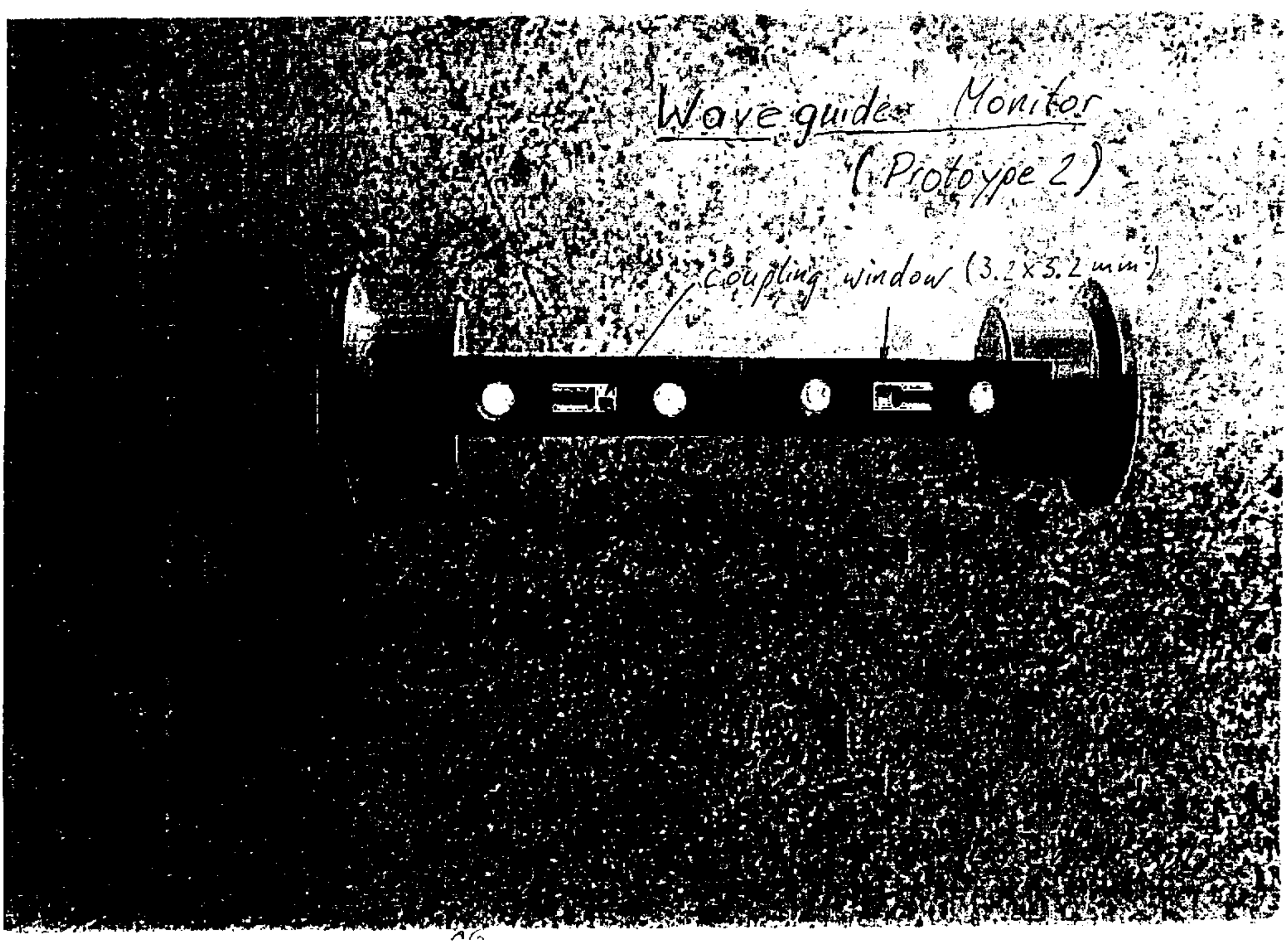
Waveguide Monitor
(Protoype 2)
coupling window (3.2 x 3.2 mm)

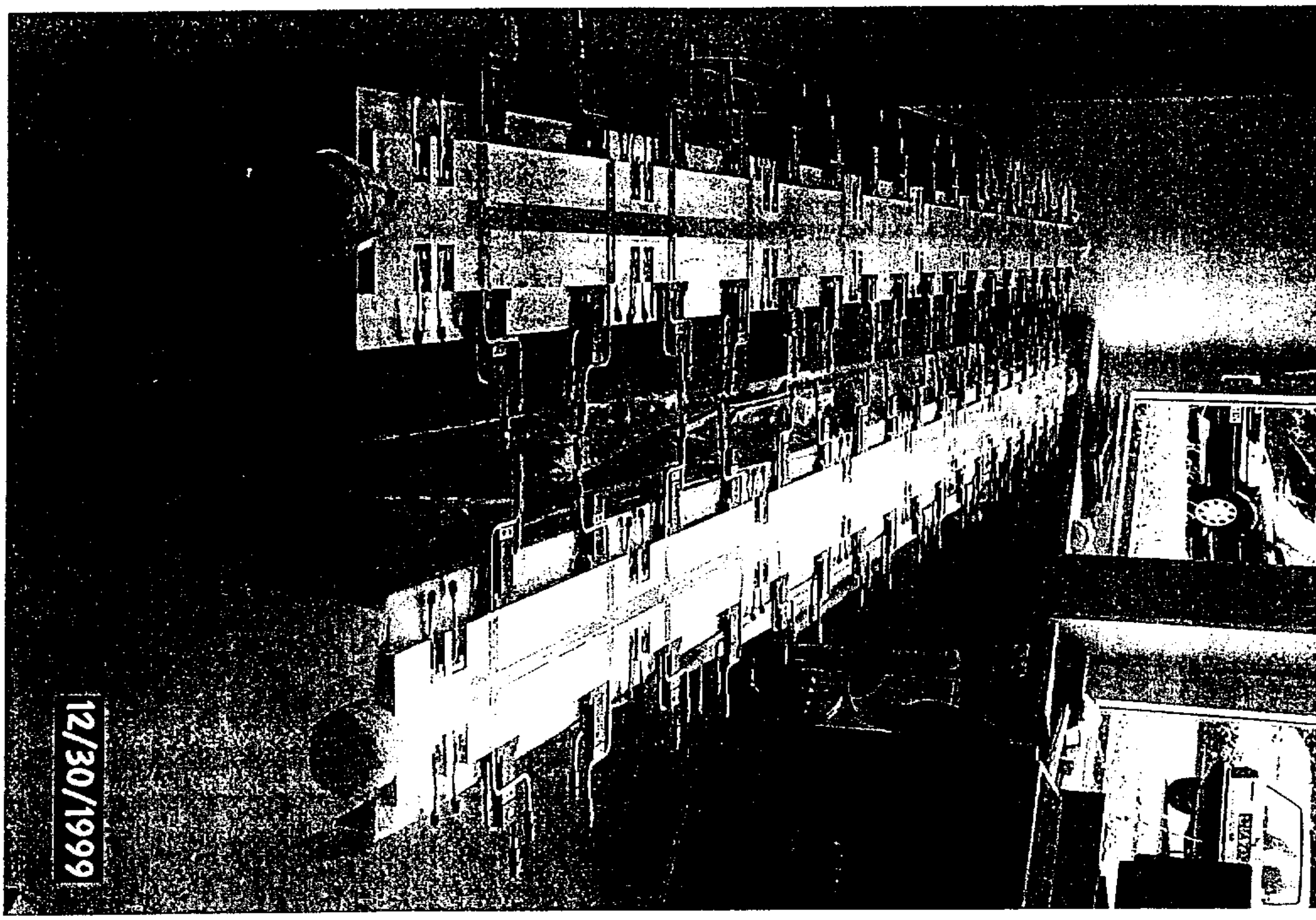
12/30/1999

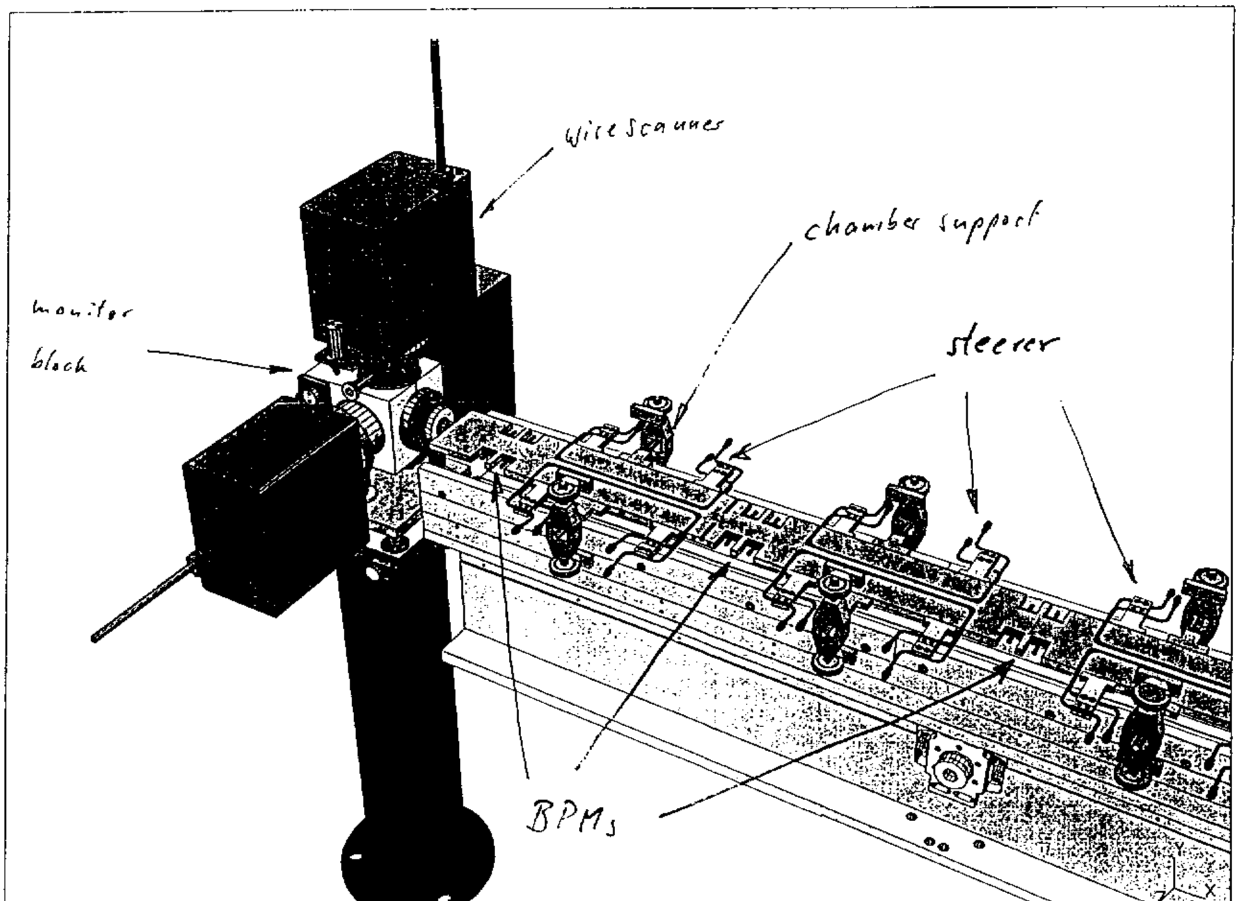
wire scanner
chamber support
monitor block
steerer
BPMs

Four Monitor Blocks

Main purpose: ***absolute*** *beam position measurement*
(goal ~ 15 μm)

1. *horizontal and vertical wirescanners with mechanical calibrated reference plate*
2. *horizontal and vertical cavity monitors (absolute after calibration)*
3. *the only position of pumping*

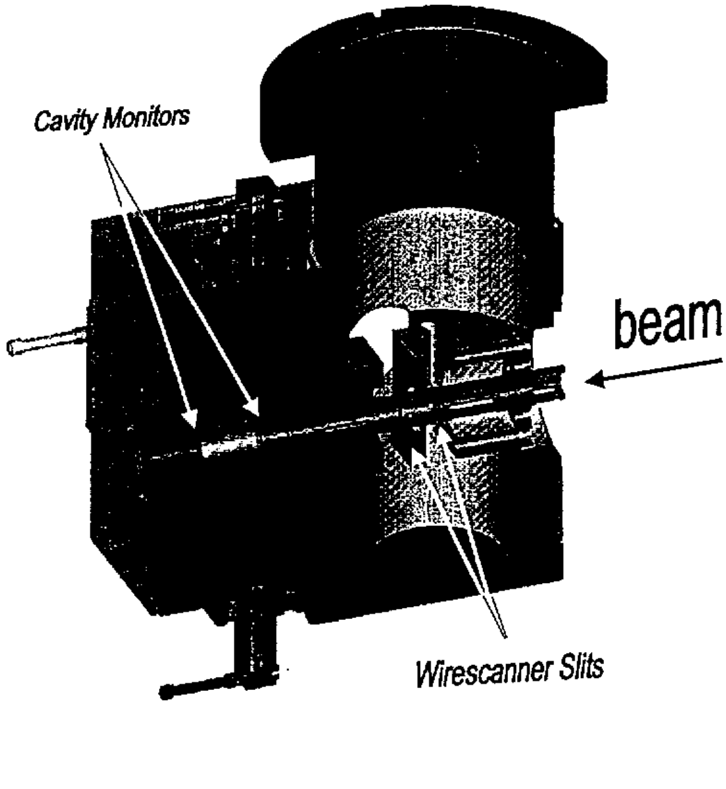

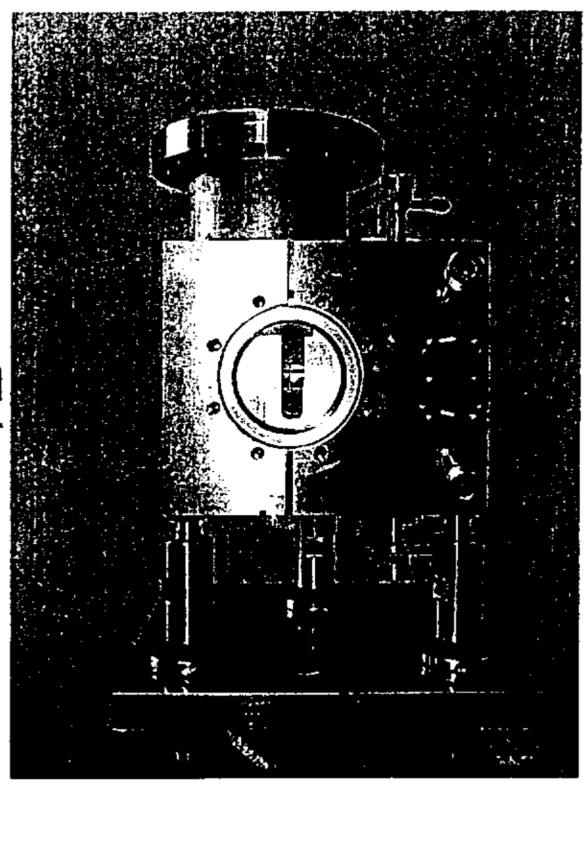

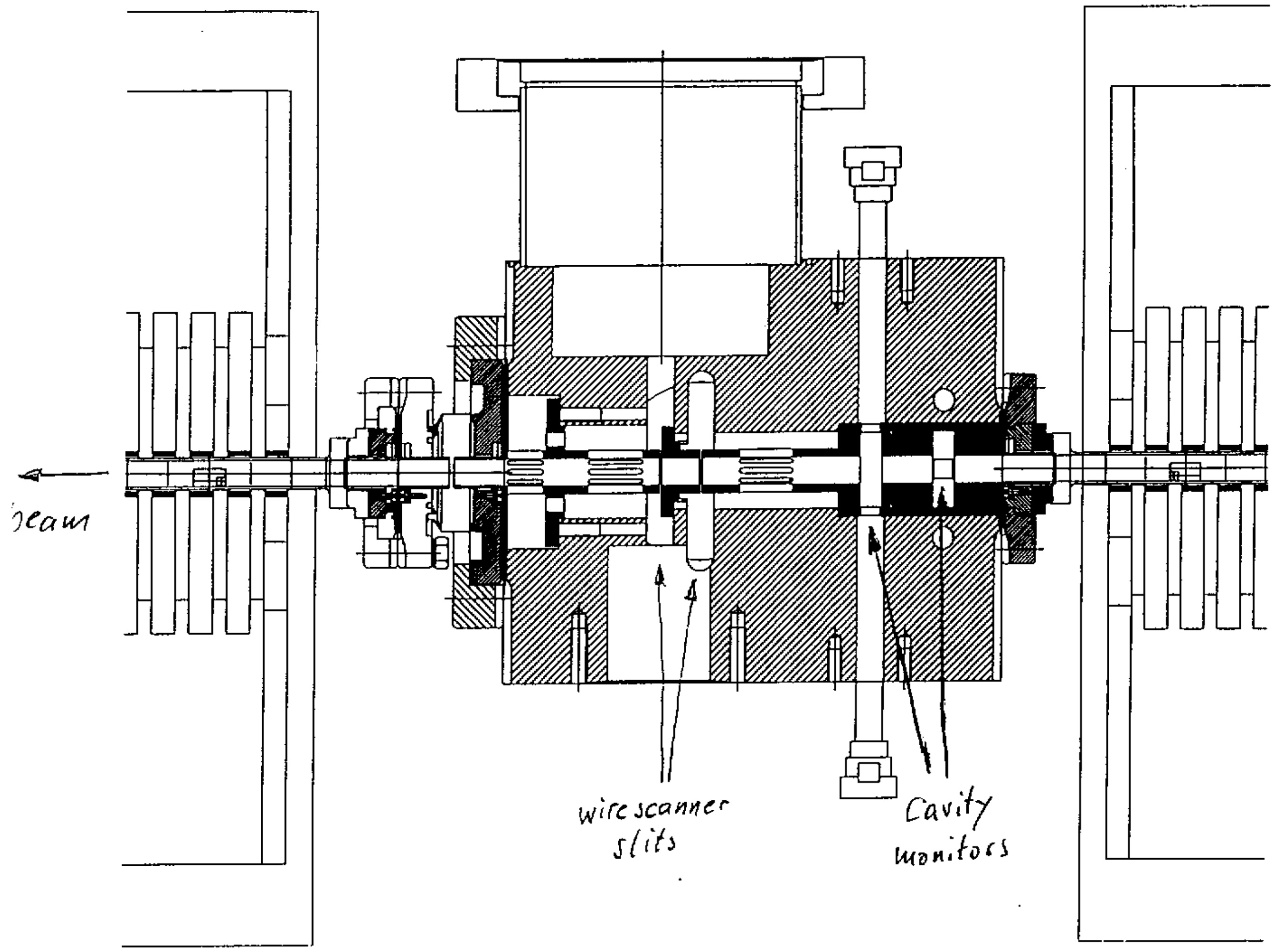
beam
wire scanner
slits
Cavity
monitors

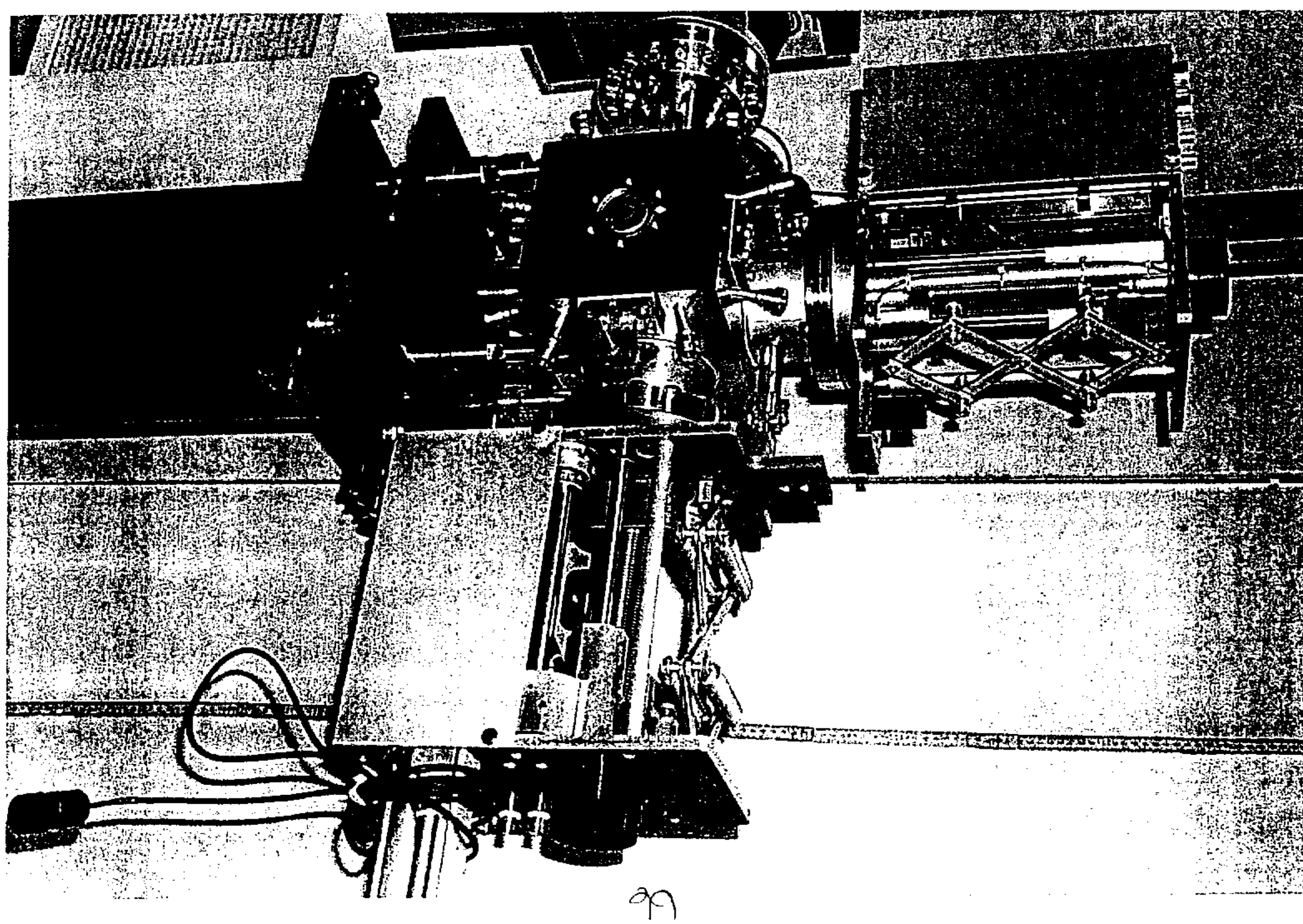

Status of the Magnet Structures

SASE 100 completed and installed in Linac	26.5.
SASE 200 completed and installed in Linac	21.6.
SASE 300 completed and to be installed in Linac	9.7.

UNDULATOR Setup in the Linac

Vacuum connection	6. – 23.7
Prealignment	12. – 16. 7.
Set up of Laserinterferometer	12. – 23. 7.
Infrastructure: Connecting monitors, correctors Water, etc.	12. – 23. 7.

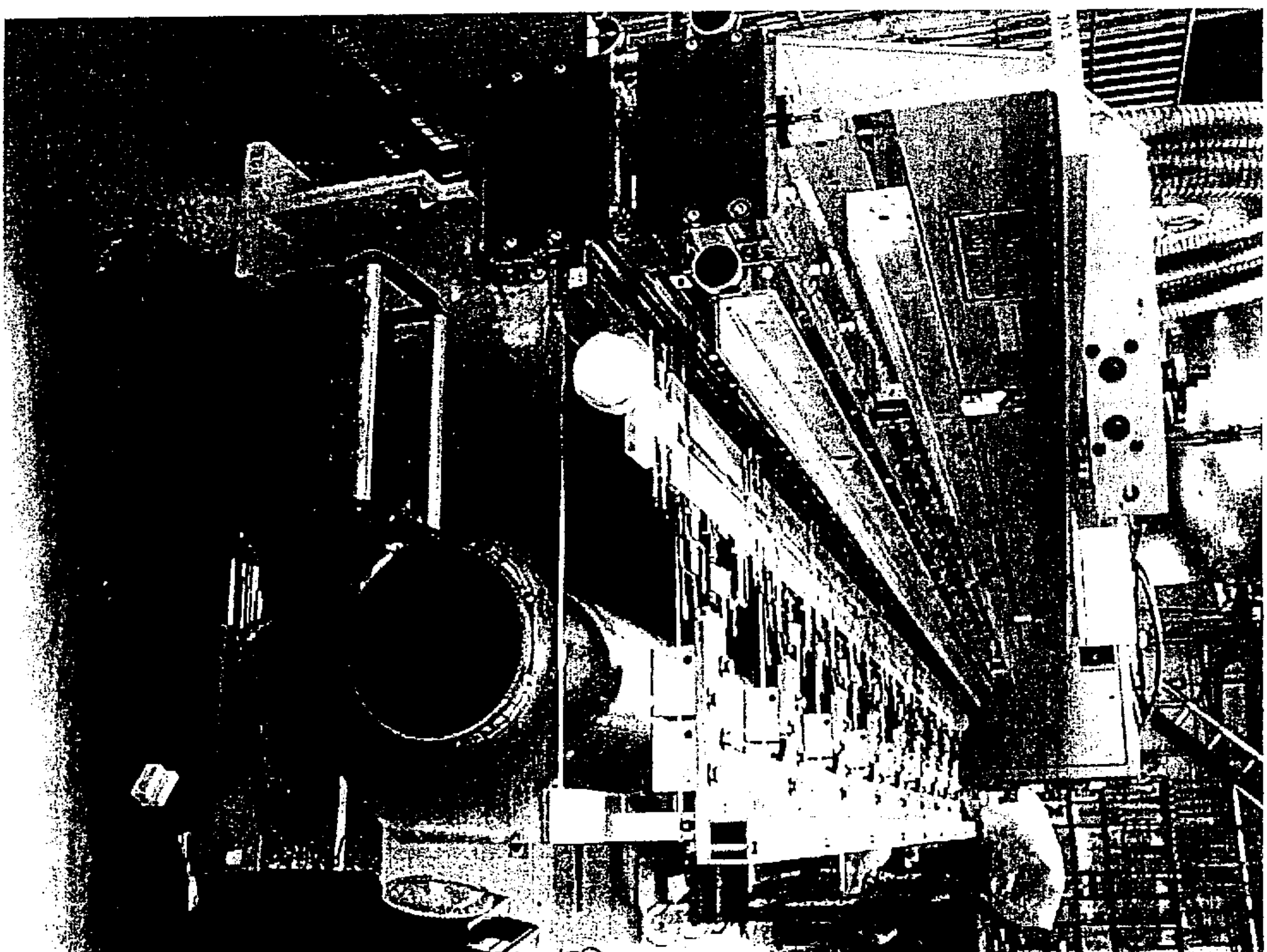

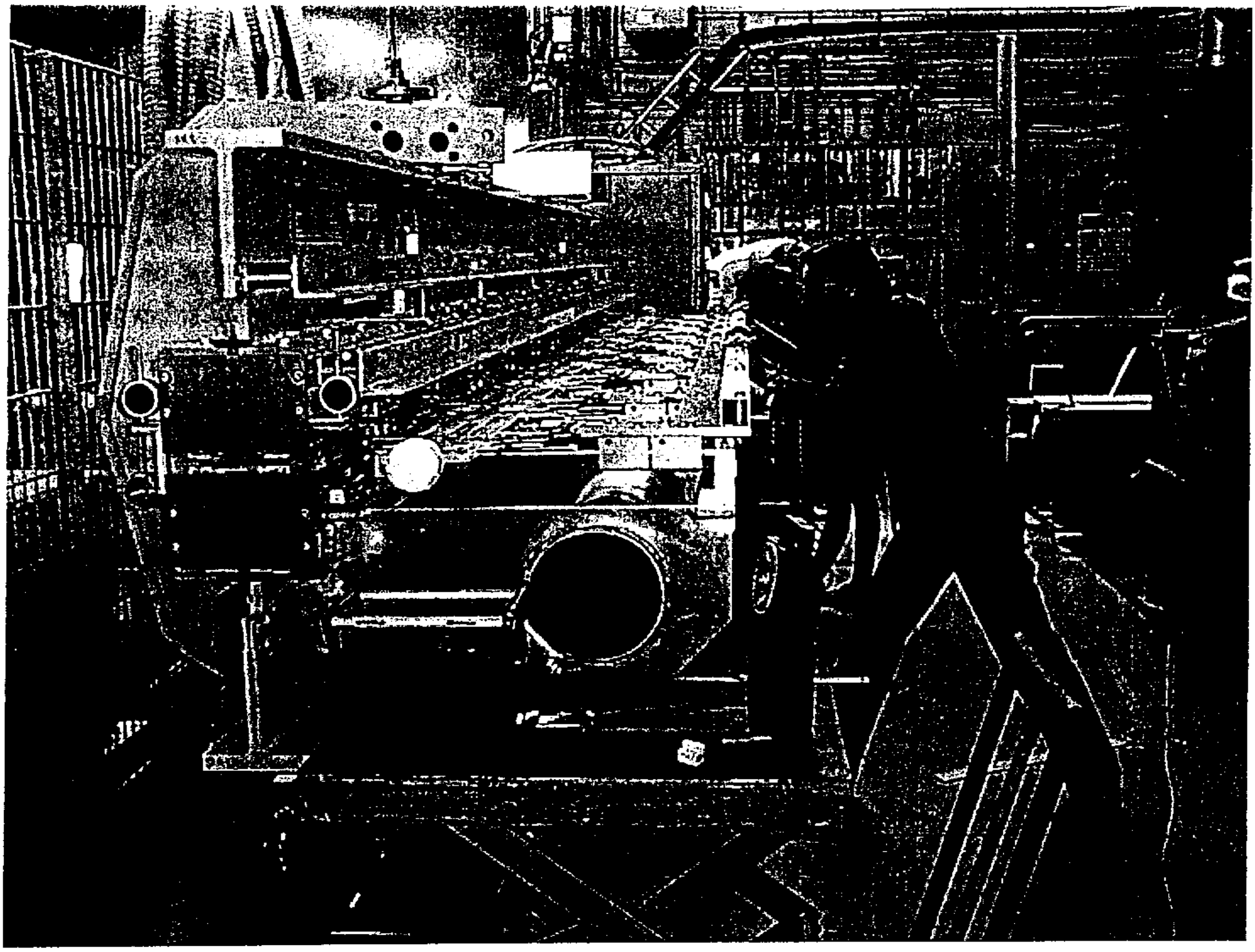

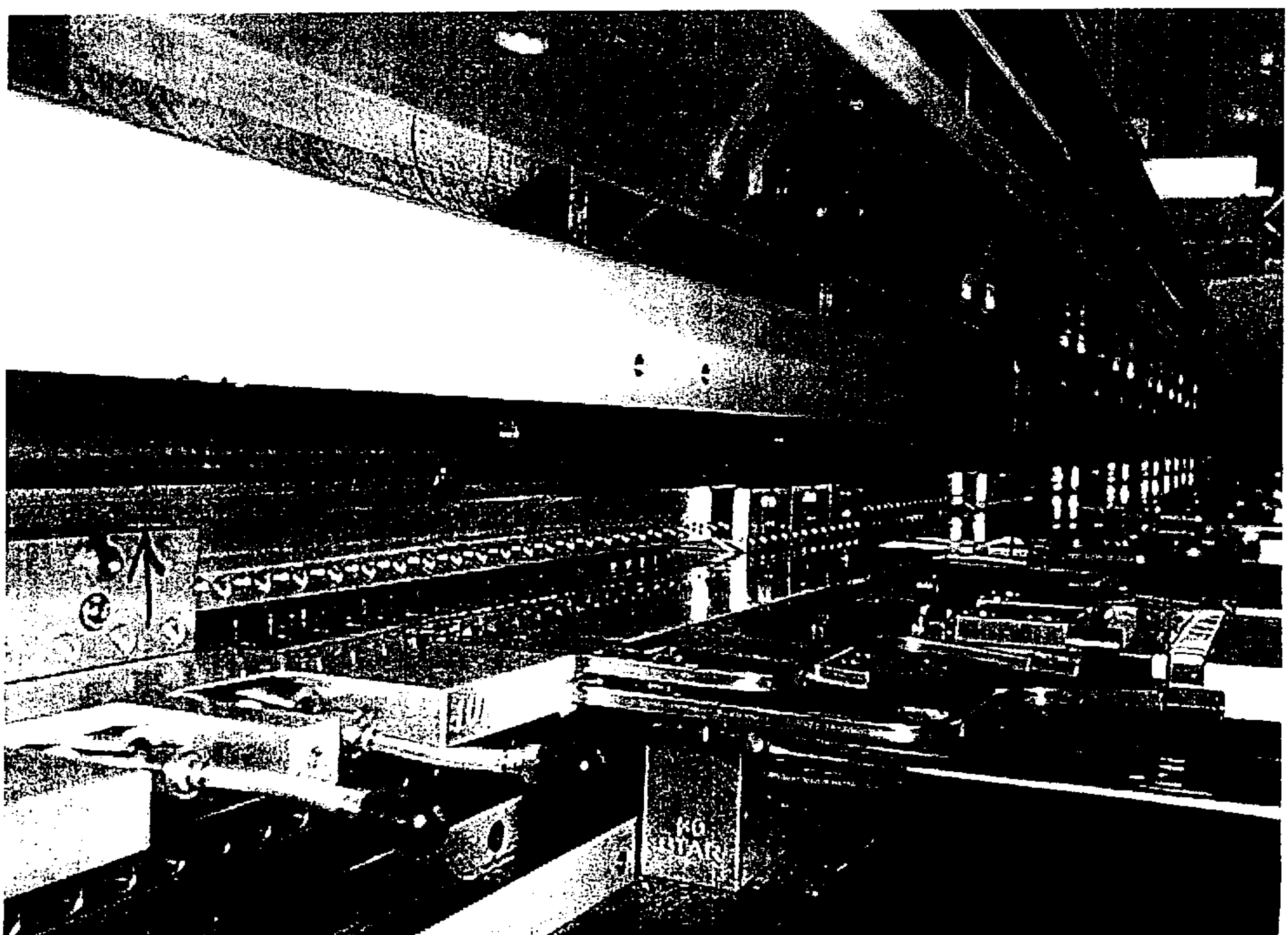
KG

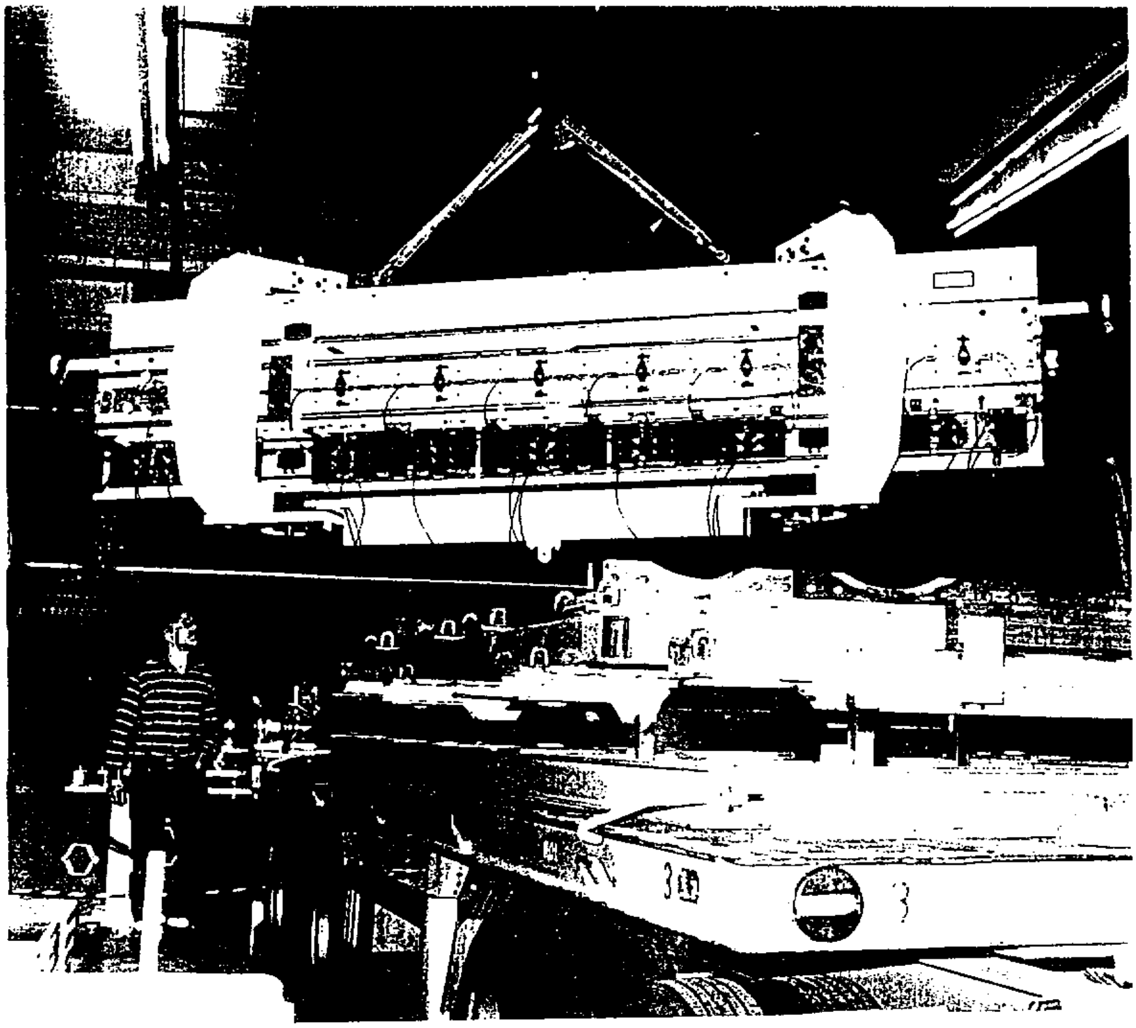

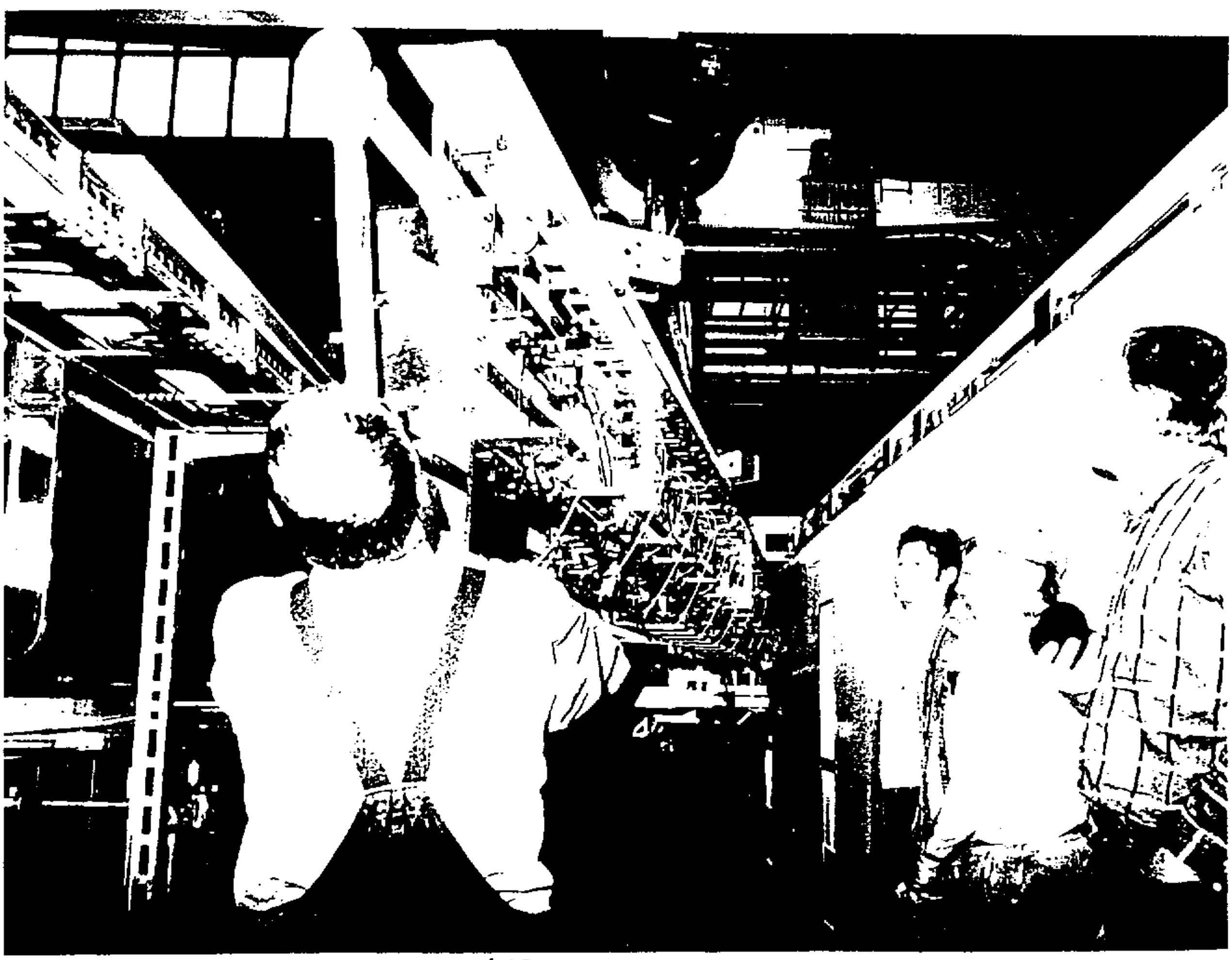

Conditions for laserinterferometric precision alignment of undulators and wirescanners

(~ two weeks)

Undulator installed & prealigned, Infrastructure connected
Vacuum system evacuated
Air conditon running at least two weeks
Tunnel closed
Concrete shielding and all heavy itoms in undulator region in place
Lasersystem & software running

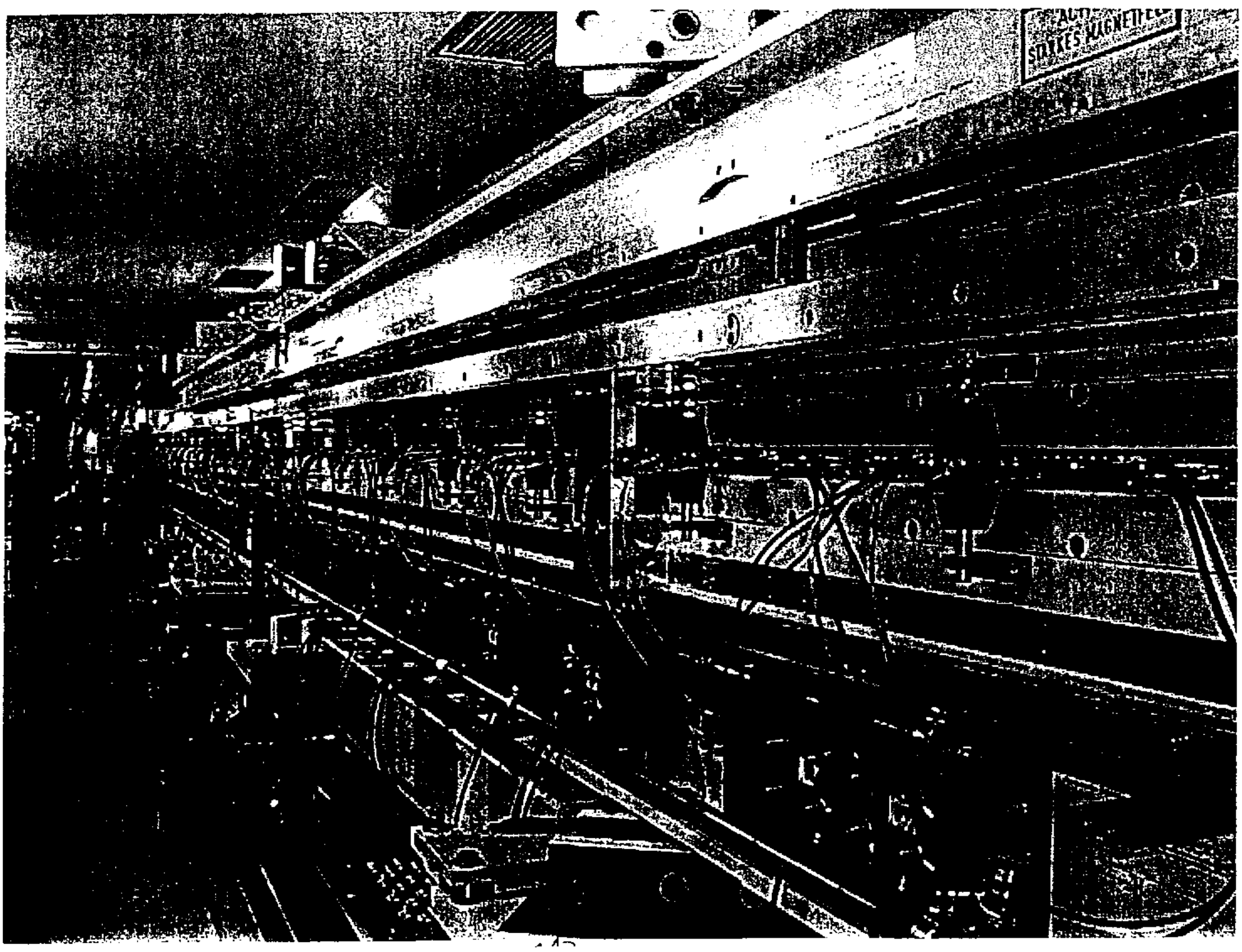

Photon Beam Diagnostics for the SASE-FEL at TTF Phase I

Rolf Treusch

HASYLAB @ DESY

114

R. Treusch

Photon Beam Diagnostics Group

Lutz Bittner
Josef Feldhaus
Ulrich Hahn
Fini Jastrow
Michael Meschkat
Rolf Treusch
Ernst Weiner
Wenxuan Xu

+ external groups from
Dublin City University
Universität Jena
Forschungszentrum Jülich
IFPAS Warszawa

115

Contents

Motivation

Main goal:

Experimental verification of the SASE (self-amplification of spontaneous emission) theory for short wavelengths in the VUV

Details:

- measure photon beam profile and integral intensity
- prove predicted gain for given e-beam and undulator parameters
- comparison of "spiked" structure in the time and frequency domain with theory
- check statistical intensity fluctuations

Experimental setup and detection techniques

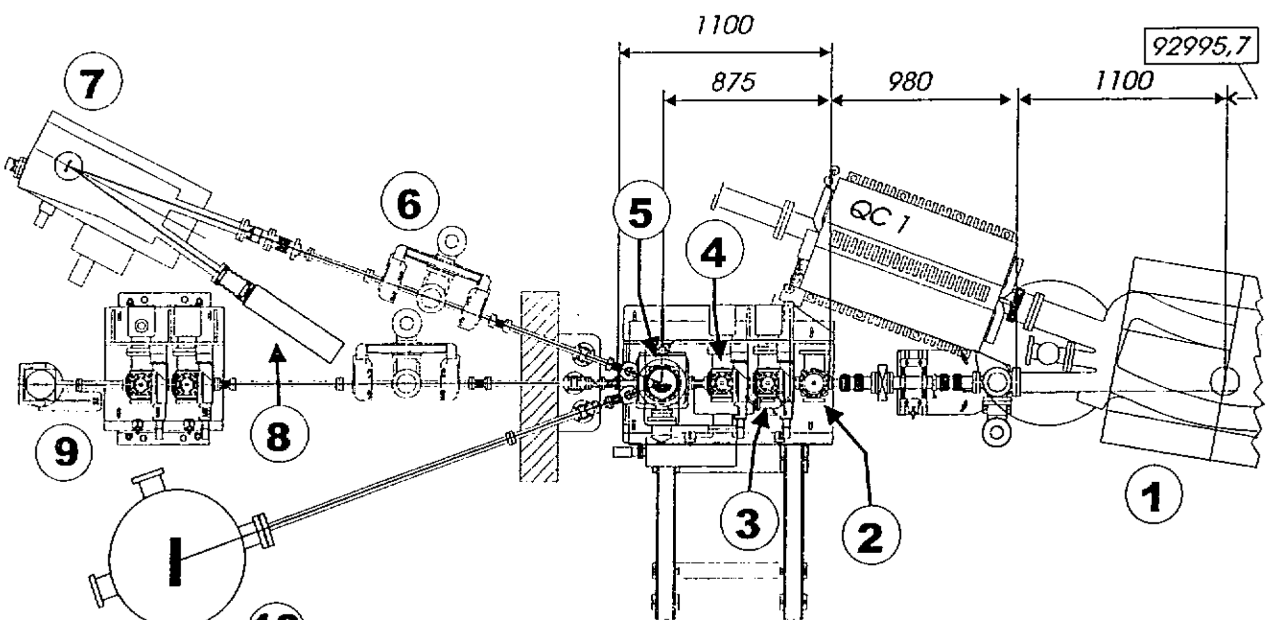

1: bending magnet, **2**: alignment laser, **3**: aperture unit, **4**: detector unit, **5**: deflecting mirror, **6**: TSP + ion pump, **7**: 1 m NIM, **8**: CCD-camera **9**: 2nd detector/aperture unit and focusing mirror (optional), **10**: beamline for autocorrelation experiments / radiation damage investigations

Intensity measurements

Expected FEL parameters:

40 nm< λ_{phot} <120 nm

1 nJ (spont. em.) < E_{pulse} < 400μJ (SASE)

$(P/A)_{max} > 1$ GW/cm^2

bunch/pulse separation: 1 μs (111 ns)

Detectors

- wires and plate (photocurrent)
- PtSi photodiodes in different sizes
- thermopiles: single one and 4×4 matrix
- fluorescent crystals viewed with CCD camera

Fast thermopile matrix detector

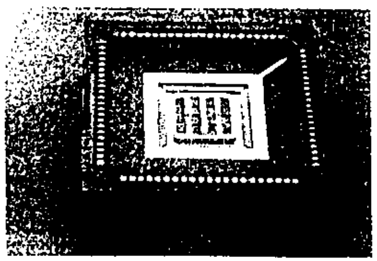

4×4 matrix (prototype)

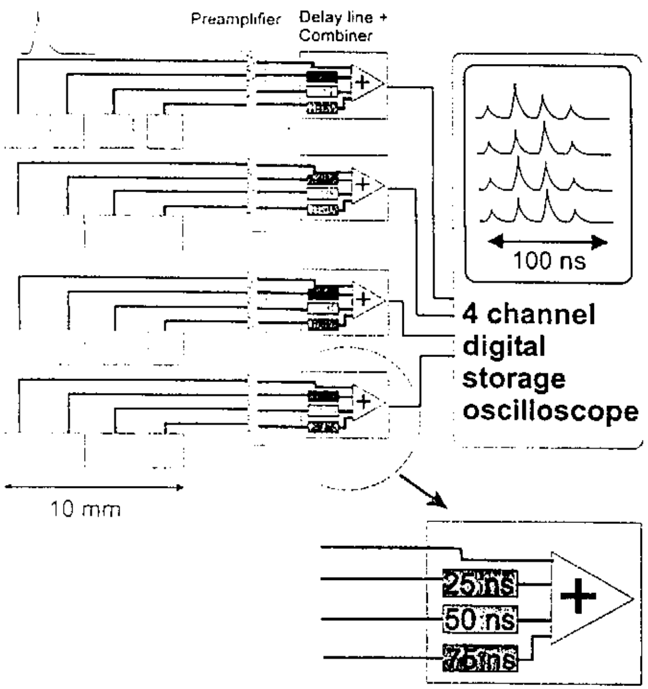

Readout

Fluorescence screens

$PbWO_4$ and Ce:YAG crystals

- fast fluorescence channel of a few / several 10 ns
- emission in the visible range (matching camera sensitivity)
- very homogeneous
- radiation hard
- UHV compatible

Frequency spectrum

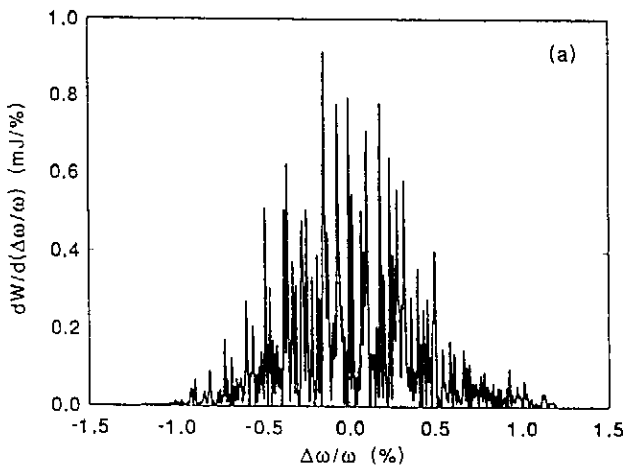

spike width $\Longrightarrow$ bunch length
envelope $\Longrightarrow$ electron energy bandwidth

Requirements for monochromator/detection:

- Resolution: $\frac{\omega}{\Delta\omega} \geq 1 \times 10^4$
- shutter faster than pulse separation

Monochromator

- 1 m normal incidence monochromator with spherical grating (up to 3600 l/mm)
- piezo controlled entrance slit (min. slit width $\approx 1\,\mu m$)
- Cameras for spectrum detection:
  - thinned back-illuminated CCD, UV sensitive
  - fast shutter (≥ 5 ns) ICCD + phosphor

Current status

- beamline front end installed
- chambers with detectors assembled
- monochromator/slit/cameras tested and ready for installation

Water cooled detector unit

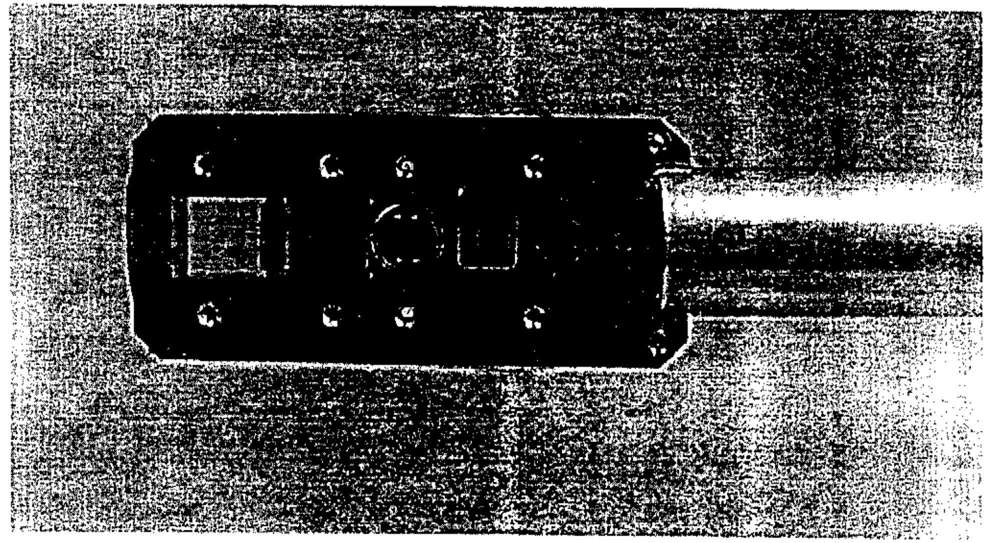

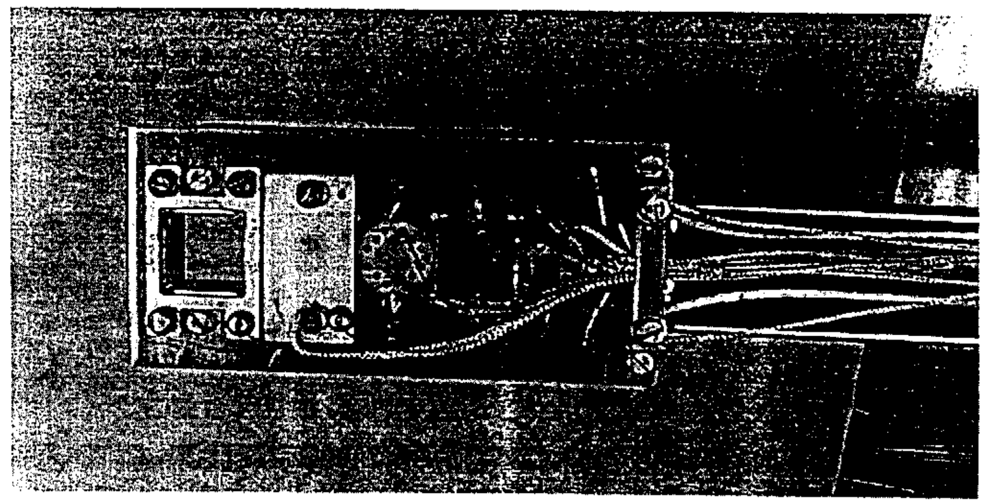

130

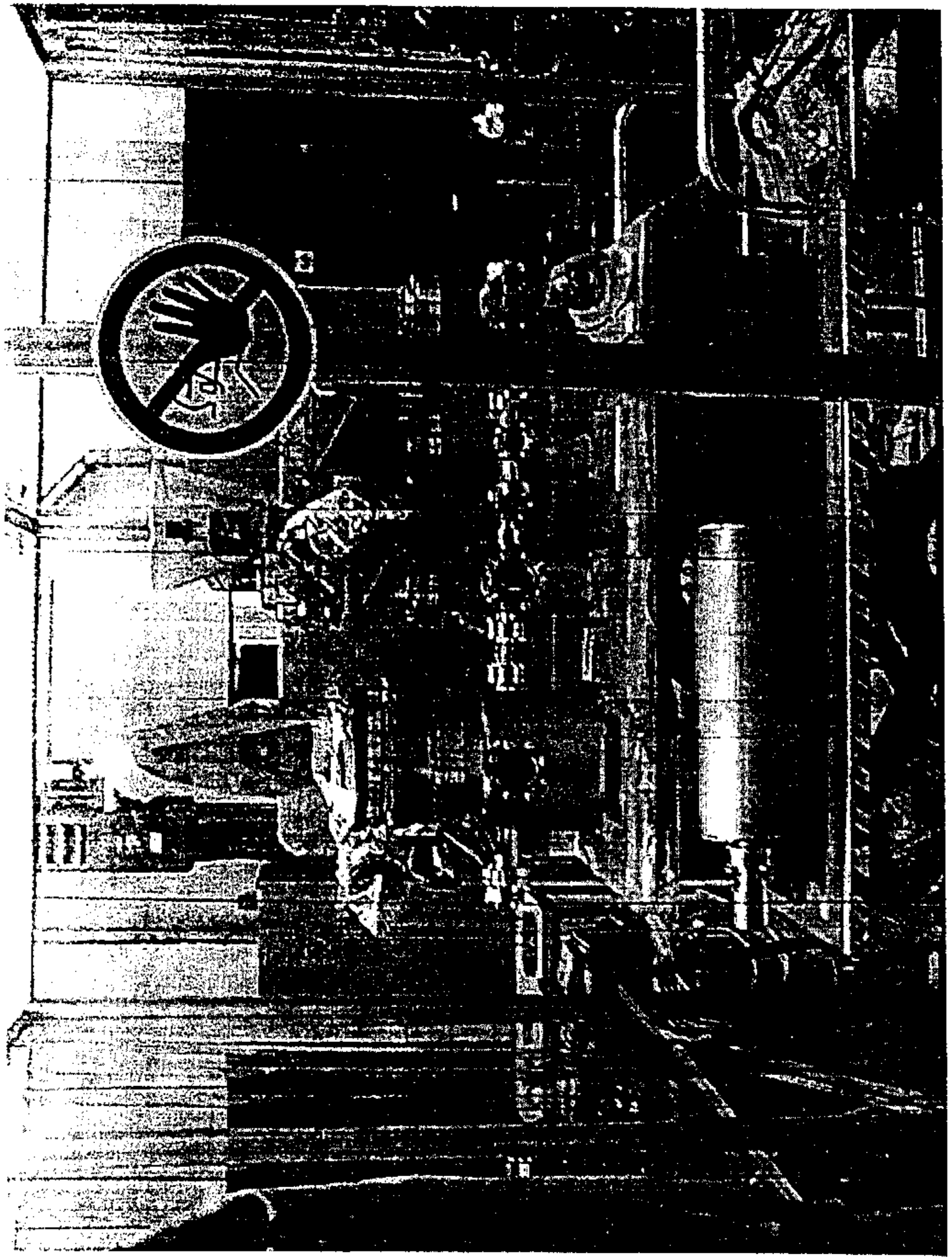

Summary

- unique properties of the FEL

  $\Longrightarrow$ new concepts for detectors

- variation of beam intensity over several orders of magnitude

  $\Longrightarrow$ manifold of different detectors necessary

- lack of experience with extremely intense VUV light

  $\Longrightarrow$ beside photon diagnostics also benchmark for detectors

FEL performance crucially depends on electron beam properties, i.e. all TTF-components. The characterization of the photon beam is also a good means of diagnostics for the e-beam and thus the performance of the machine.

Photon beam diagnostics and machine operation/commisioning will/have to be performed in a close, symbiotic collaboration.

: Curvey ORSAY/SACLAY ACTIVI
: 3/7/99

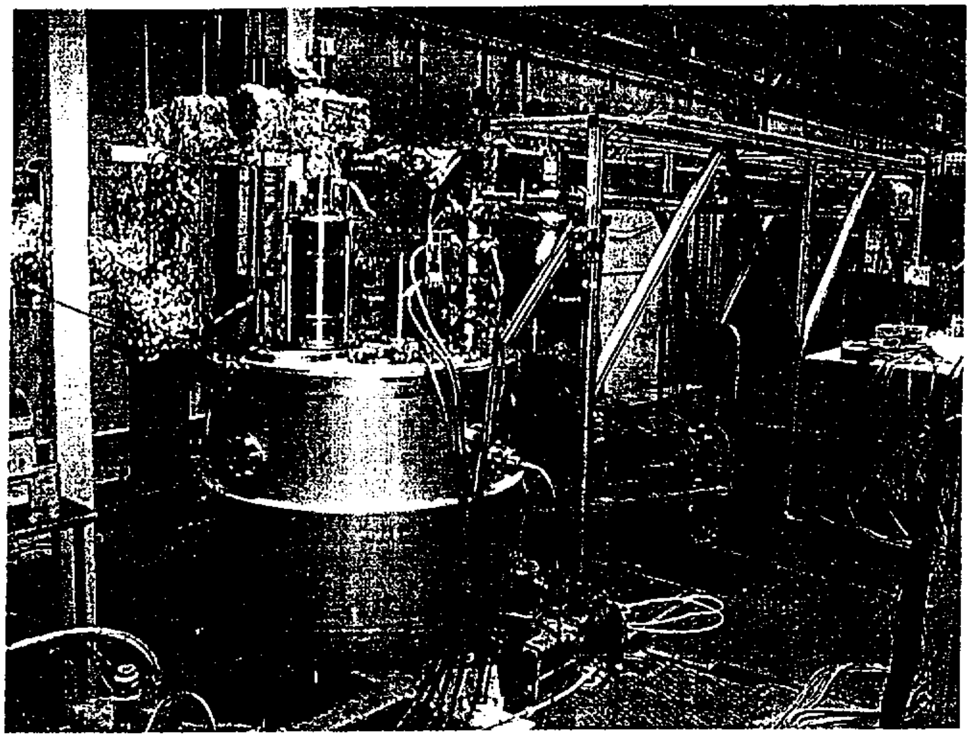

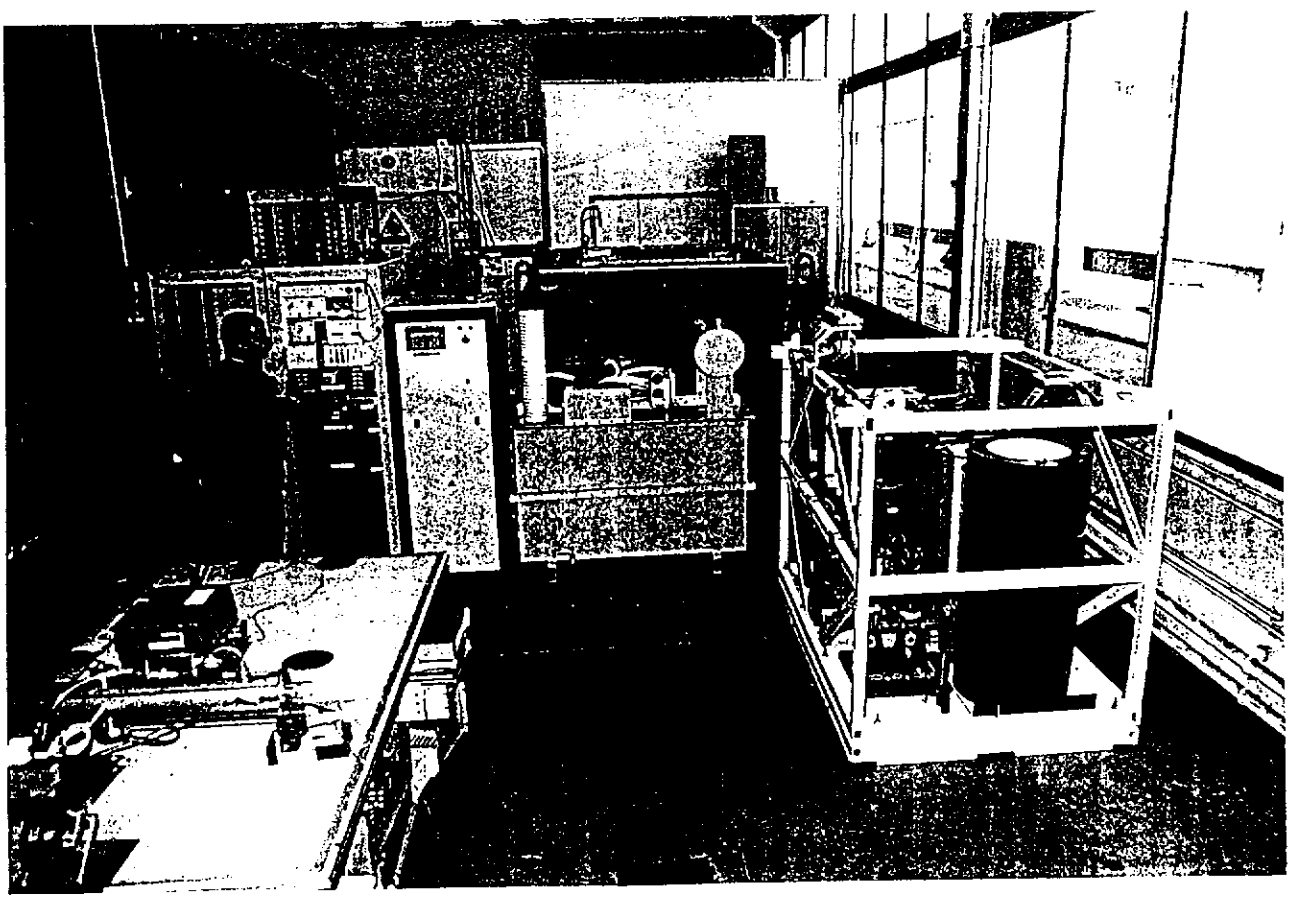

STRUCTURE OF THE TRANSITION

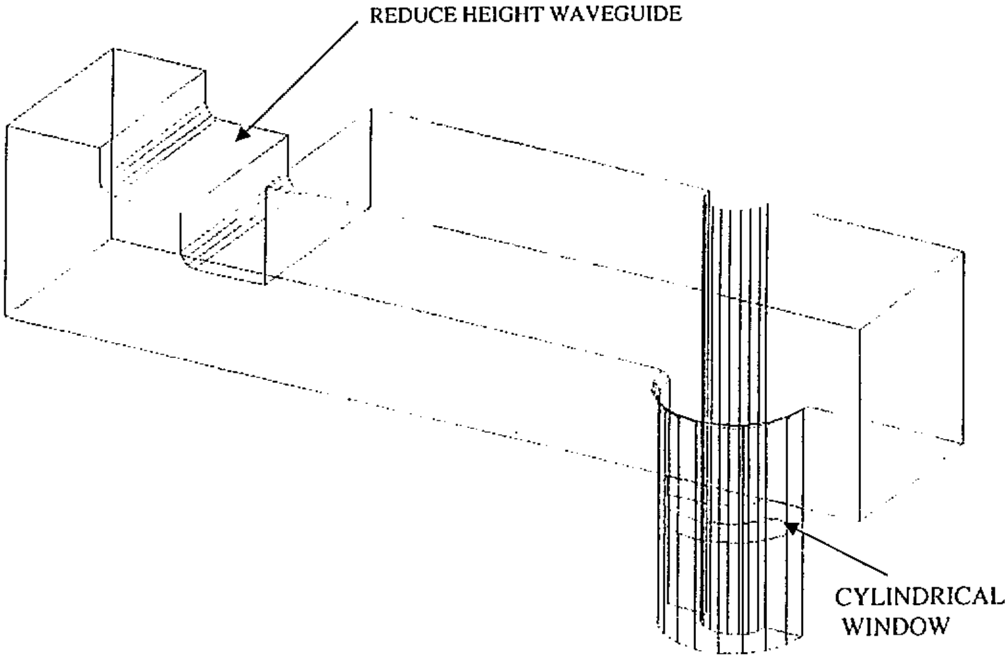

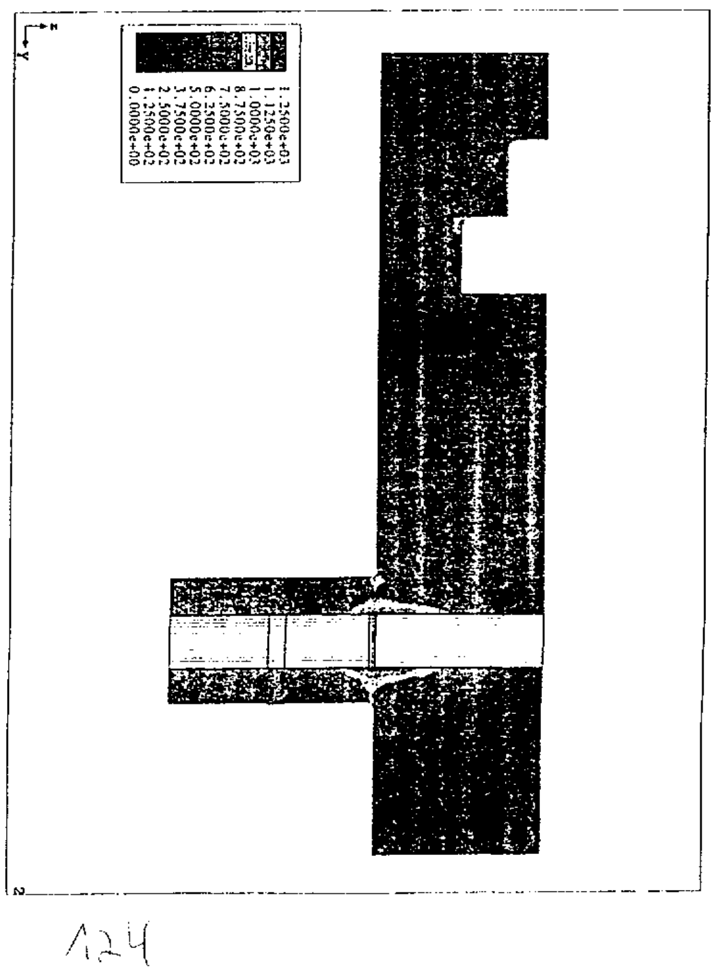

COUPLEUR PROJET TTF

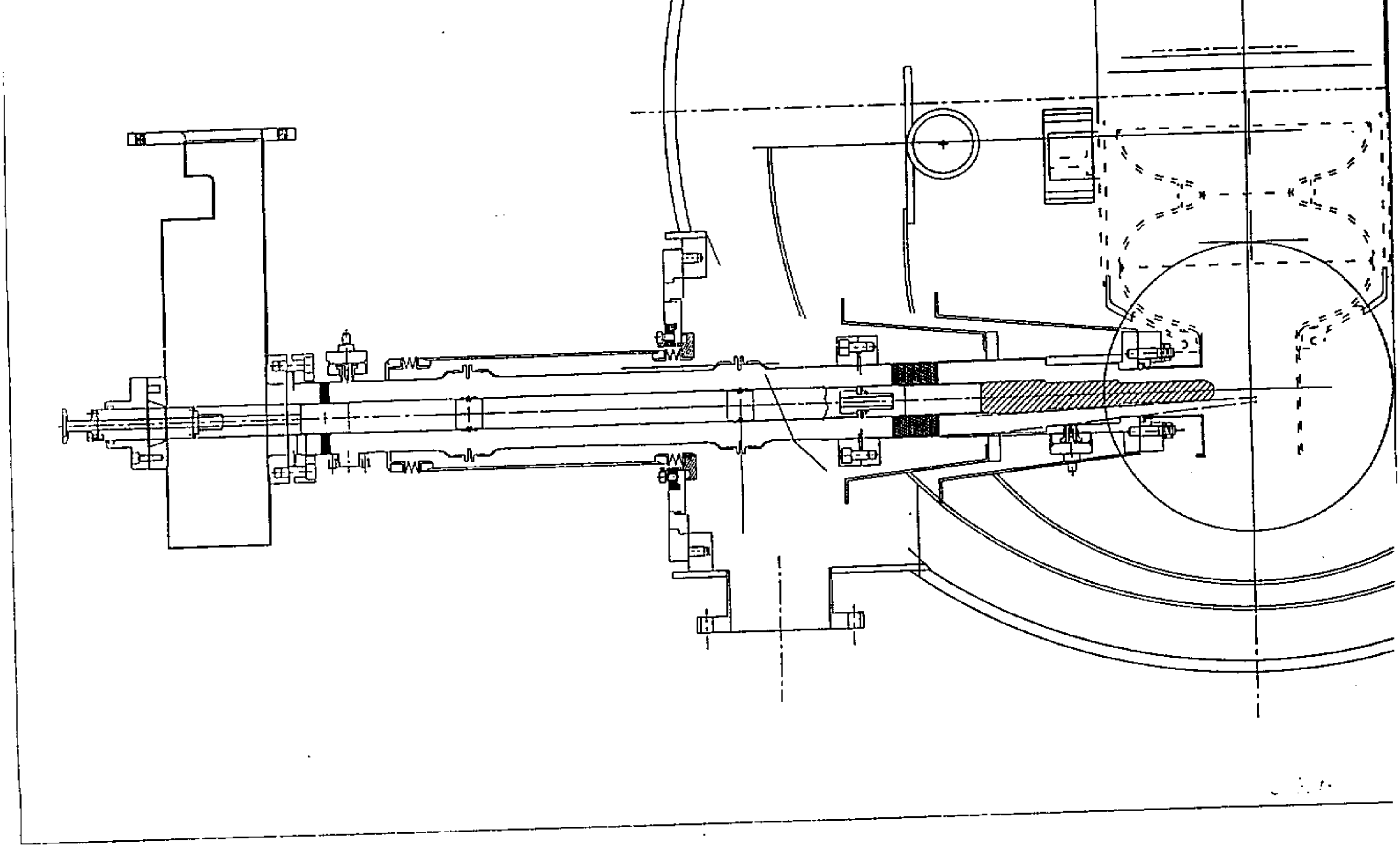

FENETRE TW

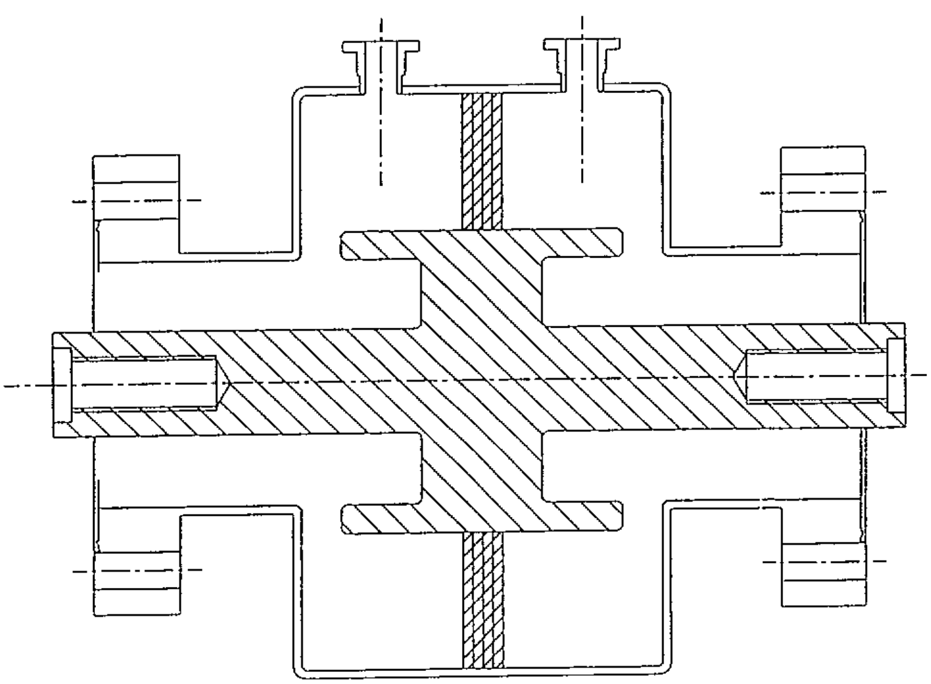

iPN

Cavity Stiffening by Thermal Spraying

CAVITY STIFFENING BY THERMAL SPRAYING:
Thermal considerations and tests on single-cell cavities

I.P.N. - ORSAY

S.Bousson, A. Caruette, M.Fouaidy, H.Gassot, J.C. Lescornet, J. Lesrel, T. Junquera

L.A.L. - ORSAY

J.L. Borne, L. Grandsire, J. Marini

C.E.A. - SACLAY

H. Safa, J.P. Charrier, M. Boloré

CNRS IN2P3

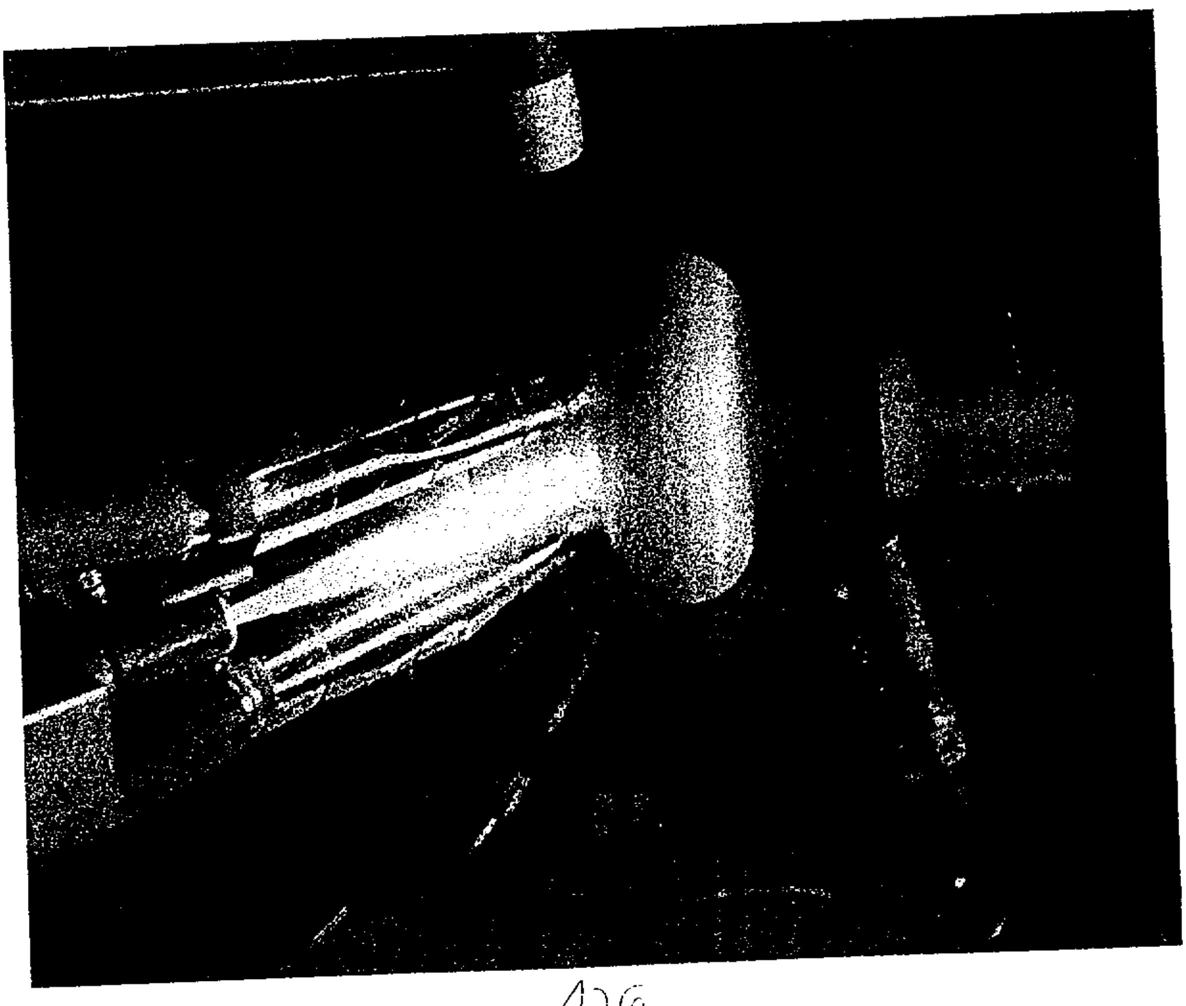

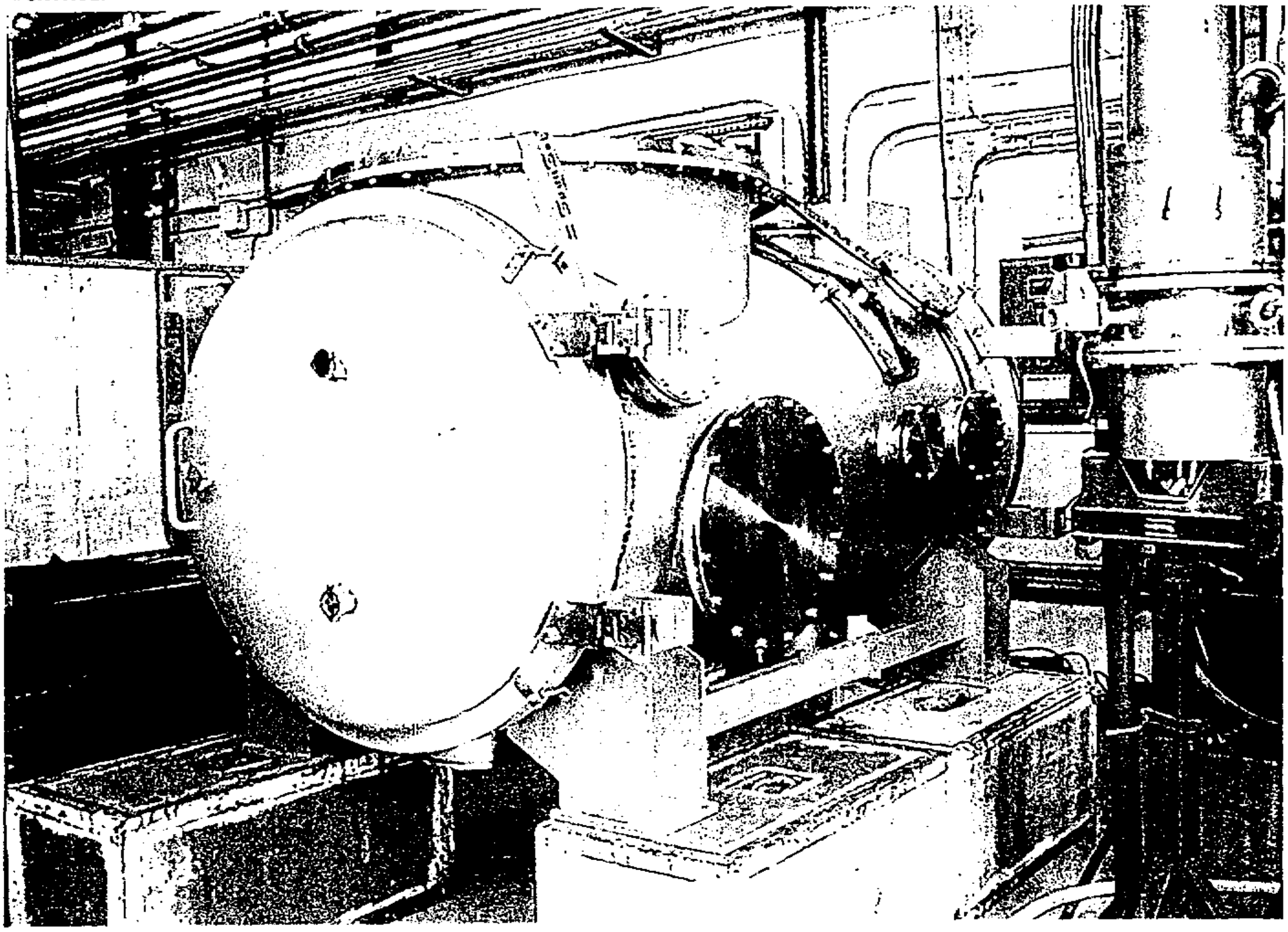

News on TTF Activities at INFN

(LNF, LNL, Milano & Roma2)

Presented by **Carlo Pagani**

128

1) Cryostat Design & Cryomodule Assemby

- Cryostats # 2 & # 3 - including WPMs
  - # 2 successfully in operation
  - # 3 assembled and ready for cooldawn
- Cryostat # 1 to # 1*
  - Delivery expected by September '99
- New Assembling Tools - in fabrication
  - Due by September '99
- Cryostats # 4 and # 5 in fabrication with WPMs
  - Expected delivery at DESY: November '99
    - Composite posts (FNAL design) in fabrication
- Cryostats # 6 in fabrication with WPMs
  - Expected delivery at DESY: April 2000

2) Photocathodes (P.Michelato)

- TTF Injector II Cathode System
  - INFN Photocathodes in operation at DESY and FNAL
  - New System for the DESY gun: ready by October '99
- R&D Activity
  - "New" photoemissive materials: K-Te & K-Cs-Te
  - Poisoning and life tests on new cathodes
  - Thermal emittance measurements: ready to start

3) Beam Diagnostics (LNF & Roma 2 groups)

- Beam instrumentation
  - OTR screens
  - Pepper pot
  - Fast electronics for the strip-lines
- Beam measurements (M. Castellano)
- New Diagnostics
  - Diffraction radiation experiment installed

4) Cavity Fabrication

- Standard Cavities - A16 to A18 measured
  - A18 : 27.8 MV/m @ Q=9.7 10^9 - Average gradient > 25 MV/m
- New Fabrication Technologies -
  - Spinning at LNL
  - Plasma spray at Milano

5) Theoretical activity (M. Ferrario)

- Beam behavior in Superstructures

ELECTRON SPECTROMETER

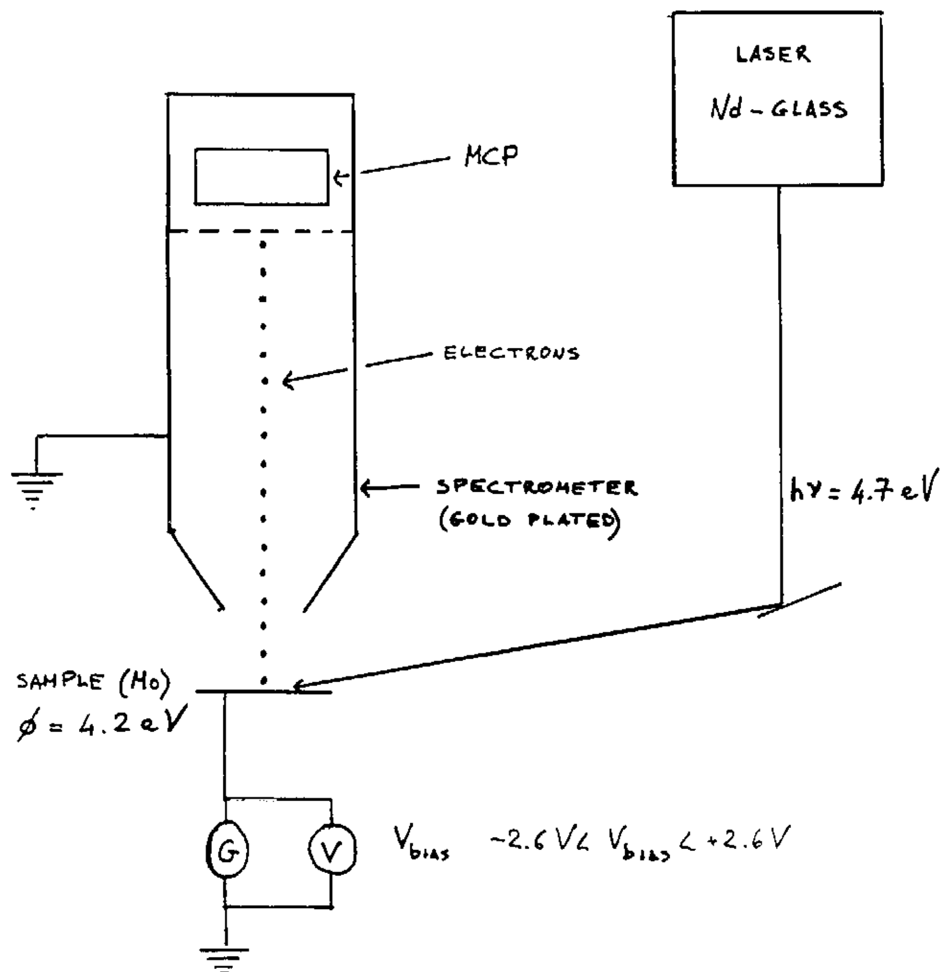

CONTACT POTENTIAL NEUTRALIZATION ⇔ V_{bias}

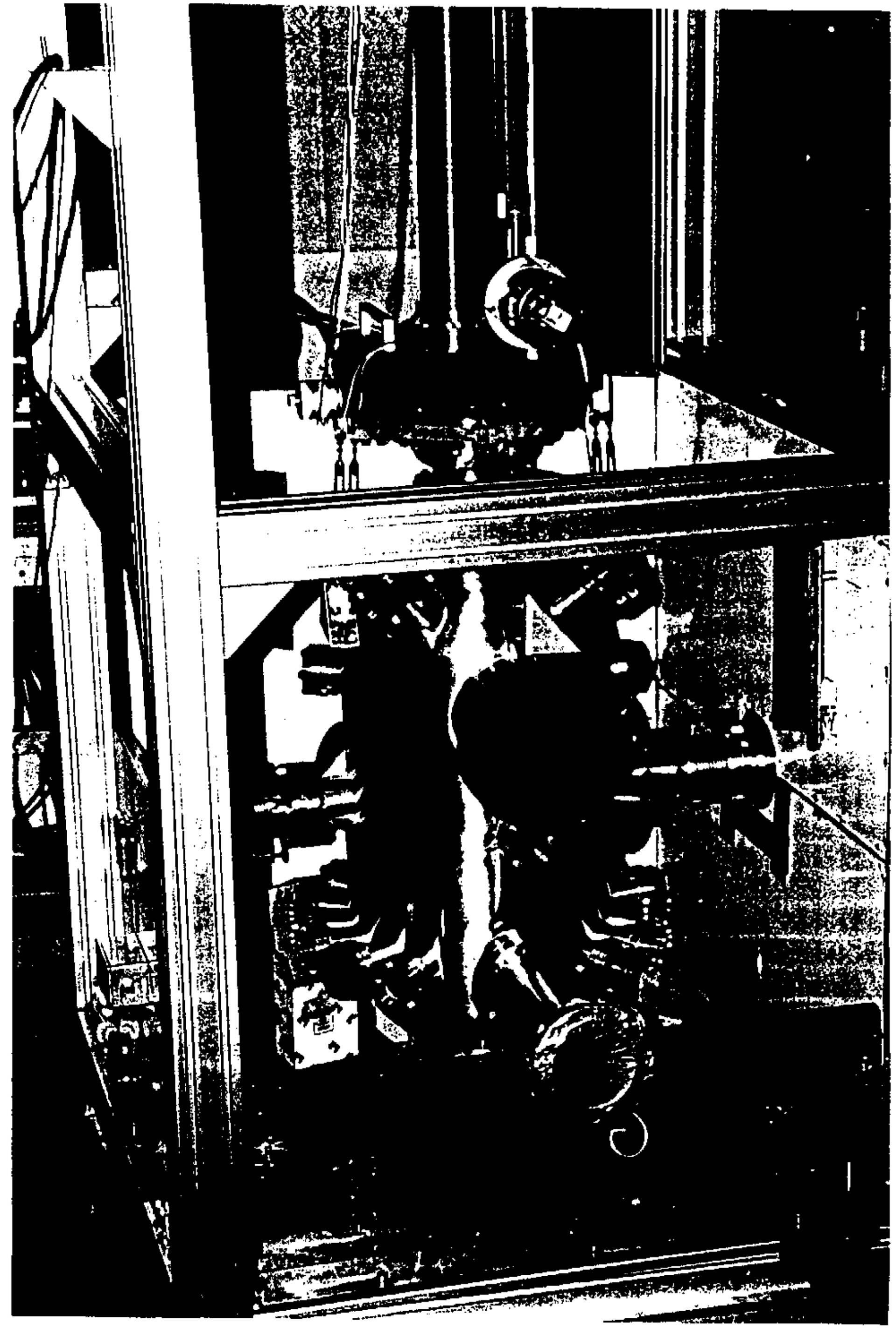

MUMETAL CHAMBER FOR THE TOF SPECTROMETER $|B| \leq 20$ mGauss

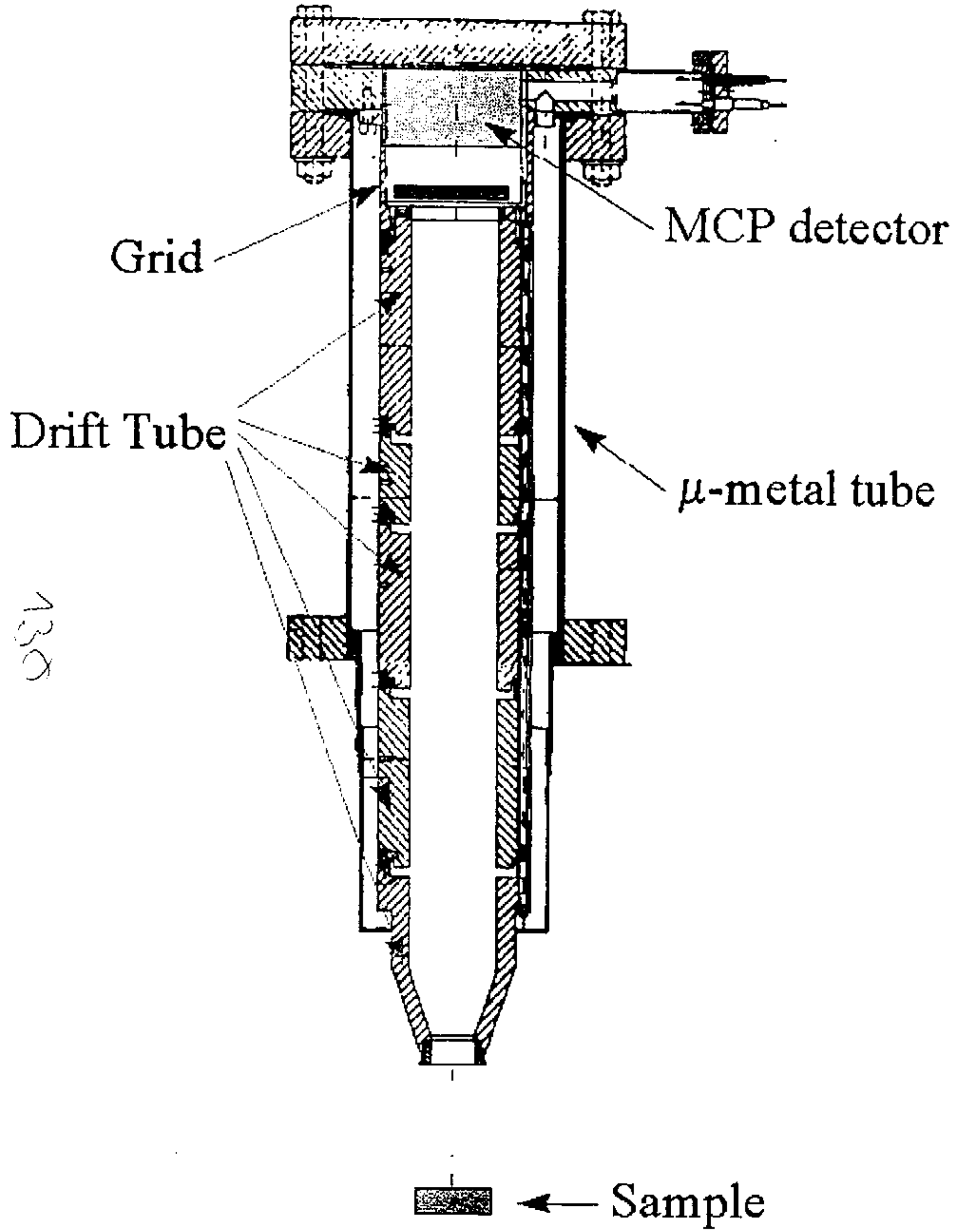

130

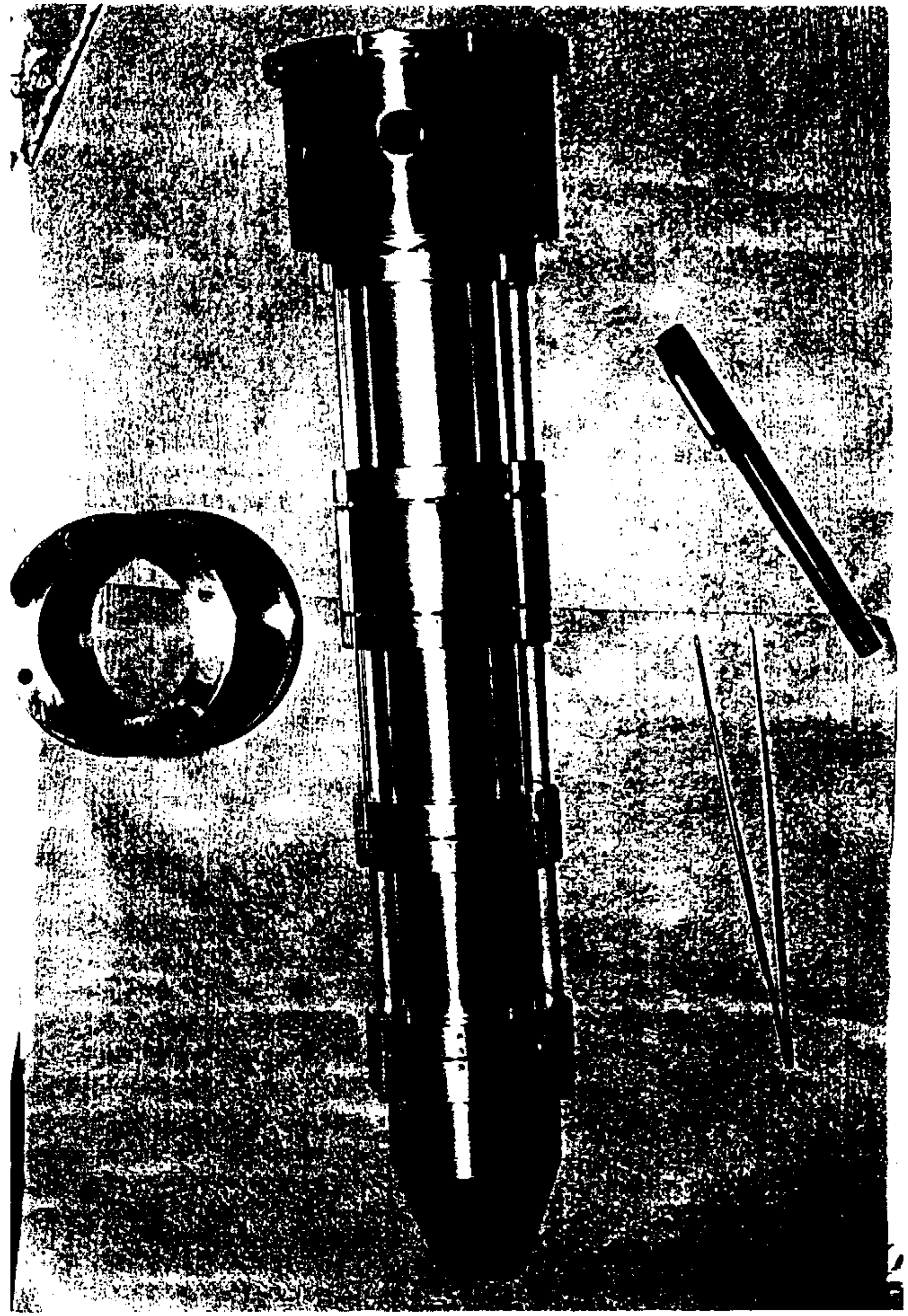

ToF SPECTROMETER

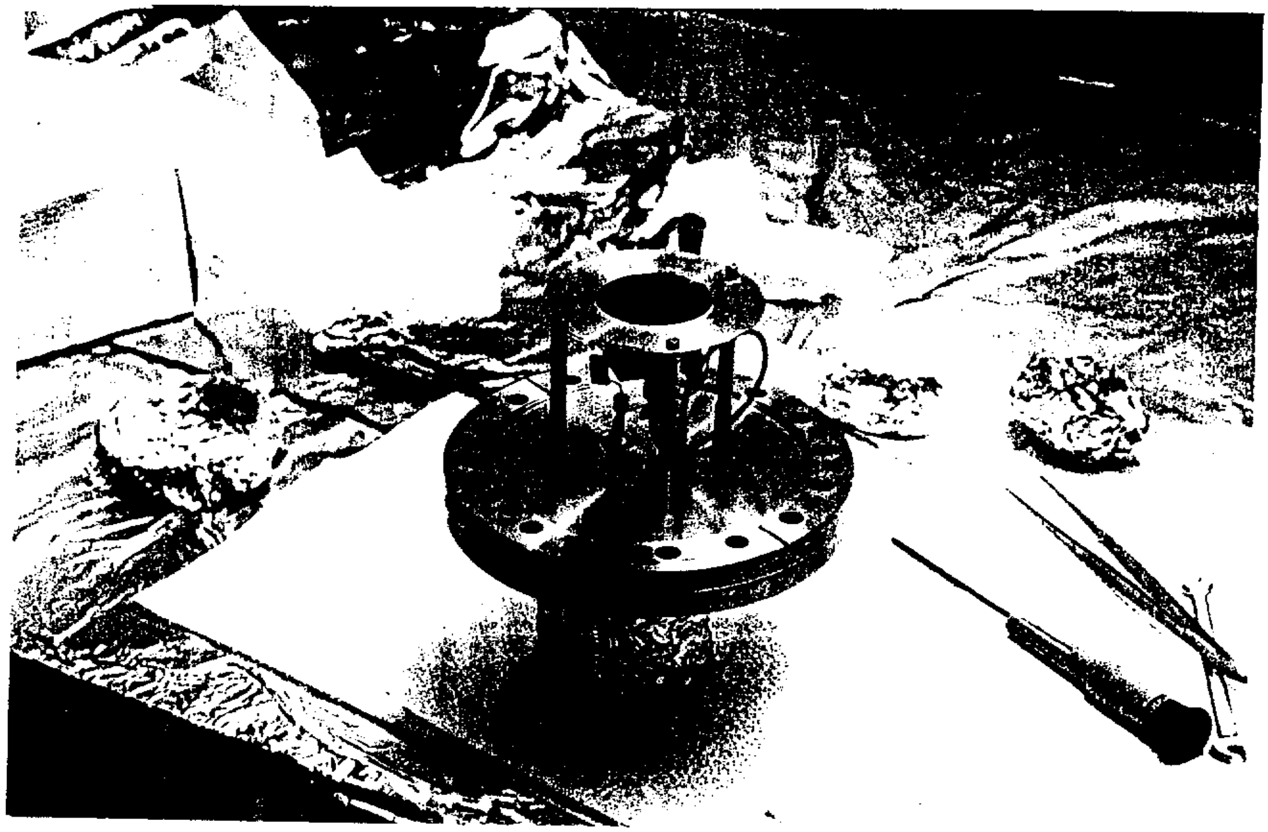

MCP DETECTOR

Mo Φ: 4.2eV hν = 4.7eV
Time of flight of photoemitted electrons from Mo (different bias potentials)

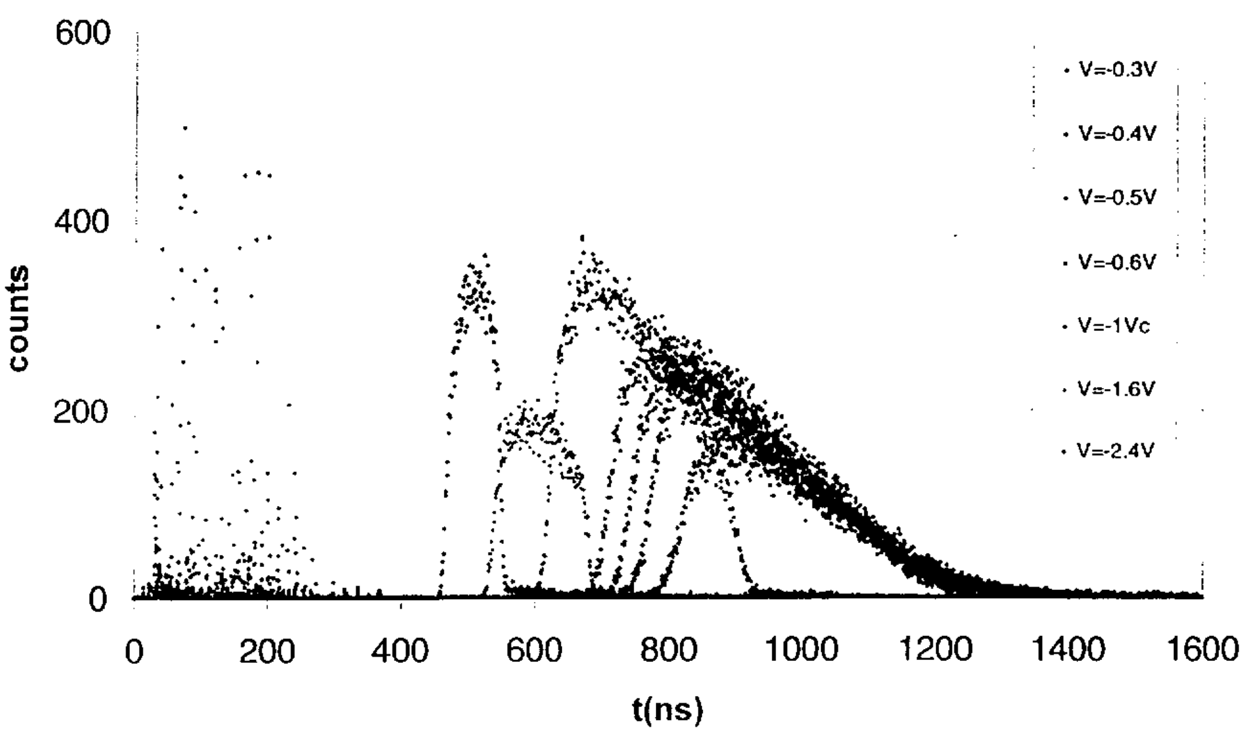

Mo Φ: 4.2eV hν = 4.7eV

Energy spectrum of photoemitted electrons from Mo (different bias potentials)

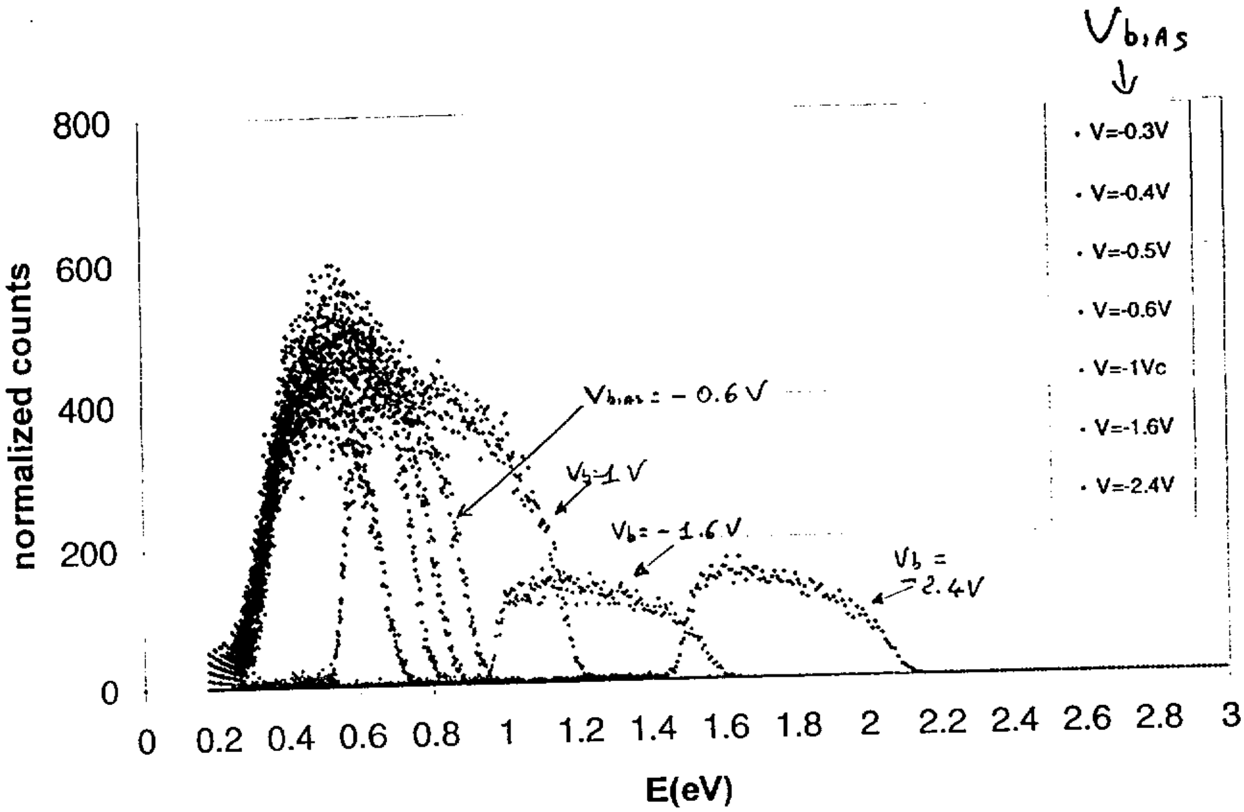

132

Test without HPR at CERN

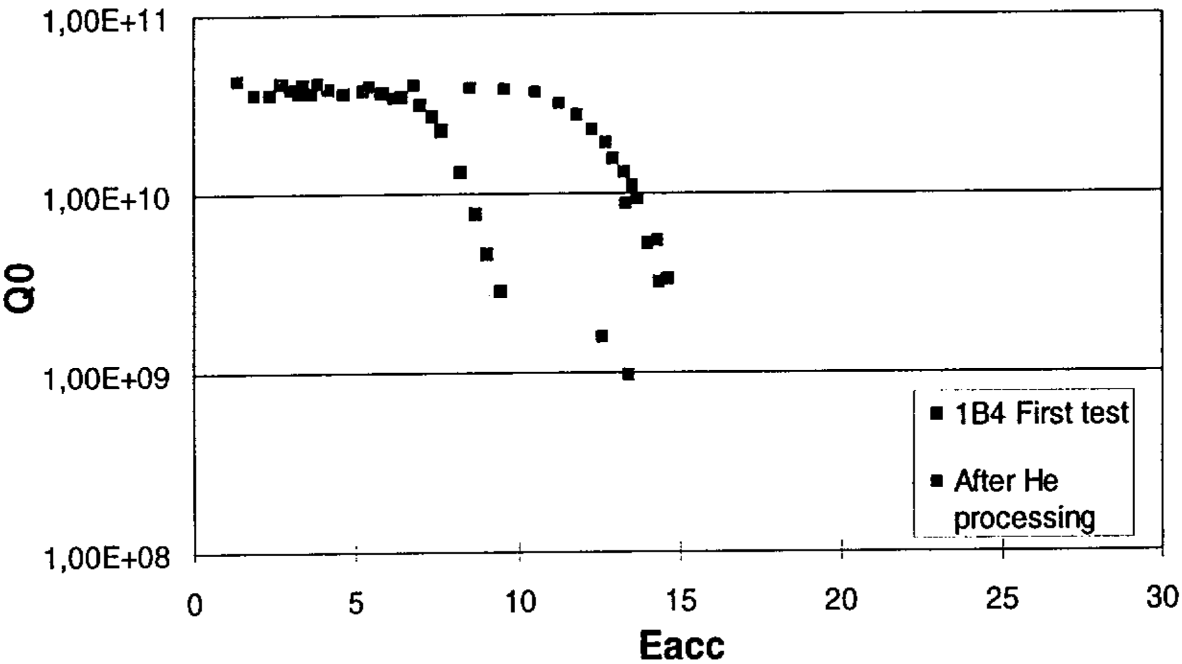

05.07.99 Lutz Lilje DESY -FDET-

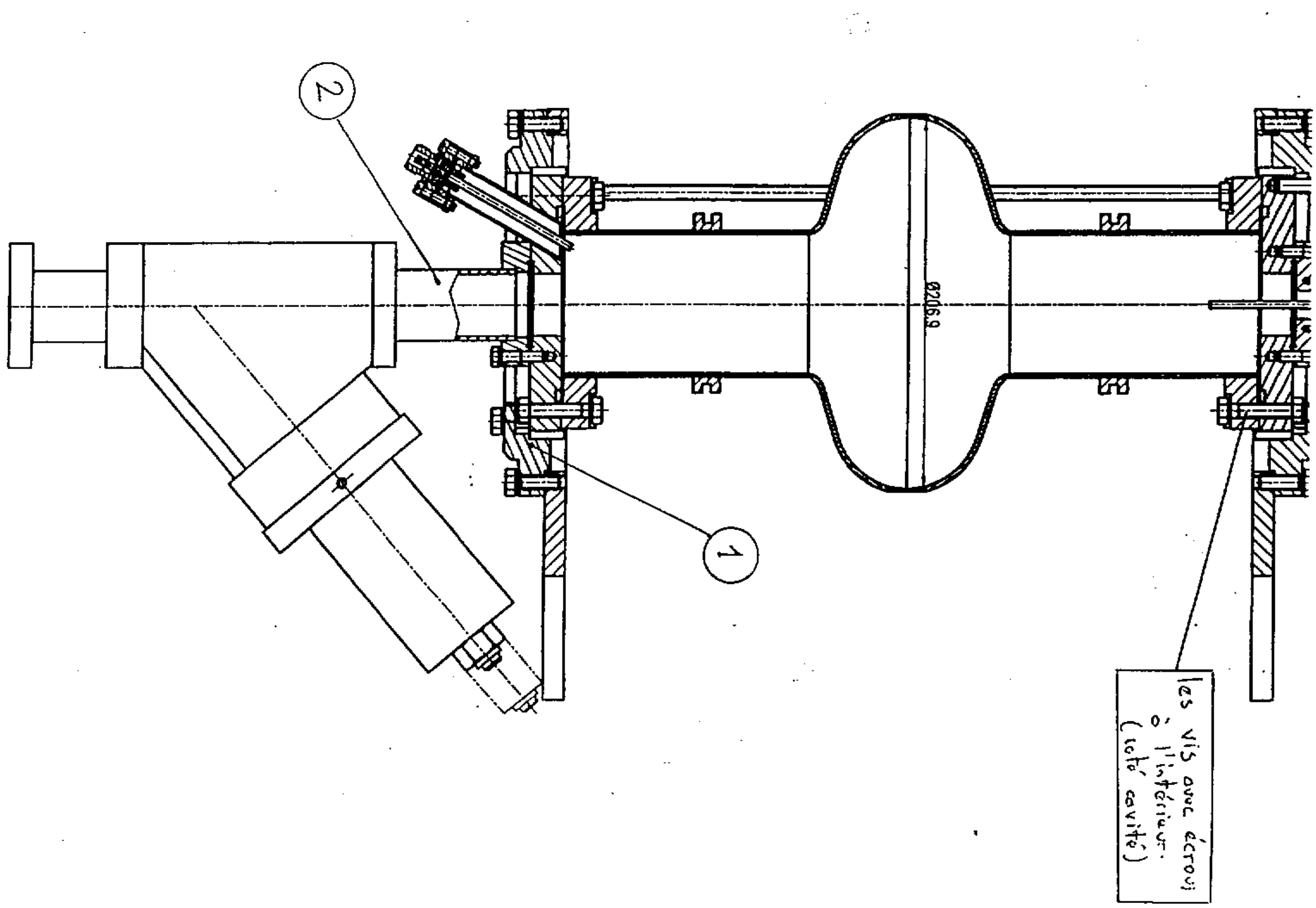

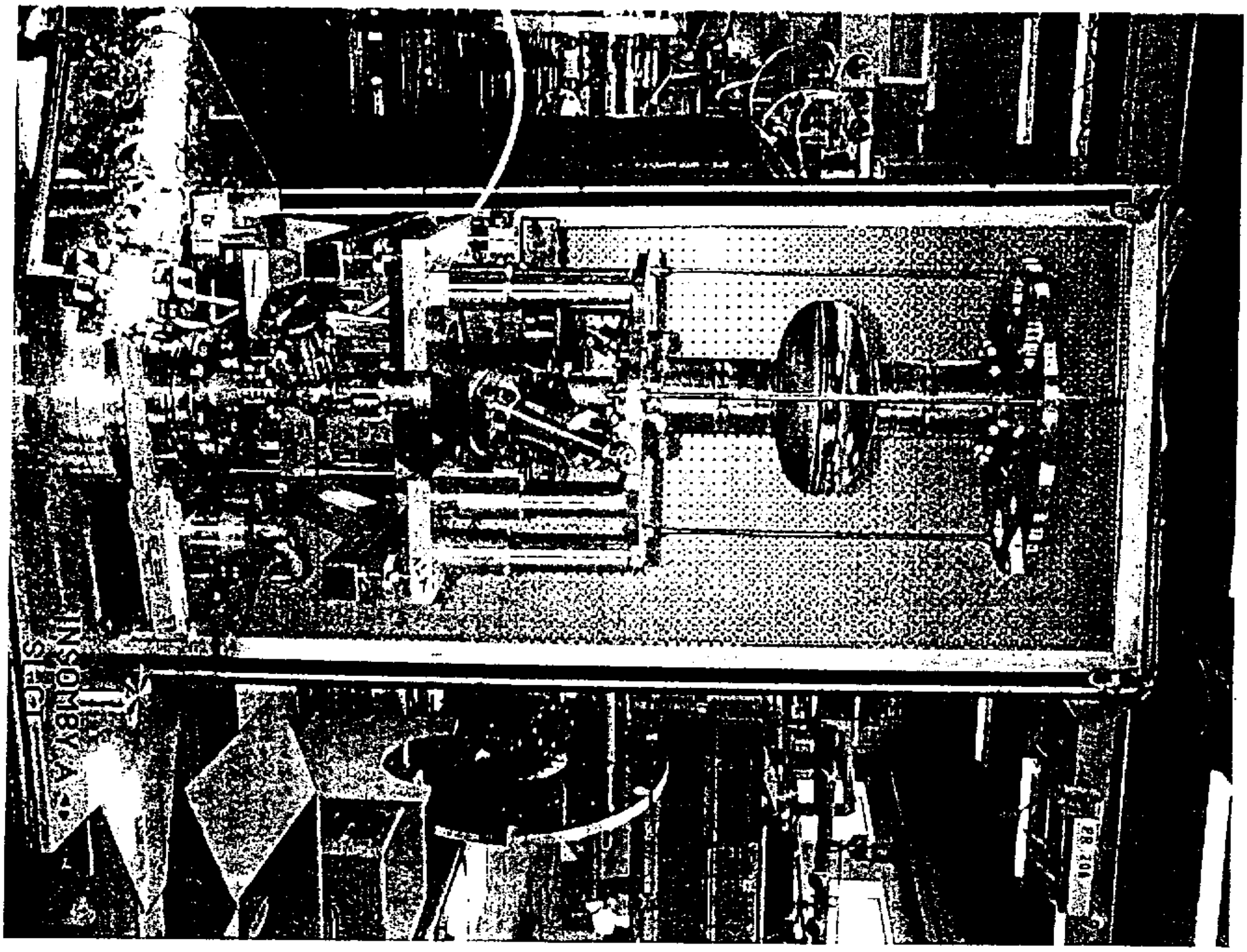

Test with HPR at CERN

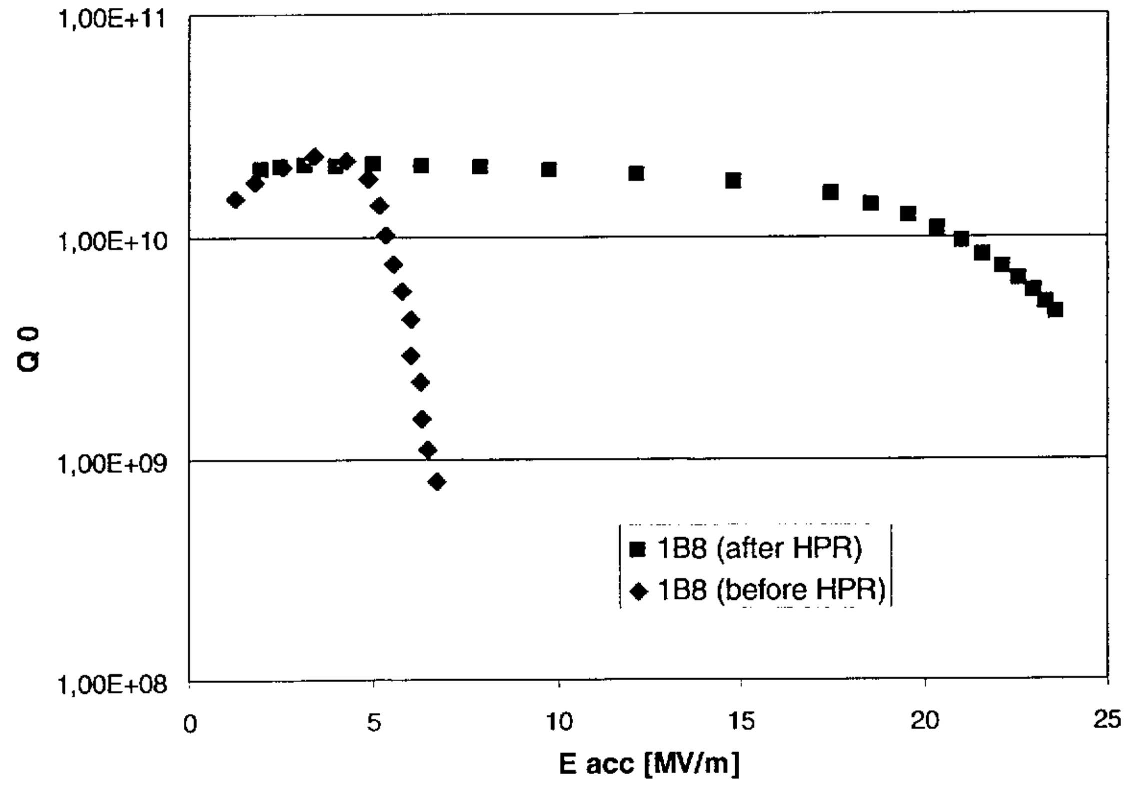

Results at CERN

- 1,3 GHz test stand is operational
- Water rinsing system is operational, minor problems during first setup
- First one-cell EP possible next week
  - mechanics finished
  - leak check done

Forschungszentrum Karlsruhe
Technik und Umwelt

OVERVIEW OF THE "SMES" MODULATOR DEVELOPMENT (Feb 26, 1999)

	STATUS	SCHEDULE	July 8, 1999 status/sched
POWER SUPPLIES FOR SMES AND CAPACITOR	ORDERED	10/99 DELIVERY	10/99 first tes in Eston
POWER PULSE FORMER UNIT	BEING ORDERED BY COMPONENTS	11/99 DELIVERY	ordered 11/99 start age -03/00 test in Est
PULSE TRANSFORMER	DELIVERED	1/99 DELIVERY	delivered
SAFETY SYSTEM	SPECIFICATIONS READY	11/99 DELIVERY	12/99-01/00
CONTROL SYSTEM	UNDER WORK	11/99 DELIVERY	03/00
SC MAGNET SYSTEM	MODEL COIL SUCCESSFULLY TESTED	9/99 DELIVERY	first coil ready 11/99 2nd coi
CRYOSTAT incl. CURRENT LEADS	BEING ORDERED	10/99 DELIVERY	ordered, 12/99 deliver 01-03/00 assem
MODULATOR CONSTRUCTION		12/99 – 2/00	- 03/00
SYSTEM TEST AT FZK	PREPARATIONS	3/00 - 4/00	04-05/00
TRANSPORT & MOUNTING		5/00	06/00
SYSTEM TEST AT DESY		6/00	07/00

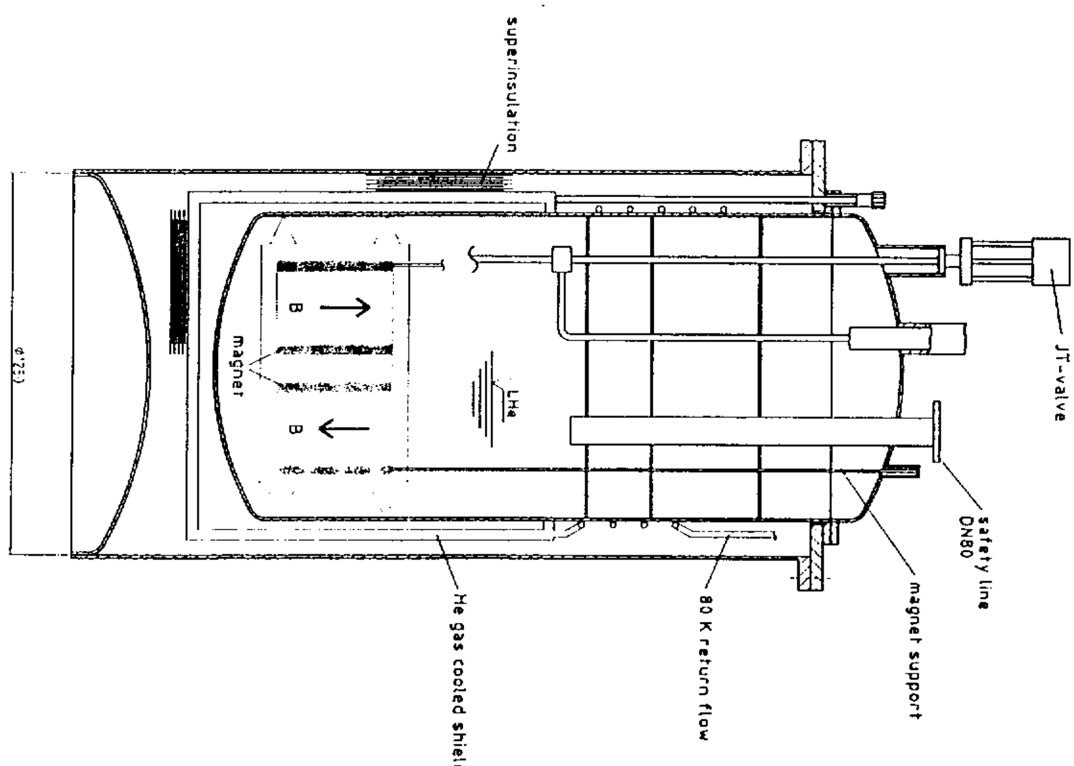

25 MW SMES Modulator Cryostat

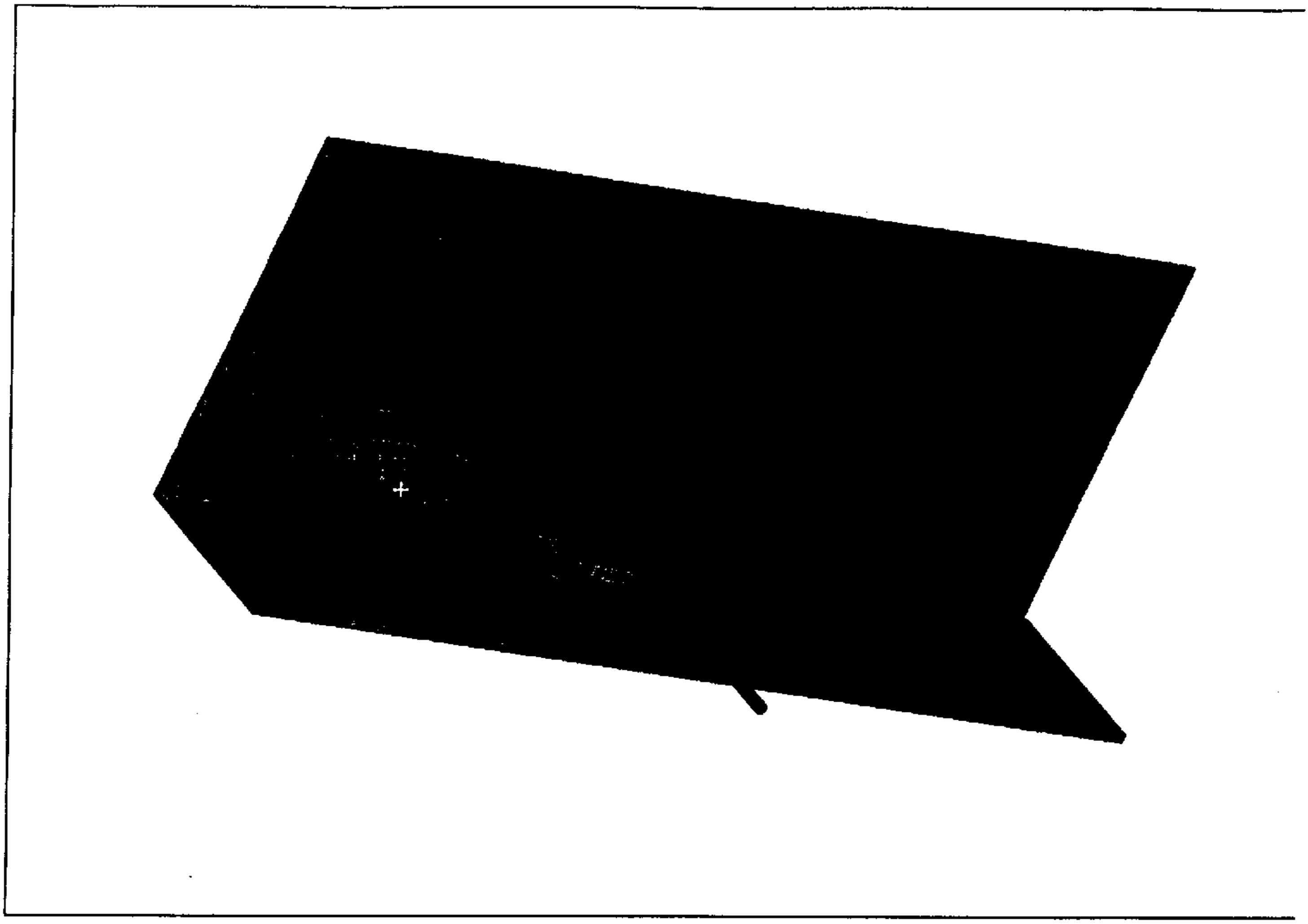

The patented modulator scheme is shown:

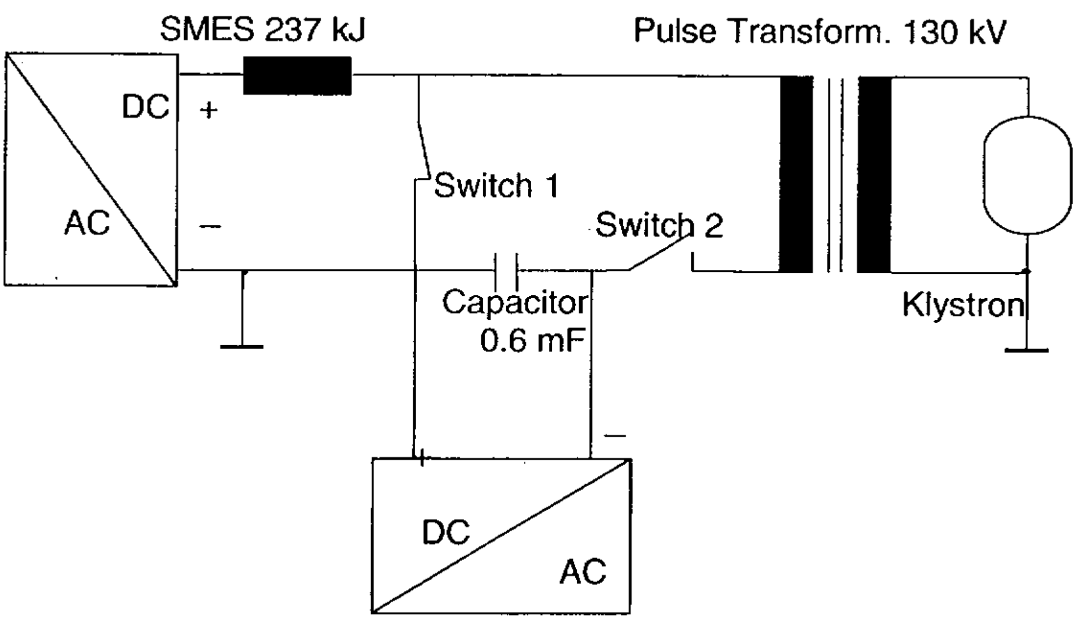

Simplified diagram

A new proposed accelerating structure consists of two standing wave coupling resonator systems

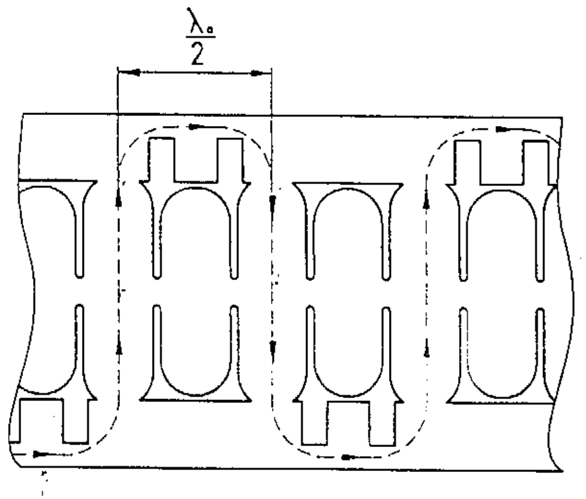

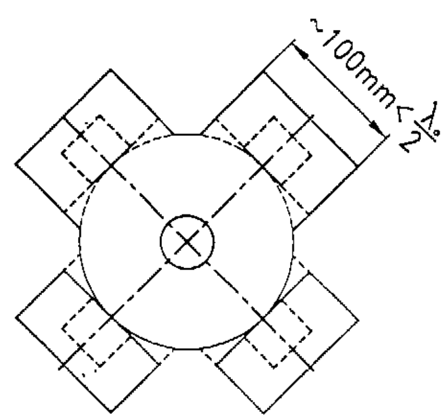

Advantages of new configuration

1. High accelerating gradient

   $\text{Acc.gradient}_{\text{New config.}} \approx 2 * \text{Acc.gradient}_{\text{TESLA}}$

2. No problem with trapped modes

   a) transverse

   b) longitudinal

3. Easy tolerance (according to P. Avrakhovs simulations)
   ↓8m ↓4m
   0.5 ÷ 1 MHz - for accelerating resonators
   4 ÷ 8 MHz - for coupling resonators

4. Few input couplers

   (1 per 8 meters)

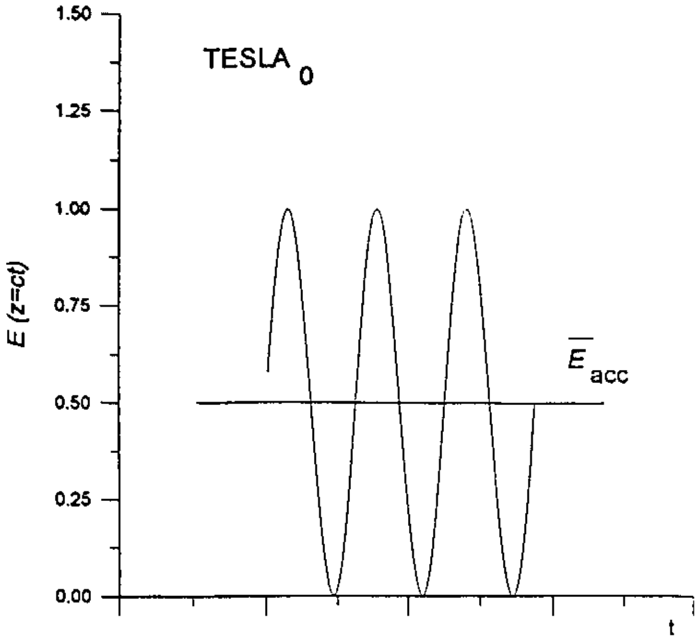
TESLA 0
E (z=ct)
1.50
1.25
1.00
0.75
0.50
0.25
0.00
$\overline{E}_{acc}$
t

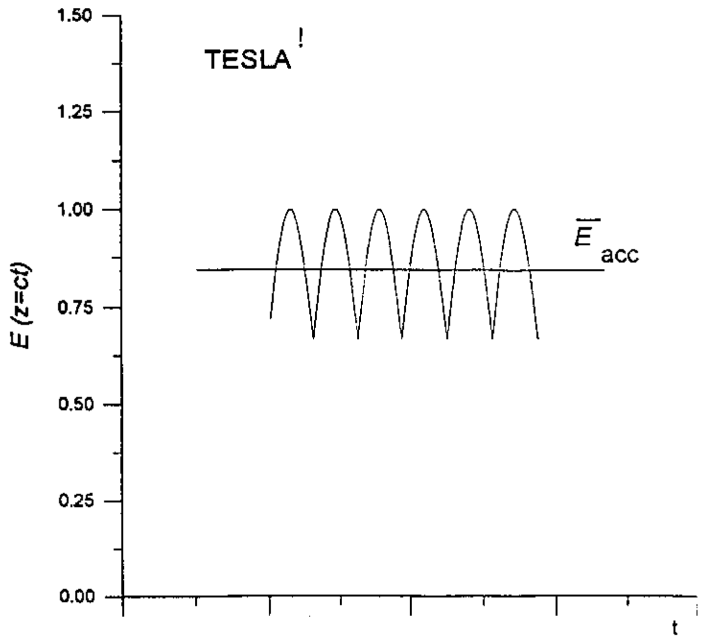
TESLA !
E (z=ct)
1.50
1.25
1.00
0.75
0.50
0.25
0.00
$\overline{E}_{acc}$
t

Progress on the FEL (DESY) gun

- new location of test stand
  (operation during linac shutdown)

- rf gun 2 (tuned to 1.3 GHz) conditioned
  - 5 Hz, 30 μs FT (total 40 μs) → 2.7 MW
    (circulator, clystron)
  - 5 Hz, 490 μs FT (total 500 μs) → 2.0 MW
    (higher <P>, cooling)

- continue until July 12th

- next shut down of linac:

  → operation with beam
  (cathode system)

- future: HGF application (MBI, BESSY, TUD, DESY)

  → independant test stand (hall II)
  for
  - rf guns (low ε, small σ_z)
  - FEL injector
  - flat beams (damping rings)

Low energy test beam Line

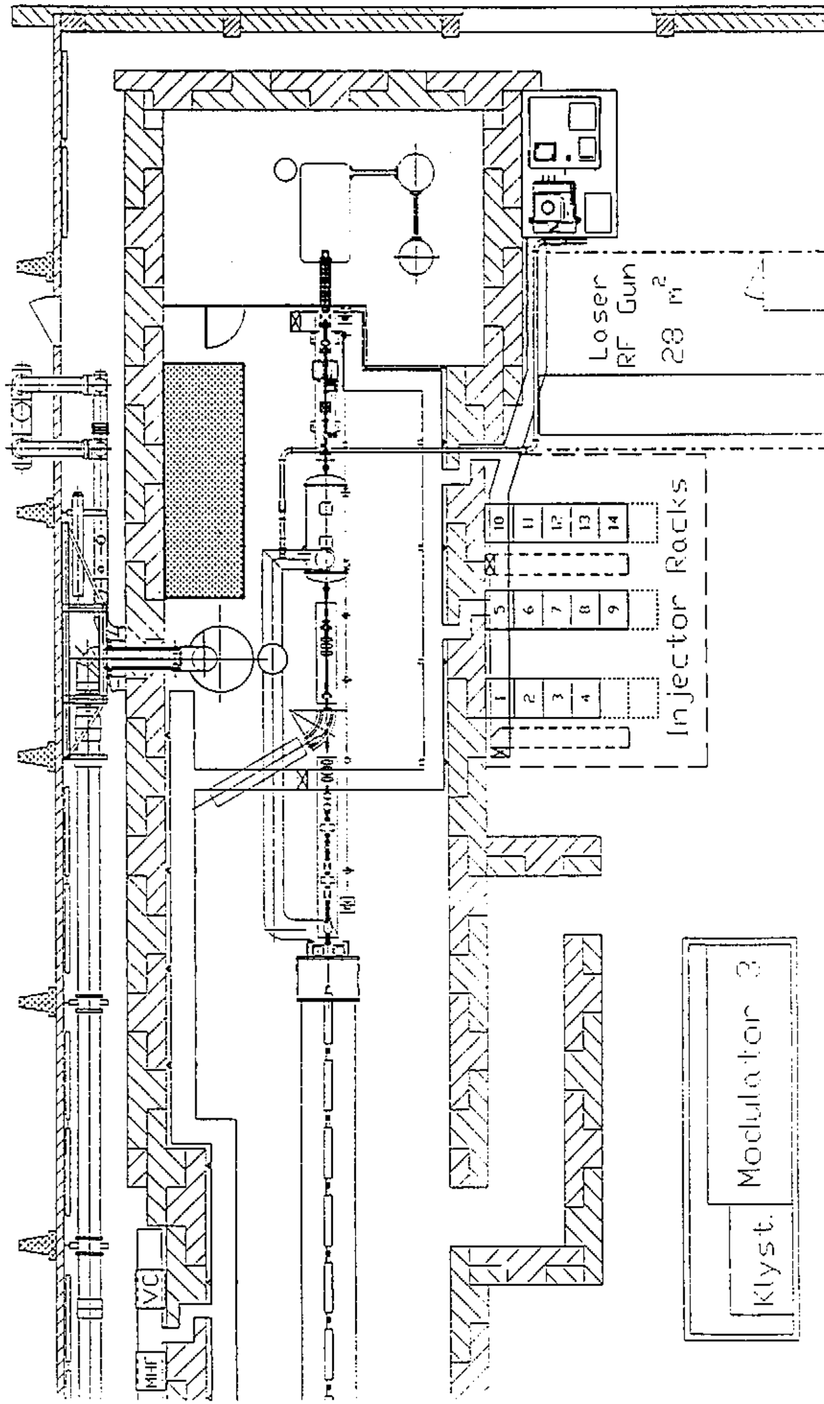

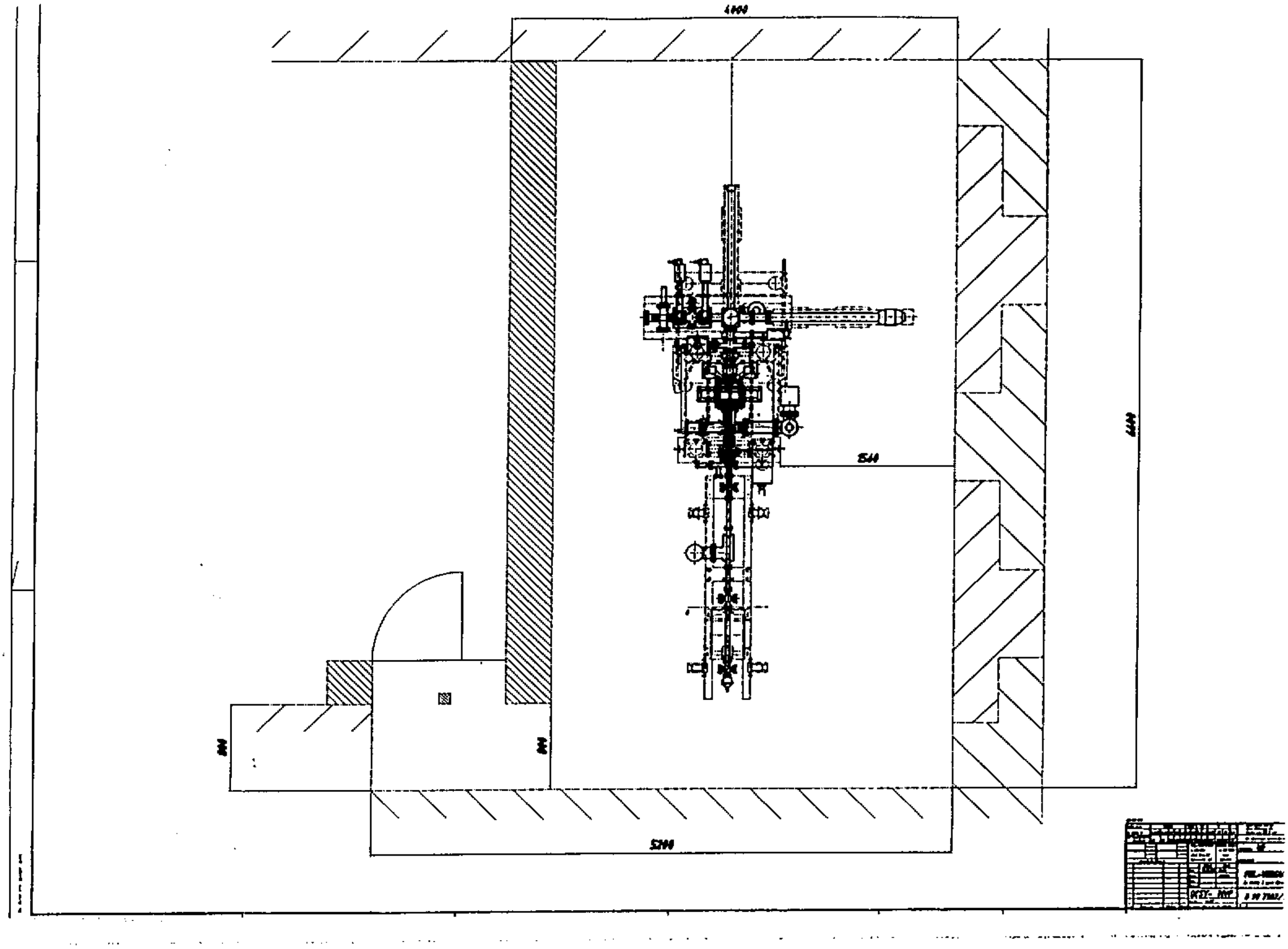

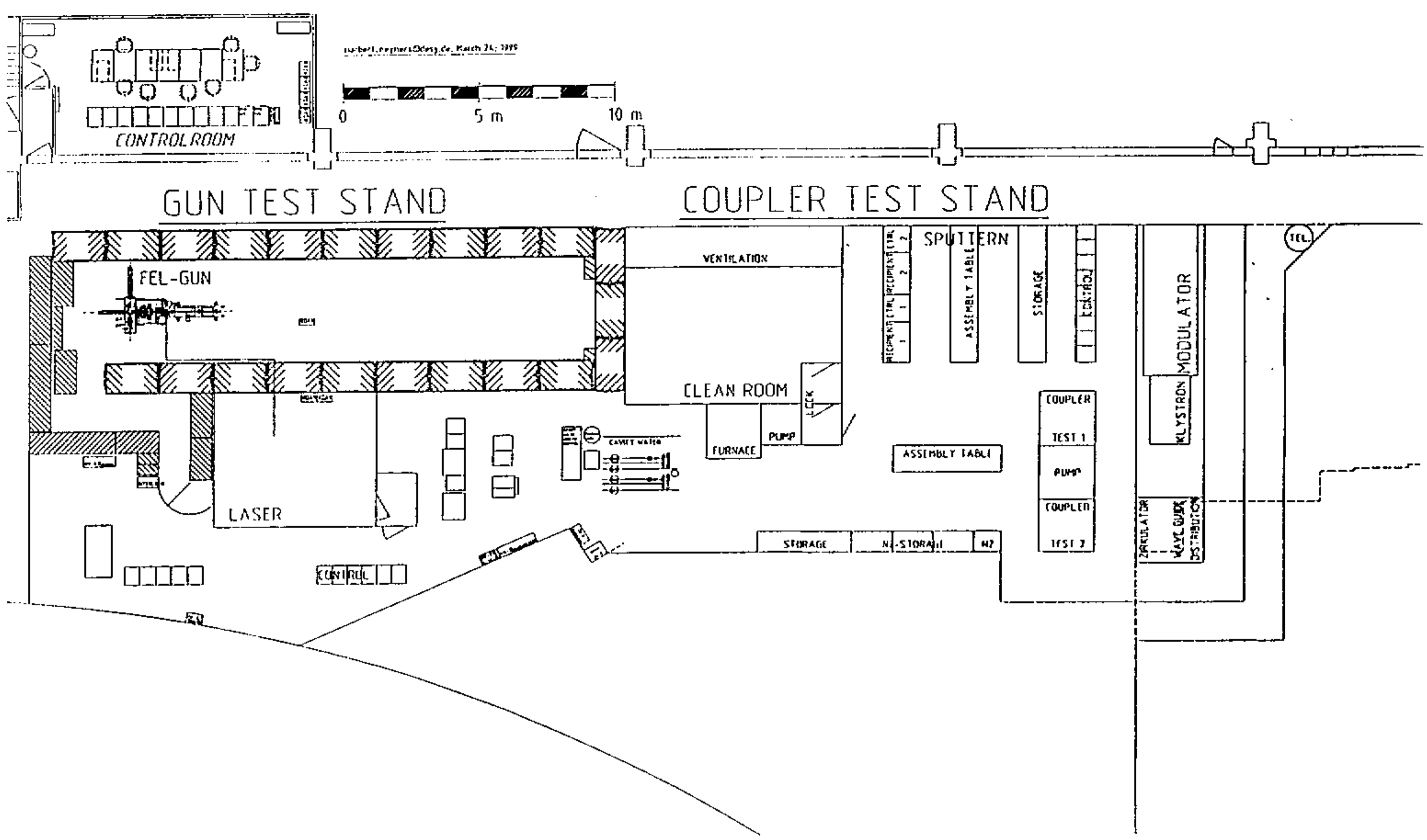
0
5 m
10 m
CONTROLROOM
GUN TEST STAND
COUPLER TEST STAND
FEL-GUN
VENTILATION
SPUTTERN
ASSEMBLY TABLE
STORAGE
MODULATOR
KLYSTRON
CLEAN ROOM
FURNACE
PUMP
LOCK
LASER
CONTROL
ASSEMBLY TABLE
COUPLER TEST 1
PUMP
COUPLER TEST 2
STORAGE
N2-STORAGE
N2
ZIRKULATOR
WAVE GUIDE DISTRIBUTION
TEL.

MODE MEASUREMENTS AT THE WARM TTF - MODULE 1 AND INFLUENCE OF INPUT COUPLERS

NICOLETA BABOI, HANS-WALTER GLOCK, GUENNADIE KREPS, FRANK MARHAUSER

(DESY, UNI - ROSTOCK, UNI - FRANKFURT)

REVIEW : "COLD" & "WARM" MEASUREMENTS
TRANSMISSION MEASUREMENTS AT THE WARM MODULE
INFLUENCE OF INPUT COUPLERS
EFFECT OF CHANGING BELLOW LENGTHS

NICOLETA BABOI
TTF-MEETING, DESY, 7-9 JULY '99

REVIEW

"WARM" EXPERIMENTS (WITH BEAM) AT MODULE 1

SOMMER '98 : S. FARTOUKH, O. NAPOLY ET AL. (SACLAY)

CHARGE MODULATION ; 800 μs ;

=> CAVITY 3 $f = 2.584980$ GHz $Q \cong 10^6$

CAVITY 6 $f \simeq 2.586$ GHz $Q \sim 10^5$

FEBRUARY '99 : CAVITY DETUNING ($f_{HOM} = n f_b$

30 BUNCHES ;

=> CAVITY 3 $f = 2.584970$ GHz $R/Q \overset{?}{\cong} 15.3\ \Omega/cm^2$

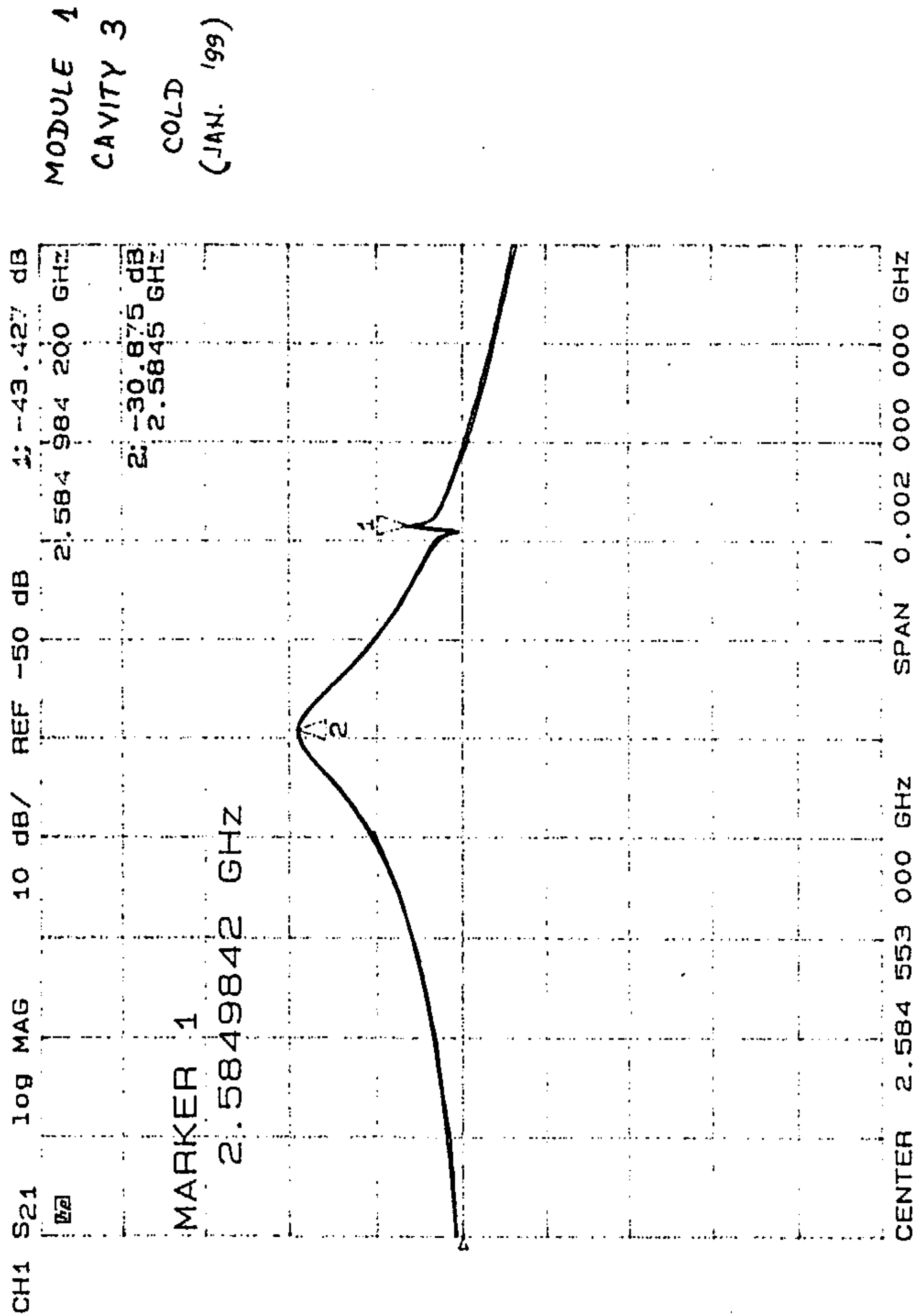

MEASUREMENTS AT THE WARM TTF - MODULE 1

(TRANSMISSION BETWEEN PAIRS OF HOM COUPLERS)

- FREQUENCY SHIFT COLD - WARM :
  ~ −5,5 MHz (AT ~2,58 GHz)
- PASSBAND SLIGHTLY WIDER
- FOR CAVITY 3, THE HIGH-Q MODE ($Q_{COLD} \simeq 10^6$, $Q_{WARM} \simeq 8000$) AT 2.579 GHz CAN STILL BE SEEN AND DISTINGUISHED FROM THE OTHER POLARISATION
- MODE PATTERN OVER 3 CAVITIES

MEASUREMENTS AT THE WARM TTF-MODULE 1 WITH NO INPUT COUPLERS IN PLACE

MODE PATTERN OVER 3 CAVITIES DISSAPPEARED

INFLUENCE OF INPUT COUPLER ON THE HIGH-Q MODE, BUT NOT ON THE OTHER POLARIZATION

CHANGE OF BELLOW LENGTHS

⇒ MODES MOVE TOGETHER IN FREQUENCY

⇒ NO CHANGE IN FIELD PATTERN

EFFECT OF BELLOW LENGTH CHANGING ON MODES FREQUENCY

MODULE 1
WARM

C3K1-C4K1

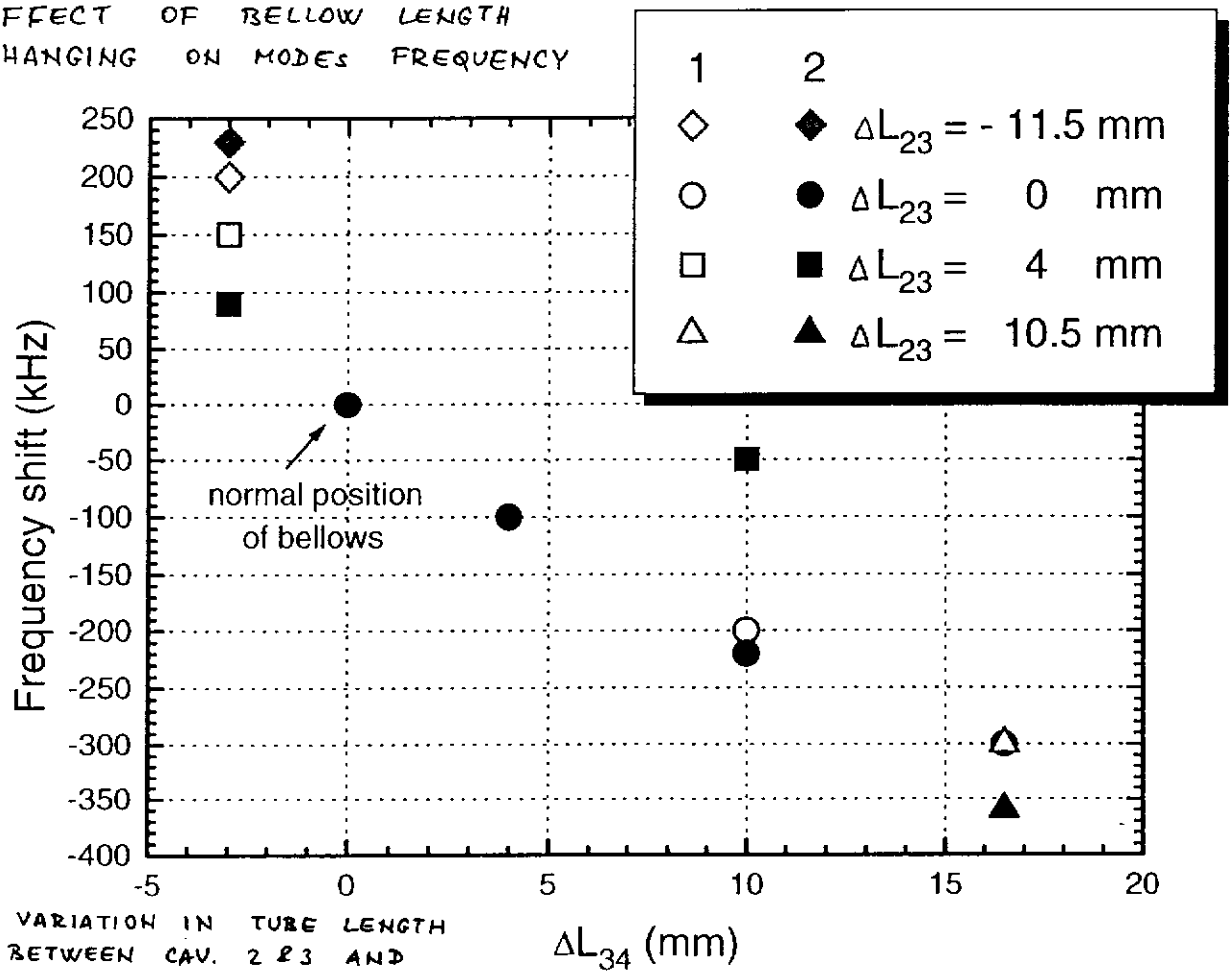

$\left.\begin{matrix}\Delta L_{23} \\ \Delta L_{34}\end{matrix}\right\}$ - VARIATION IN TUBE LENGTH BETWEEN CAV. 2 & 3 AND 3 & 4

CONCLUSIONS

- INPUT COUPLERS INDUCE
  - COUPLING OF MODES TO THE NEIGHBOURING CAVITIES
  - CHANGE IN FREQUENCY OF THE HIGH - Q MODE , BUT LESS INFLUENCE ON THE OTHER POLARIZATION
- IN THE WARM MODULE 1
  - MODE PATTERN STILL EXTENDS OVER 3 CAVITIES
- IN TESTS WITH A 4 CAVITIES CHAIN WE COULD NOT REPRODUCE A FIELD PATTERN OVER 3 CAVITIES, BUT ONLY ONE INPUT COUPLER AND FEW HOM COUPLERS

FUTURE PLANS

(+ FRENCH TEAM)

- 5 CAVITIES STRING (MODULE 1 – 3 GOOD D-CAVITIES)
- FIELD MEASUREMENTS (3 CAVITIES)
- POLARIZATION OF HOMs INDUCED BY INPUT COUPLERS (CAVITIES FROM MODULE 1 + COPPER CAVITY)

Johann Wolfgang Goethe-Universität
Frankfurt am Main
Institut für Angewandte Physik

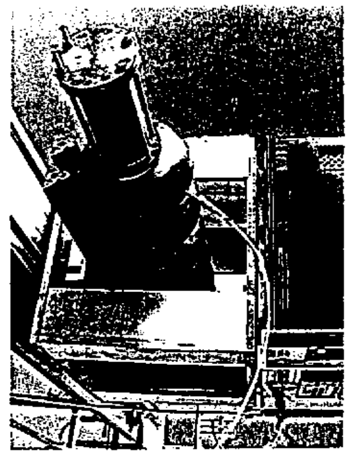

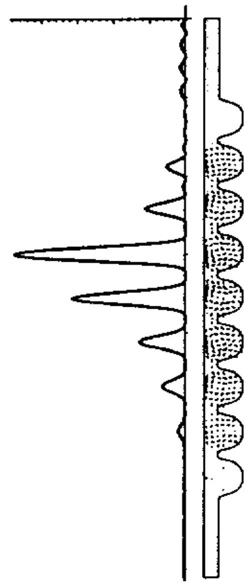

New Results on Trapped Modes in 9-cell TESLA-Cavities

Frank Marhauser
Peter Hülsmann
W.F.O. Müller

TESLA-Meeting
7.-9. July 1999
DESY, Hamburg

Frequency Shift of Monopole-TM Modes in Dependence on the Length of the Beampipes

- MAFIA-Calculation: Reference-Length: Cavity with 37,292 cm Beampipes -

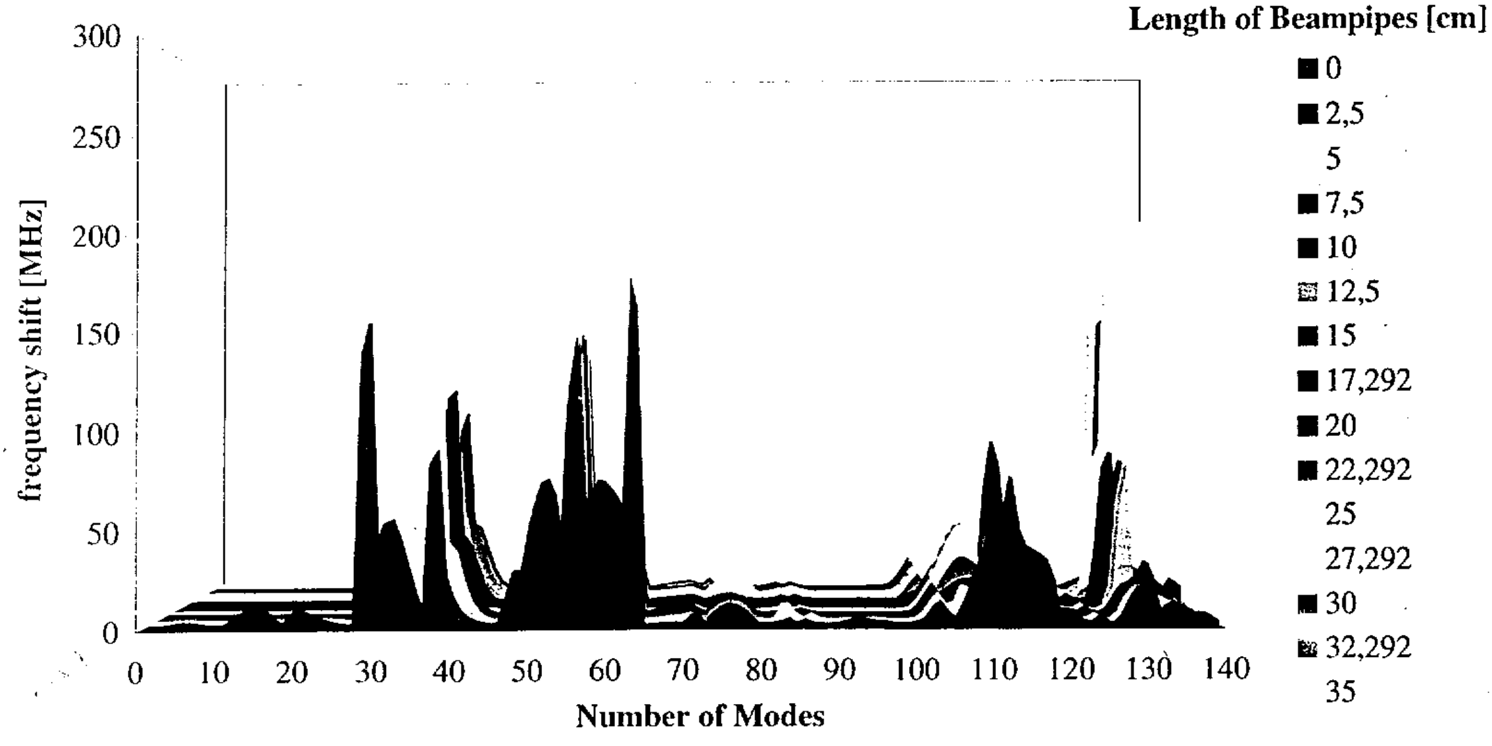

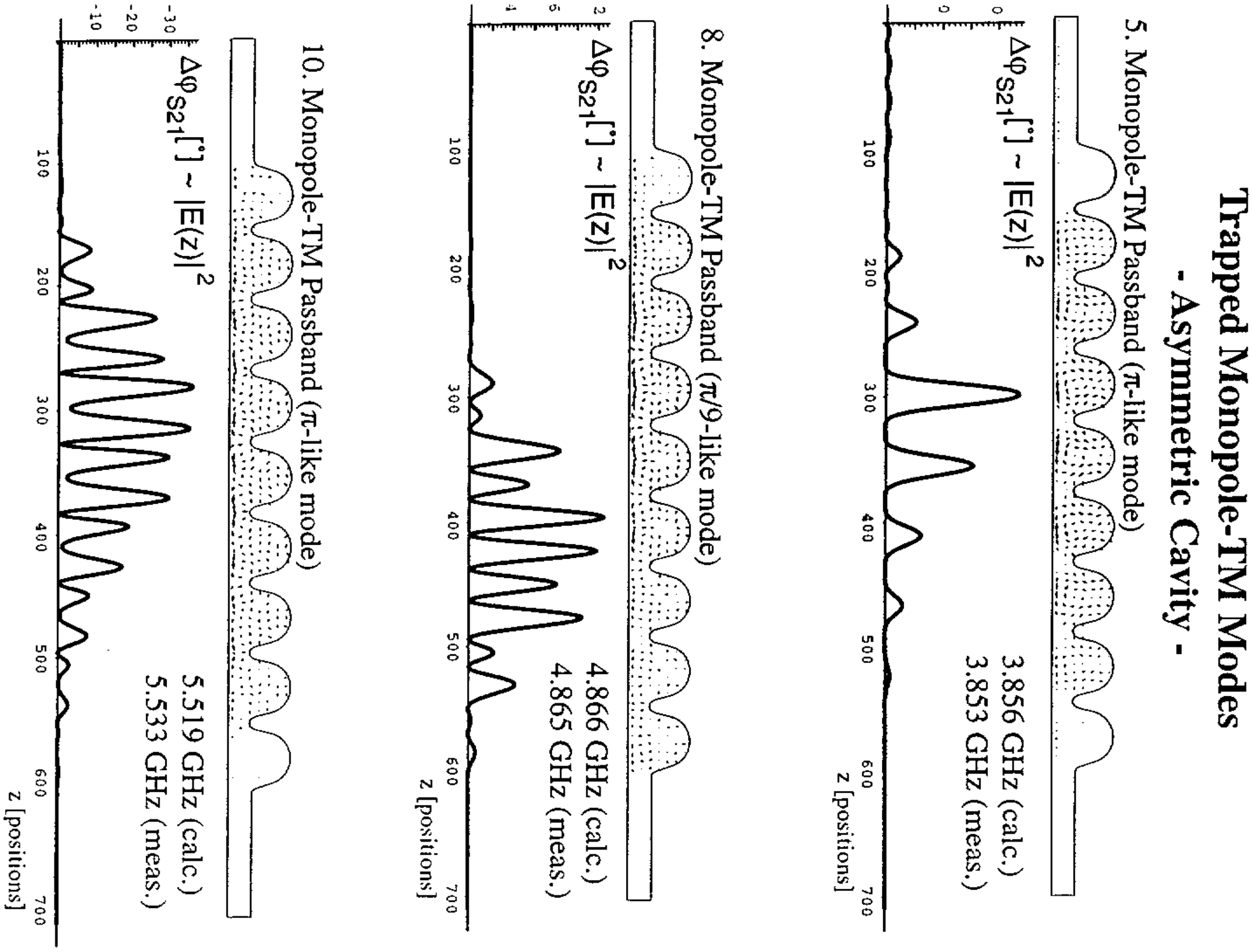

passband	frequency f [GHz]		R/Q [Ω]' without phasefactor		difference	R/Q [Ω]'	loss-factor
	calculated	measured	calculated	measured	[%]	v=c	$\kappa = \omega_0/4 \cdot R^{\parallel}/Q$ [V/nC]
5	3,856	3,853	716	514	28	51,5	311,9
8	4,866	4,865	1414	1020	28	0,09	0,7
10	5,519	5,533	1565	974	38	0,09	0,8
11	5,893	5,915	1826	900	51	0,2200	2,0
11	5,897	5,921	1814	1305	28	0,4500	4,2
11	5,904	5,926	1894	1157	39	1,3900	12,9
11	5,913	5,936	1973	963	51	8,2600	76,7
11	5,923	5,942	1978	1621	18	4,4000	40,9
11	5,932	5,948	1982	1959	1	0,1600	1,5
11	5,941	5,964	1932	1657	14	0,1100	1,0
11	5,948	5,969	1931	1700	12	0,0400	0,4
11	5,955	5,970	1735	1622	7	0,0100	0,1
15	6,693	6,712	1396	1210	13	4,33	45,5
18	7,342	7,362	1767	353	80	0,03	0,3

W-G. CAVITIES (I)

1 - Cavities for modules I* and 4

2 - Superstructure - Discussions -

3 - "Trapped modes" in module I
   results of measurements (N. Baboi)

4 - Trapped modes in 9-cell cavity
   (Frankfurt)

5 - New Structure - V. Balakin

Superstructures

- Discussion on some technical points:

  * Tuner

  * SC Gaskets : only for prototype

future: find a "clean" welding technique

  * HOM couplers:

→ one or two btw cavities ?

× one may be sufficient

× evaluate risk vs cost

→ Worry about power on fundamental mode

CAVITIES for next MODULES

2 modules to be prepared:

- module I* → module III
- module IV → tunnel extension → Expo

Problem under lively discussion:

- if module IV equipped with 8 cavities installed before march 2000

⇒ No chance to install module III with high gradient cavities !!!

Decision (strong recommandations!)

- Install Module III with 25 MV/m cavities (around spring 2000)
- Find a scenario for module IV (install 8 "average" cavities ($\lesssim$ 20 MV/m) or just dummy things)

Measurements in module I
(2.58 GHz mode)

- Measurements made on warm module and string of cavities.
- Influence of input coupler, beam tube.
- Next measurements with some cavities –

Discussion:

- Pb: explain transmission of the mode in the chain of cavities
  - → Rotation of the polarisation of the mode?
  - → Field pattern different for the two polarisations ($\Delta f \simeq$ 400 kHz)
- (consider the 8 cavities as a "superstructure"

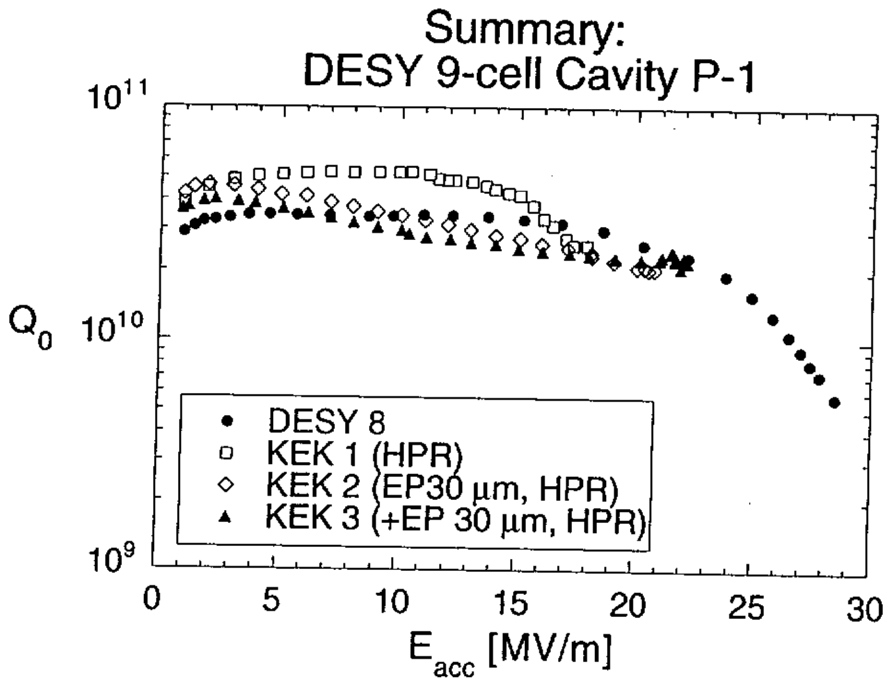

Summary:
DESY 9-cell Cavity P-1
Q0
10^11
10^10
10^9
DESY 8
KEK 1 (HPR)
KEK 2 (EP30 µm, HPR)
KEK 3 (+EP 30 µm, HPR)
0 5 10 15 20 25 30
Eacc [MV/m]

KEK

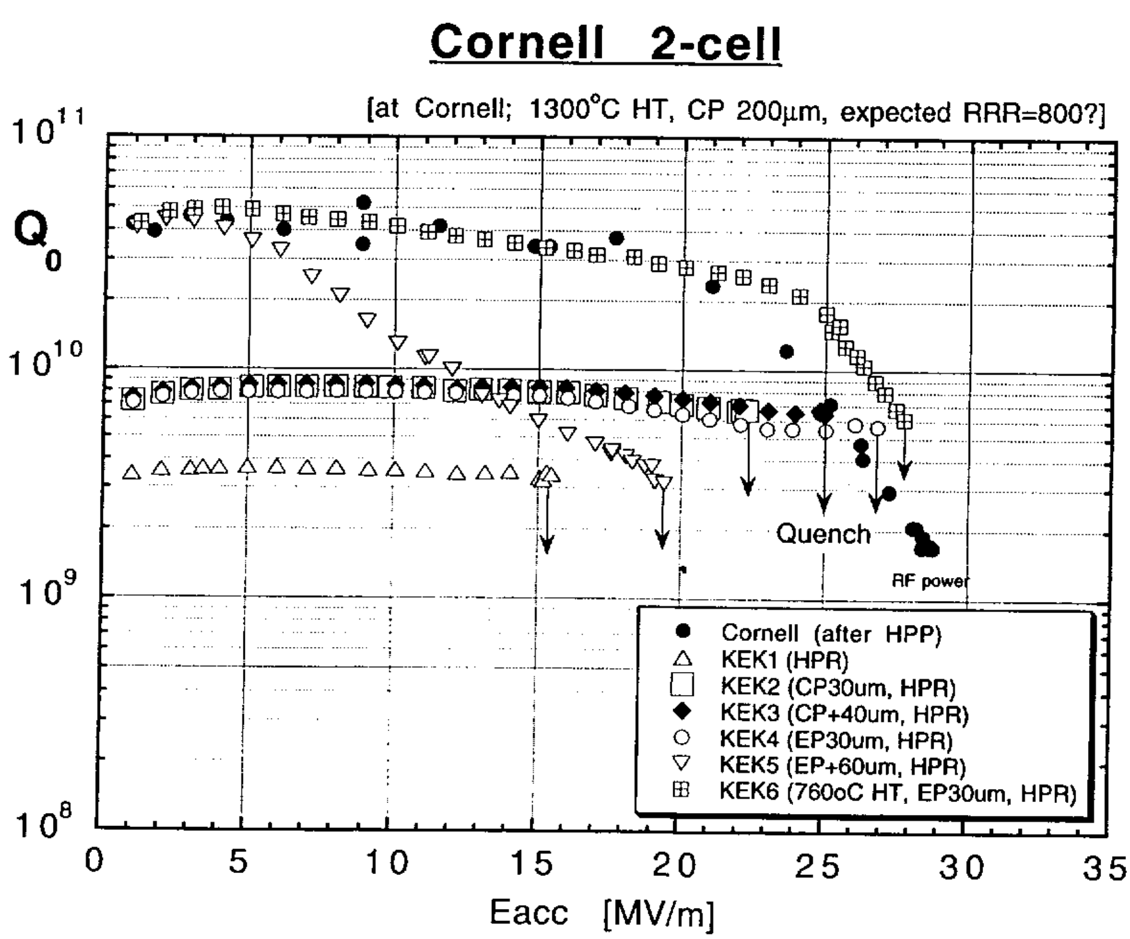

Cornell 2-cell
[at Cornell; 1300°C HT, CP 200µm, expected RRR=800?]
Q0
10^11
10^10
10^9
10^8
Quench
RF power
Cornell (after HPP)
KEK1 (HPR)
KEK2 (CP30um, HPR)
KEK3 (CP+40um, HPR)
KEK4 (EP30um, HPR)
KEK5 (EP+60um, HPR)
KEK6 (760oC HT, EP30um, HPR)
0 5 10 15 20 25 30 35
Eacc [MV/m]

KEK

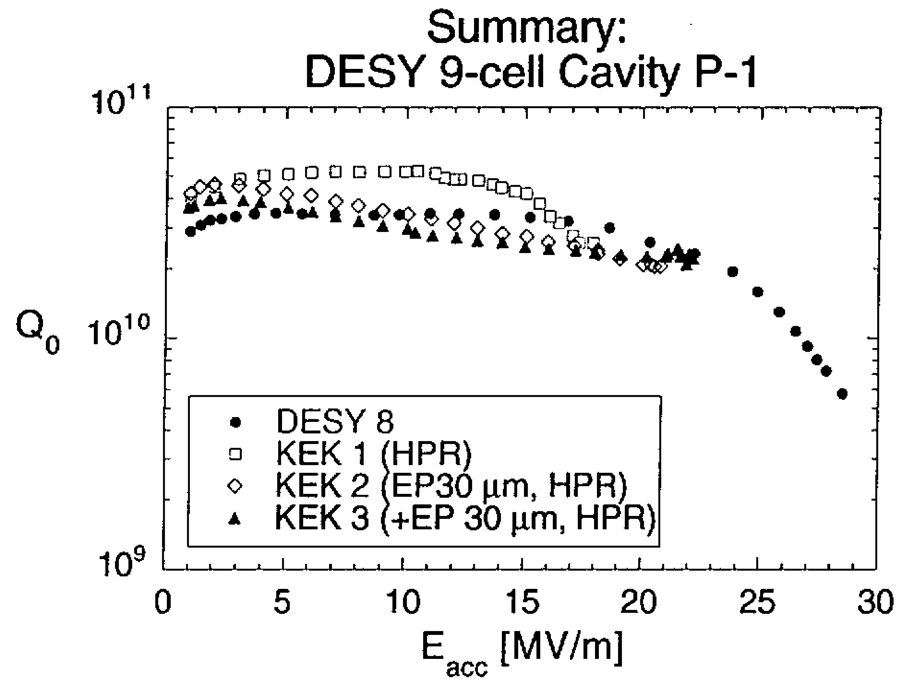

BCP cavities

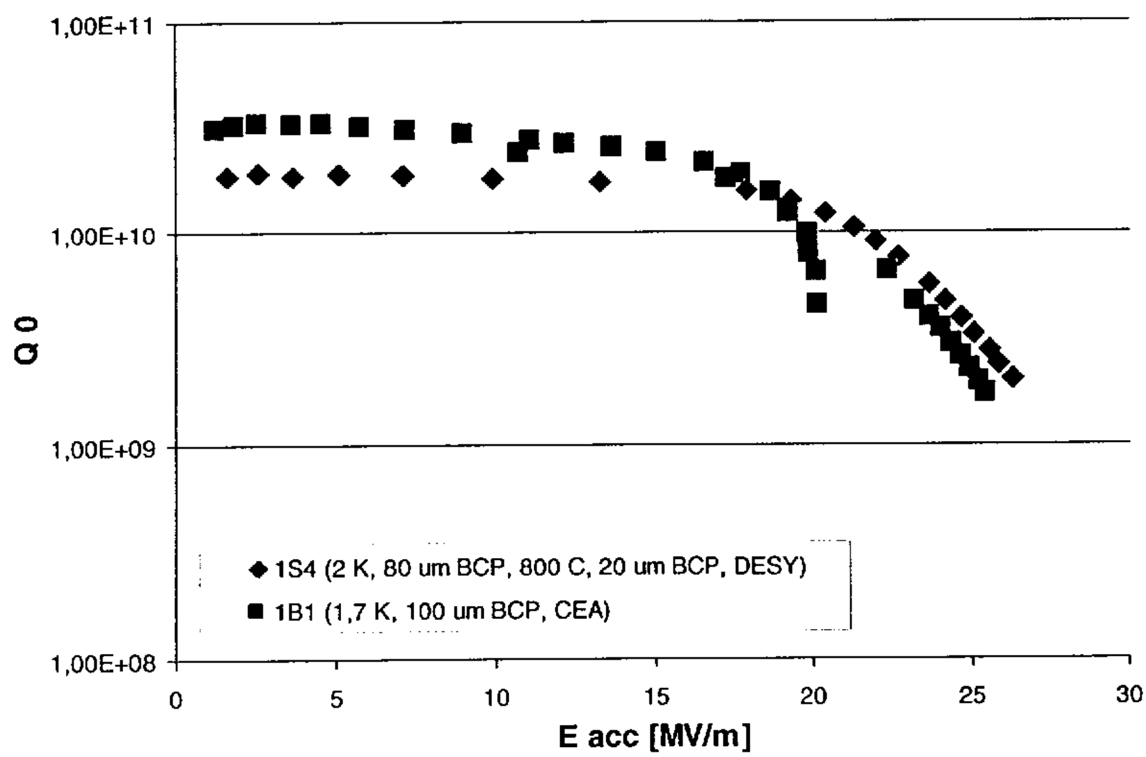

1-cells

´EP´ cavities

EP, welding at CERN

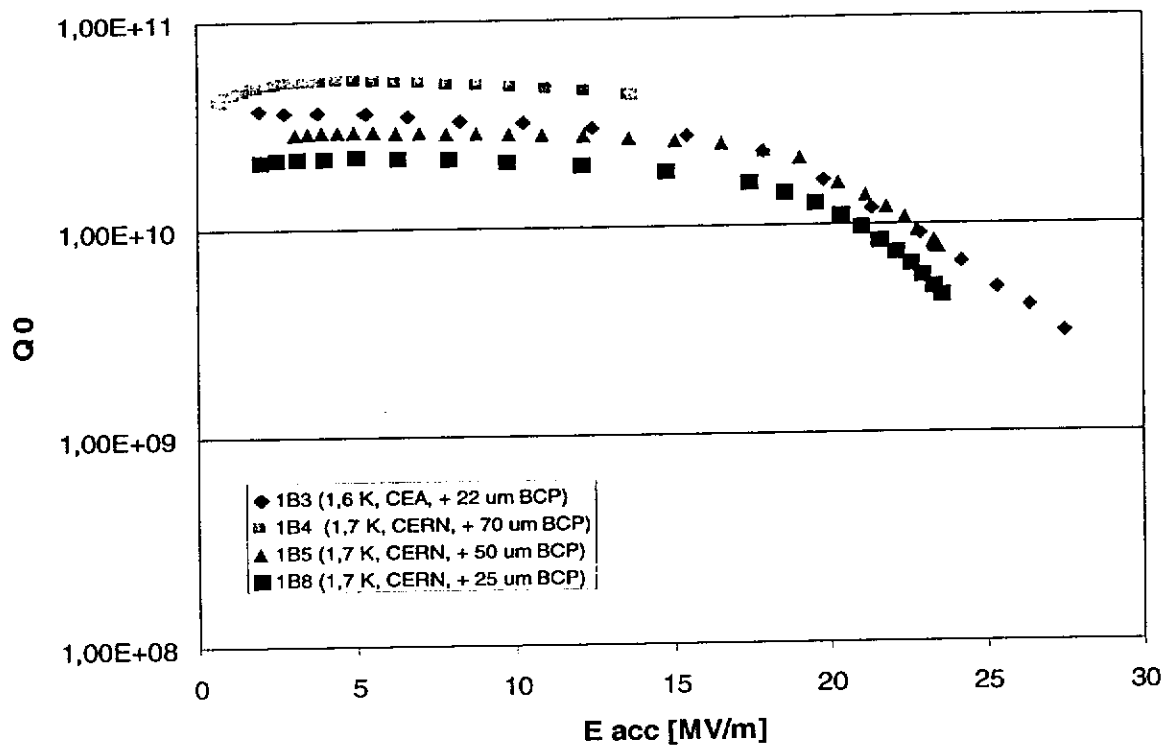

05.07.99 Lutz Lilje DESY -FDET-

Lutz Lilje (DESY)

Electropolishing

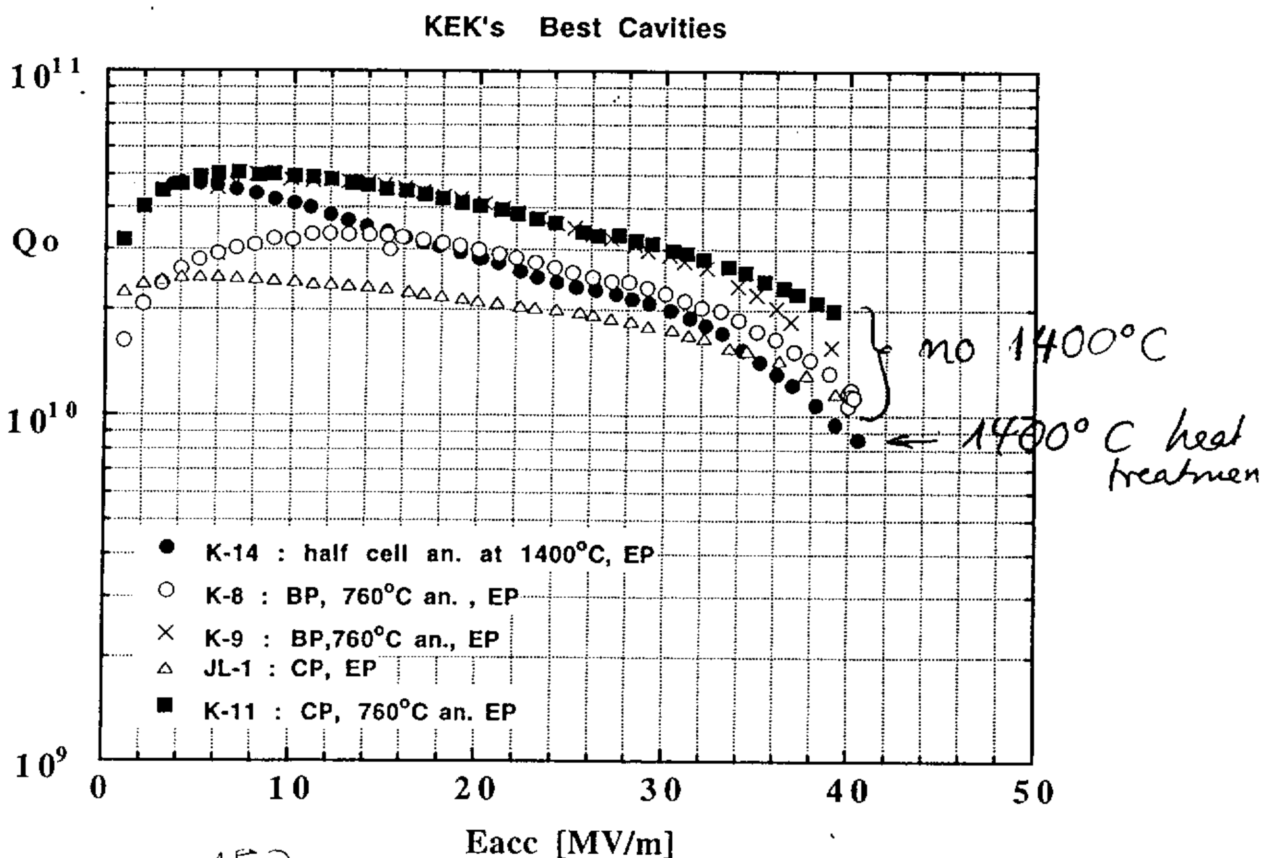

152

CAVITY STIFFENING BY THERMAL SPRAYING

Cavity Stiffening by Thermal Spraying

I.P.N. - ORSAY

S.Bousson, A. Caruette, M.Fouaidy, H.Gassot, N.Hammoudi, J.C. Lescornet, J. Lesrel, T. Junquera

L.A.L. - ORSAY

J.L. Borne, L. Grandsire, J. Marini

C.E.A. - SACLAY

H. Safa, J.P. Charrier, M. Boloré, Y.Gasser, J.P. Poupeau

CNRS CENTRE NATIONAL DE LA RECHERCHE SCIENTIFIQUE — IN2P3 — Université de Paris-Sud

CAVITY STIFFENING BY THERMAL SPRAYING

GOAL: Cavity stiffening without lowering RF performances

☞ **↘the cavity sensitivity to Lorentz forces detuning**

☞ **do not affect the cavity thermal stability**

1. **Single-cell cavity tests (1.3 and 3 GHz)**
   Cu "rough" APS, Cu HVOF, and Cu APS
2. **Thermal characterization of different coatings:**
   Cu HVOF, Cu "rough" APS and Ti APS
3. **Young modulus of different coatings:**
   Cu HVOF, Cu "rough" APS and Ti APS
   Thermal stress (measured on Nb tube with Cu coating)

Introduction
Goal
1. Cavity RF Tests
"Rough APS"
HVOF
APS
2. Mechanical Tests
Thermal stress
Young modulus
3. Thermal Tests
Simulations
Procedure
Results
Conclusion
Future

SINGLE-CELL CAVITY PROTOTYPES

Up to now, 3 different cavity prototypes have been realized:

Process	Performer	Frequency	Comments
" Rough APS "	French Firm Mallard	1.3 GHz & 3 GHz	Hand-made, Bonding Layer,
HVOF	LERMPS Laboratory	1.3 GHz	Low Porosity, High oxidation.
APS	Ecole des Mines Laboratory	3 GHz	

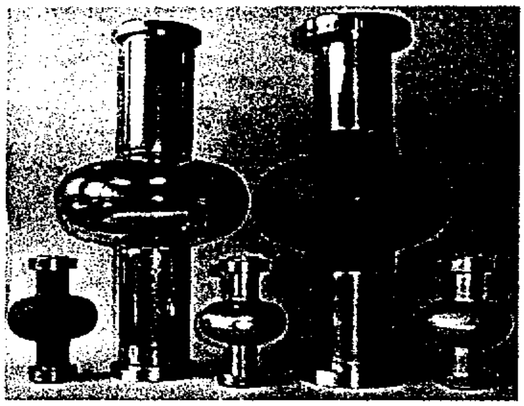

1.3 and 3 GHz Nb and Cu/Nb cavities

Introduction
Goal
1. Cavity RF Tests
"Rough APS"
HVOF
APS
2. Mechanical Tests
Thermal stress
Young modulus
3. Thermal Tests
Simulations
Procedure
Results
Conclusion
Future

THE NON-OPTIMIZED APS RESULTS

Sum-up of RF tests on APS coated cavities

3 Ghz Cavities:

Cavity	Eacc Max before coating	Eacc Max After Cu coating
#3	-	10 MV/m
#4	16.5 MV/m	16.5 MV/m
#5	14.5 MV/m	13.5 MV/m

1.3 Ghz Cavities:

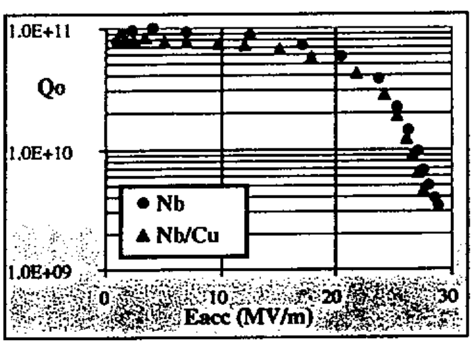

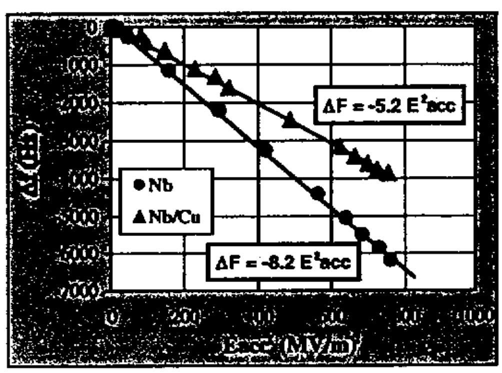

Introduction
Goal
1. Cavity RF Tests
"Rough APS"
HVOF
APS
2. Mechanical Tests
Thermal stress
Young modulus
3. Thermal Tests
Simulations
Procedure
Results
Conclusion
Future

Jean LESREL
Sebastien BOUSS
DESY
7-9 July
TESLA

The H.V.O.F. RESULTS

1.3 Ghz Cavities:

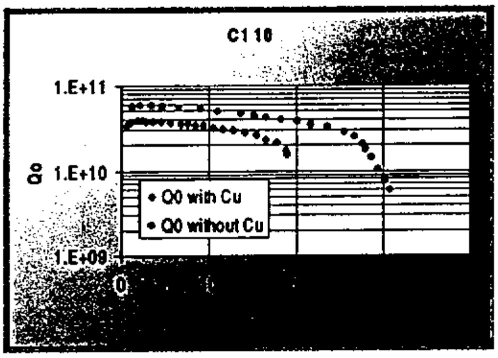

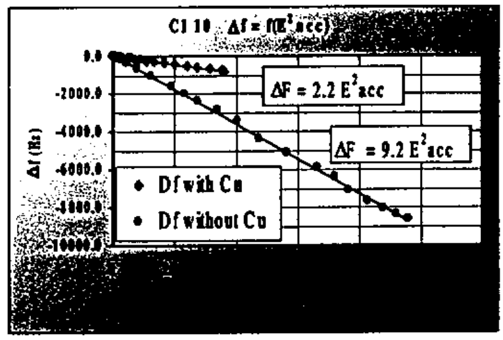

During the test with copper there was electron emission

☞ Great stiffening improvement with Cu HVOF

☞ Qo level almost not affected

Introduction
Goal
1. Cavity RF Tests
"Rough APS"
HVOF
APS
2. Mechanical Tests
Thermal stress
Young modulus
3. Thermal Tests
Simulations
Procedure
Results
Conclusion
Future

MEASUREMENTS RESULTS

	RRR Coating	Porosity	Δ Rg $K.m^2/W$	Δ Rg / Rk (Nb)	Young modulus GPa	Estimated Eacc max
Cu APS Non-opt.	3	~ 20 / 30 %	$6\ 10^{-4}$	~ 4	27	Stiffening 33 MV/m
Ti APS	3	> Cu APS non-opt.	$4.2\ 10^{-4}$	~ 3	18	Stiffening
Cu HVOF	3	2 %	$1.2\ 10^{-3}$	~ 10	53	Thermal 30 MV/m
Cu APS	4		-	-		
GOAL			$2.8\ 10^{-4}$	2	95	Stiffening 40 MV/m

☞ Layer thermal conductivity is closely related to the porosity

☞ Cu HVOF has to be improved (reduced oxidation)

PRELIMINARY RESULTS ON
THERMAL SPRAY OF Cu on Nb

P. MICHELATO
INFN-LASA

⊙ INFN + ENEL (CISE) + SAES GETTERS

+ CHOICE OF THE DEPOSITION TECHNIQUE

↳ MODIFIED ARC

↳ HVOF

⊕ ANALYSIS

↳ METALLOGRAPHIC MICROSCOPE

- Nb-Cu INTERFACE
- Nb
- Cu → POROSITY ↗ (≪ 1% HVOF) / → (≈ 6% ARC)

↳ SEM – (SECONDARY ELECTRONS / SAMPLE CURRENT)

- ELEMENT IDENTIFICATION (X RAY)

↳ SURFACE ANALYSIS (AES)

- Nb-Cu INTERFACE
- O_2 on Cu
- O_2 on Nb
- O_2 on the INTERFACE

} AES IMAGING

"ARC" TECH

Cu

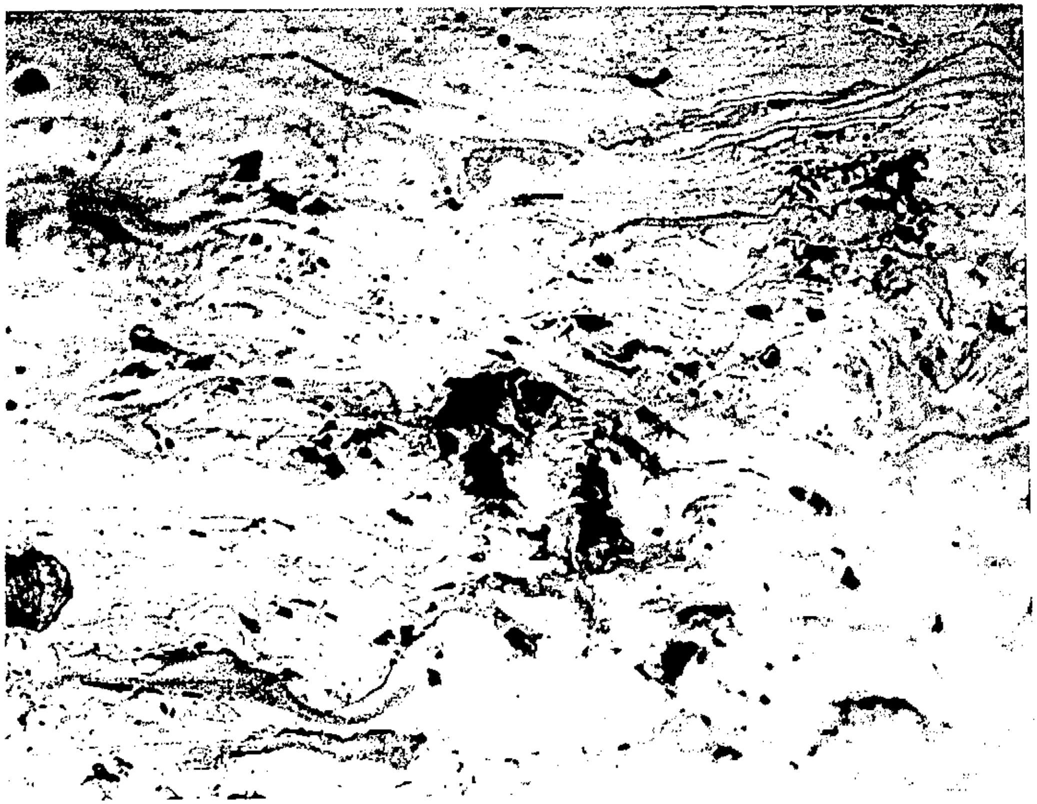

0.1 mm

HVOF

?

Cu Nb

200 μm

SEM

HVOF- Cu

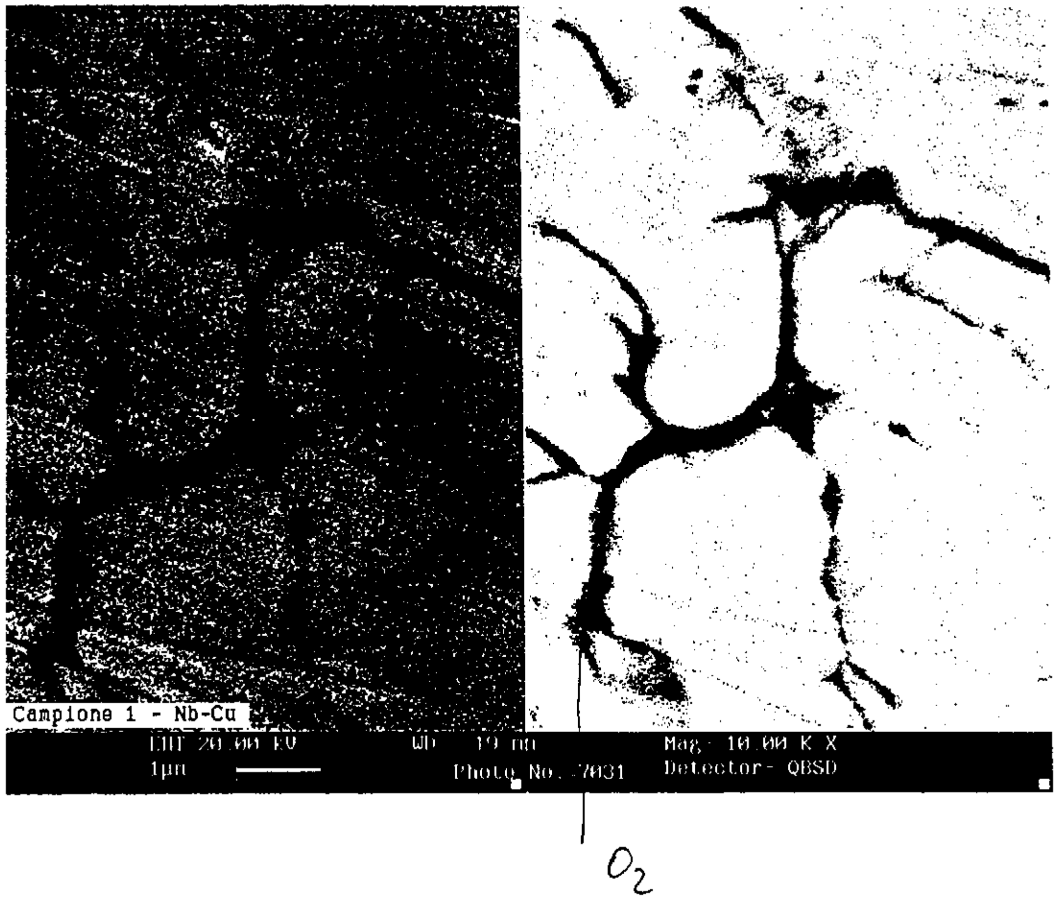
Campione 1 - Nb-Cu
EHT 20.00 KV
1µm
WD 19 mm
Photo No. 7031
Mag 10.00 K X
Detector- QBSD
O_2

159

Commissioning and Experimental Program for the TTF Linac

M. Castellano, T. Garvey, G. Schmidt

Topics:
- Status of components
- Time schedule

1) Status of components

Status of cold and warm cavity BPM's (R. Lorenz) ✓
Status of stripline BPM's (F. Tazzioli) ✓ new electronics
Status of OTR and screens (M. Castellano) ✓
Status of ~~Reentrant Cavity~~ Pickup BPM's (M. Wendt) November or later → Scope
Status of Waveguide Monitors and (Reentrant) Cavity BPM's (R. Lorenz) 2 in August → September / October → scope or 1 electronic
Status of Wire Scanners (G. Schmidt) ✓
Status of Toroids (H. Schlarb) ✓ new timing for ADC
Status of collimator diagnostics (H. Schlarb) ✓
Reentrant Cav BPM electronic might be late

Status of timing system and fast ADC (K. Rehlich) 6 ADC boards beginning of August

New Tools for the optics and orbit of TTF (P. Castro) - slow orbit feedback - optic calculation available

=> 2 hrs

⇒ Delay of nearly all electronics of the undulator BPMs
⇒ No beam based alignment available

Some new tools for TTF control

Pedro Castro / MPY

1. Optics on-line,
   Beam-based alignment,
   Orbit correction
2. Data-base, documentation
3. Orbit feedback
4. What's done and
   What needs to be done.

G. Schmidt, -MPY-, 6.07.99

2) Time schedule until FEL conference (23 -28 August) and beyond

With Goal: Electron beam through the undulator before the FEL Conference 99

- Startup of the injector (F. Stephan)
  Goal: Reproduce settings of last run. Not optimizing everything, only get reasonable beam for FEL test.
  ->injector ready to deliver beam (1nC, 8nC for rf calibration) 6.8.99 // undulator alignment   starting day at 12.00

- 4 shifts needed for phase adjustment of cavities in module 1 and 2. Calibration of gradient with an
  8 nC beam with 10 pulses
  only if the charge is not sufficient pulse length could be up to 30 pulses
  Equal power distribution between module 1 and 2 will be used.
  Goal energy is 260 MeV. 15 MV/m

- Then without longer investigations try to get beam through the collimator/undulator.
  Bunch compressor should be off for first test.
  Can then if necessary be switched on during one shift.

- Hasylab could look onto the photon beam.

  Optimize angle and position in the undulator with the diagnostics available.

  ... to be decided depending on situation

160

What has to be done for a (quick and dirty) startup of the injector until Mo. August 9th, 1999 ?

F. Stephan,
TTF meeting, July 8th

- **week 1:** Mo. July 12th → Fr. July 16th
  - switch DESY gun → FNAL gun
    - solenoids
    - technical interlock
    - water
    - rf system: WG, llrf, cable attenuation
      need power meter, GPIB interface
  - change capton foil in WG
  - (new directional coupler ← check for leak tightness)
  - enable laser beamline (remove aluminium)
  - test of llrf system (changes were done)
  - pull cable for fast technical interlock and fast DSP control to klystron 3
  - check frame grabber, motors and video signals of screens in injector
  - check injector magnets (running or not, hall probe)
  - prepare CC for operation (hardware changes?)
  - MBI people set up the laser

week 2: Mo. July 19th → Fr. July 23rd

- finish installation of persons interlock in complete tunnel
- get CC modulator working
- check laser interlock
- Tu. July 20th : tunnel closure
  - check persons interlock
    (klystron needs to be working)
- get solenoids running (technical interlock, hardware, control system)
- 161 check gun solenoids (current measurement, hall probe, field profile (M. Schmitz))
- put rf in the gun: condition with DSP control up to 100 μs with 2.2 MW ($\hat{=}$ 35 MV/m)

  (~ 2 days ?!)
- check dark current

week 3: Mo. July 26th → Fr. July 30th

- Mo. July 26th : modules and CC cold
- get CC working (new electronics, 2-3 days, Mo. → Wed. ?)
- in parallel :
  - get laser beam on cathode
    (2 fixed points on entrance window and wall)
  - check QE
- get correct timing for ICT integrators
- check ICT connection, calibration
- phase scan of rf gun cavity with 1nC and 8nC
- phase scan of CC (1nC / 8nC)
- get beam in dispersive section
- measure + optimize : energy + energy spread (1nC)
- get beam to FC in front of first module

week 4: Mo. August 2nd → Fr. August 6th

- each day: check gun phase
  check CC phase
  check energy + energy spread
  get beam to FC in sector 600
- Mo. → Th.: 1 nC, Fr.: 8 nC
- get new pepperpot working
- do emittance scans with pepper pot (sector 400)
- " " " " tomography (sector 400)
- " " " " " (sector 600)

↑ scan parameters: – main solenoid current
– secondary " "
(– gun phase)
(– ...)

do this with a fixed choice for the laser iris diameter (e.g. 3mm)

- Friday: get 8nC or more to the first module

162

General remarks

Continuos operation over longer periods to reduce the time to set up the machine for different experiments.
Improve the stability.
Special experiments at the end of the run or in blocks between work on the FEL.

Requests for beam time for special experiments
-HOM, measure without rf in cold module (parallel to injector work (September?)
if HOM exists close to beam frequency: 1week measurement time.

•Balakin (?, pulse length needed, charge?)
•Processing time for modules(maybe during the FEL conference)
-Kryo Loss measurements (if possible at the end of the run
-Wake field experiment (in November), vacuum chamber must be exchanged, ->to be decided.
-September time needed for experiment with diffraction radiator (1 week roughly).
- end of the run: prepare and test 54 MHz modulation of the laser beam (3 weeks)

- Discussion on Emittance or/and Emittance diagnostic problem.
  → No clear answer
  → Many questions
  → Investigations needed for FEL
  → maybe answer for FEL

TESLA-500 Working Group, Thursday/July 8, Room 5 Bld. Ib, 9.00h

Morning Session 9.00h, convener: R. Brinkmann

	Spent beam line and collimation	E. Merker, I. Yazynin
	Positron injector linac	V. Paramonov
~10.30h	*Coffee break*	
	Damping ring design update	W. Decking
	Muli-bunch instabilities in the damping ring	C. Burnton
	Positron source before the IP	R. Brinkmann
	Discussion on spent beam losses, extraction lines and related issues	all participants
~13.00h	*Lunch break*	

Afternoon Session 15.00h, convener: O. Napoly

	Multi-bunch beam dynamics in main linac	N. Baboi
	Beams with different energies (FEL/collider)	V. Tsakanov
	Estimate of beam halo	R. Brinkmann
~16.30h	*Coffee break*	
	Beam position measurement at the IP	T. Scholz
	Discussion on work to be done for TDR	all participants

TESLA Working Group Summary

e^+ Source

V. Paramonov : Positron injector line

E. Merker, I. Yazinin : e^- capture after IP

R. Brinkmann : Positron soure before IP ?

Damping rings

W. Decking : Design for the high luminosity parameters

C. Burnton : Multibunch dynamics

LINAC

N. Baboi : Multibunch dynamics with superstructure

V. Tsakanov : FEL / collider beam automatic

R. Brinkmann : Estimate of beam halo

IP

T. Scholz : IP Beam position monitor

e^+ source

V. Paramonov : Positron injector linac

- 260 MeV Linac, 18 × LBand SW cavities + 9 × 10 MW Klystrons

+(e⁻-separation, e^+ collimation) optics

- → ~ 22% capture efficiency, $L_{Tot.} = 60$ m, $P_{Tot.} = 600$ kW

E. Merker, I. Yazinin : Spent beam line collimation

- 9% e^- losses, 7% e^+ losses → ~ 1 MW on collimators
- 7 × 4 m long Al collimators (profile optimisation)
- IP instability ~ $10\,\sigma_y^*$ ⇒ collimator damaged in 1 pulse

R. Brinkmann : e^+ source before IP

- pro : e^+ polarisation, localized dumps, e^+ commissioning, ...
- con : e^-, $\Delta p/p \sim 3 \cdot 10^{-3}$, e^+ transport through detector hall.

... $e^\pm$ extraction lines, BDS redesign

V. Paramonov

"Positron injector linac"

Institute for Nuclear Research
Russian Academy of Sciences
60th October Anniversary Prospect, 7A
Moscow, 117 312, Russia

Conceptual Design of a Positron Pre-Accelerator for TESLA Linear Collider

Moscow-Hamburg, 1999

165

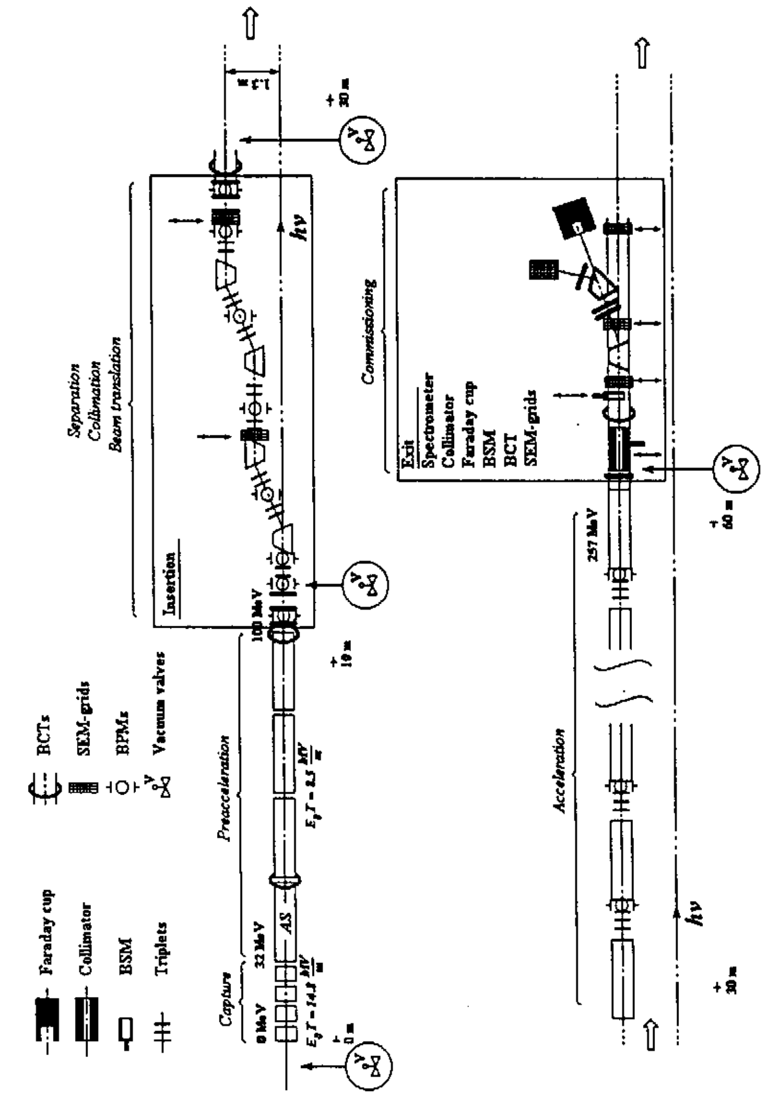

Figure 8.1. The PPA general scheme.

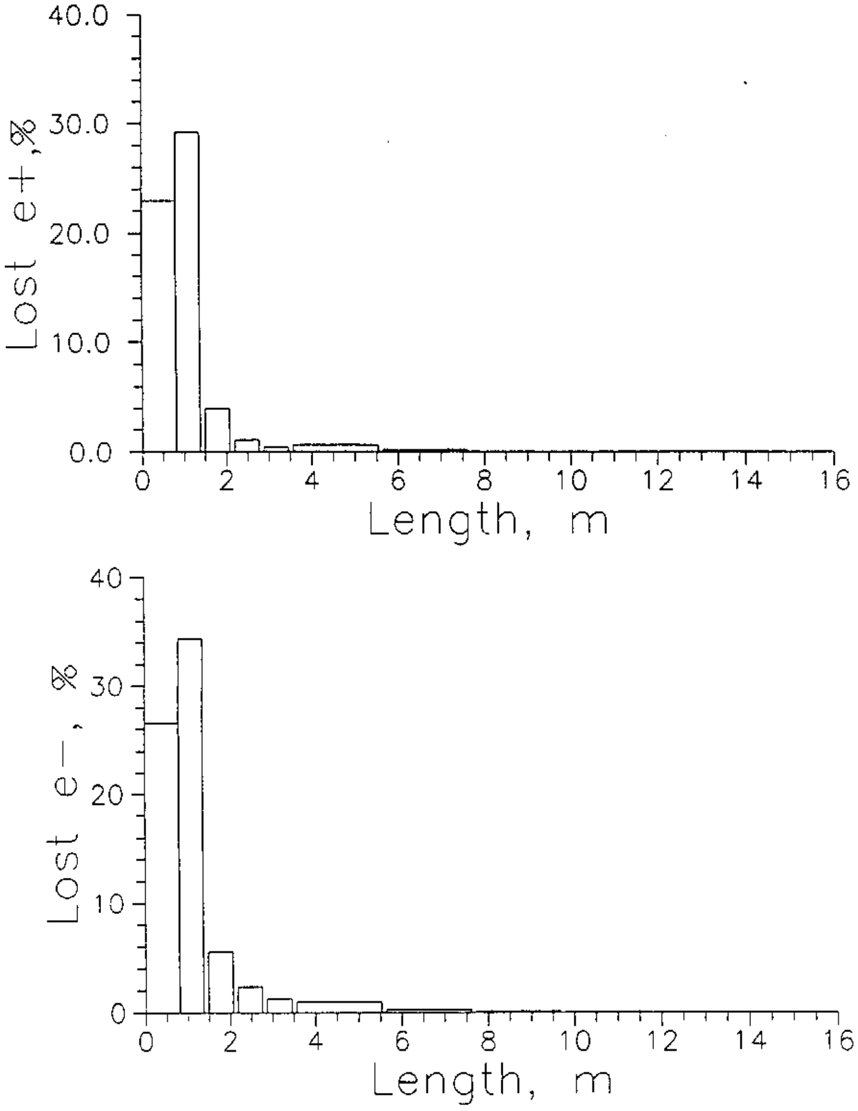

Figure 2.4.1: Particle loss distribution along the PPA.

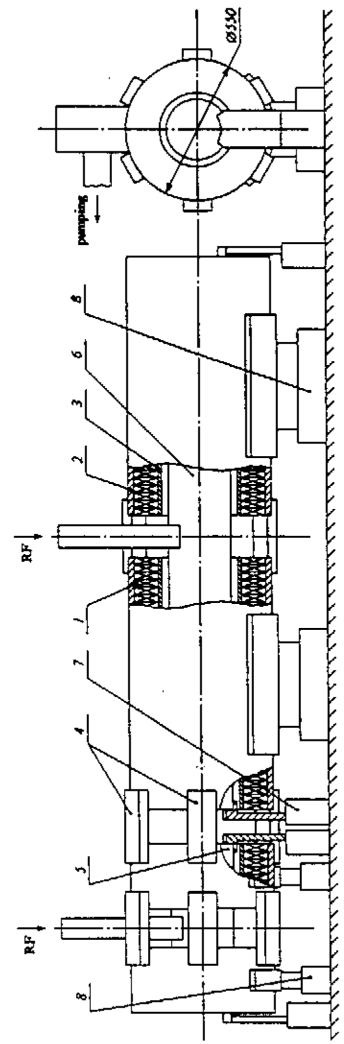

Figure 8.2. The proposal scheme for the PPA beginning design. 1- 'pancake' in the solenoid, 2- yoke, 3- support, 4- lowcarbon steel plate, 5- short AS, 6- long AS, 7- AS position adjustment, 8- solenoid adjustment.

166

Table 2.3.1: Accelerating sections parameters

Section type	Type #1	Type #2
Number of sections	4	14
Number of cells per section	5	17
Accelerating gradient E_0T, MV/m	$< 14,88$	$< 8,5$
Shunt impedance Z_{sh}, MΩ/m	31,92	35,38
Transit time factor, T	0,78393	0,79657
Length, m	0,5765	1,9602
Dissipated power, MW	< 4	< 4
Quality factor	~23690	~23580
Aperture diameter, mm	52	52

Aperture diameter of the cavity D= 52 mm
Field strength of the solenoid B= 0,24 T
AMD length 0,8 m

In this case PPA acceptance will be about twice the DR acceptance. This reserve permits to optimize the capture efficiency carefully. If it will be necessary the transverse phase space can be cut out of PPA.

107

Table 3.4.1: CDS structure parameters.

Parameter	Unit	$E_0T = 14.8 MV/m$	$E_0T = 8.5 MV/m$
Operating frequency	MHz	1300.0	1300.0
Phase velocity	relative	1.0	1.0
Aperture radius a	mm	26.0	26.0
Total web thickness	mm	30.0	30.0
Gap length g	mm	75.863	69.984
Drift tube cone angle	deg.	20.0	20.0
Lower drift tube radius r_1	mm	8.41	2.62
Upper drift tube radius r_2	mm	8.41	2.62
Upper cell radius r_3	mm	12.0	12.0
Outer cell radius R_c	mm	89.13	87.70
Effective shunt impedance Z_e	MO/m	34.35	37.45
Coupling coefficient k_c	%	5.1	8.9
Quality factor Q_0		24100	23800
Transit time factor T		0.780	0.790

P_h	η	t_h	δf_a	δf_c	S_{stmax}
kW/m	$W/(m^2C^o)$	C^o	kHz	kHz	kg/cm^2
5.7	7250	18.55	76	91	460
5.7	9000	17.44	68	84	418
26.0	9000	47.30	-255	296	980
26.0	12600	44.16	-210	221	901
26.0	12600	44.16	-210	221	901

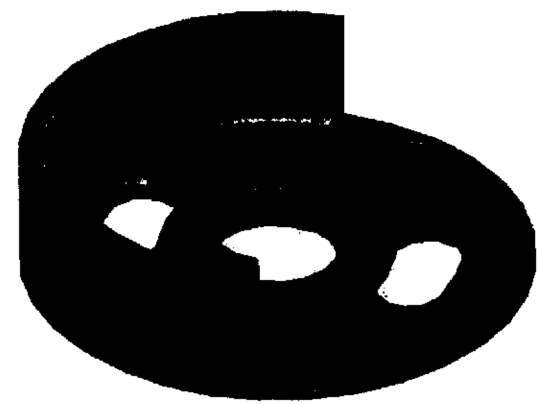

Figure 3.6.2: The cup of the CDS structure with straight chanel.

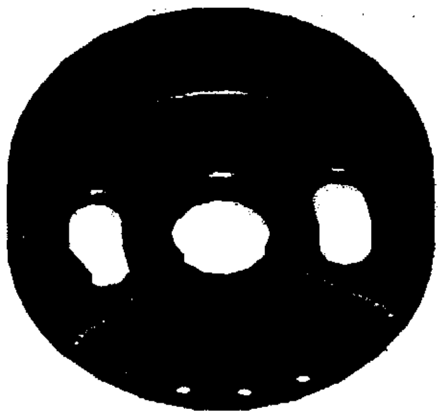

Figure 3.6.4: The cooling scheme for the second CDS cup option.

2.4 Proposal of the CDS structure design. Manufacturing and tuning procedures

The tuning procedure for the CDS structure was developed and described in [?].
As usual, tuning of compensated accelerating structure should have three procedures:
- tuning of the accelerating mode frequency f_a to f_0 one;
- tuning of the coupling mode frequency f_c to confine with f_a (closing of the stop-band);
- tuning of the accelerating field distribution (if needed).

Due to large k_c value, during the mode frequencies tuning there is no tuning of individual cells.

3 RF power system based on TESLA standard equipment

To reduce the total linac cost, to simplify maintenance it is supposed that the PPA rf system should be based on standart powerful TESLA equipment [?] - the same $10MW$ klystron with two waveguide outputs, powerful circulators after the klystron output windows, anode modulator and standard WR650 waveguide as Transmission Line (TL).

3.1 Special requirements

But PPA rf system should take into account PPA particularities. Differing from regular TESLA rf system, for PPA each klystron feeds only two normal conducting Accelerating Sections (AS), which parameters (wall rf power dissipation, Q-factor) are identical. Due to not so big AS Q_0-factor value (≈ 23000), the field rise-time for PPA AS is short enough

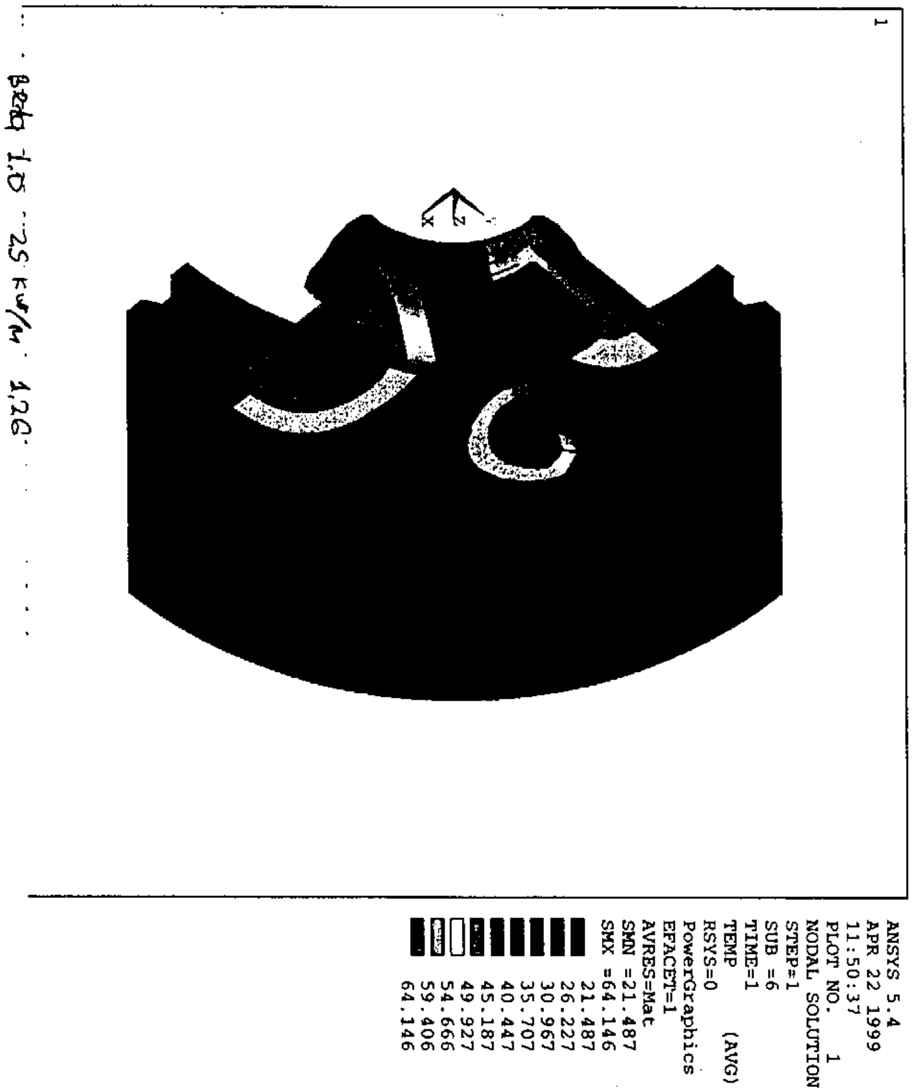

169

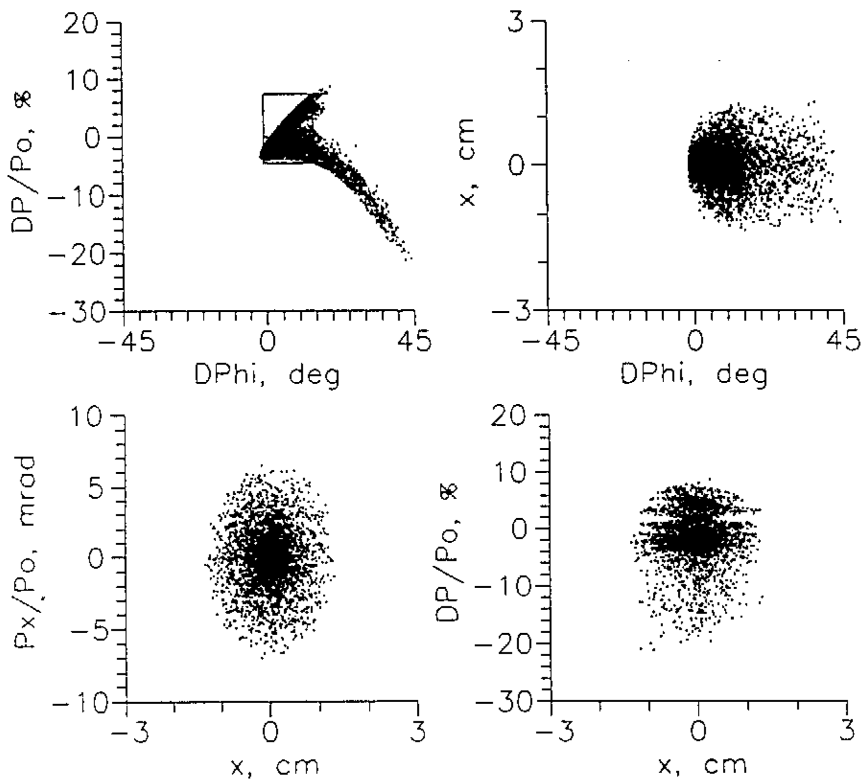

Figure 2.6.5. Output positron phase space portraits for PPA with collimating separator.

E. Merker,
I. Yazynin

"Spent beam line
collimation"

P_B = 8 MW CDR
= 11 MW $\sqrt{s}$ = 500 GeV
= 12 MW $\sqrt{s}$ = 800 GeV

The collimators must intercept that part of spent beam what can't be captured by the lines and will be lost. The total beam losses are about 9 % in electron and 7 % in positron lines. The power of them is 720 kW and 560 kW correspondingly.

The main functional requirements:

-they should intercept that and only that particles, which can't be captured by the beam lines;
-they must accumulate as much as possible energy of the intercepted particles;
-they should be able to dissipate the energy of the intercepted beam.

To be able to fulfill this task they must:

-have acceptable dimension;
to bear the maximum arising steady state temperature;
to bear the maximum arising instantaneous temperature jump.

These demands can be fulfilled only by the rational choice as the collimator material so as their configuration and geometric dimensions.

The max instantaneous specific energy deposition jump must satisfy the relation

$$K \times dE/dV < c \times \rho \times \Delta t_{max}, \quad (1)$$

where $\Delta t_{max} = \sigma_{0.2}/(E \times \alpha)$ and K is constant for all material ($\sigma_{0.2}$- plasticity limit, E-elastic module, α-coefficient of linear thermal expansion).

It can be shown, that the relation 1 will be fulfilled, if is right

$$F \times (dE/dZ)_{max} / (R_m \times c \times \rho \times \Delta t_{max}) < 1$$

where F takes into account the intensity and dimension of the beam and the geometry of the collimator. The other date are parameters of material. We have compared this relation for Al, Fe and Cu and have installed that it is better fulfilled for Al.

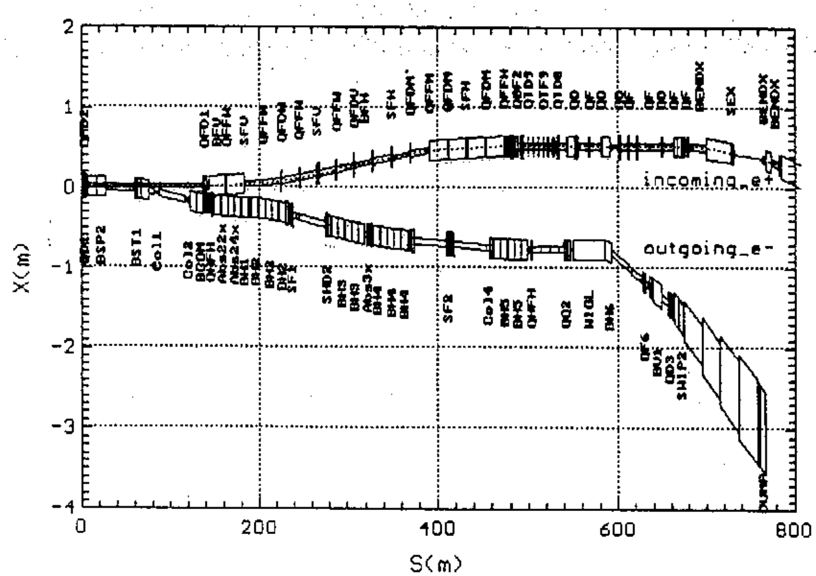

Fig.1: Layout of electron beam line.

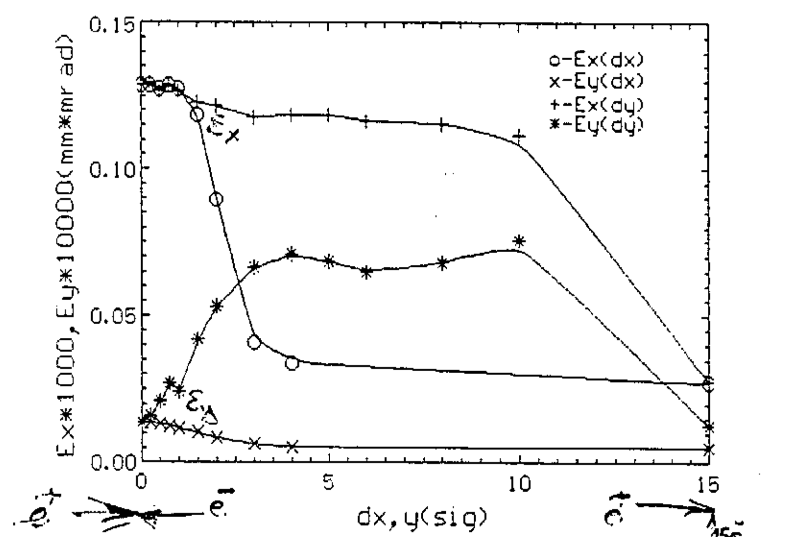

Fig.1: Beam emittance versus beam separation in IP.

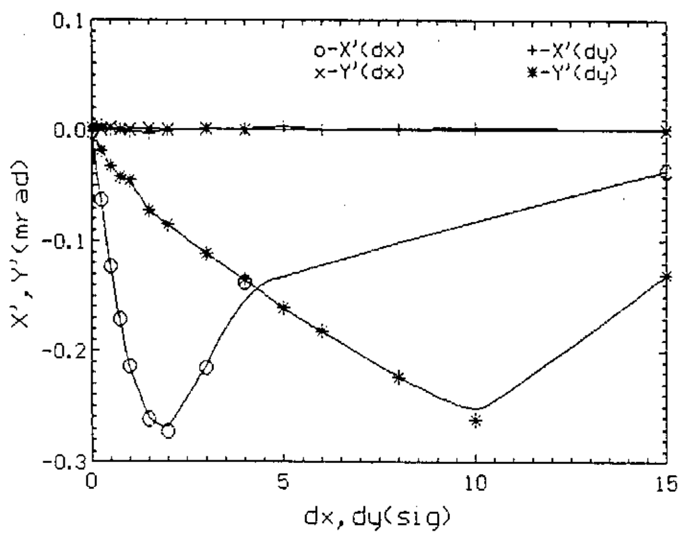

Fig.2: Angle beam deviation versus beam separation in IP.

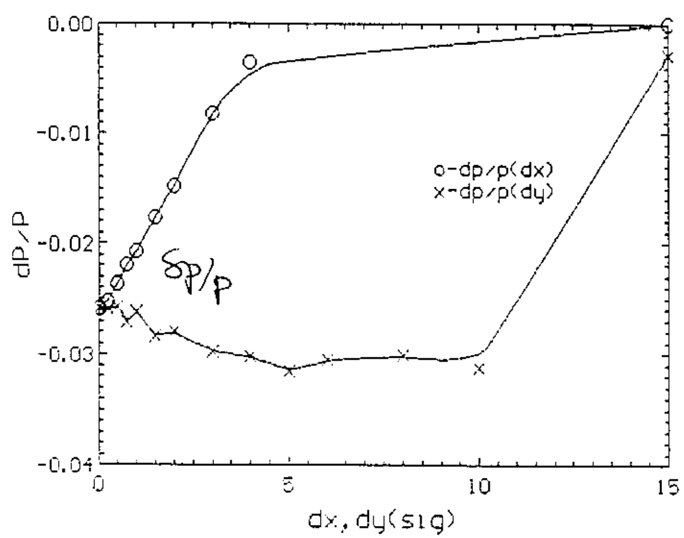

Fig.3: Average dP/P beam value versus beam separation in IP.

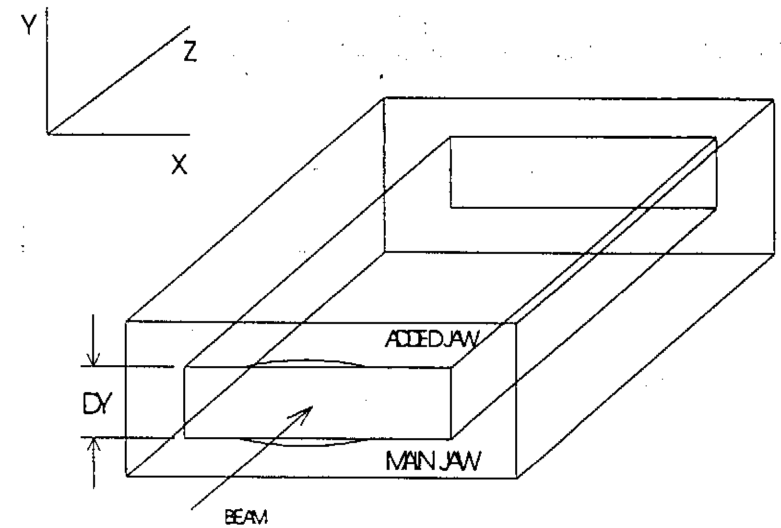

Fig. 2: Layout of variant A.

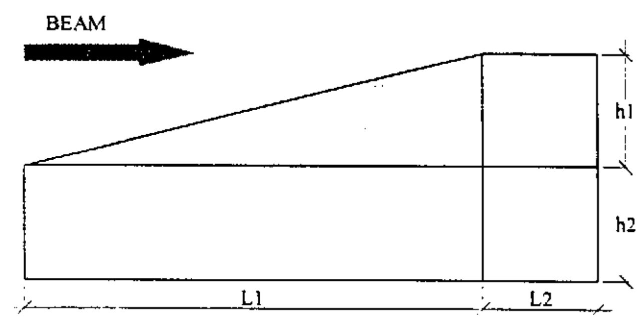

Fig. 3: Layout of variant B.

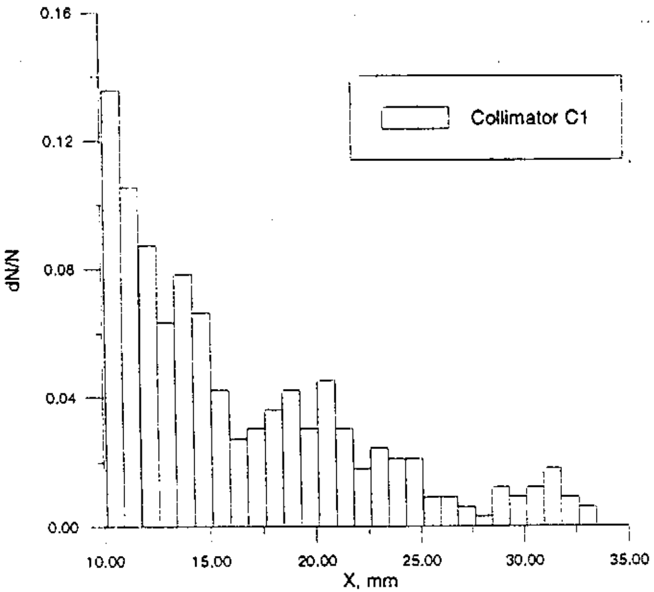

Fig. 4: Beam distribution on collimator 1 in horizontal direction.

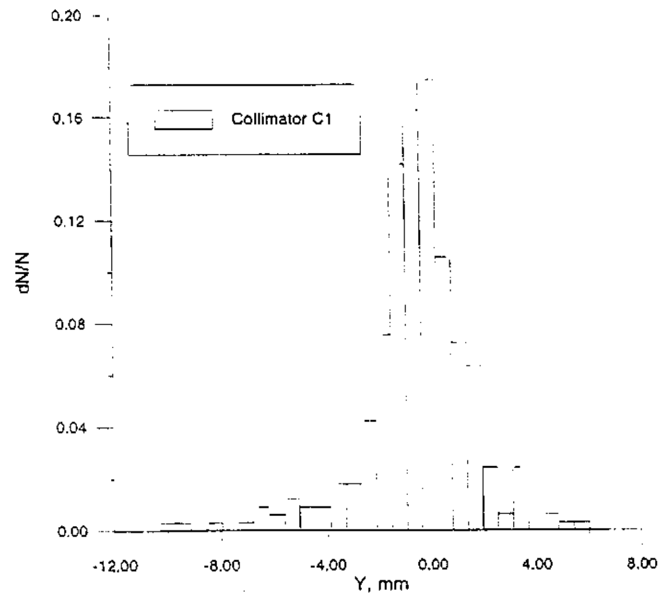

Fig. 5: Beam distribution on collimator 1 in vertical direction.

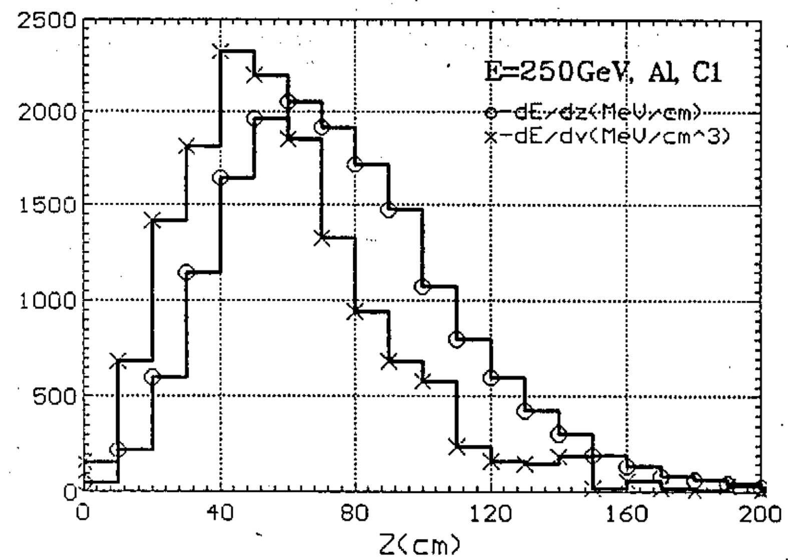

Fig. 8: Distribution of energy deposition in Al collimator 1 (variant a).

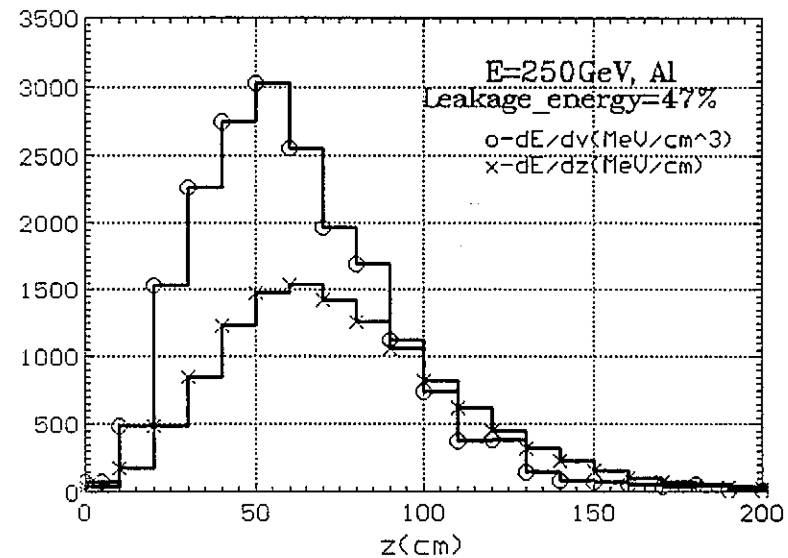

Fig. 9: Distribution of energy deposition in Al collimator 4 (variant a).

172

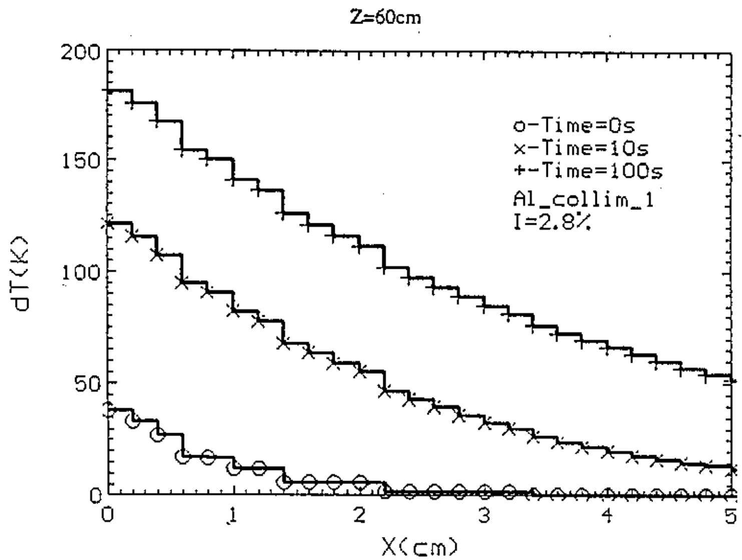

Fig. 30: Change of temperature in collimator 1in horizontal direction in section with max dE/dV.

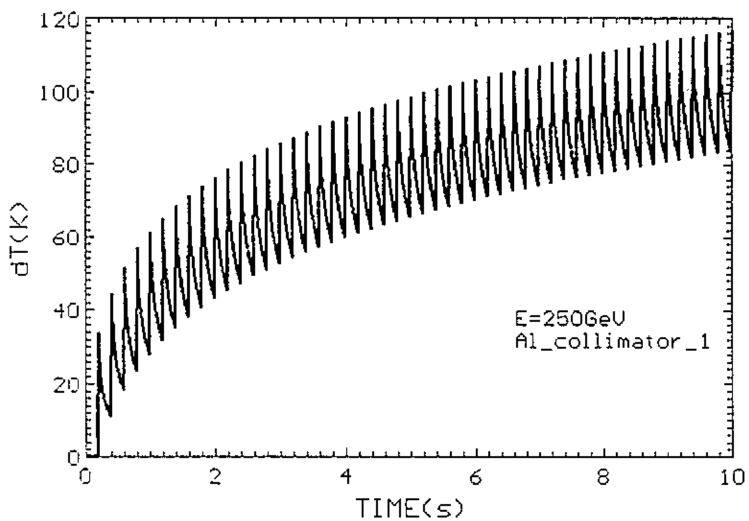

Fig.31: Change of temperature in collimator 1in horizontal direction in the section with max dE/dV (I = 2.8 %, Nb = 2.8×10^{11}c).

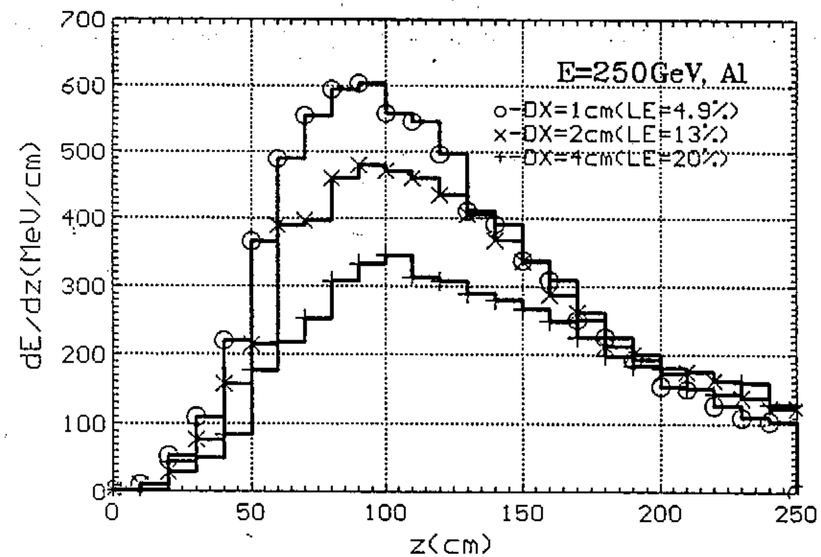

Fig. 14: Distribution of deposited energy in additional to collimator 4 jaws (variant a) with 1,2,4 cm separation.

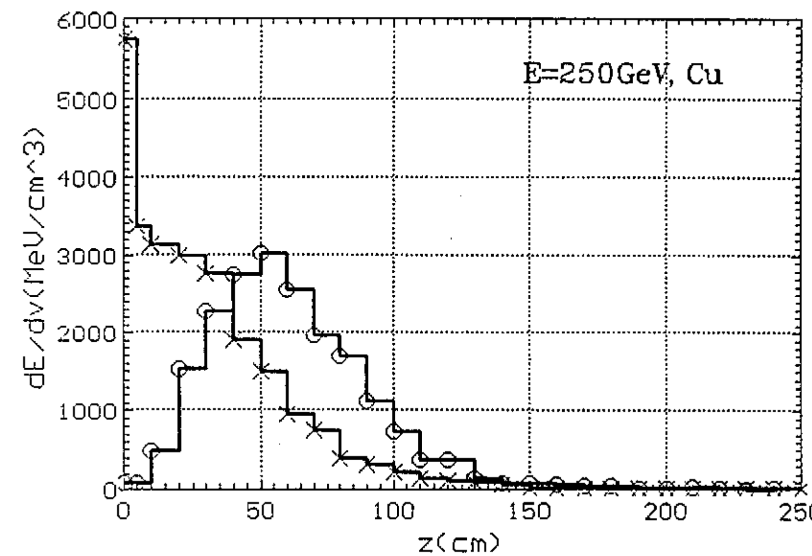

Fig. 14a: Distribution of energy density deposition in Al collimator 4 with 5 cm of copper (variant a).

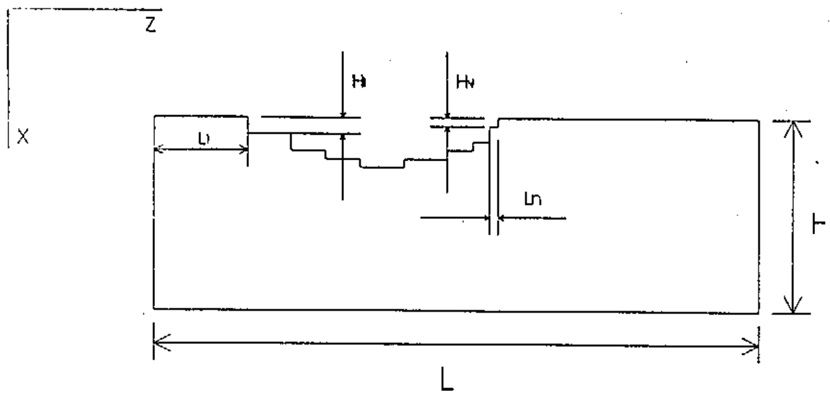

Fig. 18: Layout of variant C.

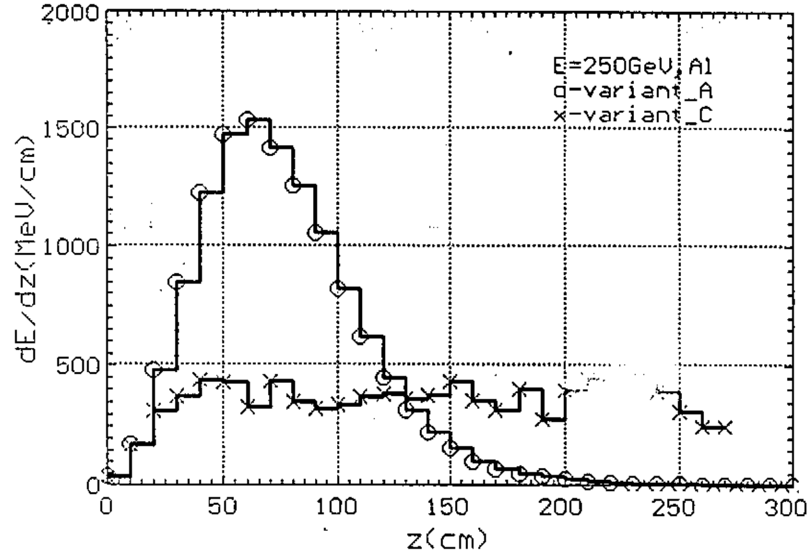

Fig. 20: Distribution of energy deposition in collimator 4 (variant c).

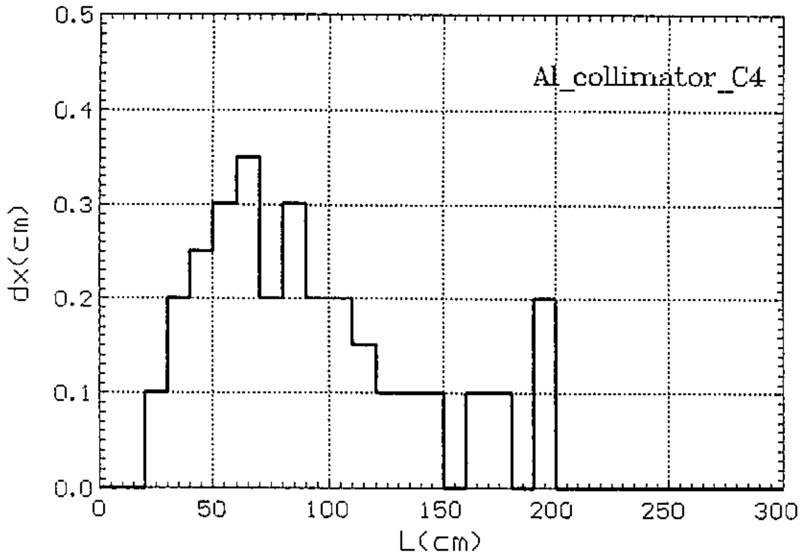

Fig. 19: Changing of H along collimator 4 (variant c).

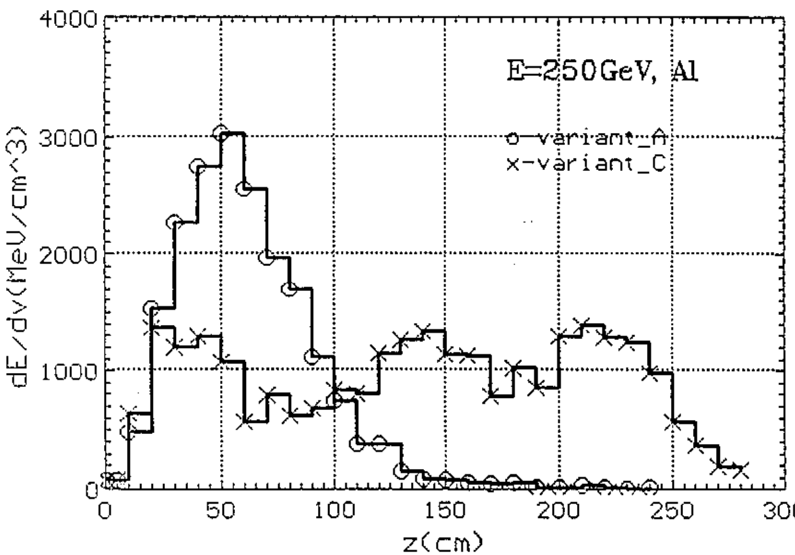

Fig. 21: Distribution of energy density deposition in collimator 4 (variant c).

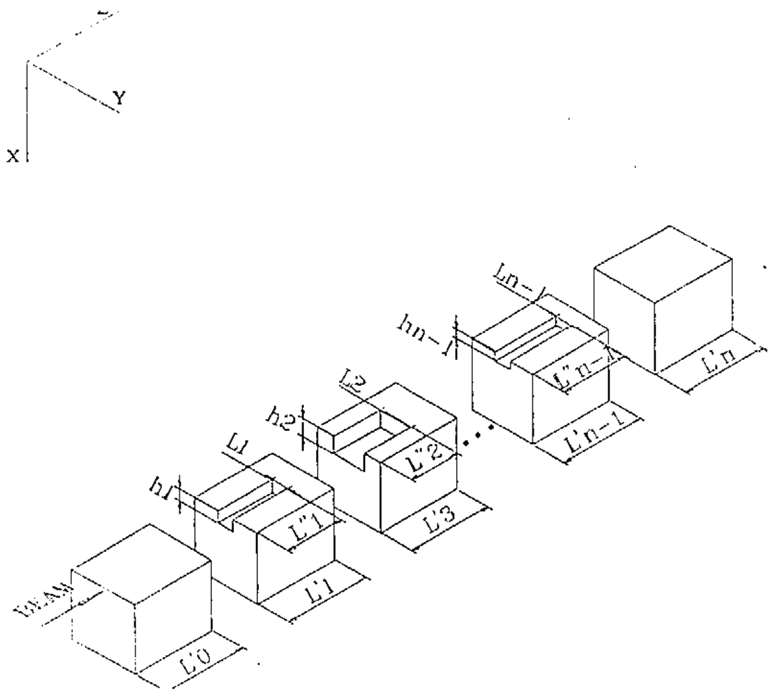

Fig. 22: Layout of variant D.

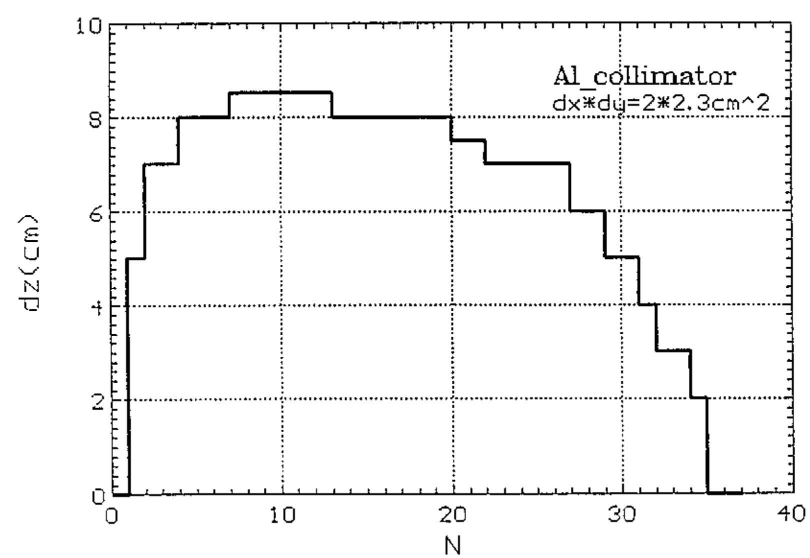

Fig. 23: Changing of L along collimator 4 (variant d).

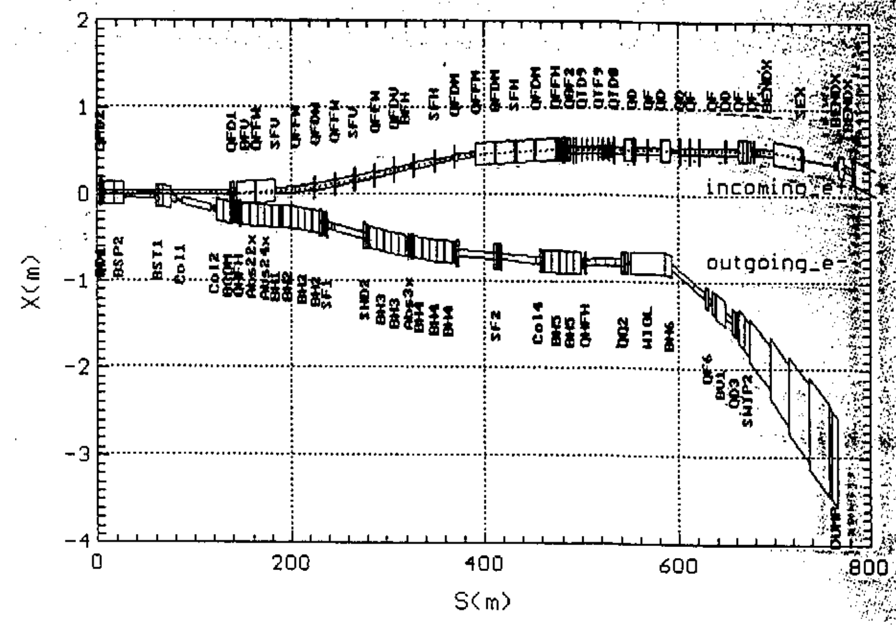

Fig.1: Layout of electron beam line.

N collim.	1	2	3	4(up)	4(down)	5(up)	5(down)
I [%]	2.79	1.07	1.26	0.70	0.78	1.14	1.08
X [mm]	-10.5	-18.0	14				
Y [mm]				3	-3	1.5	-1.5
L [m]	4	4	4	4	4	3	3
S [m]	82.01	117.42	242.33	453.71	453.71	546.86	546.86
Δ [mm]	6.13	3.84	6.06	.1.3	1.65	1.40	1.46

Table: 1 Parameters of the collimators for electron beam line.

Material	A	Z	ρ, g/cm³	L_{rad}, cm	$L_{99\%}$, cm	L_{max}, cm	$R_{99\%}$, cm	$R_{95\%}$, cm
Be	9.01	4.0	1.848	34.69	369.69	99.66	24.33	13.90
C(graphite)	12.01	6.0	1.73	24.68	460.6	188.9	23.7	13.6
Mg	24.305	12.0	1.74	14.39	207.43	54.66	29.26	14.43
Al	26.98	13.0	2.7	8.9	190.8	74.2	16.8	9.6
Ti	47.88	22.0	4.54	3.56	59.53	15.54	10.95	6.25
Fe	55.85	26.0	7.87	1.76	42.4	15.8	6.36	3.6
Cu	63.55	29.0	8.96	1.43	34.9	12.9	5.7	3.2
Be-B	9.44*)	4.23*)	1.92	31.80*)	558.67*)	234.99*)	23.28*)	13.30*)
Be-Al-Ti	18.05*)	8.34*)	2.6	13.65*)	273.20*)	109.46*)	17.53*)	10.02*)

Table 2: Atomic and nuclear properties of evaluated materials

175

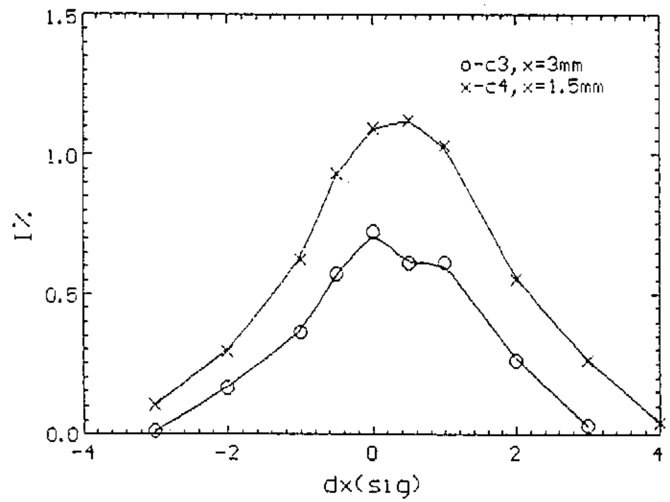

Fig.8: Beam losses on the collimators versus beam separation in IP.

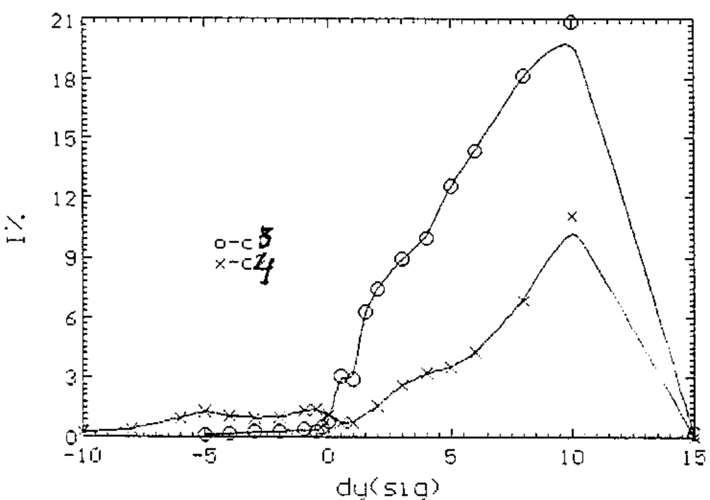

Fig.9: Beam losses on the collimators versus beam separation in IP.

Z=60cm

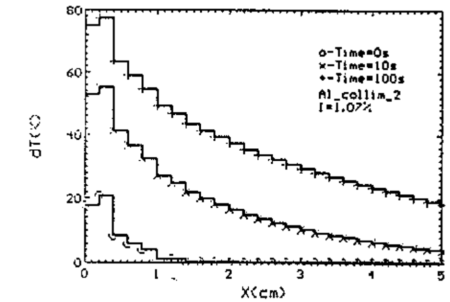

Fig. 34: Change of temperature in collimator 2 in horizontal direction in section with max dE/dV.

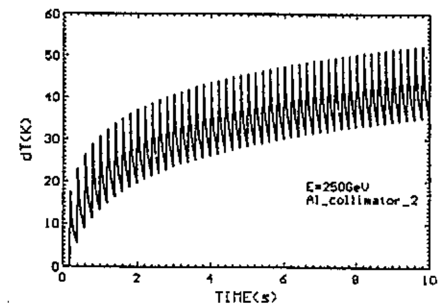

Fig.35: Change of temperature in collimator 2 in section with max dE/dV (I = 1.07 %).

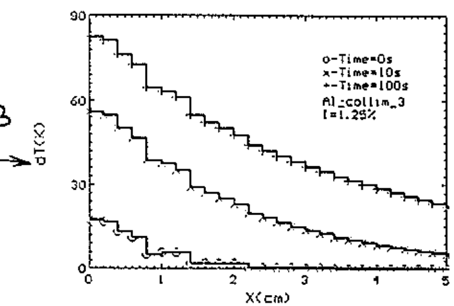

Fig. 36: Change of temperature in collimator 3 in horizontal direction in section with max dE/dV.

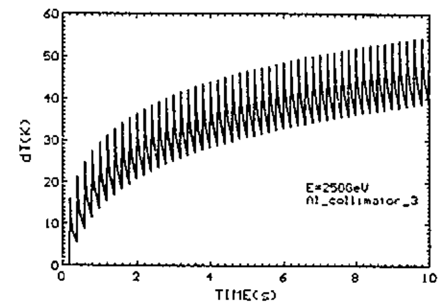

Fig.37: Change of temperature in collimator 2 in section with max dE/dV (I = 1.25 %).

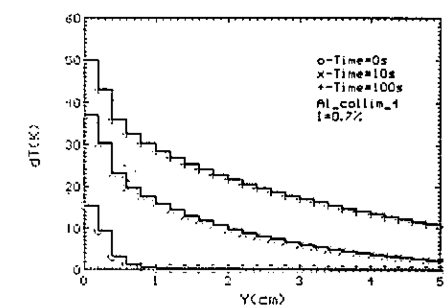

Fig. 38: Change of temperature in collimator 4 in vertical direction in section with max dE/dV.

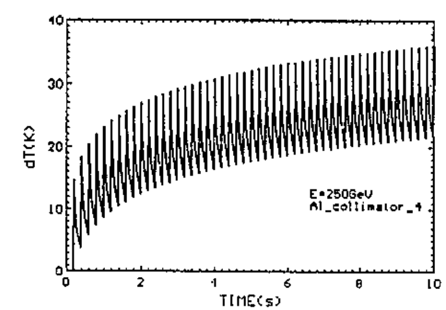

Fig.39: Change of temperature in collimator 4 in section with max dE/dV (I = 0.7 %).

R. Brinkmann

"Positron source before the IP"

177

Concept: **concentrate all large beam losses (10MW main beam, 300kW beamstrahlung, ~150kW γ's from e+ target, parasitic e- from e+ target (?)) in main beam dump hall at ~250m from IP**

Advantage for the site-layout: reduced spacing between dump halls (now ~500m), makes the site more compact (smaller) if we shift the IP ~300m north-wards

It looks feasible to use this solution, but there are many details concerning beam line layout to be studied (e.g. for modified beam delivery system, e+ transfer under the experimental hall, etc.)

Urgent: layout of spent beam line → dump without boundary conditions for e+ production (must avoid excessive beam loss!)

178

Re-consider this option mainly for the following reasons:

- Collimation of ~1MW spent beam power (average) is a serious technical problem
- Even if collimators work, strong activation of beam line components unavoidable
- Several meter concrete shielding required for radiation protection of soil/ground water
- Shower of particles from collimators may make beam diagnostics difficult or impossible

In addition, there are advantages of the upstream-source:

- Excellent beam quality of incoming beam allows for polarized positrons
- Limitations on beamstrahlung from e+ source point of view removed (room to move in parameter space for optimum luminosity)
- Can commission e+ damping ring and linac without need of sending e- beam through the IR

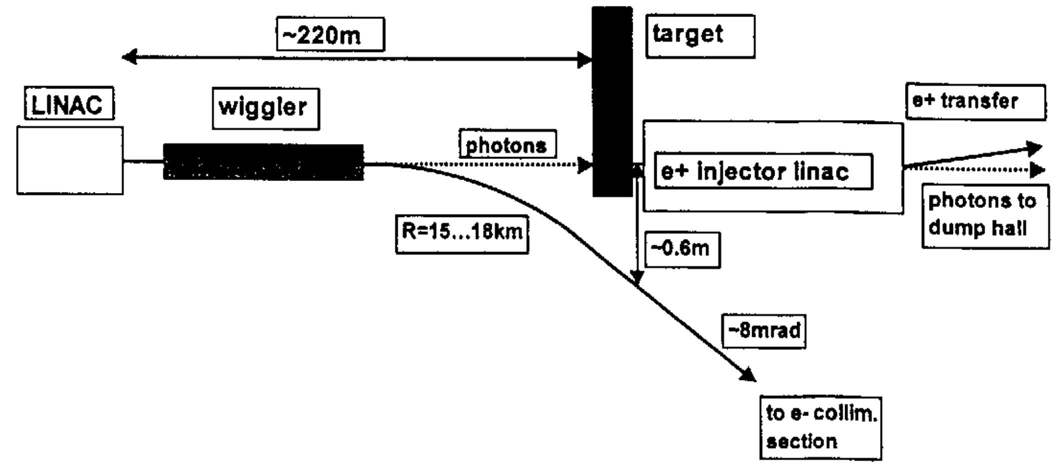

E_{beam} [GeV]	250
B_{rms}(wiggler) [T]	0.9
L_w [m]	60
λ_w [cm]	2.5
$\sigma_{r,\gamma}$(target) [mm]	1
$\eta_{capture}$ [%]	17
N_{e+}/N_{e-}	2
$\langle dE(e-)/E \rangle$ [%]	-1.6
$\sigma_E(e-)/E$ [%]	0.18
$\gamma \cdot \Delta\varepsilon(e-)$ [m]	$<10^{-8}$

W. Decking

"Damping ring design update"

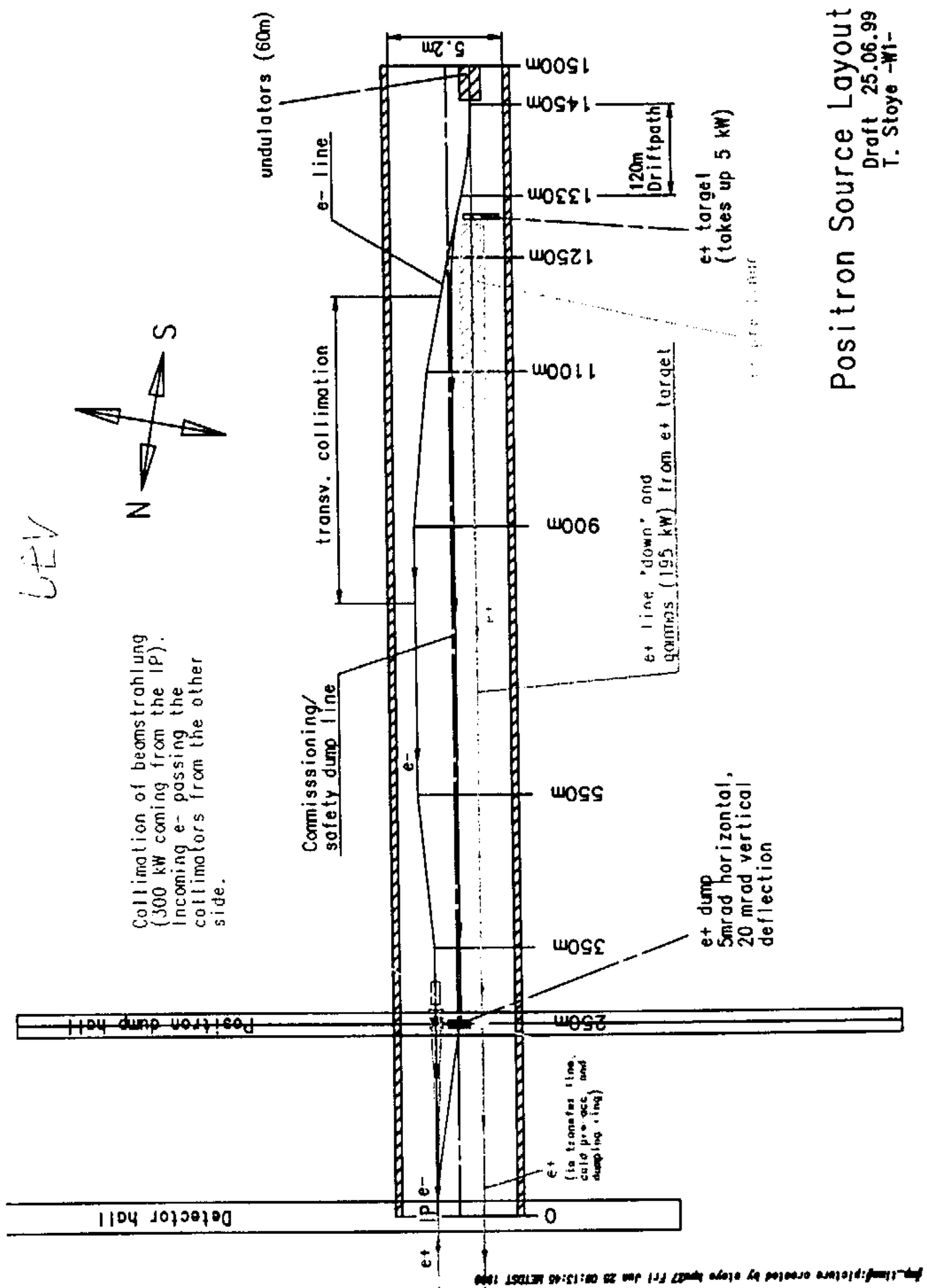

Damping Rings

W. Decking: DR design update

- E_0: 3.2 GeV ↗ 5 GeV removes Space-charge tune-shift instability (?)
- Optimisation of (Arc & Wiggler & StraightSection) Cells
- Dynamic aperture OK
- Problems: • tolerances (time varying B_x stray fields)
  • injection / extraction kickers (stability over 1 ms)

C. Burnton: Multibunch dynamics

- new parameters → RF × 2 w.r.t. CDR (16 or 23 cavities)
- HOM instability OK
- "nearly-mode" instability faster than damping

Introduction

New Parameters To Allow For Increased Luminosity:

	CDR	new set	determined by
hor. extracted emittance $\gamma\varepsilon_x$	12×10^{-6} m	8×10^{-6} m	luminosity
ver. extracted emittance $\gamma\varepsilon_y$	0.2×10^{-6} m	0.02×10^{-6} m	luminosity
eq. bunch length σ_z	< 0.01 m	< 0.01 m	bunch compressor
eq. momentum spread σ_p/P_0	$\approx 0.1\,\%$	$\approx 0.1\,\%$	bunch compressor
transverse acceptance $\gamma A_{x,y}$	> 0.05 m	> 0.05 m	$> 5 \times \gamma\varepsilon_{x,y;inj.}$
momentum acceptance A_p	$> 0.5\,\%$	$> 0.5\,\%$	
cycle time T_c	200×10^{-3} s	200×10^{-3} s	repetition rate
number of bunches n_b	1130	2820	bunch train
bunch spacing $\Delta\tau_b$	50×10^{-9} s	20×10^{-9} s	kicker raise/fall time
particles per bunch N_e	3.6×10^{10}	2×10^{10}	luminosity

Problem: Incoherent Space Charge Tune Shift

- Large ring length and relative low energy leads to huge incoherent space charge tune shift:
$$\Delta Q_{y;incoh} \approx -\frac{r_e N_e C}{(2\pi)^{3/2}\sqrt{\varepsilon_x \varepsilon_y}\sigma_z \gamma^2}$$
- $\Delta Q_{y;incoh} \approx 0.2$ for CDR parameters
- $\Delta Q_{y;incoh} \approx 0.43$ for high luminosity parameters
- Cures:
  - * Increase ring energy
    - \- Needs lattice redesign
    - \- Higher rf-costs
    - \+ Need less wiggler length
  - * Decrease ring circumference
    - \- Kicker technology not available (?)
  - * Increase bunch volume through local coupling and/or dispersion
    - \- Additional coupling in a small coupling ring
    - \+ Probably low cost solution
    - ⇒ Needs more study

Arc Cell

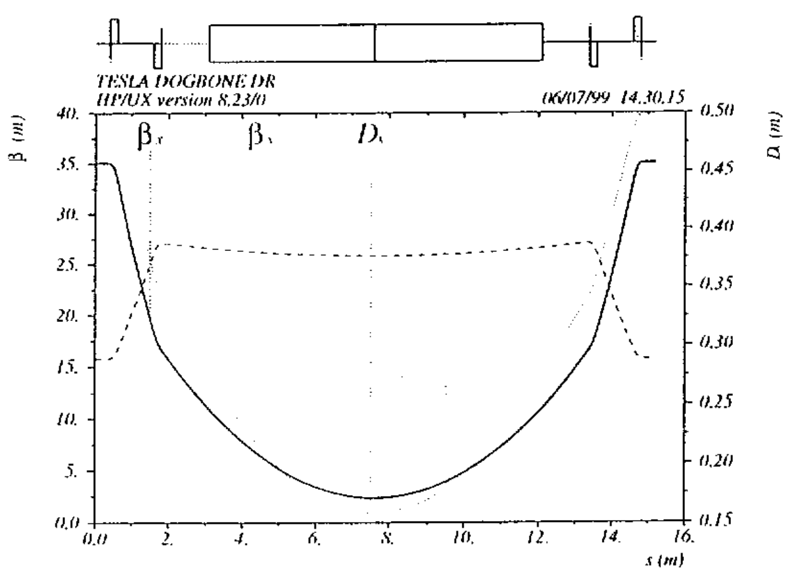

- 'detuning' $\varepsilon_r \approx 4$
- long dipole to increase β, η, α_c
- QF split for best placement of sextupole
- $\nu_x = 0.4, \nu_y = 0.1$ cancels 1^{st} order nonlinear terms after 5 cells
- $\theta = 6\,\text{deg}$ gives $\gamma\varepsilon_{x;0} = 35\,\mu\text{m}$ at $5\,\text{GeV}$
- $U_0 = 1.1\,\text{MeV/turn}$

Wiggler Cell

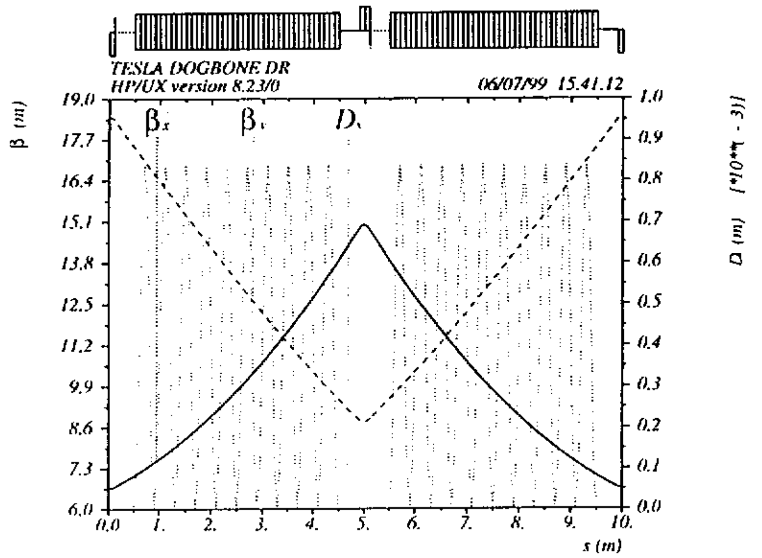

- $B = 1.5\,\mathrm{T}$, $\lambda = 0.4\,\mathrm{m}$
- cell length of $10\,\mathrm{m}$ and $\nu_x = 0.166$ gives $< \beta_x > \approx 10\,\mathrm{m}$
- $\varepsilon_{x;wig} = 7\,\mu\mathrm{m}$ at $5\,\mathrm{GeV}$
- Total of 36 cells leads to $U_0 = 18\,\mathrm{MeV/turn}$

Straight Section Cell

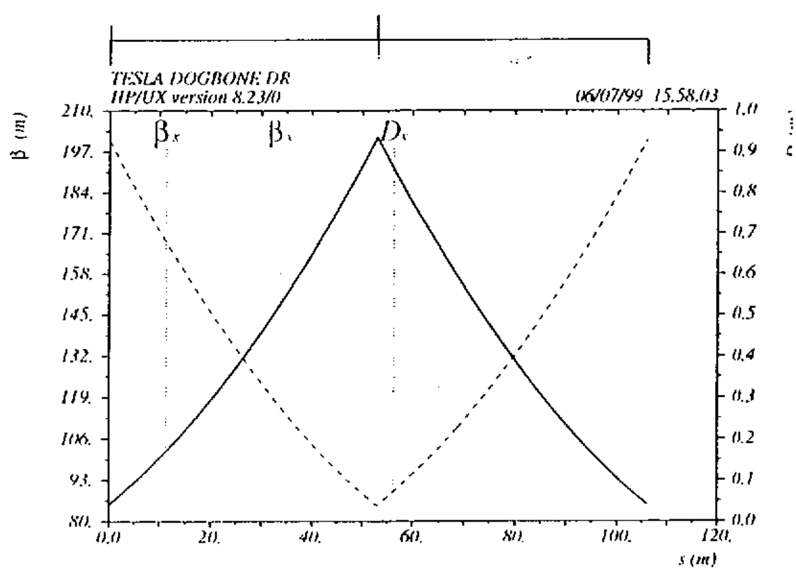

- long cell length reduces $\#_{Quads}$
- $\nu_x = \nu_y = 0.125$ to reduce chromaticity contribution
- enough space for injection, circumference correction, RF, ...
- due to high β very sensitive to errors (stray fields, ...)

Dynamic Aperture

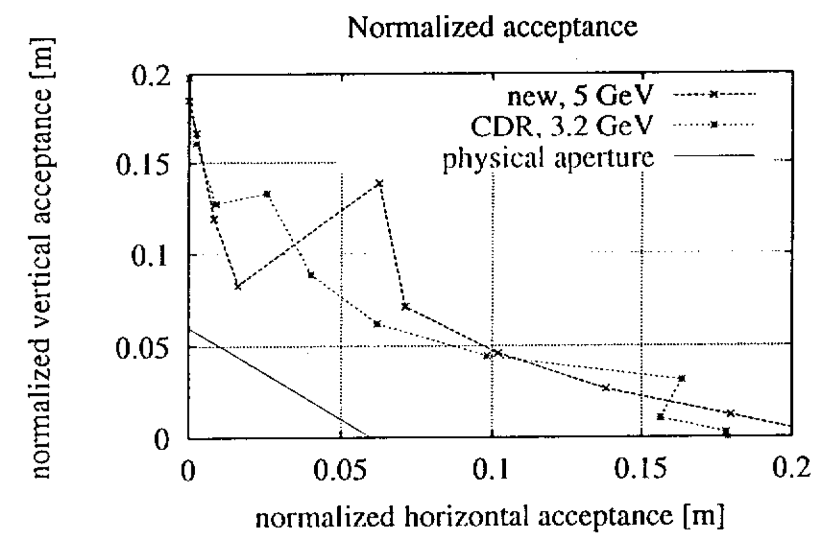

- tracked with sextupoles misaligned to introduce optics distortion and coupling

Layout

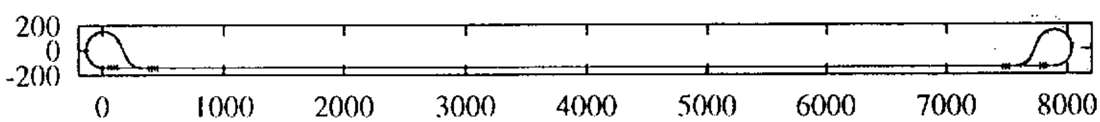

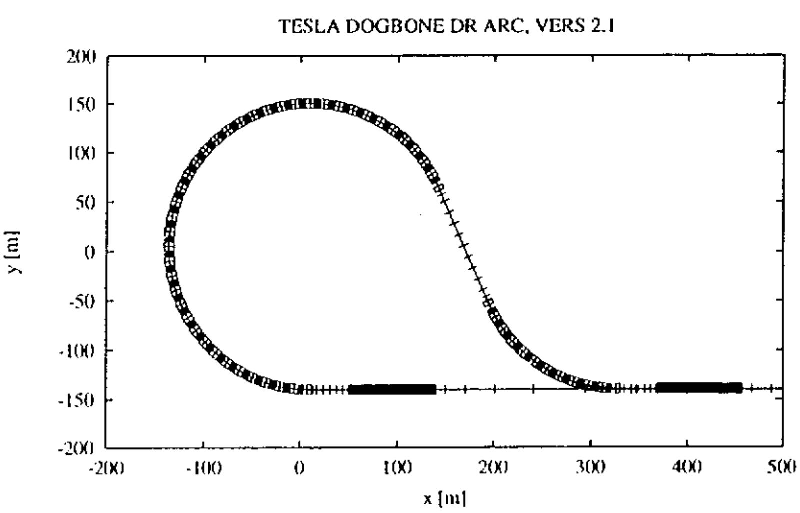

- Arc length 920 m
- Wiggler length 288 m
- $\xi_{x;arc} = -90$, $\xi_{x;straight} = -30$
- $\xi_{y;arc} = -32$, $\xi_{y;straight} = -30$

183

- Tolerances as in CDR allow to reach $\gamma\varepsilon_{y;0} = 0.1\,\mu\mathrm{m}$

transverse position of elements :	$0.1\,\mathrm{mm}$
roll angle :	$0.2\,\mathrm{mrad}$
BPM resolution :	$0.01\,\mathrm{mm}$

- For $\gamma\varepsilon_{y;0} \approx 0.01\,\mu\mathrm{m}$ vertical dispersion correction is needed to a level of $D_{y;rms} \leq 2mm$ (need a $0.5\,\%$ momentum shift to measure with BPMs with $0.01\,\mathrm{mm}$ resolution)
- Tolerances for time-varying stray fields in the long straights are a few nT; first measurements (Jensen, Pillat) show values up to $100\,\mu\mathrm{T}$ in typical accelerator environments
- Need of circumference correction to adjust for tides, wiggler on/off (?)

$$\frac{\Delta C}{C} = \alpha_c \frac{\Delta p}{P} \leq 0.1 \times \sigma_p/P \rightarrow \Delta C \leq 270\,\mu\mathrm{m}$$

C Burton

"Multi-bunch instabilities in the damping ring"

1K4

Parameters		
	CDR	New (WD)
E_b / GeV	3.2	5
σ_E	0.1×10^{-2}	0.13×10^{-2}
U_0 / MeV	10.3	20.3
V_{rf} / MeV	25	50
α_c	3.4×10^{-4}	1.2×10^{-4}
σ_z / mm	9.5	6
α_ε / Hz	59	71

Major Cavity HOM

$Q = 1100$ (damped), $R \approx 60\,\mathrm{k\Omega}$, $f_{\mathrm{HOM}} \approx 782\,\mathrm{MHz}$

$$N_{\mathrm{cav}} \sum_{p=-\infty}^{+\infty} \frac{f_{pk}}{\mathrm{GHz}} \frac{\Re e Z_{\parallel}^{\mathrm{cav}}(\omega_{pk})}{\mathrm{k\Omega}} e^{-(\omega_{pk}\sigma_z/c)^2} < \begin{cases} \mathrm{cdr}: & 930 \\ \mathrm{new}: & 2450 \end{cases}$$

$$\mathrm{HOM}: \begin{cases} \mathrm{cdr}: & 380 \\ \mathrm{new}: & 760/1090\,(N_{\mathrm{cav}} = 16, 23) \end{cases}$$

$$\text{or} \quad \text{HOM growth rate} \begin{cases} \mathrm{cdr}: & 24\,\mathrm{Hz} \\ \mathrm{new}: & 22\,\mathrm{Hz}/31\,\mathrm{Hz} \end{cases}$$

Nearby-mode Growth rate

		16 Cavities		23 Cavities	
f_{rf} / MHz	ν_{s}	$\lvert\Delta f\rvert$ / Hz	τ^{-1} / Hz	$\lvert\Delta f\rvert$ /Hz	τ^{-1} / Hz
433.33	0.065	4530	91	6512	306
400	0.063	4182	67	6012	221
350	0.059	3661	41	5263	131
325	0.056	3400	31	4888	98

Note: $\nu_{\mathrm{s}} \propto \sqrt{f_{\mathrm{rf}}}$; $R/Q = 225\,\Omega$

N. Baboi

"Multi-bunch beam dynamics in main linac"

186

LINAC

N. Baboi: Multibunch dynamics with superstructures

- HOMs R/Q & Q from Jack's calculations
- Slightly better than with 9-cell cavities

V. Tsakanov: Beam with different energies (FEL / Collider)

- $E_{acc} = 18$ MV/m for FEL (w.r.t. 25 MV/m)
- $\mu_{Coll} = 60°$ ↗ $\mu_{FEL} \simeq 90°$
- Vertical dispersion oscillates if Linac is "curved"
- replace "curved" linac by 18 m, 7 mrad dipole @ ~ 50 GeV
- beam dynamics studies

R. Brinkmann: Estimate of beam halo

- Important for $\mu^{\pm}$ background in detector
- $< 10^4$ p/bunch ⇒ $< 6\ \mu^{\pm}$ in TPC / 50 μs

  (halo from DR, beam gas scatt., intra-beam scatt., dark current)
- Dark current halo negligible at 5 GeV injection (7 p/bunch) !!

SUPER - STRUCTURE

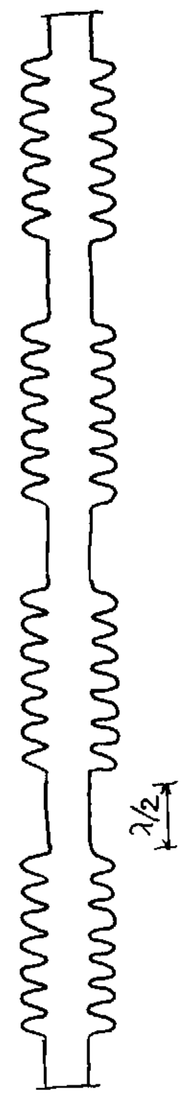

4 × 7 CELLS → IN SIMULATION AS ONE ACCELERATING STRUCTURE

3 SUPER-STRUCTURE / MODULE

TESLA CAVITY : 10 MOST "DANGEROUS" HOMs FROM CDR

9 CELLS

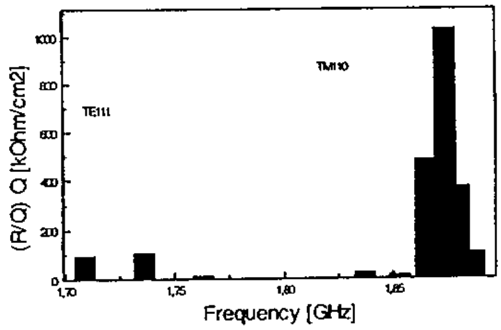

SUPER-STRUCTURE : MOST "DANGEROUS" MODES (MEASURED)

7 × 4 CELLS (FACTOR 3 COMPARED TO TESLA)

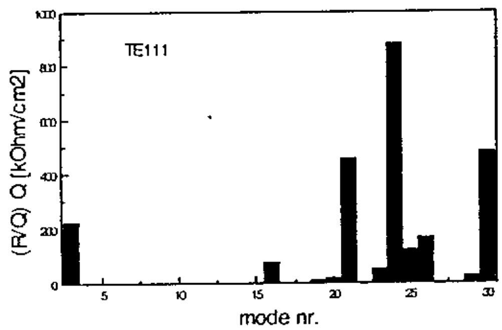

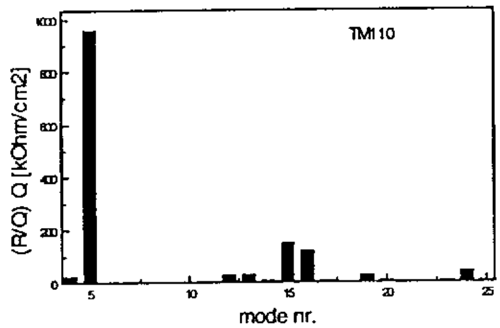

SOME RESULTS

BUNCH TRAIN AT END OF LINAC

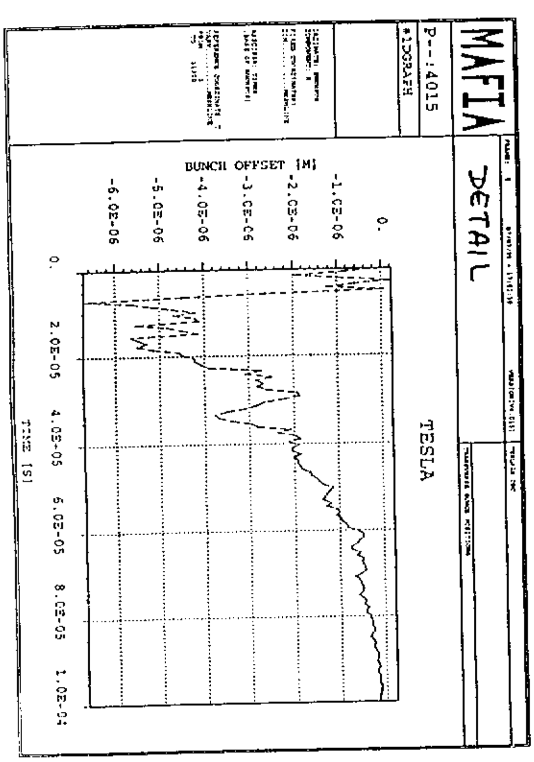

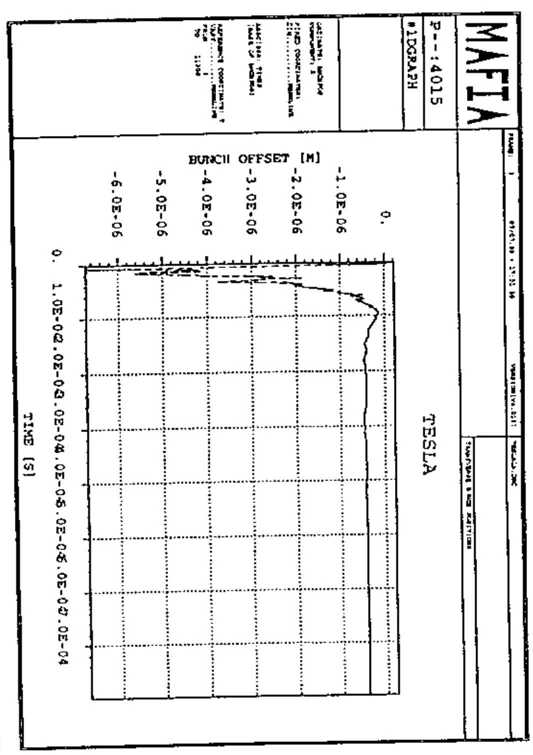

EMITTANCE

ALONG THE LINAC

~ 1% EMITTANCE GROWTH FROM MULTIBUNCH EFFECTS

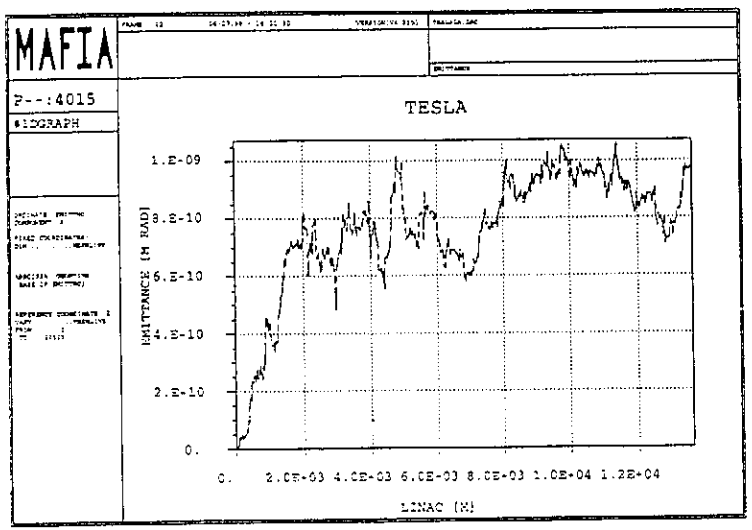

SUPER - TESLA

≤ 1 % EMITTANCE GROWTH FROM MULTI-BUNCH EFFECTS

BUNCH TRAIN AT END OF LINAC

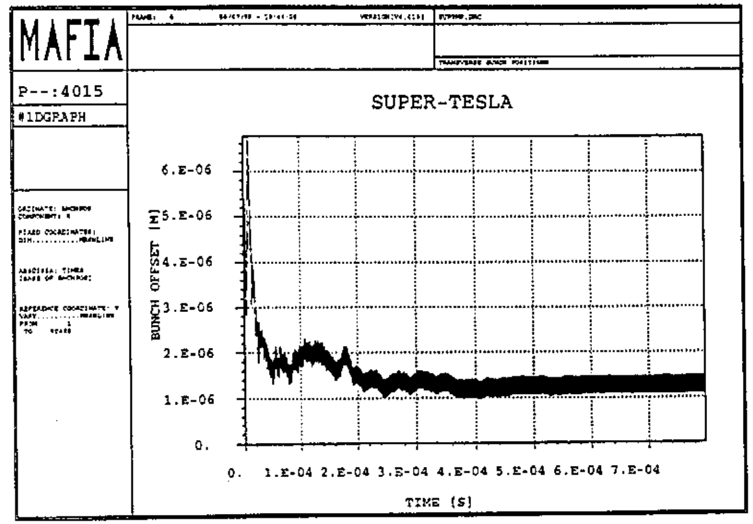

δE = 0,1%

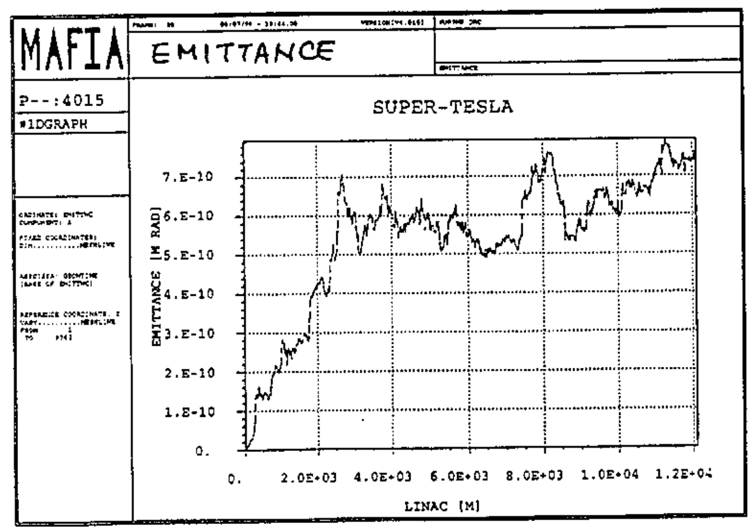

V. Tsakanov

"Beams with different energies (FEL/Collider)"

Beams with different energies (FEL/Collider)

V.M. Tsakanov

Yerevan Physics Institute, Armenia

1. Introduction
2. Present performance (CDR)
   * Linear optics
   * Emittance preservation
   * Conclusions
3. Wide TESLA/FEL energy spread
   * New parameter set
   *Linear opotics
   * Emittance preservation
   * Conclusions

559

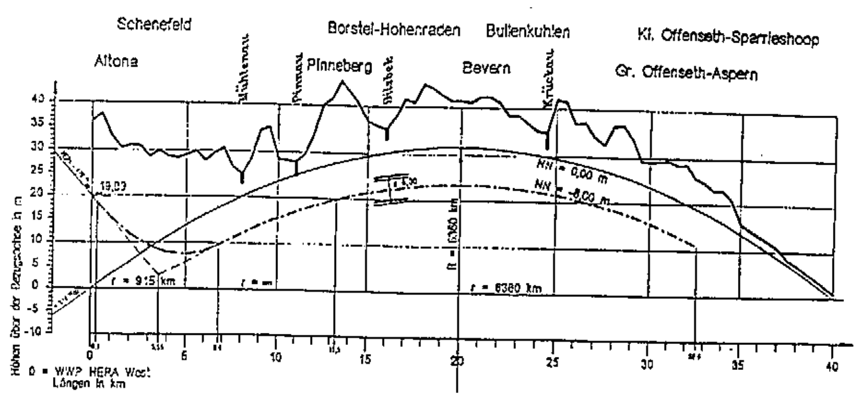

Figure 3.10.3: *Expanded profile of the Linear Collider area North-Northwest of DESY.*

1 Linear optics

$$\sin(\mu_F/2) = \frac{U_T}{U_F}\sin(\mu_T/2) \tag{1}$$

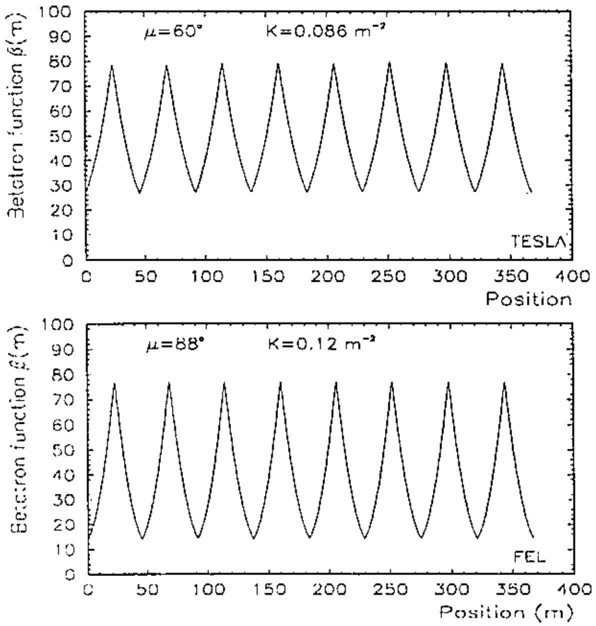

Fig.2 *The betatron functions of the TESLA and FEL beams.*

The phase ellipses of injected beams for TESLA and FEL operations have to be matched with machines ellipses to prevent the emittance dilution of the beta-mismatch

$$\frac{\Delta\varepsilon}{\varepsilon} = \frac{1}{2}\left[\frac{\beta}{\beta^*} + (\alpha - \alpha^*)^2\frac{\beta^*}{\beta} + \frac{\beta^*}{\beta}\right] \tag{2}$$

where α, β machine initial Twiss parameters, α^*, β^* the Twiss parameters at the end of injection chanels. As an example, if the matching point is at the middle of the quadrupole ($\alpha = 0$), for the 5% of emittance dilution we get

$$\alpha^* \leq 0.22, \qquad 0.75 \leq \frac{\beta^*}{\beta} \leq 1.27 \tag{3}$$

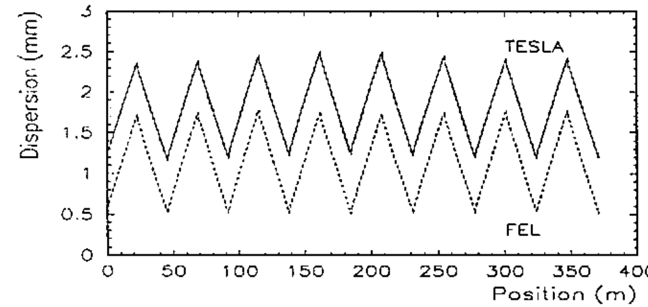

Fig.3 *The periodic dispersion functions of the TESLA (solid line) and FEL (dashed line) beams.*

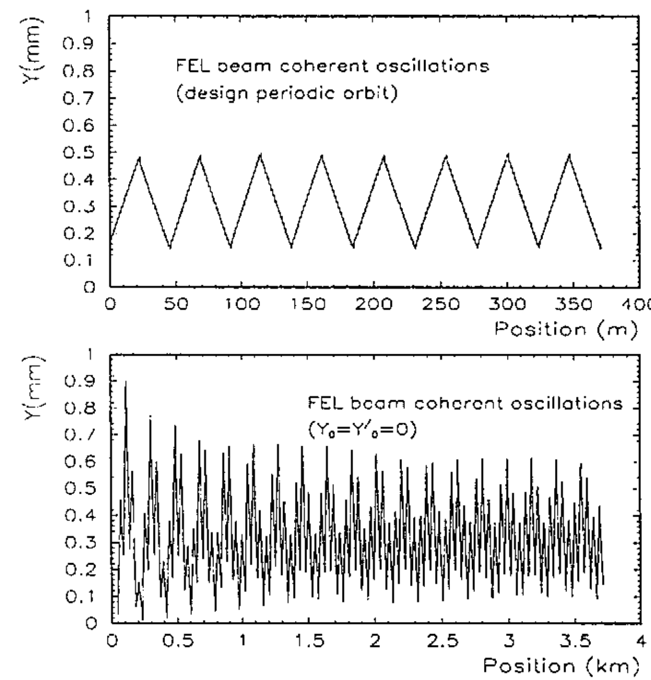

Fig. 4 *The FEL beam design periodic orbit (a) and the coherent oscillations of the beam with initial zero amplitudes (b)(on axis injection).*

1.1 Emittance preservation

a) *Dispersive effects. Coherent oscillations*

Fig.5 shows the emittance dilution of the beam caused by injection jitter and initial uncorrelated energy spread for one sigma offset of the injected beam with respect to FEL beam design orbit. For comparison we show also the dispersive emittance dilution when the FEL beam injected along the axis of the main linac. Thus, to stabilized the emittance dilution of the FEL beam with the accuracy better than 5%, the uncorrelated energy spread limited by 1% and the injection jitter by one sigma offset with respect to FEL design orbit.

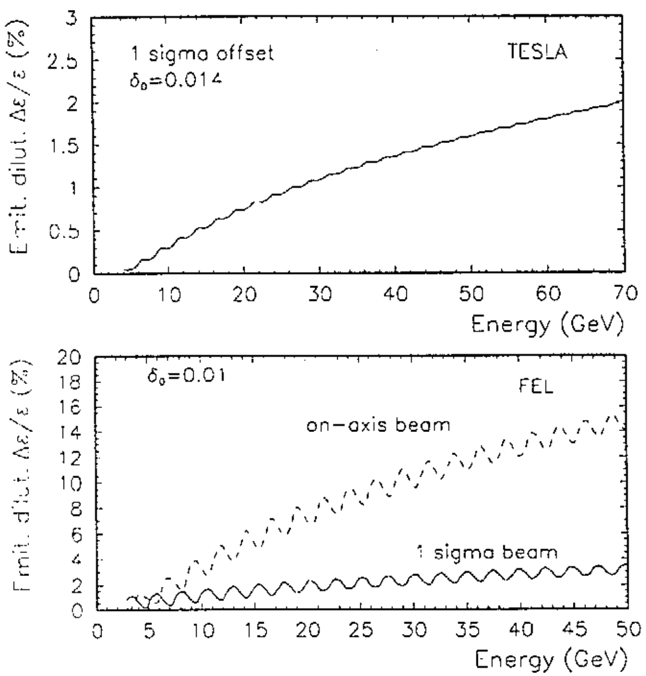

Fig.5 *The dispersive emittance dilution caused by initial uncorrelated energy spread and injection jitter. Shown are the cases of one sigma initial offset (solid line) and on-axis injected (dashed line) FEL beam.*

b) *Wake fields effects.*

The wake fields caused emittance dilution of the TESLA and FEL beams is shown in Fig.6. The high energy beam performs coherent betatron oscillation with one standard initial offset. For the FEL beam are shown the cases when the beam follow the design orbit (matched beam) and the beam injected at the axis of the main linac. The effect is in order of few percent for TESLA beam and negligible (in order of 10^{-4}) for FEL beam .

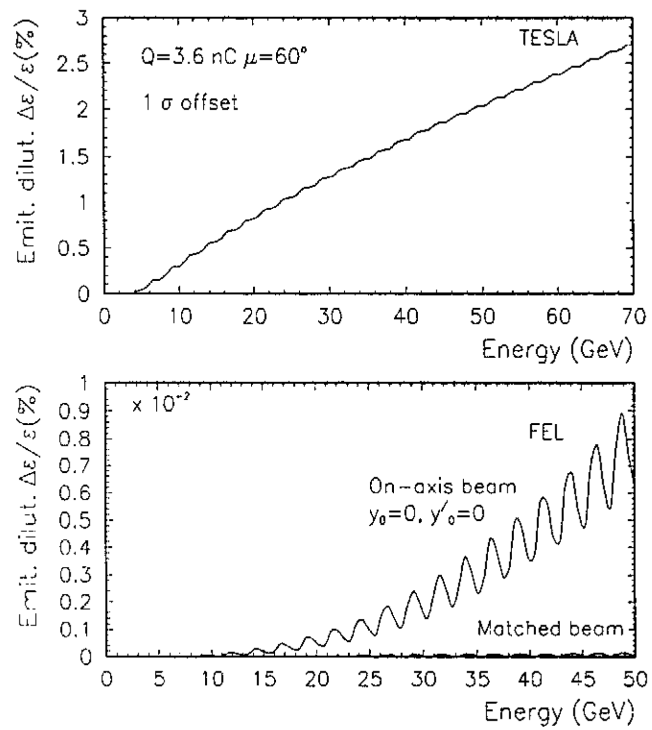

Fig.6 *The wake field emittance dilution of the TESLA and FEL beams. Coherent oscillations with matched and on-axis injected FEL beam.*

c) Trajectory correction

The quadrupole misalignments of the linac affect both trajectories of the TESLA and FEL beams. Note, that if one of the beams is corrected, the second beam with the large energy shift experiences an additional kick in quadrupoles which is proportional to the corrected trajectory offset of the first beam $\Delta x_2' \approx K x_1$. Thus the second beam not follow the dispersion trajectory but performs additional beating , the amplitude of which could be substantially growth leading to large emittance growth. We will return to this problem in the next section. Fig.7 shows the **TESLA** and **FEL** beams trajectories when the high energy beam is corrected by using one-to-one correction technique. Note, that the dispersion functions exactly follow the trajectory of the beams.

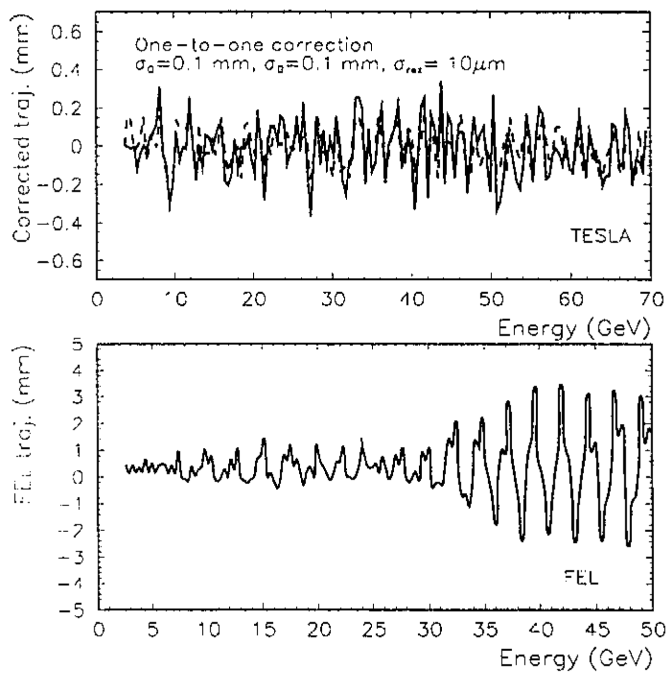

Fig.7 *The beating of the FEL beam with the one-to-one correction of the TESLA beam. Shown the quadrupoles misalignment-dashed line, and the TESLA one-to-one corrected trajectory solid line (top) and the coherent oscillations of the FEL beam (bottom).*

1.2 Machine performance

Beam dynamics:

* the **FEL beam should be matched with the design orbit to prevent** the emittance dilution of **injection jitter;**

* the **dispersions of the TESLA and FEL beams should be matched** to obtain the minimum periodic dispersion of the machine;

* the periodic dispersion is still large (**2.5 mm**) and the application of the **beam based trajectory correction becames problematic.**

Machine performance:

* each **FODO cell should be geometrically curved by about 0.05** mrad to be linked with the **design trajectory of the TESLA beam. In** turn, the each **cell should be aligned with the accuracy better than** $100\mu m$;

* the **option of the further colliding of the TESLA electron beam** with **HERA proton beam needs some reconstruction of the machine** elements as far as the **correction dipoles with the maximum magnetic** field 44 m **T could not provide the corresponding bend of the electron** beam at **energies 250-500 GeV.**

To **prevent all these aspects of the machine performance and beam** dynamics issues, the **part of the main linac with parallel operation** of collider and **FEL beam is reasonable to be straight with further** bending of the collider beam by angle **7.5 m rad in achromat cell after** the **separation of colliding and FEL beams (Fig.1). The energy of** the collider beam is then at the **level of 70 Gev . The FEL beam is** extracted from the linac at the **different energies by the fast kicker** setup at energies **15, 25 and 50 GeV and is transported to the user** laboratories.

193

2 Wide band energy spread and high luminosity TESLA

TABLE 1: Parameter list

1. TESLA (FEL) injection energy - 5 GeV (2.2 GeV).
2. Vertical emittance $\gamma\varepsilon_y$ - $0.03 mm \cdot mrad$, $(0.7 mm \cdot mrad)$
3. Charge per bunch - $2 \cdot 10^{10}$, $(6 \cdot 10^{9})$
4. Bunch length - 0.4 mm ($25 \mu m$)
5. Initial uncorrelated energy spread - 0.01 (0.01)

a) Linear optics

$$\sin(\mu_T/2) = \sin(\mu_1/2)\left(\frac{E_{0T}}{E_{0F}}\frac{E_F(n)}{E_T(n)}\right)^{\alpha} \quad (4)$$

$$\sin(\mu_F/2) = \sin(\mu_{1T}/2)\left(\frac{E_{0T}}{E_{0F}}\right)^{\alpha}\left(\frac{E_T(n)}{E_F(n)}\right)^{1-\alpha} \quad (5)$$

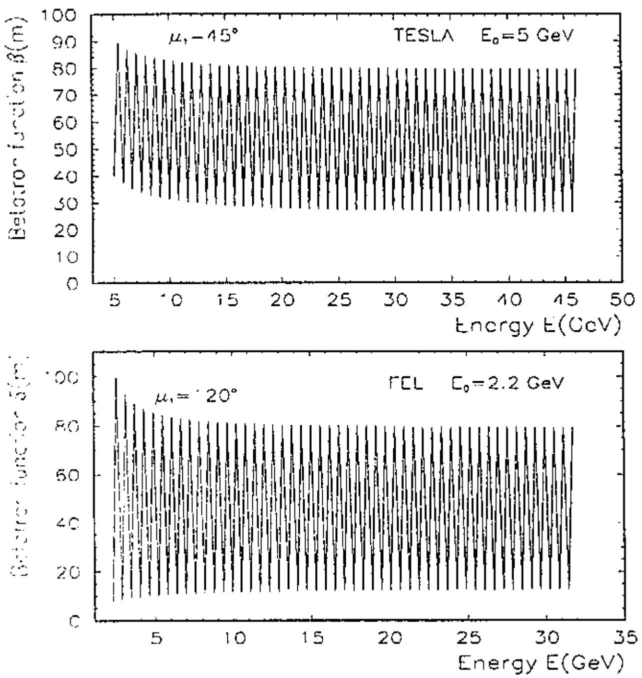

Fig.7 *The betatron functions for TESLA and FEL beams.*

b) Free coherent oscillations. Dispersive effects

$$\frac{\Delta\varepsilon}{\varepsilon}(z) = 2\delta_0^2\tan^2(\mu/2)\left(\frac{\gamma_0}{\Delta\gamma}\right)^2\ln^2\frac{\gamma(z)}{\gamma_0} \quad (6)$$

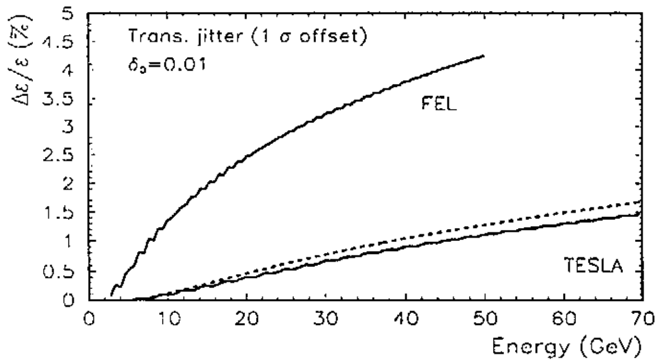

Fig.8 *The dispersive emittance dilution caused by injection jitter and initial uncorrelated energy spread. The beam performs free coherent oscillations with one sigma initial offset ($\sigma_T = 15 \mu m, \sigma_F = 120 \mu m$). The dashed line shows the analytical prediction for TESLA beam with constant beta lattice ($\mu = 60^\circ$).*

c) Free coherent oscillations. Wakefield effects

$$\frac{\Delta\varepsilon}{\varepsilon}(z) = \frac{1}{2}\frac{a_0^2}{\varepsilon_0}\left(\frac{eQW_dL_c}{8G}\right)^2\frac{1}{\sin^2\mu}\ln^2\frac{\gamma(z)}{\gamma_0}, \quad (7)$$

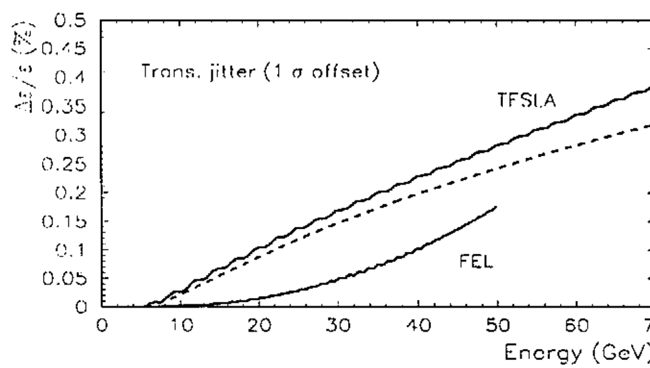

Fig.9 *The wakefield caused emittance dilution. The beam performs free coherent oscillations with one sigma initial offset. Dashed line -analytical prediction for TESLA beam.*

d) *Accelerator section misalignments*

$$\frac{\Delta\varepsilon(z)}{\varepsilon} = \frac{< y_a^2 >}{2N_{cav}\varepsilon_0}\left(\frac{eQW_D}{4G}\right)^2 \frac{\Delta\gamma}{\gamma_0}\frac{L_c}{\sin\mu}\ln\frac{\gamma(z)}{\gamma_0} \qquad (8)$$

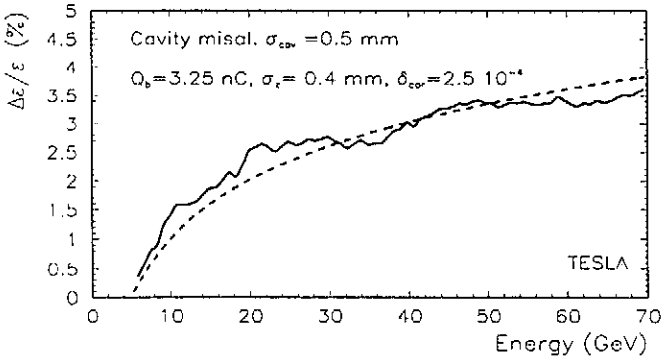

Fig 10. *Emittance dilution of the TESLA beam because of the cavity misalignments. Dashed line -analytical prediction.*

e) *One-to-one correction*

$$\frac{\Delta\varepsilon}{\varepsilon} = 8\delta^2_{0_{rms}}\frac{< y_c^2 >}{\varepsilon_0 L_c}\frac{\gamma_0}{\Delta\gamma}\tan\frac{\mu}{2}\cdot\ln\frac{\gamma(z)}{\gamma_0} \qquad (9)$$

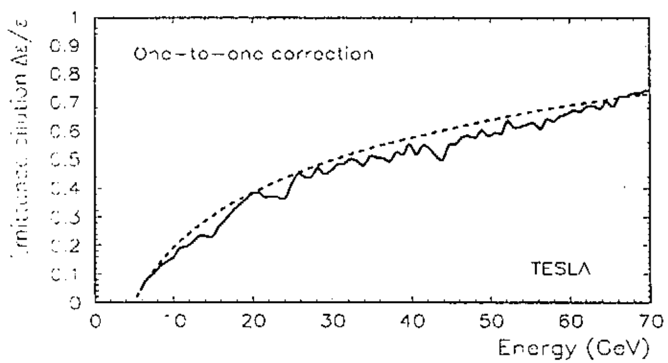

Fig 11. *Uncorrelated dispersive emittance dilution of the TESLA beam with one-to-one correction (σ_q = 100μm, σ_b = 100μm, σ_r = 10μm). Dashed line - analytical prediction.*

f) *Two beam operation*

$$< \Delta y^2 >= \bar{\delta}^2 < y_t^2 > \frac{\beta(z)}{\gamma(z)}\sum_k K_{fk}^2 L_q^2 \beta_k \gamma_k \sin^2[\phi(z) - \phi(z_k)] \qquad (10)$$

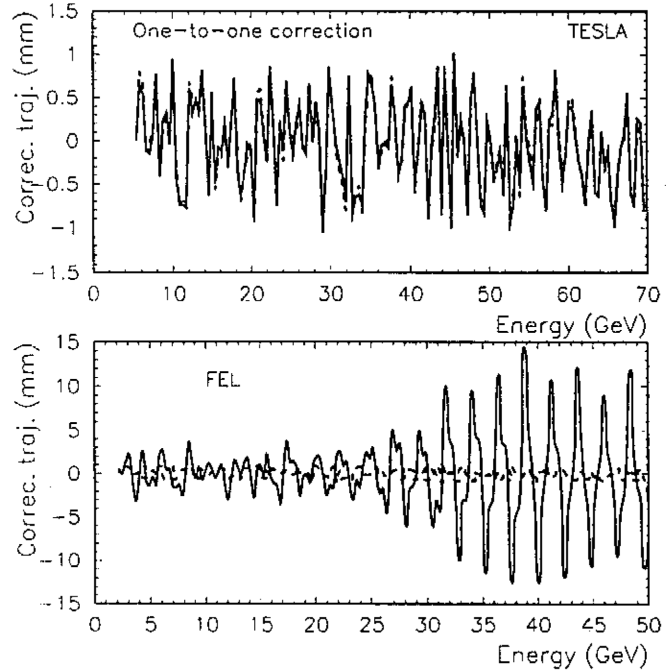

Fig.12 *The TESLA beam corrected trajectory (one-to-one correction, σ_q = 0.5mm, σ_b = 0.1mm, σ_r = 10μm) and the coherent oscillations of the FEL beam.*

Summary

*** the two-beam operation part of the main linac need to be straight to prevent the dispersion caused errors for beam based correction technique;**

*** the use of the one-to-one correction technique for one of the beams accompanies by the large coherent oscillations of the second beam ;**

*** the operation of the machine with two beams with different energies - use to use on-line two-beam based trajectory correction.**

R. Brinkmann

"Estimate of Beam halo"

196

<u>Halo from damping ring</u>

As (pessimistic) estimate for beam halo in the D.R. I assume a fraction of 10^{-3}

A low-energy collimation system reduces that by at least a factor 10^4 (according to calculations for high-energy system)

→ expect ~ 10^3 halo particles/bunch at linac entrance

<u>Beam-gas in the linac</u>

1. single Coulomb scattering

total cross section for scattering angle larger than acceptance θ_A:

$$\sigma(\gamma) = 2\pi\left(\frac{2Zr_e}{\gamma}\right)^2 \cdot \int_{\theta_A}^{\pi} d\theta \frac{\sin\theta}{\theta^4}, \qquad \theta_A = n_\sigma \sqrt{\frac{\varepsilon_y}{\gamma\cdot\beta}}$$

approximately: $$\sigma(\gamma) \approx \frac{4\pi Z^2 r_e^2 \beta}{n_\sigma^2 \varepsilon_y \gamma}, \quad \sigma_{tot} = \int_{Linac} \sigma(\gamma) ds$$

gas density (@2K): $n_{gas} = 3.6 \cdot 10^{24} m^{-3} \cdot P/mbar$, example $P(He)=10^{-10}$ mbar, $\beta=100m$, $\varepsilon_y=3 \cdot 10^{-8}m$, $n_\sigma=30$:

# of Coulomb scattering events p. electron = $5.7 \cdot 10^{-8}$

→ **$1.2 \cdot 10^3$ halo particles per bunch**

2. Bremsstrahlung

→ **negligible compared to Coulomb scattering**

Touschek effect

Hard intra-beam scattering with momentum transfer >3% (BDS acceptance)

→ **negligible (~ 1 particle per bunch)**

Dark current

Phase space distribution of dark current obtained from PhD thesis by C. Stolzenburg (using field emission model for one 9-cell resonator)

Question: how much of that is transported to high energy in the TESLA linac?

Depends strongly on the "nominal" (i.e. main beam) energy at which the field emission takes place (most particles get lost downstream due to over-focusing in the linac lattice)

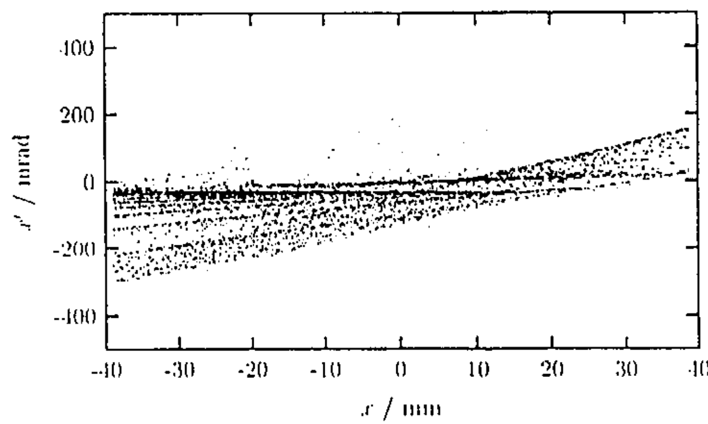

One 9-cell cavity, g = 25MV/m:

$\langle E \rangle = 11 MeV$, $\langle \varphi_{rf} \rangle = 40$ deg., $\varepsilon = 4 \cdot 10^{-4}$ m determine fraction of stable phase-space volume by tracking large # of particles through the linac, as function of main beam energy at the position of the emitting cavity

assume 60 deg. FODO lattice, 16 cavities between quads, 1st cav. is d.c. source

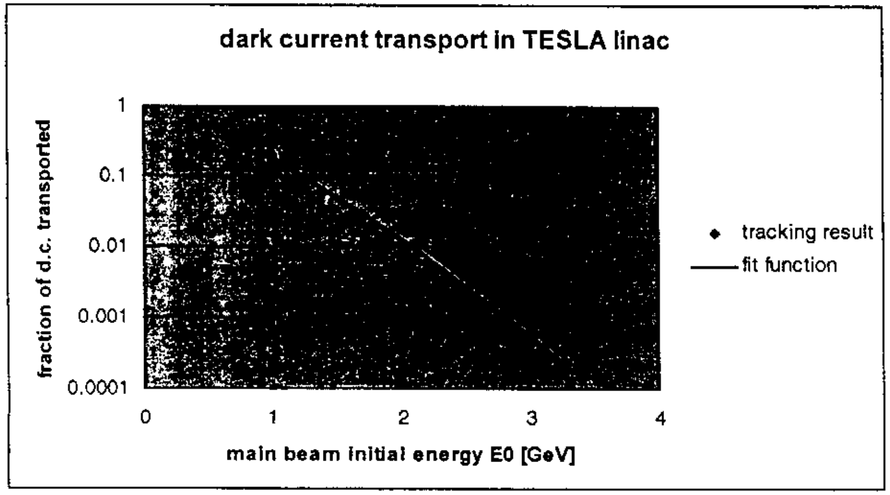

Fit function:

$$\frac{I_{stable}}{I_{initial}} = \exp(-1.7 E_0^{1.35})$$

total dark current at end of linac:

$$I_{d.c.}(E_0) = \int_{E_0}^{E_f} I_{stable}(E) \frac{dI_{emit}}{dE} dE$$

rough estimate: dI/dE = 40μA/GeV (i.e. 1μA p. cavity)

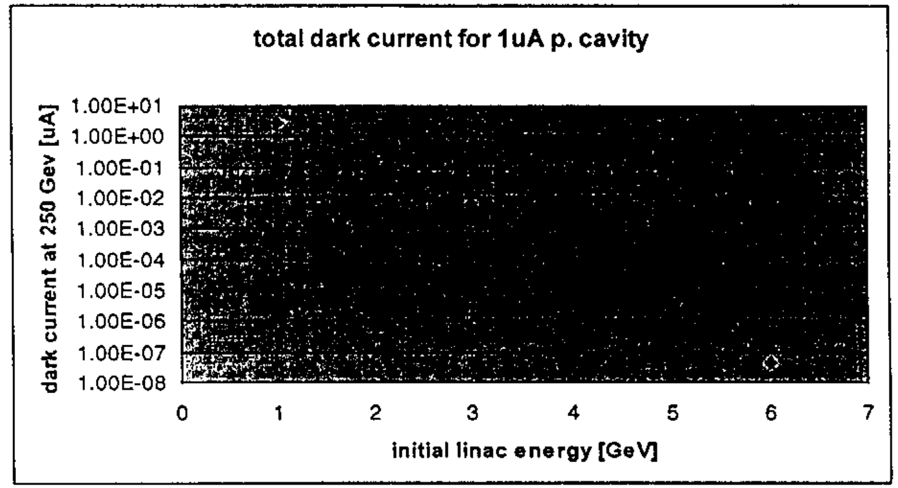

→ # of halo particles p. pulse

$4 \cdot 10^7$ for 3 GeV damping ring (1.4·10^3 p. bunch)
$2 \cdot 10^4$ for 5 GeV damping ring (7 p. bunch)

+ low-energy particles from the last few GeV of the linac

INTERACTION POINT

T. Scholz: BPM for IP feedback

- needs 2 × 3 BPM in last doublet
- compact design fits in cryostat
- 5 μm resolution possible (one dimension)
- can measure both incoming e^+ & outgoing e^- beams: $\Delta\tau = 20$ ns
- e^+e^- pair background ??

T. Scholz

"Beam position measurement at the IP"

Design of a Beam Position Monitor for the Interaction Point (IP) in TESLA

Principle of Working

- technical drawings

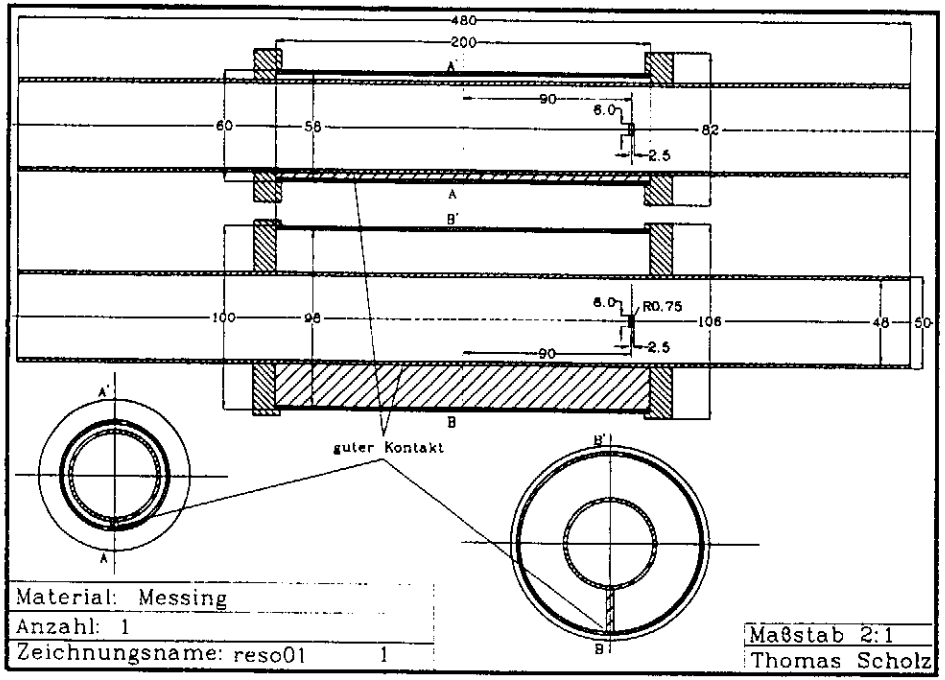

- prototypes

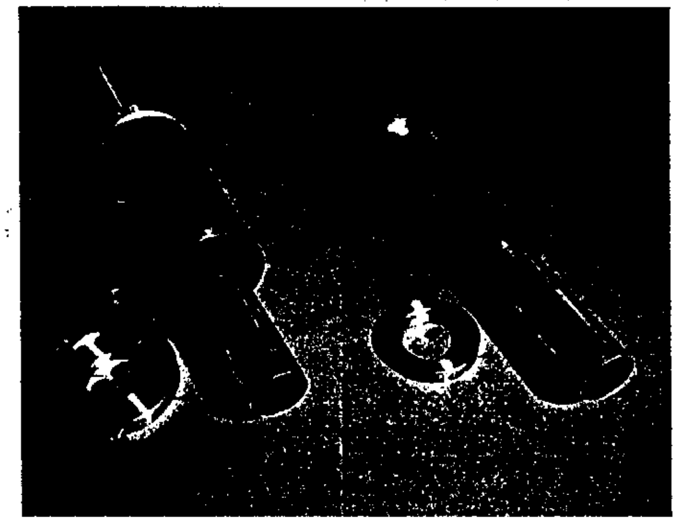

- coupling in / out, magnetic field of the dipole mode

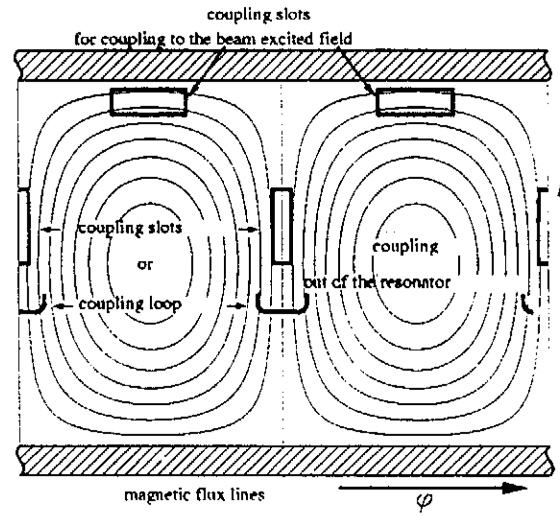

- alternatives for coupling:
  - waveguides
  - inductive loops
- 3D-configuration:

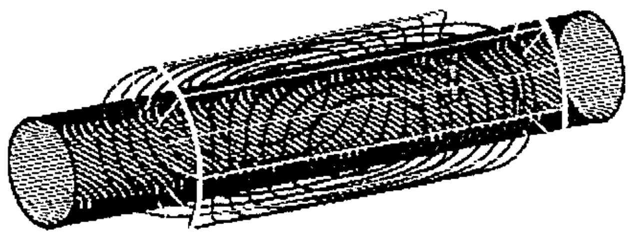

- modes

	monitor A		monitor B	
mode	calculat.	measurem.	calculat.	measurem.
	[GHz]	[GHz]	[GHz]	[GHz]
TE_{011}	0.944	1.000	1.171	1.147
TE_{021}	1.372	1.520	1.949	1.936
TE_{012}	1.605	1.677	1.748	1.729

- quality numbers:
  - prototype A: 5600,
  - prototype B: 850 (500).

201

- prototype B

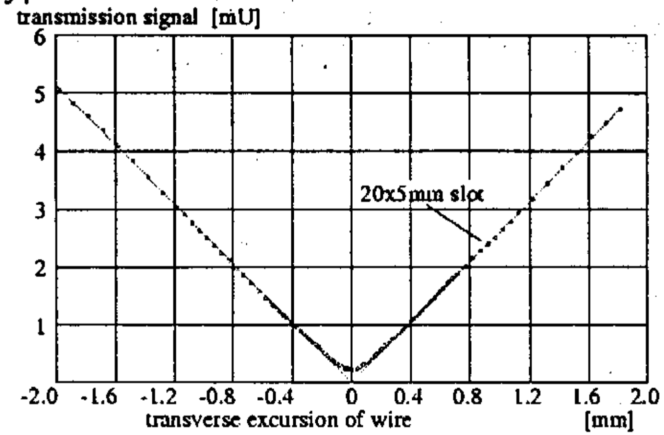

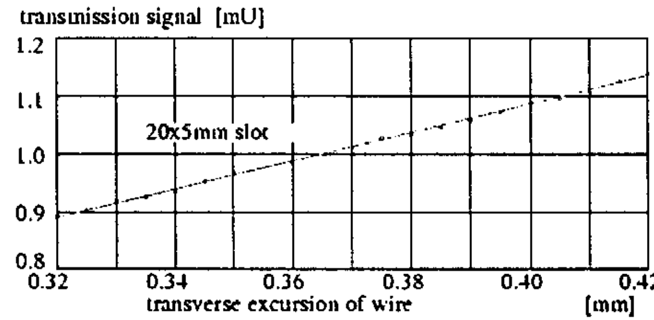

– mask for radiation shielding:

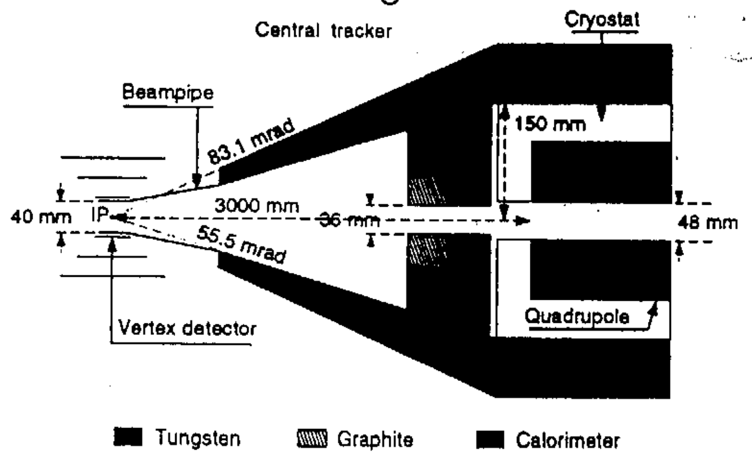

– proposed arrangement of the 3 planned BPM:

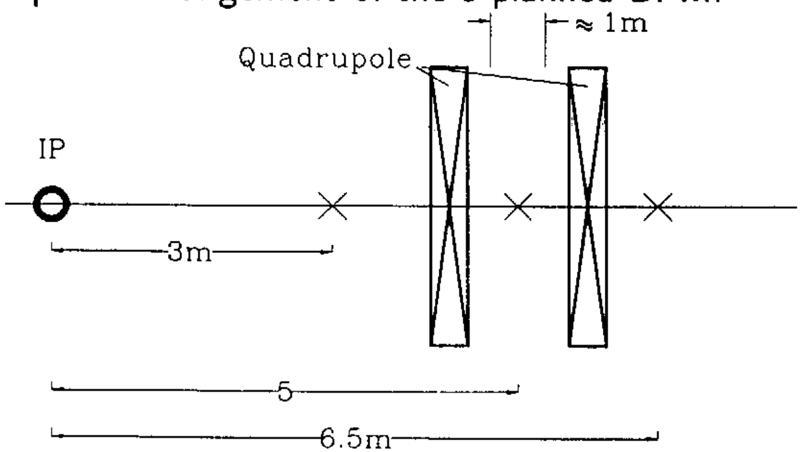

Time Response

- time structure at the BPM's:
  - periodic signals for the distances $20ns$, $33ns$, $43ns$ ($\nu = 1.95GHz$, $Q = 850$):